

ISSN 1408-7073



RMZ

**MATERIALS AND
GEOENVIRONMENT**

MATERIALI IN GEOOKOLJE

Volume
Letnik 55

Ljubljana, June 2008

No. 2
Št.

RMZ - Materials and Geoenvironment

RMZ - Materiali in geookolje

Old title: Rudarsko-metalurški zbornik (Mining and Metallurgy Quarterly),
ISSN 0035-9645, 1952-1997.

Is issued quarterly by the *Faculty of Natural Sciences and Engineering, Ljubljana, Velenje Coal Mine, Velenje and Institute for Mining, Geotechnology and Environment (IRGO), Ljubljana.*

Izdaja *Naravoslovnotehniška fakulteta Univerze v Ljubljani, Premogovnik Velenje, Velenje ter Inštitut za rudarstvo, geotehnologijo in okolje (IRGO), Ljubljana, štirikrat letno.*

Financially supported also by *Ministry of Higher Education, Science and Technology of Republic of Slovenia.*
Pri financiranju revije sodeluje tudi *Ministrstvo za visoko šolstvo, znanost in tehnologijo Republike Slovenije.*

Editor-in-chief (Glavni urednik):

Peter Fajfar

Editorial management (Odgovorni urednik):

Jakob Likar

Advisory Board (Uredniški odbor):

Vlasta Čosović, Sveučilište u Zagrebu
Evgen Dervarič, Premogovnik Velenje
Meta Dobnikar, Univerza v Ljubljani
David John Lowe, British Geological Survey
Borut Kosec, Univerza v Ljubljani
Jakob Likar, Univerza v Ljubljani
Ilija Mamuzić, Sveučilište u Zagrebu
Milan Medved, Premogovnik Velenje
Primož Mrvar, Univerza v Ljubljani
Sebastiano Pelizza, Politecnico di Torino
Daniele Peila, Politecnico di Torino
Andrej Šmuc, Univerza v Ljubljani
Milan Terčelj, Univerza v Ljubljani
Radomir Turk, Univerza v Ljubljani
Milivoj Vulić, Univerza v Ljubljani
Nina Zupančič, Univerza v Ljubljani
Franc Zupanič, Univerza v Mariboru

Editorial Office (Uredništvo):

Barbara Bohar Bobnar

Gregor Vesel

Nives Vukič

Digital Layout (Priprava za tisk):

Tiskarna ACO, Litija

Print (Tisk): Tiskarna ACO, Litija

RMZ - Materials and Geoenvironment

Aškerčeva cesta 12, p.p. 312

1001 Ljubljana, Slovenia

Telefon: +386 (0)1 470 45 00

Telefaks: +386 (0)1 470 45 60

Articles published in journal »**RMZ M&G**« are indexed in international secondary periodicals and databases:
Članki objavljeni v periodični publikaciji »**RMZ M&G**« so indeksirani v mednarodnih sekundarnih virih:

Civil Engineering Abstracts, CA SEARCH® - Chemical Abstracts® (1967- present), Materials Business File, Inside Conferences, ANTE: Abstracts in New Technologies and Engineering, METADEX®, GeoRef, CSA Aerospace & High Technology Database, Aluminium Industry Abstracts, Computer and Information Systems, Mechanical & Transportation Engineering Abstracts, Corrosion Abstracts, Earthquake Engineering Abstracts, Solid State and Superconductivity Abstracts, Electronics and Communications Abstracts.

The authors themselves are liable for the contents of the papers.

Za mnenja in podatke v posameznih sestavkih so odgovorni avtorji.

Copyright © 2008 **RMZ - MATERIALS AND GEOENVIRONMENT**

Naklada 300 izvodov. Printed in 300 copies.

Online Journal/Elektronska revija: <http://www.rmz-mg.com>

Letna naročnina za posameznike v Sloveniji: 16.69 EUR, za inštitucije: 33.38 EUR

Letna naročnina za tujino: 20 EUR, inštitucije 40 EUR

Tekoči račun pri Novi ljubljanski banki, d.d. Ljubljana: UJP 01100-6030708186

Davčna številka: 24405388

ISSN 1408-7073

RMZ – MATERIALS AND GEOENVIRONMENT

PERIODICAL FOR MINING, METALLURGY AND GEOLOGY

RMZ – MATERIALI IN GEOOKOLJE

REVIJA ZA RUDARSTVO, METALURGIJO IN GEOLOGIJO

Historical Review

More than 80 years have passed since in 1919 the University Ljubljana in Slovenia was founded. Technical fields were joint in the School of Engineering that included the Geologic and Mining Division while the Metallurgy Division was established in 1939 only. Today the Departments of Geology, Mining and Geotechnology, Materials and Metallurgy are part of the Faculty of Natural Sciences and Engineering, University of Ljubljana.

Before War II the members of the Mining Section together with the Association of Yugoslav Mining and Metallurgy Engineers began to publish the summaries of their research and studies in their technical periodical *Rudarski zbornik* (Mining Proceedings). Three volumes of *Rudarski zbornik* (1937, 1938 and 1939) were published. The War interrupted the publication and not until 1952 the first number of the new journal *Rudarsko-metalurški zbornik - RMZ* (Mining and Metallurgy Quarterly) has been published by the Division of Mining and Metallurgy, University of Ljubljana. Later the journal has been regularly published quarterly by the Departments of Geology, Mining and Geotechnology, Materials and Metallurgy, and the Institute for Mining, Geotechnology and Environment.

On the meeting of the Advisory and the Editorial Board on May 22nd 1998 *Rudarsko-metalurški zbornik* has been renamed into “*RMZ - Materials and Geoenvironment (RMZ -Materiali in Geokolje)*” or shortly *RMZ - M&G*.

RMZ - M&G is managed by an international advisory and editorial board and is exchanged with other world-known periodicals. All the papers are reviewed by the corresponding professionals and experts.

RMZ - M&G is the only scientific and professional periodical in Slovenia, which is published in the same form nearly 50 years. It incorporates the scientific and professional topics in geology, mining, and geotechnology, in materials and in metallurgy.

The wide range of topics inside the geosciences are welcome to be published in the *RMZ -Materials and Geoenvironment*. Research results in geology, hydrogeology, mining, geotechnology, materials, metallurgy, natural and antropogenic pollution of environment, biogeochemistry are proposed fields of work which the journal will handle. *RMZ - M&G* is co-issued and co-financed by the Faculty of Natural Sciences and Engineering Ljubljana, and the Institute for Mining, Geotechnology and Environment Ljubljana. In addition it is financially supported also by the Ministry of Higher Education, Science and Technology of Republic of Slovenia.

Editor in chief

Table of Contents – Kazalo

Increasing of hot deformability of tool steels – preliminary results

Povečanje vroče preoblikovalnosti orodnih jekel – preliminarni rezultati

VEČKO PIRTOVŠEK, T., FAZARINC, M., KUGLER, G., TERČELI, M. 147

Heat treatment and fine-blankin Inconel 718

Toplotna obdelava in precizno štančanje Inconela 718

ČESNIK, D., BRATUŠ, V., KOSEC, B., ROZMAN, J., BIZJAK, M. 163

Shape memory alloys in medicine

Materiali z oblikovnim spominom v medicini

BROJAN, M., BOMBAČ, D., KOSEL, F., VIDENIČ, T. 173

Artificial tooth and polymer-base bond in removable dentures: the influence of pre-treatment on technological parameters to the bond's strength

Vez med umetnim zobom in polimerno osnovo v snemljivi zobni protezi: vpliv tehnoloških parametrov pred-obdelave na trdnost nastale vezi

PAVLIN, M., RUDOLF, R., JEROLIMOV, V. 191

The onset of Maastrichtian basinal sedimentation on Mt. Matajur, NW Slovenia

Začetek maastrichtijske bazenske sedimentacije na Matajurju, SZ Slovenija

MIKLAVIČ, B., ROŽIČ, B. 199

Analitical surface water forecasting system for Republic of Slovenia

Analičen sistem napovedovanja pretokov površinskih vod v Republiki Sloveniji

VIŽINTIN, G., VIRŠEK, S. 215

Rodoretto talc mine (To, Italy): studies for the optimization of the cemented backfilling

PEILA, D., OGGERI, C., ORESTE, P., POLIZZA, S., MONTICELLI, F. 225

Determination of environmental criteria for estimation of land development using GIS

Uporaba GIS-a za določitev naravnih kriterijev možnosti okoljskega razvoja

VIŽINTIN, G., STEVANOVIČ, L., VUKELIČ, Ž. 237

Construction of the Šentvid tunnel

Gradnja predora Šentvid

POPIT, A., RANT, J. 259

Strateški vidiki oskrbe centralne in jugovzhodne Evrope z električno energijo z oceno vloge premoga ter premogovnih tehnologijStrategic aspects of electricity power supply in central and south - eastern Europe -
The role of coal and coal technologies evaluation

MEDVED, M., DERVARIČ, E., SKUBIN, G. 277

Author`s Index, Vol. 55, No. 2 296**Instructions to Authors** 297**Template** 300

Increasing of hot deformability of tool steels – preliminary results

Povečanje vroče preoblikovalnosti orodnih jekel – preliminarni rezultati

TATJANA VEČKO PIRTOVŠEK¹, MATEVŽ FAZARINC¹, GORAN KUGLER¹, MILAN TERČELJ¹

¹University of Ljubljana, Faculty of Natural Sciences and Engineering, Aškerčeva cesta 12, SI-1000 Ljubljana, Slovenia; E-mail: tpirtovsek@metalravne.com, matevz.fazarinc@guest.arnes.si, goran.kugler@ntf.uni-lj.si, milan.tercelj@ntf.uni-lj.si

Received: December 11, 2007

Accepted: May 29, 2008

Abstract: The influences on the hot deformability of ledeburitic tool steels are very complex since many processing parameters in process chain of steel are involved. For increasing the hot deformability of tool steels thus several research steps should be carried out, i.e. determination of an appropriate soaking temperature, the ranges of safe hot deformation and optimal hot working conditions, optimisation of chemical composition of tool steels, appropriate dimensions of the ingot (cooling rate), etc. The results presented in the contribution demonstrate the importance of the suggested approach for increasing the hot deformability and were obtained on base of industrial practice and of experiments carried out on a Gleeble 1500D thermo-mechanical simulator.

Izveleček: V tem prispevku so prikazani nekateri koraki, ki jih moramo izvesti na ledeburitnih orodnih jeklih, da bi zvišali njihovo plastično sposobnost v vročem, t.j. določitev primerne temperature ogrevanja, določitev območij varnega vročega preoblikovanja ter najbolj optimalnih pogojev preoblikovanja, optimiranje kemične sestave, določitev primerne temperature litja, optimalne dimenzije ingota (hitrost ohlajanja), itd. Na posameznih primerih izbranih orodnih jekel so prikazani rezultati, ki ilustrirajo pomen predlaganega pristopa pri zvišanju plastičnih sposobnosti orodnih jekel. Rezultati, ki potrjujejo omenjeni pristop, so bili dobljeni tako v industrijski praksi kot tudi na simulatorju termomehanskih metalurških stanj Gleeble 1500D.

Keywords: tool steels, cooling rate, hot compression, soaking temperature, chemical composition, neural networks

Ključne besede: orodna jekla, ohlajevalna hitrost, vroče stiskanje, temperature ogrevanja, kemična sestava, nevronske mreže

INTRODUCTION

The occurrence of surface cracking during hot forming (hot deformability) of ledeburitic tool steels is still an insufficiently investigated research area; it is influenced as much by processing and geometrical as by intrinsic (material) properties. Alloying elements (V, Cr, Mo, etc) in tool steels form carbides that improve hardenability, control grain growth, increase strength, hardness, wear resistance, etc. and decrease hot deformability and make hot working temperature range very narrow in comparison to conventional steels. Additionally the majority of tool steels are nowadays produced from scrap material and thus besides carbide-forming elements other elements such as copper and tin have a strong influence on hot deformability of tool steels when their concentration is not in the acceptable range. Their presence can form eutectic phases with low melting points or phases that are brittle and are predominantly precipitated on grain boundaries. Thus, determination of the acceptable chemical composition of any tool steel is an important step at increasing hot deformability. The relatively low hot deformability of tool steels is characterized by the production of external (surface) as well as of internal cracks during hot forming. This reduces the profitability of the production process, as well as the useful mechanical properties of the tool steel since the defects in the tool material originate in general from inadequate low hot deformability as well as from inappropriate hot working conditions^[1-9].

Publications in the literature with regards to hot deformability of low alloyed steels

as well as those regarding tool steels, are predominately of a partial nature. Namely, they study only the influence of particular factors on hot deformability i.e., determination of the upper and lower temperatures of hot working, determination of the limit of hot plasticity, influence of deformation parameters on hot deformability, precipitation of carbides, etc. Moreover, hot tension, hot compression, hot torsion and laboratory hot rolling tests were applied and the materials were predominately in the wrought (deformed) state; the influence of thermo-mechanical parameters (cooling rate, casting temperature, variable chemical composition, soaking temperature) in previous processing chains usually were not considered. Any contribution in this research area in which the occurrence of cracking during hot forming is studied by more integral approach and in which the basic points which characterize the relevant processes that take place in the materials in the whole processing chain of steel production, will be defined, is important and valuable. It is important to mention that the values of the chosen processing parameters in previous processing chains should have a positive influence on hot deformability; any eventual negative influence can be partly compensated by appropriately chosen hot deformation parameters. Modern practice proves that the above mentioned thermo-mechanical processing parameters significantly influence the chosen deformation parameters and thus they cannot be constant.

The investigation of the presented paper is dealing with processing of tool steels BRM2, OCR12VM, CRV3 and BRCMO2. Some steps that should be applied in order

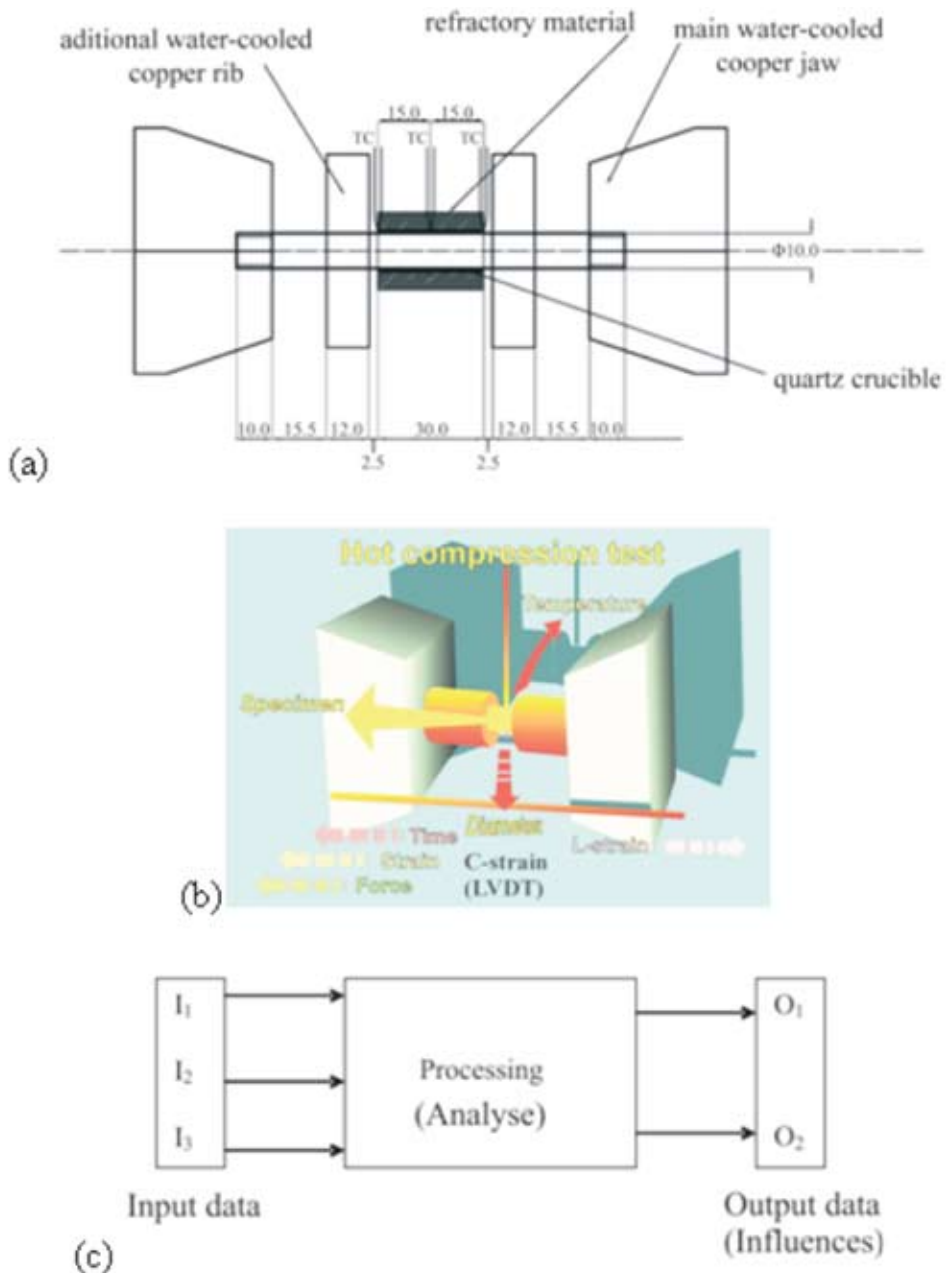


Figure 1. Applied method and tests: solidification test (a)^[12], hot compression test (b), schematic presentation of analysis of influences on hot deformability by CAE neural networks (c)

Slika 1. Uporabljene metode in testi: test strjevanja (a)^[12], tlačni preizkusi v vročem (b), shematski prikaz analize vplivov parametrov na vročo preoblikovalnost s CAE nevronskimi mrežami (c)

to increase their hot deformability, i.e. determination of optimal casting temperature, cooling rate, soaking temperature, working range or safe hot deformation and determination of acceptable chemical composition are suggested. Thus, an extension of hot deformability and consequently improvement in the applied mechanical properties of tool steels can be achieved.

EXPERIMENTAL

Applied methods and equipment

Gleeble 1500D was applied so for simulation of solidification process at various rates as well as for hot compression. Specially developed test, presented in Figure 1a^[12], was used for simulation of solidification process; the test is computer guided thus various process paths and resulting microstructures can be obtained with varying of solidification and cooling rates. Upper and lower temperature range of safe hot deformation was obtained by hot compression tests (Figure 1b). The applied criterion was occurrence or non-occurrence of cracks on deformed specimens at compression strain of 0.9. The data on hot deformability was collected in industrial conditions as well as in laboratory. Analyse of influences on hot deformability was carried out by CAE neural networks (see Figure 1c). The data base consists of industrial as well as of laboratory results. Optical microscopy (Olympus BX61) was used for observation of microstructure.

Description of applied tool steels

The proposed new approach will be illustrated with particular results obtained in thermo-mechanical processing of ledeburitic tool steels, i.e. BRM2 (HSS), OCR12VM (cold working tool steel), CRV3 (cold working tool steel) and BRC-MO2 (super HSS). All these steels contain C and carbide-forming elements (Cr, W, Mo and V, chemical composition is given in Table 1). The microstructure of these steels consists of a martensitic matrix in which the ledeburitic and secondary carbides are present. These tool steels have specifically useful mechanical properties such as high hardness, wear resistance and high tempering resistance on one hand and higher flow stress and lower hot deformability on the other. The morphology, size, distribution and type of carbides influence on the behaviour of the material during hot forming were studied. During heating, soaking and hot deformation various processes take place: decay (decomposition) of carbide phases and formation of new carbide phases (secondary phases) and dissolution of carbides and of alloying elements. All these processes and properties of particular phases, their volume fraction (proportion) and chemical composition result in hardening during hot deformation that decreases hot deformability^[2-7]. In Figure 2a-b typical microstructures of ledeburitic tool steels for as-cast and wrought (deformed) states are presented, respectively. Figure 2c shows the approximate values of microhardness of the relevant carbides.

Table 1. Chemical composition of applied tool steels (wt.%)**Tabela 1.** Kemična sestava preiskovanih orodnih jekel (mas.%)

	C	Si	Mn	Cr	Mo	V	W	Co
BRM2	0.90	0.30	0.30	4.05	5.10	1.95	6.35	-
BRCMO2	1.09	0.26	0.25	3,81	9.32	1.09	1.40	8.20
OCR12VM	1.52	0.25	0.32	11.65	0.80	0.89	-	-
CRV3	1.17	0.24	0.26	11.3	1.35	1.48	2.24	-

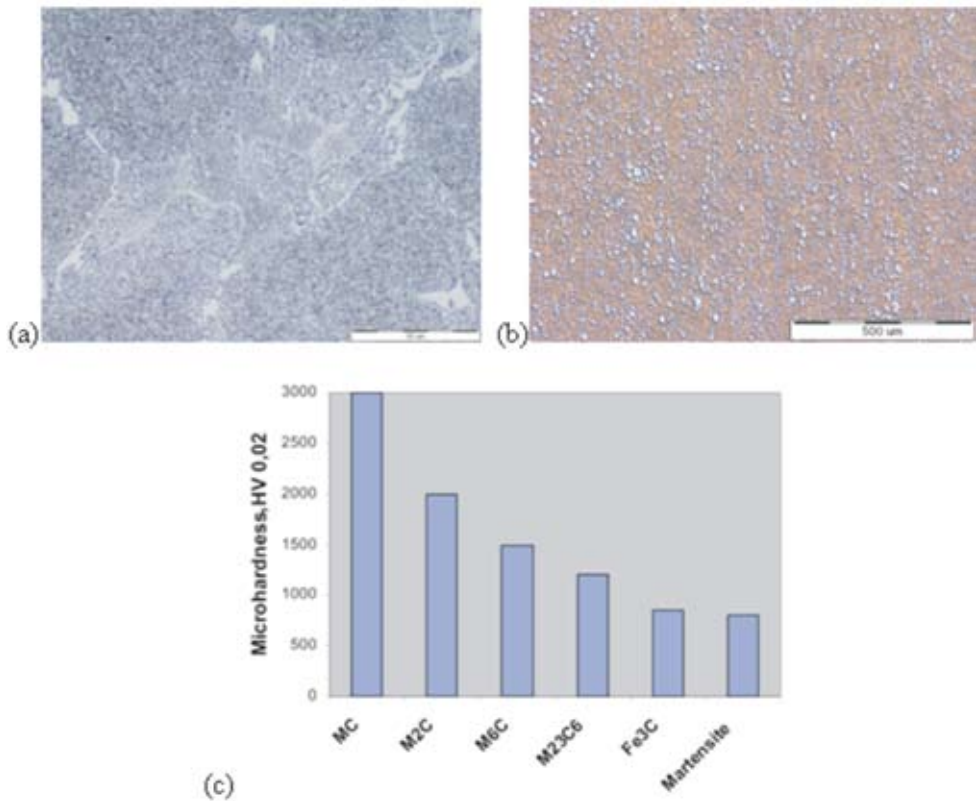


Figure 2. Typical microstructures of tool steels: BRCMO2 as-cast state (a), BRCMO2 in wrought (deformed) state (b), and microhardness values of carbides^[4] (c)
Slika 2. Tipična mikrostruktura orodnih jekel: BRCMO2, lito stanje (a), BRCMO2 predelano stanje (b) in mikrotrdote posameznih karbidov^[4] (c)

RESULTS ON EXPERIMENTAL AND COMPUTATIONAL STEPS NEEDED FOR INCREASING OF HOT DEFORMABILITY

Determination of an appropriate casting temperature and cooling rate

The casting temperature and cooling rate during solidification influence the diffusion processes. Depending on the cooling rate, precipitation of different types of carbides with different chemical composition, morphology and distribution may occur during solidification. This results in different microstructures with different proportion of particular phases with various

properties and different hot deformability. In the ingot due to different cooling rates in the cross section, different microstructures are formed. The measured cooling rate^[11] of the ingot core was approximately 0.36 K/s. Figure 3 presents the microstructure obtained at various cooling rates on solidification of super high speed steel (BRCMO2). In the vicinity of the ingot surface, where the cooling rate was the highest (>0.36 K/s), in the soft annealed microstructure of spheroidal perlite, M_2C type of eutectic carbides with fine lamellar morphology can be hardly visible (Figure 3a). In Figure 3b the microstructure ob-

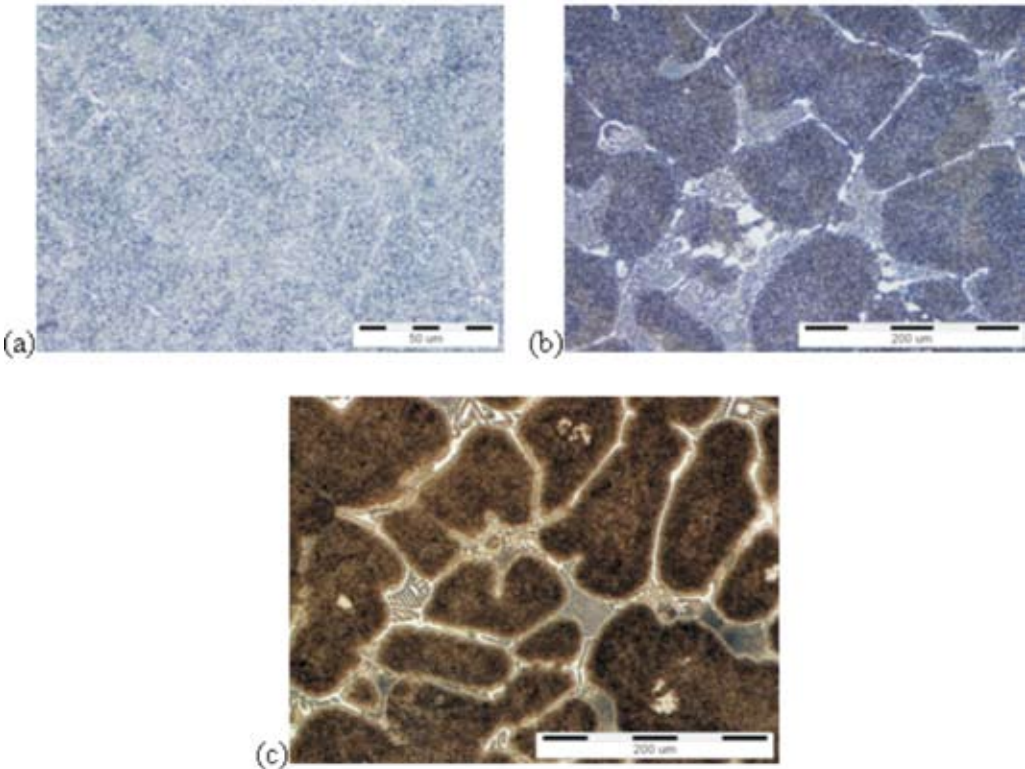


Figure 3. Microstructures obtained at various cooling rates of BRCMO2 tool steel, >0.36 K/s (a), 0.36 K/s (b) and 0.16 K/s (c)

Slika 3. Mikrostrukture dobljene pri različnih ohlajevalnih hitrostih za jeklo BRCMO2, >0,36 K/s (a), 0,36 K/s (b) in 0,16 K/s (c)

tained 50 mm from the ingot centre where the cooling rate was approximately 0.36 K/s is presented. In the soft annealed basic microstructure coarse eutectic cells of coarser lamellar eutectic type M_2C and primary carbides is visible (compared to Figure 3a). The microstructure in Figure 3c was obtained by simulation of the solidification process at a cooling rate of 0.166 K/s; the solidification process was carried out on the Gleeble 1500D thermo-

mechanical simulator as reported in^[12]. In the microstructure beside M_2C eutectic carbides, the eutectic carbide M_6C with fish bone morphology can also be observed. It is obvious that the morphology, proportion of various types of carbides and their chemical composition are different at different cooling rates. Thus the weight and dimensions of ingots influences the obtained microstructures and consequently also the hot deformability.

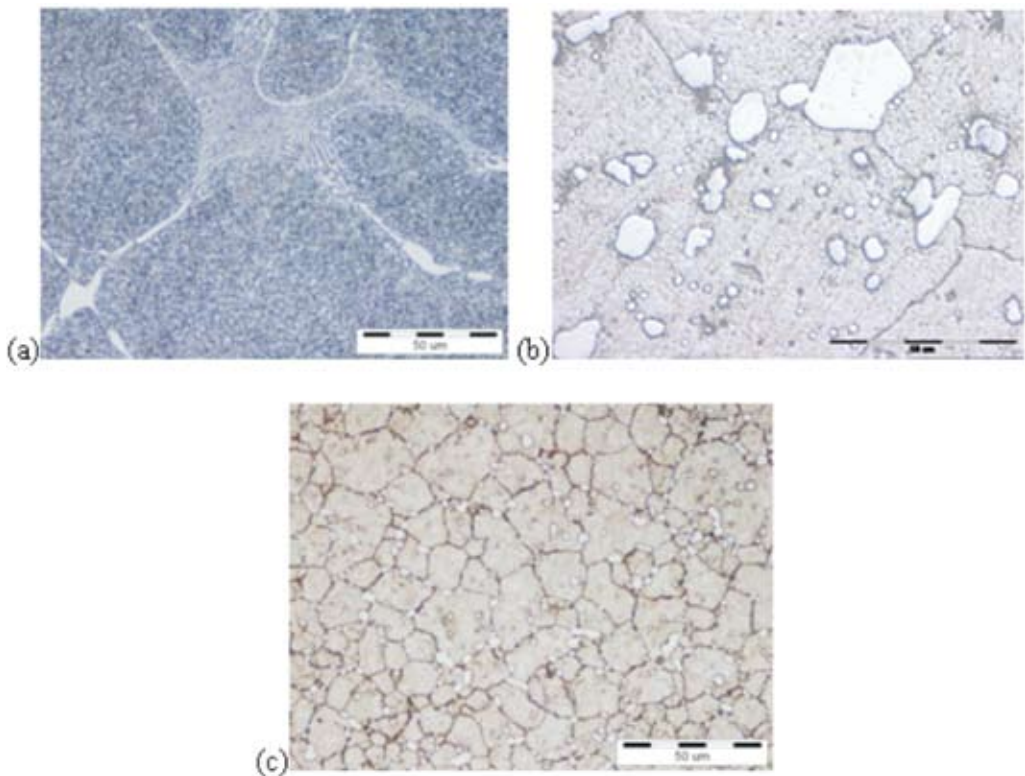


Figure 4. Initial as-cast microstructure of ingot (a); microstructure obtained in rolled piece at inappropriate soaking temperature (b); microstructure obtained in rolled piece at appropriate soaking temperature (c); BRCMO2 tool steel

Slika 4. Začetna mikrostruktura vlitega ingota (a); mikrostruktura dobljena iz končnega, valjanega dela, ogrevanega pri neprimerni temperaturi (b); mikrostruktura dobljena iz končnega, valjanega dela, ogrevanega pri primerni temperaturi (c); orodno jeklo BRCMO2

Assessment of an appropriate soaking temperature

Before conducting the hot compression tests, the appropriate soaking temperatures for as-cast and for the deformed initial state were assessed. This step is presented for the case of hot forming of BRCMO2 tool steel. The criterion for its assessment was the appearance of cracks on the compressed specimen surface at a strain of 0.9. The soaking temperature influences the processes of dissolution of fine carbides, coagulation and growth of coarse carbides, proportion of equilibrium phases, and growth of austenitic grains. The fine lamellar as-cast microstructure of an ingot (BRCMO2, Figure 4a) in the case of inappropriate (too high) soaking temperature deformed by hot rolling (in end rolled piece) with a microstructure consisting of coarse grains and coarse eutectic carbides (Figure 4b). In the case of an appropriate soaking temperature the initial microstructure can be deformed into an end piece with fine grained microstructure with fine and homogeneously distributed eutectic carbides (Figure 4c). Thus the soaking temperature does not influence only the hot deformability but also the mechanical properties of the product. Further, hot compression testing (using the proposed criterion) revealed that the appropriate soaking temperature for a deformed microstructure (same chemical composition, same charge) differs from that for the as-cast state.

The soaking temperature also influences the lower limit of the temperature range for safe hot forming. This example is presented for the case of hot forming of OCR12VM tool steel in Figure 5. In the case of an appropriate soaking tempera-

ture it was possible to deform at 850 °C without the occurrence of micro-cracks in the deformed piece (Figure 5a-b). In the case of an inappropriate soaking temperature and hot forming at the same temperature (850 °C), micro- (on triple points and along grain boundaries) and macro-cracks occurred (Figure 5c-e). Thus the working temperature range is narrowed due to the shift of lower temperature of safe hot forming to higher values. This could be explained by intensive precipitation of secondary carbides along the grain boundaries (Figure 5e) during the deformation phase; coarser eutectic carbides are formed as a consequence of the inappropriate soaking temperature that decreases hot deformability. It is general known that too coarse carbides precipitated on grain boundaries decrease the hot deformability especially on lower limit of working range.

Determination of safe hot working range

This step is illustrated on CRV3 tool steel for wrought (deformed) initial state. After the determination of the optimal soaking temperature, hot compression tests were carried out in order to determine the flow stresses and range of safe hot deformation. Physical simulation of the hot working process was carried out on the Gleeble 1500D thermo-mechanical simulator. Cylindrical specimen dimensions of $\phi=10$ mm \times 15 mm were applied. The following testing conditions were chosen: temperature range 850-1180 °C, strain rates 0.001-6 s⁻¹ and true strains 0-0.9 (Table 2). On the basis of the obtained flow curves, the range of safe hot deformation was estimated by Prasad's processing map. This was developed on the basis of a dynamic

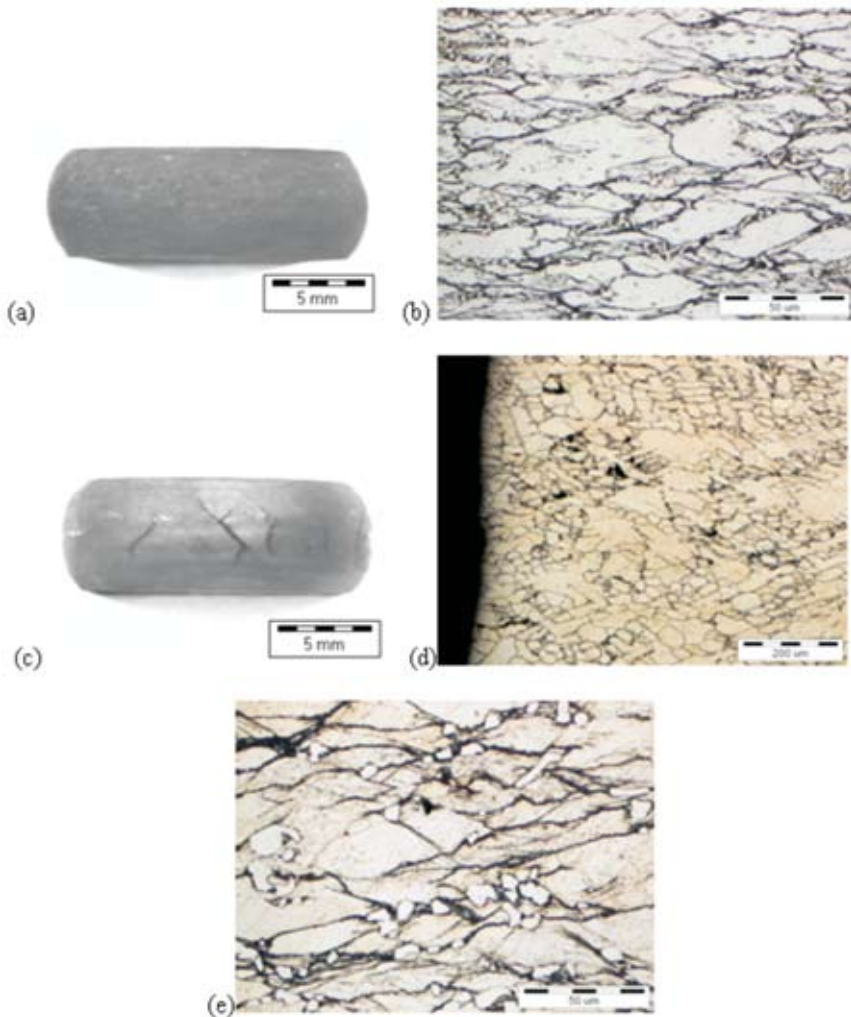


Figure 5. Influence of soaking temperature on hot deformability at 850 °C for OCR12VM, macro view of deformed specimen (soaked at an appropriate temperature) (a), microstructure of deformed specimen (soaked at an appropriate temperature) (b), macro-cracks on deformed specimen soaked at an inappropriate temperature (c), formation of micro-cracks on grain boundaries (soaked at an inappropriate temperature) (d), precipitated carbides on grain boundaries and coarser eutectic carbides (soaked at an inappropriate temperature) (e)

Slika 5. Vpliv ogrevne temperature na vročo deformacijo pri 850 °C za jeklo OCR12VM, makroposnetek deformiranega vzorca (ogrevanega na primerno temperaturo) (a), mikrostruktura deformiranega vzorca (ogrevanega na primerno temperaturo) (b), makro razpoke na površini deformiranega vzorca (ogrevanega na neprimerno temperaturo) (c), nastanek mikro razpok na mejah zrn deformiranega vzorca (ogrevanega na neprimerno temperaturo) (d), izločeni karbidi na mejah zrn in grobi evtectski karbidi (ogrevano na neprimerno temperaturo) (e)

material model (DMM). The processing map of the material can be described as an explicit representation of its response to the imposed process parameters. This is a superimposition of the efficiency of power dissipation (equation 1) and an instability map (equation 2).

$$\eta = \frac{2m}{m+1} \quad (1)$$

$$\xi \left(\frac{\dot{\epsilon}}{\epsilon} \right) = \frac{\partial \ln(m/(m+1))}{\partial \ln \dot{\epsilon}} + m > 0 \quad (2)$$

In equations 1 and 2, η is efficiency of power dissipation, m is strain rate sensitivity, ξ is parameter expressing stability or instability of flow behaviour ($\xi < 0$ indicates on instable flow behaviour) and $\dot{\epsilon}$ is average strain rate.

One can find details about processing maps in^[10]. In Figure 6a-b the efficiency of power dissipation and the instability map

at strains of 0.2 and 0.4 are presented, respectively. The relatively low values for the efficiency of power dissipation indicate smaller microstructural changes (dynamic recrystallization and recovery) and consequently also possible lower hot ductility. Unstable areas of hot deformation occur at lower strain rates (approximately at 0.01 s⁻¹) and lower deformation temperatures (below 950 °C) as a consequence of precipitation of secondary carbides on grain boundaries (Figures 7a-b).

Laboratory assesment of the upper and lower limit of the working range

At the upper limit of the working range for CRV3 tool steel, due to the increase (up to 40 °C) of specimen temperature during deformation, local melting and precipitation of thin films of eutectic carbides took place along the grain boundaries, resulting in a rapid decrease of hot deformability. In this case precipitated new eutectic has lamellar morphology (Figure 8). On

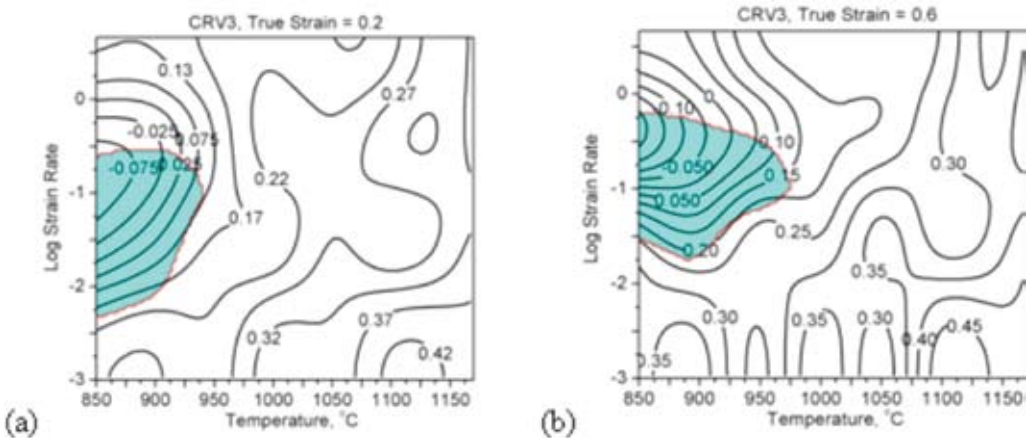


Figure 6. Superimposition of efficiency of power dissipation and instability map for CRV3 tool steel for deformed state at strain of 0.2 (a) and at strain of 0.6 (b)

Slika 6. Učinkovitost porabe moči in mape nestabilnosti za CRV3 orodno jeklo, pri deformaciji 0,2 (a) in 0,4 (b)

Table 2. Testing (hot compression) conditions for CRV3 tool steel**Tabela 2.** Tesni pogoji za tlačne preizkuse v vročem za CRV3 orodno jeklo

Deform. temp./ °C	Strain rate / s ⁻¹
850, 900, 950, 1000, 1050, 1100, 1150, 1160, 1170, 1180	0.001, 0.01, 0.1, 1.0, 6.0

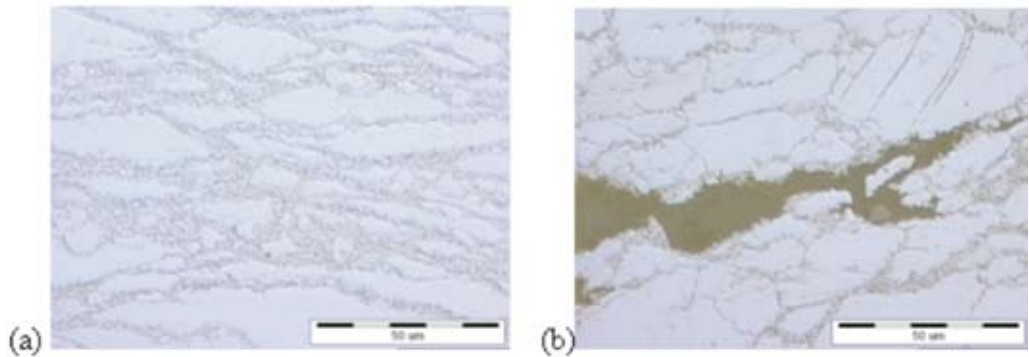


Figure 7. Microstructure of deformed specimen obtained at 850 °C, showing precipitation of carbides on grain boundaries (a), and occurrence of cracking on grain boundaries (b); strain rate 0.01 s⁻¹, CRV3 tool steel

Slika 7. Mikrostruktura vzorca deformiranega pri 850 °C z izločki na mejah zrn (a) in pojavom razpok na mejah zrn (b); hitrost deformacije 0,01 s⁻¹, orodno jeklo CRV3

the same figure cracking caused by grain boundary melting is also presented. At the lower limit of the working range the carbides that have precipitated during hot deformation along grain boundaries (Figure 7a) are responsible for the occurrence of cracking (Figure 7b). Carbides inhibit the movement of grain boundaries as well as processes of dynamic recrystallization, leading to occurrence of cracking at higher strains ($\epsilon = 0.6$). Thus examination of the microstructure confirms the position of the instability area shown in Figure 6.

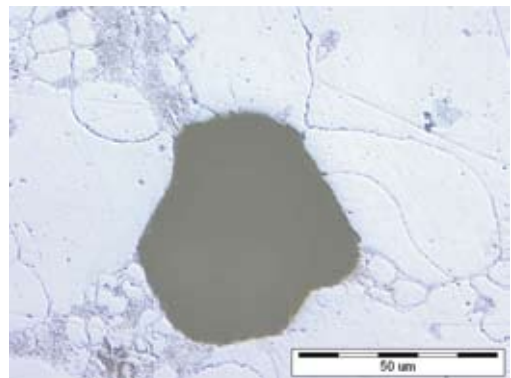


Figure 8. Formation of eutectic with lamellar morphology and grain boundary cracking

Slika 8. Tvorba eitektika z lamelarno morfologijo in pokanje na mejah zrn

Precipitation of carbides along grain boundaries is also expressed by the increasing of maximum flow curve values at lower strain rates. Namely, at lower strain rates the processes of carbides precipitation during hot deformation is more emphasised in comparison to higher strain rates, leading to higher values of the flow curves (peak values, Figure 9). The processes of hardening are so intense during the deformation at 850-950 °C that the values of peak stresses at lower strain rates intersect the values of peak stresses obtained at higher strain rates. Chemical composition of tool steel effects on upper limit of working range, since the temperature of precipitated eutectic carbides can vary up to 20 °C.

Determination of optimal chemical composition

Neural networks enable analysis of each individual parameter, as well analysis of the simultaneous influence of several parameters on hot deformability. The last step which contributes to increase of hot deformability is optimisation of chemical composition in the framework of its allowable variations. But at least two ranges should be considered separately, i.e. upper limit of working range and medium of working range. For analysis of the influence of chemical composition on hot deformability, the application of artificial neural networks is more appropriate than classical statistical methods. Beside the presence of carbides in the microstructure, other elements (oligo elements, trace elements) also influence the hot deformability.

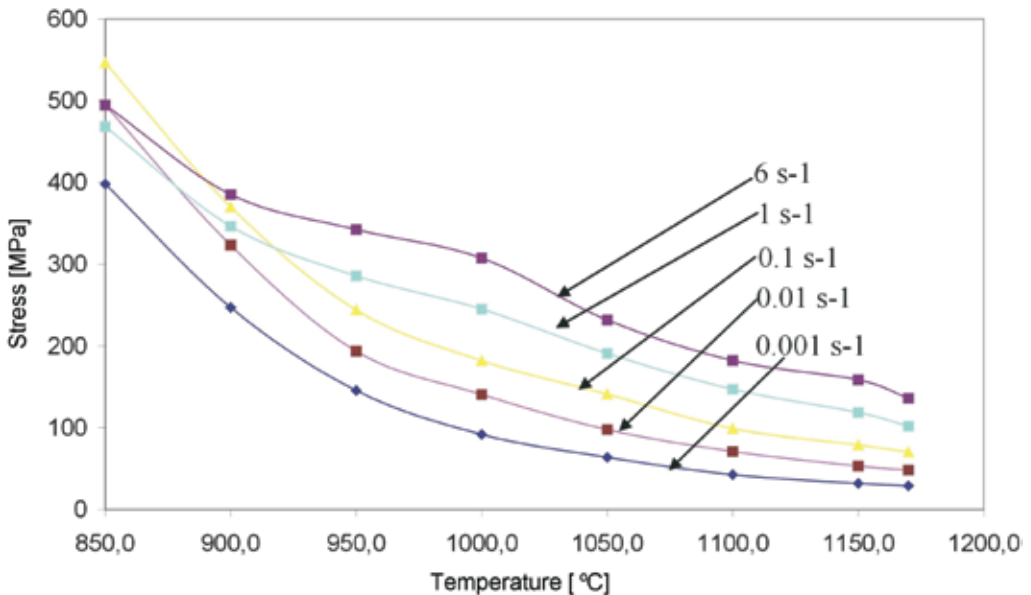


Figure 9. Influence of strain rates and temperatures on peak values of flow curves, CRV3 tool steel

Slika 9. Vpliv hitrosti deformacije in temperature na maksimalne napetosti tečenja za orodno jeklo CRV3

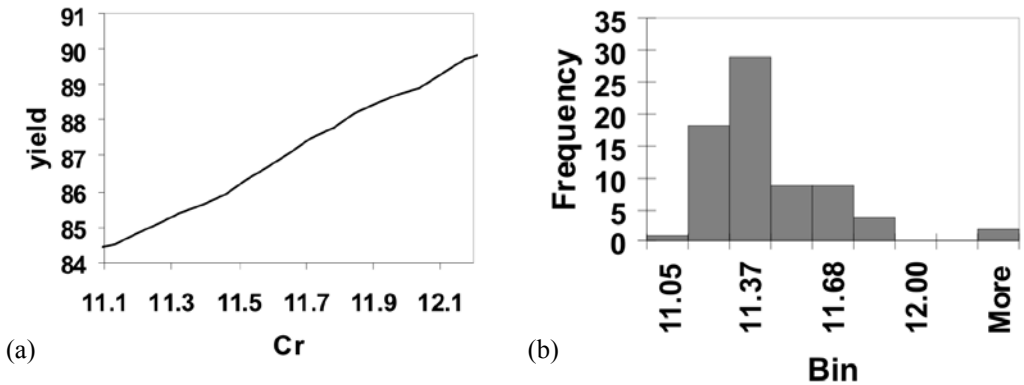


Figure 10. Influence of Cr on yield of hot rolling (influence on upper working range) (a) and frequency of distribution of Cr (b), OCR12VM tool steel

Slika 10. Vpliv Cr na izplen vročega valjanja (a), frekvenca razporeditve Cr (b) za orodno jeklo OVR12VM

Optimisation of chemical condition considering upper limit working range

Upper limit of working range is determined by occurrence of incipient melting, i.e. usually presence of eutectic carbides and phases with low melting point are decisive factors. On base of industrial data (yield and chemical composition) for OCR12VM tool steel where the ingots were soaked on upper limit of the temperature range and after this also hot rolled, and by means of CAE NN the results of influence of Cr on hot deformability (yield) is given in Figure 10a. On Figure 10b the frequency of Cr distribution is given. From the Figure 10a it is visible that increased content of Cr results in increased yield. The result was proven also by thermocalc calculation; increased content of Cr also increases temperature of precipitation of eutectic carbides. Also other chemical elements (especially carbide-forming) influence the temperature of precipitation of eutectic carbides. The results indicate that upper limit of work-

ing range can vary in range of about 25 °C thus chemical composition should be considered as a determining factor in processing parameters.

Optimisation of chemical condition considering medium working range

For BRM2 tool steel hot torsion tests (medium working range, temperature of deformation 1060 °C, strain rate 1s⁻¹) were carried out in order determine hot deformability (number of spins up to breakdown of the tested specimen^[9]). In this analysis 128 various test specimens (deformed state) with different chemical composition were included. On Figure 11a-b the influence of carbon and vanadium on hot deformability are presented. Allowable variation of carbon is in range 0.86-0.94 wt.% and of vanadium 1.7-2.1 wt.%. From Figure 11 it apparent that the optimal value for carbon is 0.88 wt.%, while the values of vanadium should be at the lower limit of the allowable variation.

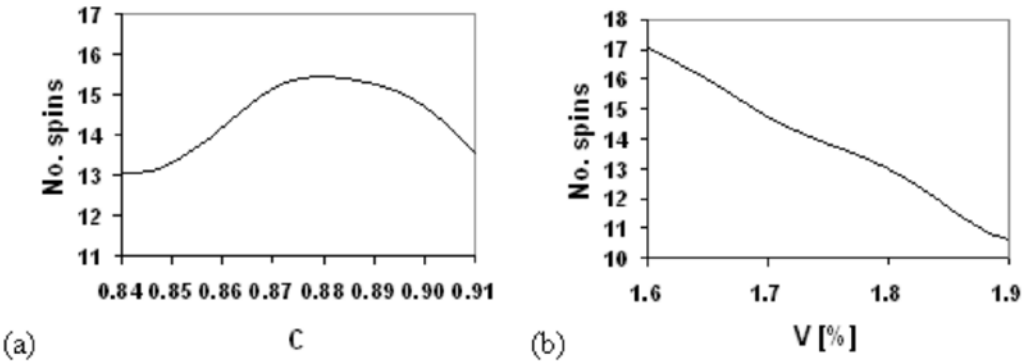


Figure 11. Hot deformability (plasticity) as function of content of chemical elements for medium working range: (a) carbon (C), (b) vanadium (V), BRM2 tool steel
Slika 11. Vroča plastičnost kot funkcija vsebnosti kemijskih elementov za orodno jeklo BRM2: ogljik (a) in vanadij (b)

CONCLUSIONS

The influences of processing parameters (factors), chemical composition, etc on the hot deformability of ledeburitic tool steels are very complex. Many processing parameters (in all process chains) of steel production (including soaking and hot forming) are involved thus integral research approach should be applied in order to increase hot deformability. In this contribution some recommended steps that should be carried out for increasing hot deformability are presented. The following should be emphasised:

1. The cooling rate influences the formation of various phases and the types of carbides of differing morphology, size, chemical composition and properties.
2. Soaking temperature influences the dissolution, the growth and coagulation of carbides, growth of austenitic grains and the precipitation of carbides at lower temperatures in the working range.
3. Chemical composition, despite its variation within the allowable range, influences the hot deformability of tool steels but in different way on upper working range in comparison to medium working range.
4. The highest temperature of the working range is determined by the beginning of incipient melting, while the lowest temperature is defined by the occurrence of micro-cracking as a consequence of precipitation of carbides on grain boundaries.
5. The deformations (strains) can be higher in the range of optimal hot working condition.

POVZETEK

Povečanje vroče preoblikovalnosti orodnih jekel – preliminarni rezultati

Vplivi procesnih parametrov izdelave, kemične sestave itd. na vročo plastičnost ledeburitnih jekel so zelo kompleksni, zato je potreben bolj integralni pristop, če želimo dvigniti vročo preoblikovalnost. Rezultati raziskave so strnjeni v naslednjem:

1. Hitrost ohlajanja vpliva na formiranje različnih faz ter karbidov z različnimi morfologijami, obliko, tipom in velikostjo.
2. Temperatura ogrevanja vpliva na raztopitev, rast in koagulacijo karbidov, rast avstenitnih zrn in izločanje karbidov na spodnji meji temperaturnega območja preoblikovanja.
3. Kemična sestava, kljub variranju v dopustnih mejah različno vpliva na preoblikovalnost na zgornji meji oz. v sredini področja preoblikovanja.
4. Zgornja temperatura preoblikovanja je določena s pričetkom taljenja na kristalnih mejah, spodnja meja pa s pojavom mikrorazpok kot posledica izločanja karbidov.
5. Deformacije so lahko večje v srednjem temperaturnem območju preoblikovanja.

REFERENCES

- [1] KOPP, R., BERNRATH, G. (1999): The determination of formability for cold and hot forming conditions. *Steel Research.*; Vol. 70/(4+5), pp. 147-153.
- [2] IMBERT, C.A.C., MCQUEEN, H.J. (2001): Hot ductility of tool steels. *Canadian Metallurgical Quarterly.*; Vol. 40, pp. 235-244.
- [3] IMBERT, C.A.C., MCQUEEN, H.J. (2001): Peak strength, strain hardening and dynamic restoration of A2 and M2 tool steels in hot deformation. *Materials Science and Engineering.*; Vol. 313, pp. 88-103.
- [4] IMBERT, C.A.C., MCQUEEN, H.J. (2001): Dynamic Recrystallization of A2 and M2 tool steels. *Materials Science and Engineering.*; Vol. 313, pp. 104-116.
- [5] LIU, J., CHANG, H., WU, R., HSU, T.Y., RUAN, X. (2000): Investigation on hot deformation behaviour of AISI T1 high-speed steel. *Materials Charact.*; Vol. 45, pp.175-186.
- [6] MILOVIC, R., MANOJLOVIC, D., ANDJELIC, M., DROBNJAK, D. (1992): Hot workability of M2 high-speed steel. *Steel Research.*; Vol. 63/2, pp. 78-84.
- [7] RODENBURG, C., KRYZANOWSKI, M., BEYNON, J.H., RAINFORTH, W.M (2004): Hot workability of spray-formed AISI M3:2 high speed steel. *Materials Science and Engineering.*; Vol. 386, pp. 420-427.
- [8] IMAI, N., KOMATSUBARA, N., KUNISHIHE, K. (1997): Effect of Cu, Sn and Ni on Hot Workability of Hot-rolled Mild Steel. *ISIJ International.*; Vol. 37/3, pp. 217-223.

- [9] SZILVASSY, C.C., WONG, W.C.K. (1992): Statistical classification of chemical composition and microstructure as a function of tool-steel deformability. *Journal of Materials Processing Technology*.; Vol. 29, pp. 191-202.
- [10] PRASAD, Y.V.R.K., SASIDHARA, S. (1997): *Hot Working Guide: Compendium of Processing Maps*. ASM - International, pp. 1-24.
- [11] VEČKO PIRTOVŠEK, T., TERČELJ, M. (2007): Increasing of hot deformability of tool steels. In: J.Lamut (ed.), M.Knap (co-ed.). 13. *Conference on process metallurgy, Moravče, 17.-18. Maj 2007*. Departments of materials and metallurgy Faculty of Natural Science and Metallurgy, pp. 77-88, (in slovene language).
- [12] BRADASKJA, B., KORUZA, J., FAZARINC, M., KNAP, M., TURK, R. (2008): A laboratory test for simulation of solidification on Gleeble 1500D thermo-mechanical simulator. *RMZ-Mater. Geoenviron.*; Vol.55/1, pp. 31-40.

Heat treatment and fine-blankin Inconel 718

Toplotna obdelava in precizno štancanje Inconela 718

DAMIR ČESNIK¹, VITOSLAV BRATUŠ¹, BORUT KOSEC², JANEZ ROZMAN³, MILAN BIZJAK²

¹Hidria Institute for Materials and Technology d.o.o., Spodnja Kanomlja 23, SI-5281 Spodnja Idrija, Slovenia; E-mail: damir.cesnik@hidria.com, vito.bratus@hidria.com

²University of Ljubljana, Faculty of Natural Sciences and Engineering, Aškerčeva cesta 12, SI-1000 Ljubljana, Slovenia; E-mail: borut.kosec@ntf.uni-lj.si, milan.bizjak@ntf.uni-lj.si

³ITIS d.o.o., Lepi pot 11, SI-1001 Ljubljana, Slovenia; E-mail: janez.rozman@guest.arnes.si

Received: December 15, 2007

Accepted: June 9, 2008

Abstract: Inconel 718 is a nickel based superalloy. Functional properties of Inconel 718 can be achieved by choosing proper heat treatment. The most important kind of hardening is precipitation hardening. The process consists of solution annealing, quenching and aging. The correct heat treatment is required to ensure proper rate between γ'' and δ phases. The effect of time and temperature on microstructure and mechanical properties was determined by microstructure changes, measurement of hardness, tensile strength and toughness. Furthermore, the influences of different heat treatment procedures on mechanical properties of Inconel 718 alloy that are reflected in the loading on the tool were investigated. A force that acts on the punch during fine-blanking of parts to be used in turbochargers for automotive diesel engines was measured. The measurements were made with a force transducer composed of strain gauges, connected in a full Wheatstone bridge, placed directly on the punch. The sheet metal from which segments were produced was alloy Inconel 718. The aim was to define the time - dependence of the force.

Izvleček: Inconel 718 je superzlitina na osnovi niklja. Uporabne lastnosti Inconela 718 zagotovimo s pravilno izbiro toplotne obdelave. Glavni način utrjevanja je izločevalno utrjevanje. Postopek obsega raztopno žarenje, gašenje in staranje. Pravilna toplotna obdelava je potrebna, da zagotovimo ustrezno razmerje med fazama γ'' in δ . Vpliv časa in temperature na mikrostrukturo in mehanske lastnosti smo zasledovali s pomočjo mikrostrukturnih sprememb, meritev trdote, natezne trdnosti in udarne žilavosti. Prav tako smo zasledovali vpliv mikrostrukturnih in mehanskih lastnosti na obremenitev orodja pri preciznem štancanju Inconela 718. Vpliv smo zasledovali z meritvijo sile preciznega štancanja pri izdelovanju segmentov, ki se uporabljajo za turbopolnilnike dizelskega motorja. Silo smo merili z merilnimi lističi povezanimi v Wheatstonov mostič, ki smo jih nalepili na nož orodja. Pločevina iz katere smo izdelovali segmente je bila zlitina Inconel 718. Cilj je bil določiti časovni potek sile.

Key words: Inconel 718, heat treatment, microstructure, mechanical properties, fine-blanking, load on punch

Ključne besede: Inconel 718, toplotna obdelava, mikrostruktura, mehanske lastnosti, precizno štančanje, obremenitev orodja

INTRODUCTION

The sheet metal from which turbocharger segments were fine-blanked was a nickel base superalloy Inconel 718. Superalloy Inconel 718 is widely used for high temperature applications in aerospace, power and nuclear industry. Due to its good mechanical properties and microstructural stability at elevated temperature it has found its place also in automobile industry. It is used for parts in a turbocharger. The most important method of hardening alloy Inconel 718 is precipitation hardening. The process consists of solution annealing, quenching and aging. The temperature of solution annealing must be high enough to dissolve alloying elements in the metal matrix, which during aging forms precipitates that harden the nickel matrix. Two heat treatments are generally utilized for Inconel 718^[1,2].

A. Solution annealing at 925-1010 °C, then quenching in water, aged at 720 °C for 8 hours, then furnace cooled to 620 °C, held at 620 °C for a total aging time of 18 hours, finally air cooled.

B. Solution annealing at 1035-1065 °C, then quenching in water, aged at 760 °C for 10 hours, then furnace cooled to 650 °C, held at 650 °C for a total aging time of 20 hours, finally air cooled.

The material is machined, formed or welded in the solution annealed condition. Af-

ter fabrication, it can be heat - treated as required by the foreseen application.

Before any detailed research was done, it was believed that materials requirements for fine-blanking should be similar to those of conventional stamping. The conditions present in stamping were also assumed to be at work in fine-blanking. This assumption was found to be false. Research revealed that the process involves both metal flow and shearing. If stresses in the material are considered, the fine-blanking process is closer to deep-drawing and cold forming than to stamping. For this reason, fine-blanking calls for soft, easily cold formed materials^[3].

The purpose of this study was to determine the influence of microstructure and mechanical properties on the process of fine-blanking Inconel 718 by measuring the forces present in the process. In designing the tool it is very important to know as much as possible about the mechanical and microstructure properties and deformation abilities of the alloy that strongly depend on the chosen heat treatment.

EXPERIMENTAL

The starting samples were 3.2 mm thick sheet-metal pieces made of superalloy Inconel 718 with the chemical composition given in Table 1. The samples were used

Table 1. Chemical composition of the investigated alloy Inconel 718**Tabela 1.** Kemična sestava preiskovane zlitine Inconel 718

Element	Ni	Cr	Nb	Mo	Ti	Al	Co	C
mas. %	53.4	18.4	4.97	3.05	1.0001	0.54	0.1972	0.053
Element	Mn	Si	P	S	B	Cu	Fe	
mas. %	0.2459	0.08	< 0.005	< 0.002	0.003	0.0173	In balance	

Table 2. Heat treatment procedure for Inconel 718**Tabela 2.** Parametri toplotne obdelave Inconela 718

Samples	Heat treatment procedures	
	Solution annealing t = 1h	Ageing
A	960 °C → water	
B	1050 °C → water	
A1	960 °C → water →	720 °C/8h $\xrightarrow{2h}$ 620 °C/8h → air
A2	960 °C → water →	760 °C/10h $\xrightarrow{2h}$ 650 °C/8h → air
B1	1050 °C → water →	720 °C/8h $\xrightarrow{2h}$ 620 °C/8h → air
B2	1050 °C → water →	760 °C/10h $\xrightarrow{2h}$ 650 °C/8h → air

for analysis of microstructure, tensile test and for fine-blanking process itself. Samples were solution annealed at temperature 960 °C and 1050 °C, quenched in water and then age – hardened according to two different procedures. All of the investigated heat treatment procedures are given in Table 2.

After different heat treating procedures, the microstructure was determined using the method of electronic scanning microscopy, performed on the JEOL JSM – 5610 microscope, and the method of electronic transmission microscopy, performed on TEM JEM – 2010 F. Once the tensile tests

and measurement of hardness had been performed, the mechanical properties were determined. The tensile test was performed on the ZWICK Z250 tensile machine in conformance with standard SIST EN 10002 – 1. The Charpy test of toughness was also performed complying with standard SIST EN 10045.

Finally, the force of fine-blanking was measured with a force transducer placed as a full Weastone bridge directly on the punch of the tool (Figure 1a). For fabricate the turbocharger parts (Figure 1c), straps (Figure 1b) made of solution annealed Inconel 718 sheet metal annealed at 960 °C

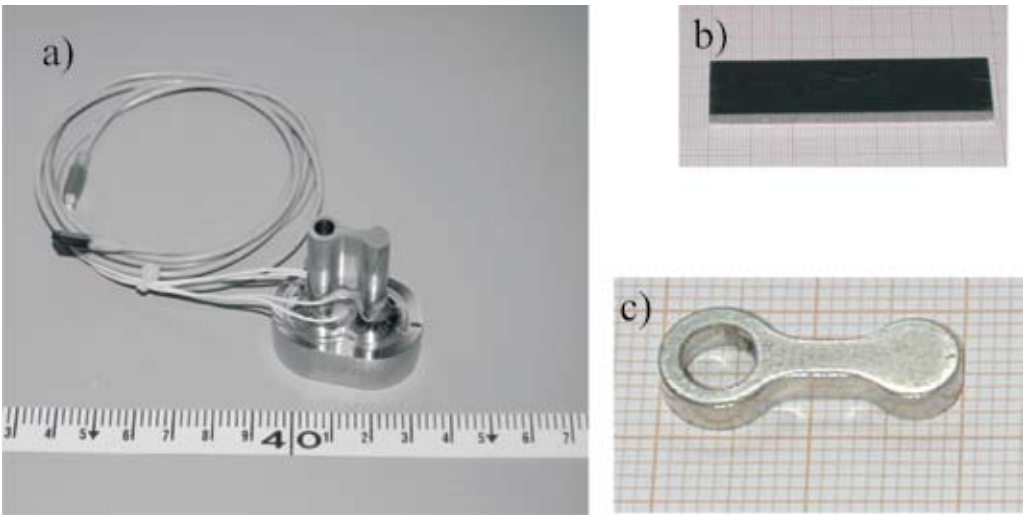


Figure 1. a) strain gauge placed on punch, b) input sample in a shape of strap, c) fine-blanked part for turbocharger

Slika 1. a) merilni lističi nalepljeni na nož, b) vhodni vzorec v obliki traku, c) precizno štančan segment turbopolnilnika

and 1050 °C and quenched in water were used. The different solution annealed straps were manually inserted into the press. During fine-blanking the force acting on the punch was being measured.

RESULTS AND DISCUSSION

Microstructure of alloy Inconel 718

The temperature of solution annealing affects the amount of intermetal solution Ni_3Nb , known as δ phase which is present in the nickel matrix. With higher temperature a higher amount of δ phases is dissolved. In the Inconel 718 microstructure, some titanium - niobium carbides - (Ti, Nb) C were observed (Figure 2). They can be seen in all other microstructures images.

After solution annealing at 960 °C, some amount of δ phase shown in Figure 3 (left),

was still present in the nickel matrix. However, after solution annealing at 1050 °C, all of the δ phase has dissolved (Figure 4). This is only reasonable. As the temperature increased, the volume of δ phase decreased. Complete solution occurred at the δ solvus temperature at 1010 °C^[4-8].

During solution annealing the growth of the grains occurs. After solution annealing at 960 °C the grains are 8.5 μm large, after solution annealing at 1050 °C the grains are 42 μm large. This agrees well with previous investigations^[4,6]. The growth of crystal grains during annealing is hindered by precipitates on the crystal grain boundaries. Significant grain growth is observed only after complete dissolution of the δ phase.

The changes in microstructure after ageing can not be observed with electronic

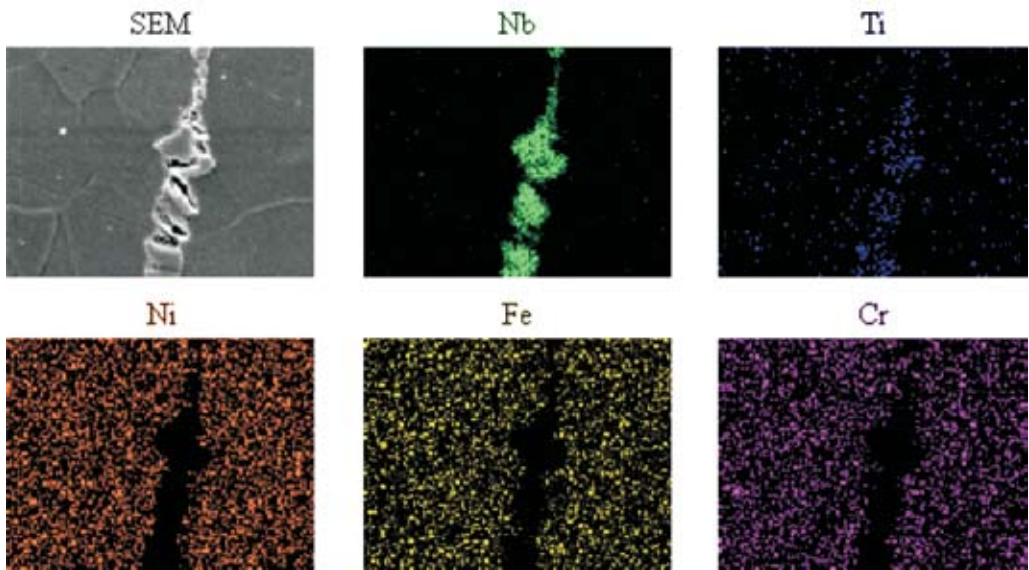


Figure 2. Mapping of carbide particle in metal matrix (SEM)

Slika 2. Kvalitativna ploskovna mikroanaliza karbidnega delca v kovinski osnovi (SEM)

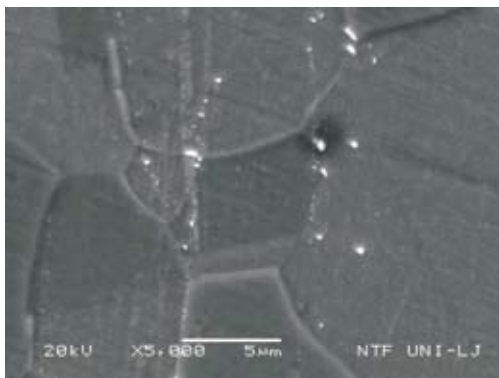


Figure 3. Microstructure obtained after solution annealing at 960 °C and quenching in water (SEM). In the microstructure are seen particles of δ phase in the nickel matrix.

Slika 3. Mikrostruktura po raztopnem žarjenju na 960 °C in gašenju v vodi (SEM). Vidni so delci δ faze v nikljevi osnovi.

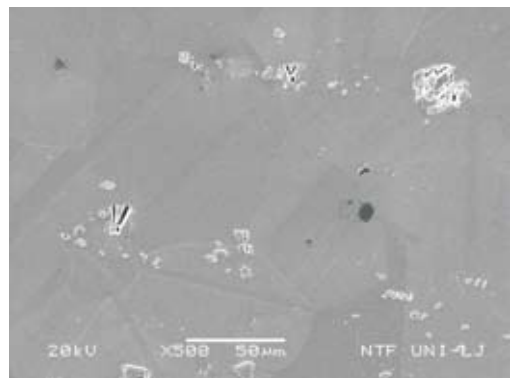


Figure 4. Microstructure after solution annealing at 1050 °C and quenching in water (SEM). In the microstructure are seen only carbide particles in the nickel matrix. All of δ phase has dissolved.

Slika 4. Mikrostruktura po raztopnem žarjenju na 1050 °C in gašenju v vodi (SEM). V nikljevi osnovi so vidni le karbidni delci. Vsa δ faza se je raztopila.

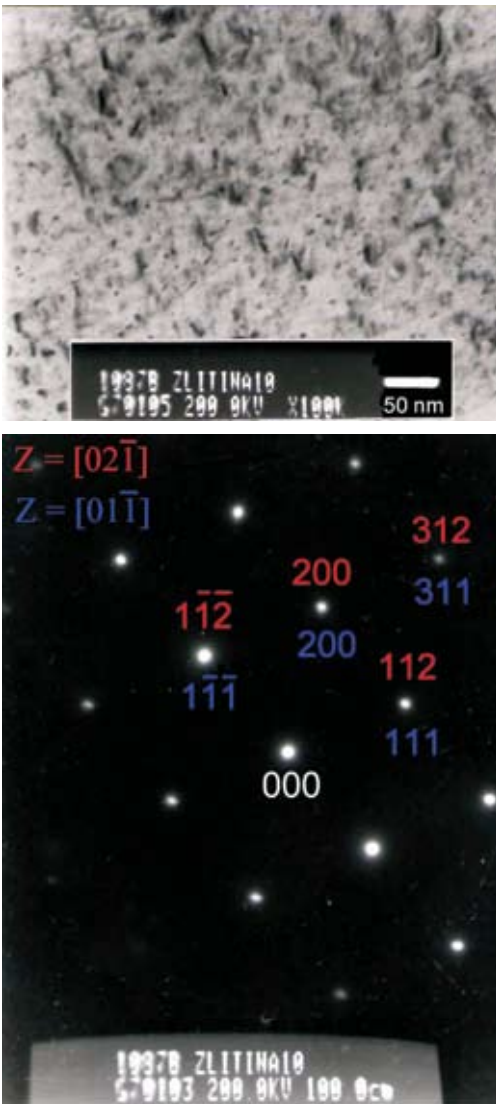


Figure 5. a) Microstructure after ageing (TEM). In the microstructure is seen γ'' phase in the nickel matrix. b) Diffraction pattern of precipitate.

Slika 5. a) Mikrostruktura po staranju (TEM). Vidni so delci γ'' v nikljevi osnovi. b) Uklonska slika precipitata.

scanning microscopy. The precipitations are only 10 nm large (Figure 5a), so the electronic transmission microscopy must be used. The diffraction pattern (Figure 5b) belongs to face centered cubic space lattice and/or tetragonal space lattice. The precipitations are γ'' phase. To the equal results came also other researchers^[4,5,9,10]. After ageing the γ'' phase is main hardening phase.

Mechanical properties of alloy Inconel 718

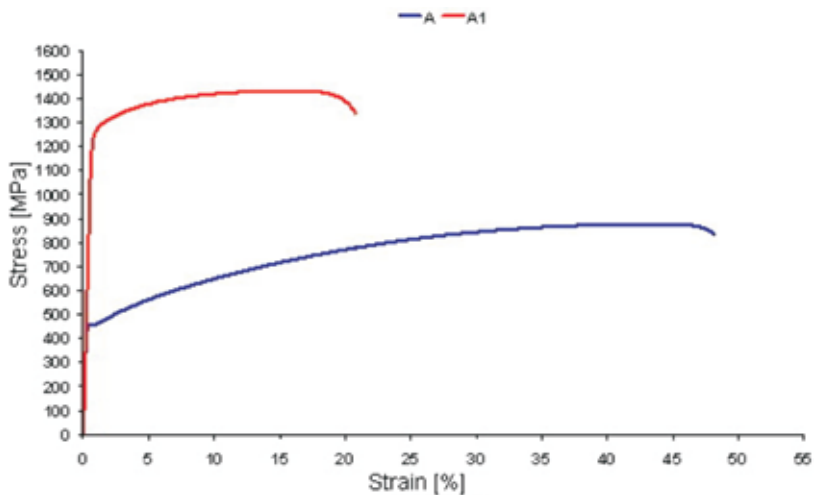
The chosen heat treatment procedure affects also the mechanical properties of Inconel 718. The mechanical properties in terms of the chosen heat treatment are given in Table 3. The changes of mechanical properties are in correlation with changes of microstructure.

During solution annealing the δ phase is dissolving, a lower amount of δ phase means lower mechanical properties. With higher temperature of solution annealing, yield stress ($R_{p0.2}$), tensile stress (R_m) and hardness (HV) become lower, but elongation (A) and toughness (KV) become higher due to lower amount of δ phase and bigger grains.

Mechanical properties of alloy become higher after ageing due to precipitations of γ'' phase. Yield stress ($R_{p0.2}$), tensile stress (R_m) and hardness (HV) become higher. On the other hand, elongation (A) and toughness (KV) become lower. The mechanical properties are in correlation with distribution of precipitations. For

Table 3. The influence of different heat treatment on mechanical properties of Inconel 718**Tabela 3.** Vpliv različnih toplotnih obdelav na mehanske lastnosti Inconela 718

Type of heat treatment	Average values						
	$R_{p0,2}$ [MPa]	R_m [MPa]	A [%]	n [1]	C [MPa]	HV0,3	KV [J]
A	443	877	48	0.39	1816	220	117.3
B	293	757	59	0.46	1572	185	147.8
A1	1230	1431	21	0.130	2134	470	61.7
A2	774	1185	25	0.192	1983	470	56.5
B1	1076	1288	21	0.136	1943	478	80.6
B2	1029	1348	23	0.157	2113	446	61.2

**Figure 6.** Stress - elongation curve for alloy Inconel 718 for different heat treatments; A – solution annealing at 960 °C, A1 – heat treating according to procedure A1

Slika 6. Inženirska krivulja napetost - raztezek različno toplotno obdelane zlitine Inconel 718; A – raztopno žarjenje na 960 °C, A1 – toplotna obdelava po postopku A1

exact understanding the role of precipitations distribution in hardening Inconel 718 a more extensive investigation is needed. The stress – strain curves for the solution annealed and aged alloy Inconel 718 are presented in Figure 6.

Force in fine-blanking

Mechanical and microstructure properties of sheet metal have an influence on the force in fine-blanking. A line graph of force versus time is presented in Figure 7. During fine-blanking of alloy A the punch is loaded with force of 255 kN. On the other hand, during fine-blanking of alloy B the punch is loaded with force of 235 kN.

The reasons for this are lower mechanical properties and higher deformation abilities of alloy B, which was solution annealed at higher temperature.

The punch touches the sheet metal at the time $t = 0$, after that time the force starts increasing. The curve can be divided into two parts: the first with elastic deformation of sheet metal (part I.), and the second when the ability of elastic deformation is exceeded and plastic deformation of sheet metal begins (part II.). The plastic deformation continues until the punch cuts through the entire thickness of sheet metal.

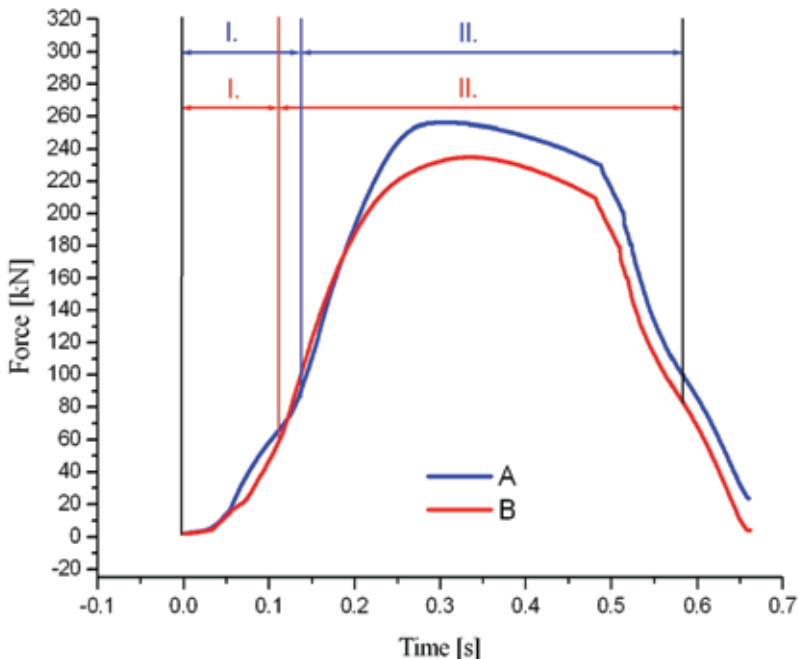


Figure 7. Curves for force versus time during the process of fine-blanking; A – solution annealed alloy Inconel 718 at temperature 960 °C, B – solution annealed alloy Inconel 718 at temperature 1050 °C

Slika 7. Časovni potek sile pri preciznem štančanju; A – raztopno žarjena zlitina Inconel 718 na temperaturi 960 °C, B – raztopno žarjena zlitina Inconel 718 °C na temperaturi 1050 °C

CONCLUSIONS

The purpose of our investigation was to determine the influence of heat treatment on microstructure and mechanical properties. The properties of the alloy were changed with different heat treatment procedures. Furthermore, the relationship between mechanical and microstructure properties of the alloy and the fine-blanking force was investigated. Action of the force that is applied on the punch during fine-blanking segments for the turbocharger from alloy Inconel 718 and the dependence of this force on time were also determined.

1. After solution annealing at 960 °C for 1 hour in the nickel matrix there is a presence of globular δ phase. After solution annealing at 1050 °C for 1 hour all of δ phase has dissolved.
2. During solution annealing at 1050 °C the growth of grains occurs. The grains grow up from 8.5 μm to 42 μm .
3. Precipitation of γ'' phase occurs during ageing.
4. Mechanical properties of alloy become higher after ageing due to precipitations of γ'' phase. Yield stress, tensile stress and hardness become higher, but elongation and toughness become lower.
5. Mechanical and microstructure properties of sheet metal have an influence on the force of fine-blanking. During fine-blanking of alloy A the punch is loaded with maximal force of 255 kN and during fine-blanking of alloy B with a maximal force of 235 kN. The Reasons for this are lower mechanical properties and higher deformation abilities of alloy B.

POVZETEK

Toplotna obdelava in precizno štancanje Inconela 718

Inconel 718 je superzlitina na osnovi niklja in je zaradi svojih dobrih lastnosti široko uporabljen. Glavni način utrjevanja zlitine je izločevalno utrjevanje. Postopek obsega raztopno žarenje, gašenje in staranje. Proces preciznega štancanja zahteva duktilne materiale, ki se z lahkoto hladno preoblikujejo

Izhodni vzorec je bila 3,2 mm debela pločevina iz zlitine Inconel 718. Vzorce smo toplotno obdelali pri različnih temperaturah in časih. Nato smo določili vpliv različnih parametrov toplotne obdelave na mikrostrukturne in mehanske lastnosti zlitine. Iz zlitine smo izdelovali segmente turbopolnilnika dizelskega motorja in pri tem merili silo s katero zlitina obremenjuje nož orodja. Na ta način smo določili časovni potek sile in vpliv lastnosti zlitine na velikost sile.

Temperatura raztopnega žarjenja vpliva na delež faze δ . Po raztopnem žarjenju na temperaturi 960 °C so v nikljevi osnovi še delci faze δ . Med raztopnim žarjenjem na temperaturi 1050 °C se v nikljevi osnovi raztopijo vsi delci faze δ . Med staranjem se iz prenasičene trdne raztopine izloča utrjevalna faza γ'' .

Mehanske lastnosti zlitine so odvisne od temperature raztopnega žarjenja. Zlitina ima po raztopnem žarjenju na 960 °C večje mehanske lastnosti od zlitine žarje-

ne na 1050 °C. Mehanske lastnosti zlitine pred staranjem so odvisne od precipitativne faze δ . Mehanske lastnosti zlitine po staranju se povečajo. Mehanske lastnosti zlitine po staranju so odvisne od porazdelitve in velikosti precipitativne faze γ'' .

Višja temperatura raztopnega žarjenja zmanjša silo in potrebno delo preciznega štancanja surovca iz zlitine Inconel 718. Maksimalna sila preciznega štancanja surovca iz raztopno žarjene na temperaturi 960 °C in gašene zlitine znaša 255 kN. Maksimalna sila preciznega štancanja surovca iz raztopno žarjene na temperaturi 1050 °C in gašene zlitine pa znaša 235 kN.

REFERENCES

- [1] DAVIS, J.R. (2000): *Nickel, Cobalt, and Their Alloys: ASM Specialty Handbook*. Materials Park: ASM International.
- [2] DONACHIE, M.J., DONACHIE, S.J. (2002): *Superalloys: a technical guide*. 2nd ed. Materials Park: ASM International.
- [3] BIRZER, F. (1997): *Forming and Fineblanking: cost effective manufacture of accurate sheetmetal parts*. Landsberg: Verlag Moderne Industrie.
- [4] MILLER, M.K., BABU, S.S., BURKE, M.G. (1999): Intragranular precipitation in alloy 718. *Materials Science and Engineering*; Vol. 270, pp. 14-18.
- [5] LI, R.B. et al. (2002): Isolation and determination for δ , γ' and γ'' phases in Inconel 718 alloy. *Scripta Materialia*; Vol. 46, pp. 635-638.
- [6] AZADIAN, S., WEI, L.Y., WARREN, R. (2004): Delta phase precipitation in Inconel 718. *Materials Characterization*; Vol. 53, pp. 7-16.
- [7] MURALIDHARAN, G., THOMPSON, R.G. (1997): Effect of second phase precipitation on limiting grain growth in alloy 718. *Scripta Materialia*; Vol. 36, No. 7, pp. 755-761.
- [8] CAI, D. et al. (2007): Dissolution kinetics of δ phase and its influence on the notch sensitivity of Inconel 718. *Materials Characterization*; Vol. 58, No. 3, pp. 220-225.
- [9] JIANXIN, D., XISHAN, X., SHOUHUA, Z. (1995): Coarsening behavior of γ'' precipitates in modified Inconel 718 superalloy. *Scripta Metallurgica et Materialia*; Vol. 33, No. 12, pp. 1933-1940.
- [10] HE, J. et al. (1998): Interfaces in a modified Inconel 718 with compact precipitates. *Acta Metallurgica*; Vol. 46, No. 1, pp. 215-223.

Shape memory alloys in medicine

Materiali z oblikovnim spominom v medicini

MIHA BROJAN¹, DAVID BOMBAC², FRANC KOSEL¹, TOMAŽ VIDENIČ¹

¹University of Ljubljana, Faculty of Mechanical Engineering, Aškerčeva cesta 6, SI-1000 Ljubljana, Slovenia; E-mail: miha.brojan@fs.uni-lj.si, franc.kosel@fs.uni-lj.si, tomaz.videnic@fs.uni-lj.si

²University of Ljubljana, Faculty of Natural Sciences and Engineering, Aškerčeva cesta 12, SI-1000 Ljubljana, Slovenia; E-mail: david.bombac@ntf.uni-lj.si

Received: December 8, 2007

Accepted: April 21, 2008

Abstract: The Shape memory alloys (SMA) are success story in medical applications market with enormous growth in usage. Huge advances from surgical point of view mean great opportunity for new commercial applications. This paper reviews the development of the shape memory alloys (SMA), constitutive behavior and use in medicine. Shape memory effect, pseudoelasticity and other basic properties of SMA are presented. Later many medical devices using shape memory effect and current commercial applications are presented. Because vast majority of current SMA medical devices is made from Nitinol, this paper also consider the factors that impinge on the associated risk analysis of using Nitinol in medical applications.

Izvešček: Materiali z oblikovnim spominom so zgodba o uspehu uporabe v medicini in še vedno pridobivajo na svoji uporabnosti. Velike prednosti s kirurškega stališča pomenijo ogromne možnosti za nove komercialne aplikacije. To delo podaja pregled fizikalnega ozadja materialov z oblikovnim spominom, njihove fizikalne zakonitosti ter uporabnost v medicini. Predstavljeni so pojav oblikovnega spomina, psevdoelastičnost in druge osnovne lastnosti materialov z oblikovnim spominom. V nadaljevanju so predstavljeni medicinski pripomočki, ki izkoriščajo oblikovni spomin in sedanja komercialna uporaba. Ker je večina takšnih medicinskih pripomočkov izdelanih iz materiala nitinol so preučeni tudi vplivi, ki zadevajo nevarnosti uporabe tega materiala v medicinskih aplikacijah.

Key words: shape memory effect, shape memory alloys, SMA medical implants, Nitinol

Ključne besede: oblikovni spomin, materiali z oblikovnim spominom, SMA medicinski vsadki, nitinol

INTRODUCTION

Smart materials have been given a lot of attention mainly for their innovative use in practical applications. One example of such materials is also the family of shape memory alloys (SMA) which are arguably the first well known and used smart material. Shape memory alloys possess a unique property according to which, after being deformed at one temperature, they can recover to their original shape upon being heated to a higher temperature. The effect was first discussed in the 1930s by ÖLANDER^[1] and GRENINGER and MOORADIAN^[2]. The basic phenomenon of the shape memory effect was widely reported a decade later by Russian metallurgist G. Kurdjumov and also by CHANG and READ^[3]. However, presentation of this property to the wider public came only after the development of the nickel-titanium alloy (nitinol) by BUEHLER and WANG^[4]. Since then, research activity in this field has been intense, and a number of alloys have been investigated, including Ag-Cd, Au-Cd, Cu-Zn, Cu-Zn-Al, Cu-Al-Ni, Cu-Sn, Cu-Au-Zn, Ni-Al, Ti-Ni, Ti-Ni-Cu, Ni-Ti-Nb, Ti-Pd-Ni, In-Ti, In-Cd and others. Crystallography of shape memory alloys have been studied for the last four decades. Only a fraction of the available literature is listed here^[5-14]. Because these materials are relatively new, some of the engineering aspects of the material are still not well understood. Many of the typical engineering descriptors, such as young's modulus and yield strength, do not apply to shape memory alloys since they are very strongly temperature dependent. On the other hand, a new set of descriptors must be introduced, such as stress rate and amnesia. That is why numerous constitu-

tive models have been proposed over the last 20 years to predict thermomechanical behaviour^[15-28].

THERMOMECHANICAL BEHAVIOR

These materials have been shown to exhibit extremely large, recoverable strains (on the order of 10 %), and it is these properties as functions of temperature and stress which allow SMAs to be utilized in many exciting and innovative applications. From a macroscopic point of view, the mechanical behavior of SMAs can be separated into two categories: the *shape memory effect* (SME), where large residual (apparently plastic) strain can be fully recovered upon raising the temperature after loading and unloading cycle; and the *pseudoelasticity* or *superelasticity*, where a very large (apparently plastic) strain is fully recovered after loading and unloading at constant temperature. Both effects are results of a martensite phase transformation. In a stress-free state, an SMA material at high temperatures exists in the parent phase (usually a body-centered cubic crystal structure, also referred as the austenite phase). Upon decreasing the material temperature, the crystal structure undergoes a self-accommodating crystal transformation into martensite phase (usually a face-centered cubic structure). The phase change in the unstressed formation of martensite from austenite is referred to as 'self-accommodating' due to the formation of multiple martensitic variants and twins which prohibits the incurrence of a transformation strain. The martensite variants, evenly distributed throughout material, are all crystallographically equivalent,

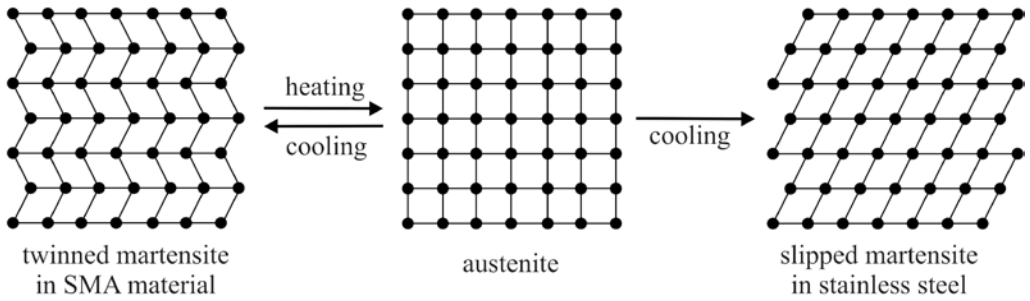


Figure 1. Martensite transformation in shape memory alloys and steels

Slika 1. Martenzitna premena v materialih z oblikovnim spominom in jeklih

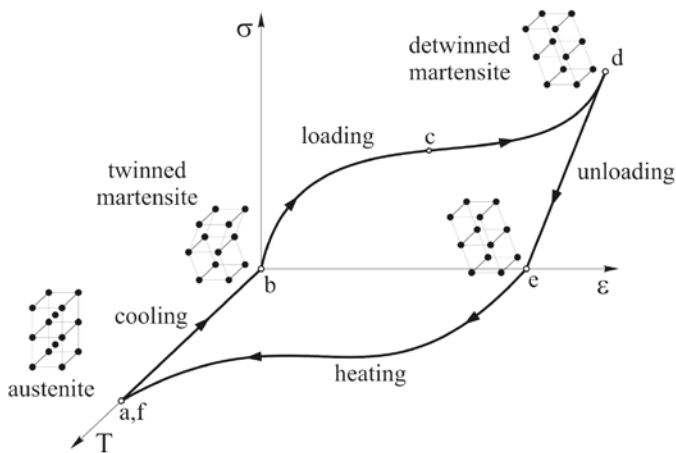
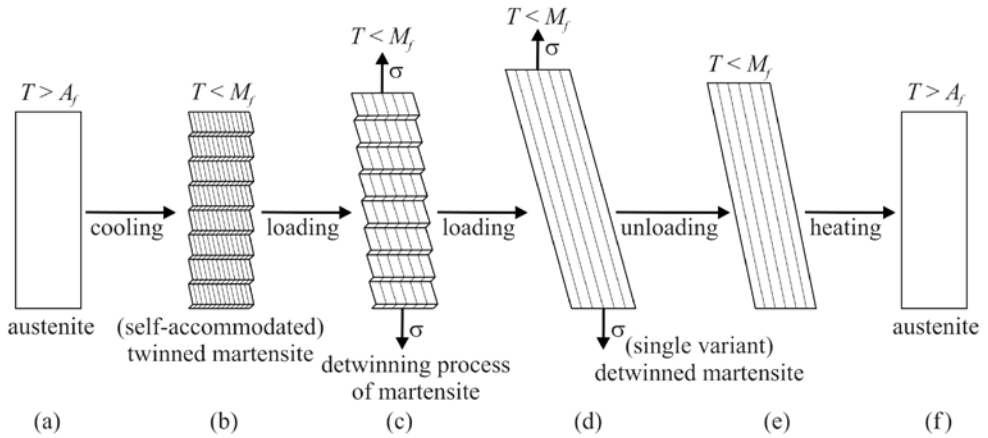


Figure 2. Shape memory effect

Slika 2. Pojav spomina oblike

differing only by habit plane. The process of self-accommodation by twinning allows an SMA material to exhibit large reversible strains with stress. However, the process of self-accommodation in ordinary materials like stainless steel does not take place by twinning but via a mechanism called slip. Since slip is a permanent or irreversible process, the shape memory effect cannot occur in these materials. The difference between the twinning and slip process is shown in Figure 1.

In the stress-free state, an SMA material has four transition temperatures, designated as M_f , M_s , A_s , A_f , i.e. Martensite Finish, Martensite Start, Austenite Start, and Austenite Finish, respectively. In the case of "Type I" materials, temperatures are arranged in the following manner: $M_f < M_s < A_s < A_f$. A change of temperature within the range $M_s < T < A_s$ induces no phase changes and both phases can coexist within $M_f < T < A_f$. With these four transformation temperatures and the concepts of self-accommodation, the shape memory effect can be adequately explained. As an example let us consider a martensite formed from the parent phase, Figure 2(a), cooled under stress-free conditions through M_s and M_f . This material has multiple variants and twins present, Figure 2(b), all crystallographically equivalent, but with different orientation (different habit plane indices). When a load applied to this material reaches a certain critical stress, the pairs of martensite twins begin "detwinning" to the stress-preferred twins, Figure 2(c). It means that the multiple martensite variants begin to convert to a single variant determined by alignment of the habit planes with the direction of loading, Figure 2(d). During

this process of reorientation, the stress rises very slightly in comparison to the strain. As the single variant of martensite is thermodynamically stable at $T < A_s$, upon unloading there is no conversion to multiple variants and only a small elastic strain is recovered, leaving the material with a large residual strain, Figure 2(e). The detwinned martensite material can recover the entire residual strain by simply heating above A_f ; the material then transforms to the parent phase, which has no variants, and recovers to its original size and shape, Figure 2(f), thus creating the shape memory effect.

The pseudoelastic effect can be explained, if an SMA material is considered to be entirely in the parent phase (with $T > A_f$), Figure 3(a). When stress is applied to this material, there is a critical stress at which the crystal phase transformation from austenite to martensite can be induced, Figure 3(b). Due to the presence of stress during the transformation, specific martensite variants will be formed preferentially and at the end of transformation, the stress-induced martensite will consist of a single variant of detwinned martensite, Figure 3(c). During unloading, a reverse transformation to austenite occurs because of the instability of martensite at $T > A_f$ in the absence of stress, Figure 3(e). This recovery of high strain values upon unloading yields a characteristic hysteresis loop, diagram in Figure 3, which is known as pseudoelasticity or superelasticity.

Many of the possible medical applications of SMA materials in the 1980's were attempting to use the thermally activated memory effect. However, temperature regions tolerated by the human body are

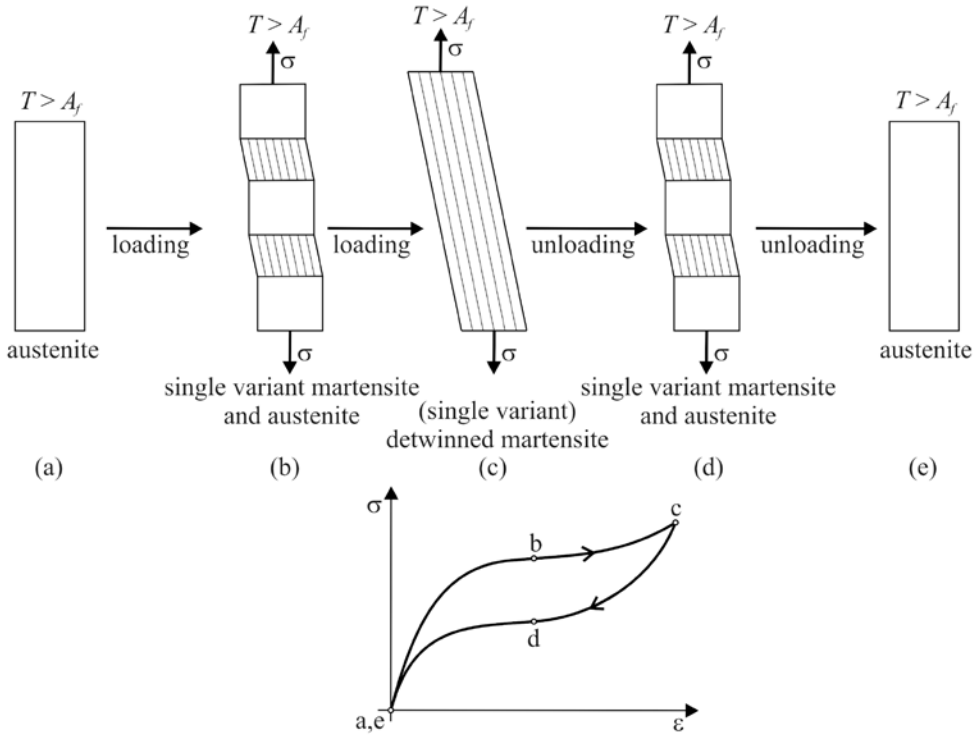


Figure 3. Pseudoelasticity or superelasticity
Slika 3. Psevdoelastičnost ali superelastičnost

very limited. Small compositional changes around the 50-50 % of Ti-Ni ratio can make dramatic changes in the operating characteristics of the alloy. Therefore very precise control of phase transition temperatures is required. On the other hand, pseudoelasticity is ideally suited to medical applications since the temperature region of optimum effect can easily be located to encompass ambient temperature through body temperature.

BIOCOMPATIBILITY

It is important to understand the direct effects of an individual component of the al-

loy since it can dissolve in the body due to corrosion and it may cause local and systemic toxicity, carcinogenic effects and immune response. The cytotoxicity of elementary nickel and titanium has been widely researched, especially in the case of nickel, which is a toxic agent and allergen^[29-31]. Nickel is known to have toxic effects on soft tissue structures at high concentrations and also appears to be harmful to bone structures, but substantially less than cobalt or vanadium, which are also routinely used in implant alloys. Experiments with toxic metal salts in cell cultures have shown decreasing toxicity in the following order: Co > V > Ni > Cr > Ti > Fe^[32]. The dietary exposure to nickel is 160-600 mg/

day. Fortunately most of it is eliminated in the feces, urine and sweat. Pure nickel implanted intramuscularly or inside bone has been found to cause severe local tissue irritation and necrosis and high carcinogenic and toxic potencies. Due to corrosion of medical implants, a small amount of these metal ions is also released into distant organs. Toxic poisoning is later caused by the accumulation, processing and subsequent reaction of the host to the corrosion of the Ni-containing implant. Nickel is also one of the structural components of the metalloproteins and can enter the cell via various mechanisms. Most common Ni^{2+} ions can enter the cell utilizing the divalent cation receptor or via the support with Mg^{2+} , which are both present in the plasma membrane. Nickel particles in cells can be phagocytosed, which is enhanced by their crystalline nature, negative surface energy, appropriate particle size (2-4 μm) and low solubility. Other nickel compounds formed in the body are most likely to be NiCl_2 and NiO , and fortunately there is only a small chance that the most toxic and carcinogenic compounds like Ni_3S_2 , are to be formed. Nickel in soluble form, such as Ni^{2+} ions,

enters through receptors or ion channels and binds to cytoplasmic proteins and does not accumulate in the cell nucleus at concentrations high enough to cause genetic consequences. These soluble Ni^{2+} ions and are rapidly cleaned from the body. However, the insoluble nickel particles containing phagocytotic vesicles fuse with lysosomes, followed by a decrease of phagocytic intravesicular pH, which releases Ni^{2+} ions from nickel containing carrier molecules. The formation of oxygen radicals, DNA damage and thereby inactivation of tumor suppressor genes is contributed by that.

On the other hand, titanium is recognized to be one of the most biocompatible materials due to the ability to form a stable titanium oxide layer on its surface. In an optimal situation, it is capable of excellent osteointegration with the bone and it is able to form a calcium phosphate-rich layer on its surface, Figure 4, very similar to hydroxyapatite which also prevents corrosion. Another advantageous property is that in case of damaging the protective layer the titanium oxides and calcium phosphate layer regenerate.

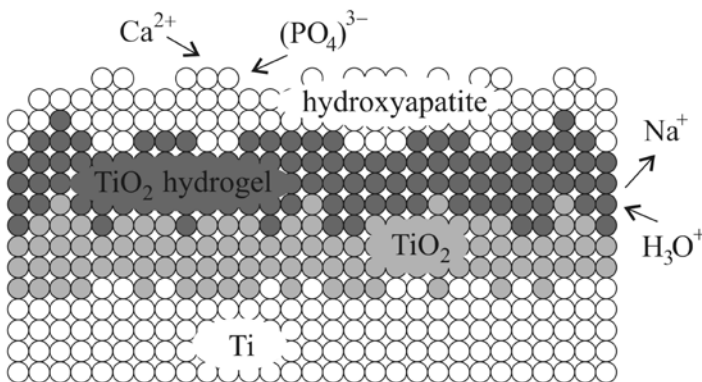


Figure 4. Formation of hydroxyapatite layer on titanium oxide film^[33]

Slika 4. Nastanek hidroksiapatitne plasti na plasti titanovega oksida^[33]

The properties and biocompatibility of nitinol have their own characteristics which are different from those of nickel or titanium alone. In vitro NiTi biocompatibility studies on the effects of cellular tolerance and its cytotoxicity have been performed on various cell culture models^[34,35]. Human monocytes and microvascular endothelial cells were exposed to pure nickel, pure titanium, stainless steel and nitinol. Nitinol has been shown to release higher concentrations of Ni²⁺ ions in human fibroblast and osteoblast cultures, which did not affect cell growth^[36-38]. Metal ion release study also revealed very low concentrations of nickel and titanium that were released from nitinol. Researchers therefore concluded that nitinol is not genotoxic.

For in vivo biocompatibility studies of nitinol effect, different experiments have been done on animals. Several in vivo nitinol biocompatibility studies which were done in the last decade disclosed no allergic reactions, no traces of alloy constituents in the surrounding tissue and no corrosion of implants. Studies of rat tibiae response to NiTi, compared with Ti-6Al-4V and AISI 316L stainless steel, showed that the number and area of bone contacts was low around NiTi implants, but the thickness of contact was equal to that of other implants. Normal new bone formation was seen in rats after 26 weeks after implantation. Good biocompatibility results of NiTi are attributed to the fact that implants are covered by a titanium oxide layer, where only small traces of nickel are being exposed.

Corrosion Behavior

The body is a complicated electrochemical system that constitutes an aggressive corrosion environment for implants which are surrounded by bodily fluids of an aerated solution containing 0.9 % NaCl, with minor amounts of other salts and organic compounds, serum ions, proteins and cells which all may modify the local corrosion effect. High acidity of certain bodily fluids is especially hostile for metallic implants. Acidity can increase locally in the area adjacent to an implant due to inflammatory response of surrounding tissues mediating hydrogen peroxide and reactive oxygen and nitrogen compounds. The local pH changes for infected tissues or near haematomas are relatively small, however these changes can alter biological processes and thereby the chemistry around the implant. It is known that small point corrosion or pitting prevails on surfaces of metallic implants. Another important feature is roughness of the surface which increases the reacting area of the implant and thereby add to total amount of corrosion. Therefore surface finishing is a major factor in improving corrosion resistance and consequently biocompatibility of medical devices^[39, 40].

Corrosion resistance of SMA has also been studied in vivo on animals. Plates and stents have been implanted in dogs and sheeps for several months. Corrosion has been examined under microscope and pitting was established as predominant after the implants were removed. Thus surface treatments and coatings were introduced.

The improvement of corrosion resistance was considerable, since pitting decreased in some cases from 100 μm to only 10 μm in diameter.

Surface

The human response to implanted materials is a property closely related to the implant surface conditions. The major problems associated with the implants currently used are inadequate implant-tissue interface properties. Parameters that characterize surface property are chemical composition, crystallinity and heterogeneity, roughness and wettability or surface free energy which is a parameter important for cell adhesion. Each parameter is of great importance to biological response of the tissue. Another problem is implant sterilization which can remarkably modify desired parameters. Steam and dry sterilization are nowadays replaced by more advanced techniques like hydrogen peroxide plasma, ethylene oxide, and electron and γ -ray irradiation.

The surface of NiTi SMA has revealed a tendency towards preferential oxidation of titanium. This behavior is in agreement with the fact that the free enthalpy of formation of titanium oxides is negative and exceeds in absolute value the enthalpy of formation of nickel oxides by at least two to three times. The result of oxidation is an oxide layer of a thickness between 2-20 nm, which consists mainly of titanium oxides TiO_2 , smaller amounts of elemental nickel Ni, and low concentrations of nickel oxides NiO. The surface chemistry and the amount of Ni may vary over a wide range, depending on the preparation method. The ratio of Ti/Ni on polished surface is around

5.5, while boiled or autoclaved items in water show decreased concentration of Ni on the surface and the Ti/Ni ratio increases up to 23 to 33 ^[41]. Different in vitro studies have shown how the physical, chemical and biocompatible properties of the implant surface can be improved^[42-46].

Surface Improvements

Some of the most important techniques for improving the properties of Ni-Ti alloy surfaces are: (1) *Surface modification by using energy sources and chemical vapors* like hydroxyapatite, laser and plasma treatment, ion implantation, TiN and TiCN chemical vapor deposits. Hydroxyapatite coatings result in the best known biocompatibility and reveal a tendency to dissolution due to its relative miscibility with body fluids. Ion implantation and laser treatments usually result in surface amorphization that improves corrosion resistance, but the obtained amorphous surface layers are often not uniform. Laser surface melting leads to an increased oxide layer, decrease of Ni dissolution and improvement of the cytocompatibility up to classical Ti level. There is also a possibility that laser melted surfaces may be enriched in nickel, and become harder than bulk and swell. TiN and TiCN coatings are known to improve corrosion resistance but large deformations caused by the shape memory effect may cause cracking of the coating. Therefore, for plates and staples a plasma-polymerized tetrafluoroethylene has been introduced. (2) *Development of bioactive surfaces* is another approach to improve biocompatibility of the SMA. Human plasma fibronectin covalently immobilised to NiTi surface improved the attachment of cells while corrosion rates were

reduced drastically. Studies showed NiTi surface improved with this method caused a development of calcium phosphate layers, which in fact eliminate the need for hydroxyapatite coatings^[43,47]. (3) *Electrochemical processing for oxidation in air/oxygen* is a most common way of metal surface treatment. The technique combines electrochemical processes and oxidation in various media. Growth of native passive films that are highly adhesive and do not crack or break due to dynamic properties of SMA is promoted with this method. Oxide films obtained in air have different colors, thickness, and adhesive properties, with TiO₂ as a predominant oxide type. (4) *Oxidation of SMA medical devices in water and steam* is also one of the surface improvement techniques. Implants are preliminary chemically etched and boiled in water. The result is a surface with a very low Ni concentration, while etching removes surface material that was exposed to processing procedures and acquired various surface defects and heterogeneity. It also selectively removes nickel and oxidizes titanium. Surfaces obtained after oxidation in steam show better properties than those oxidized in water. (5) *Electrochemical techniques* are commonly used to passivate NiTi surfaces. Surface passivation using electropolishing is often considered as a treatment of first choice just because this technique is used for surface conditioning of stainless steels, Co-Cr alloys, etc. However, the universal techniques developed for surface passivation of various alloys used for medical purposes are not necessary efficient for NiTi.

It should also be noted that the implant surface coatings are not always beneficial.

The major problem of titanium based alloys is that the formation of TiO₂, according to the chemical equation $\text{Ti} + 2\text{H}_2\text{O} \rightarrow \text{TiO}_2 + 4\text{H}^+ + 4\text{e}^-$, reduces the pH level at the titanium/coating interface. This means that if the coating is composed of hydroxyapatite, it can dissolve, which gradually leads to detachment of the coating.

MEDICAL APPLICATIONS

The trends in modern medicine are to use less invasive surgery methods which are performed through small, leak tight portals into the body called trocars. Medical devices made from SMAs use a different physical approach and can pull together, dilate, constrict, push apart and have made difficult or problematic tasks in surgery quite feasible. Therefore unique properties of SMAs are utilized in a wide range of medical applications. Some of the devices used in various medical applications are listed below.

Stents are most rapidly growing cardiovascular SMA cylindrical mesh tubes which are inserted into blood vessels to maintain the inner diameter of a blood vessel. The product has been developed in response to limitations of balloon angioplasty, which resulted in repeated blockages of the vessel in the same area. Ni-Ti alloys have also become the material of choice for superelastic *self-expanding (SE) stents* which are used for a treatment of the superficial femoral artery disease, Figure 5(a). The SE nitinol stents are produced in the open state mainly with laser cut tubing and later compressed and inserted into the catheter. They can also be produced from wire and laser

welded or coiled striped etched sheet. Before the compression stage, the surface of the stent is electrochemically polished and passivated to prescribed quality. Deployment of the SE stent is made with the catheter. During the operation procedure, when the catheter is in the correct position in the vessel, the SE stent is pushed out and then it expands against the inner diameter of the vessel due to a rise in temperature (thermally triggered device). This opens the iliac artery to aid in the normal flow of blood. The delivery catheter is then removed, leaving the stent within the patient's artery. Recent research has shown that implantation of a self-expanding stent provides better outcomes, for the time being, than balloon angioplasty^[48-50]. *The Simon Inferior Vena Cava (IVC) filter* was the first SMA cardiovascular device. It is used for blood vessel interruption for preventing pulmonary embolism via placement in the vena cava. The Simon filter is filtering clots that travel inside bloodstream^[51]. The device is made of SMA wire curved similarly to an umbrella which traps the clots which are better dissolved in time by the bloodstream. For insertion, the device is exploiting the shape memory effect, i.e. the original form in the martensitic state is deformed and mounted into a catheter. When the device is released, the body's heat causes the filter to return to its predetermined shape. *The Septal Occlusion System* is indicated for use in patients with complex ventricular septal defects (VSD) of significant size to warrant closures that are considered to be at high risk for standard transatrial or transarterial surgical closure based on anatomical conditions and/or based on overall medical condition. The system consists of two primary components; a permanent

implant, which is constructed of an SMA wire framework to which polyester fabric is attached, and a coaxial polyurethane catheter designed specifically to facilitate attachment, loading, delivery and deployment to the defect^[52]. The implant is placed by advancing the delivery catheter through blood vessels to the site of the defect inside the heart. The implant remains in the heart and the delivery catheter is removed. Instruments for minimally invasive surgery used in endoscopic surgery could not be feasible without implementation of SMA materials. The most representative instruments such as *guidewires*, *dilatators* and *retrieval baskets* exploit good kink resistance of SMAs^[53]. *Open heart stabilizers* are instruments similar to a steerable joint endoscopic camera. In order to perform bypass operations on the open heart stabilizers are used to prevent regional heart movements while performing surgery. Another employment of the unique properties of SMAs such as constant force and superelasticity in heart surgery is a *tissue spreader* used to spread fatty tissue of the heart, Figure 5(b).

In general, conventional orthopedic implants by far exceed any other SMA implant in weight or volume. They are used as fracture fixation devices, which may or may not be removed and as joint replacement devices. Bone and nitinol have similar stress-strain characteristics, which makes nitinol a perfect material for production of bone fixation plates, nails and other trauma implants^[54]. In traditional trauma surgery bone plates and nails fixated with screws are used for fixation of broken bones. Shape memory fixators are one step forward applying a necessary

constant force to faster fracture healing. *The SMA embracing fixator* consists of a body and sawtooth arms^[55]. It embraces the bone about 2/3 of the circumference, Figure 5(c). The free ends of the arms which exceed the semi-circle are bent more medially to match the requirement fixation of a long tubular body whose cross section is not a regular circle. The applied axial compression stress is beneficial for enhancing healing and reducing segmental osteoporosis caused by a stress shielding effect. Its martensitic transformation temperature is 4-7 °C and shape recovery temperature is around the body's normal temperature, 37 °C. Similar to the embracing fixator is the so called *Swan-Like Memory-Compressive Connector (SMC)* for treatment of fracture and nonunion of upper limb diaphysis. The working principle of the device is similar with one important improvement. The SMC trauma implant is able to put constant axial stress to a fractured bone^[56]. For fixation of tibial and femoral fractures nails fixated with screws are normally used. New *SMA*

inter-locking intramedullary nails have many advantages compared to traditional ones. For example, when cooled SMA inter-locking nails are inserted into a cavity, guiding nails are extracted and body heat causes bending of nails into a preset shape applying constant pressure in the axial direction of the fractured bone^[57]. The SMA effect is also used in surgical fixators made from wire. Certain device which have been developed to fix vertebra in spine fractures are similar to an ordinary staple. *Staple shaped compression medical devices* are also used for internal bone fixation^[58]. The compression staple is one of most simple and broadly used SMA devices in medicine, Figure 5(d). Since its introduction in 1981, over a thousand patients have been all successfully treated using this device. *The SMA Patellar Concentrator* was designed to treat patellar fractures, Figure 5(e). The device exerts continuous compression for the fixation of patella fracture. The shape of patellar concentrator consists of two basic patellae claws, conjunctive waist and

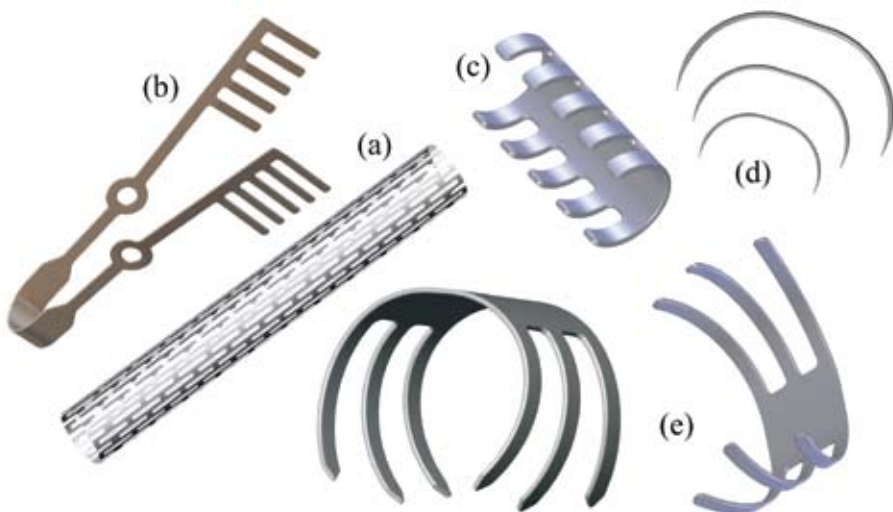


Figure 5. Examples of nitinol medical devices

Slika 5. Primeri medicinskih pripomočkov iz nitinola

three apex patellae claws. The thickness of the device may vary between 1.8 and 2.2 mm depending on different sizes of the concentrator. In clinical surgery, the claws are unfolded and put over fractured patella. Exposed to body temperature, the device tends to recover to its original state resulting in a recovery compressive force^[59].

Dentists are using devices made from SMA for different purposes. NiTi based SMA material performs exceptionally at high strains in strain-controlled environments, such as exemplified with *dental drills* for root canal procedures. The advantage of these drills is that they can be bent to rather large strains and still accommodate the high cyclic rotations^[52]. Superelastic SMA wires have found wide use as orthodontic wires as well, Figure 6(b). *NiTi orthodontic archwire* was first produced in batches and clinically used in China in the beginning of 1980's^[60]. Due to its unique property-superelasticity, the wire exerts gentle and retentive force to teeth, which is superior to stainless steel wire. Shape memory bracelet do not require as frequent visits to the dentist as the classical ones because of

their ability to self adjust. The therapeutic period is therefore cut down by 50 %.

Lately a special *fixator for mounting bridgework* has been developed, Figure 6(a). A small piece of SMA metal is notch on both sides and placed between teeth and bridgework. As the temperature rises the notched area of metal is expanded on both sides causing a permanent hold of bridge-work. The tooth fixator can also be used to prevent a loose tooth from falling out.

CONCLUSIONS

A SMA implants and medical devices have been successful because they offer a possibility of performing less invasive surgeries. Nitinol wires in medical instruments are more kink resistant and have smaller diameters compared to stainless steel 316L or polymer devices. Research to develop composite materials, containing SMA which will prove cost efficient and porous SMAs which will enable the transport of body fluids through its bulk is currently underway.

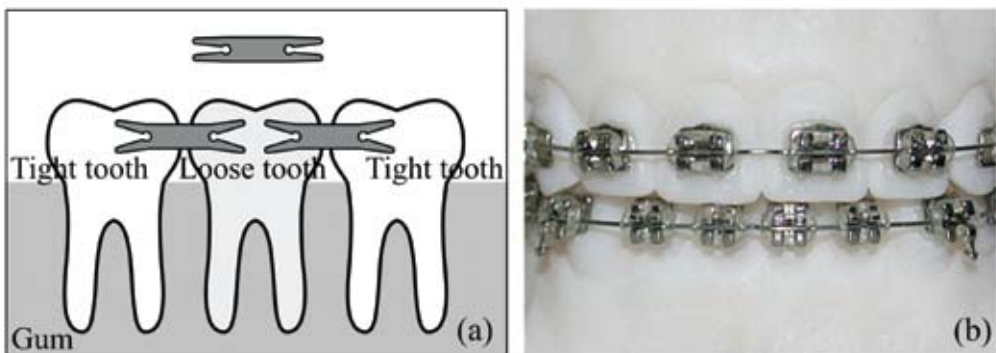


Figure 6. Dental applications of nitinol
Slika 6. Zobozdravstvene aplikacije nitinola

POVZETEK

Materiali z oblikovnim spominom v medicini

Materiali z oblikovnim spominom so zgodba o uspehu uporabe v medicini in še vedno pridobivajo na svoji uporabnosti. Velike prednosti s kirurškega stališča pomenijo ogromne možnosti za nove komercialne aplikacije. To delo podaja pregled razvoja materialov z oblikovnim spominom, njihove fizikalne zakonitosti ter uporabnost v medicini. Predstavljeni so pojav oblikovnega spomina, psevdoelastičnost in druge osnovne lastnosti s spominom oblike. V nadaljevanju so predstavljeni medicinski pripomočki, ki izkoriščajo oblikovni spomin in sedanja komercialna uporaba. Ker je večina takšnih medicinskih pripočkov izdelanih iz materiala nitinol so preučeni tudi vplivi, ki zadevajo nevarnosti uporabe tega materiala v medicinskih aplikacijah.

Medicinski implantati in ostali pripomočki iz materialov z oblikovnim spominom so uspešni predvsem zaradi zmožnosti izvajanja manj invazivnih kirurških posegov. Žice in nitinola in medicinski instrumenti so bolj odporni proti prepogibom in imajo v primerjavi z nerjavečim jeklom ali polimeri manjše prečne premere. V teku so številne raziskave, ki se ukvarjajo z razvojem in uporabnostjo kompozitnih materialov, ki v svoji sestavi vsebujejo tudi materiale s spominom oblike. Porozni materiali s spominom oblike, ki bi omogočali prehod telesnih sokov skozi prerez, pa so trenutno tik pred tem, da preidejo v uporabo za komercialne namene.

REFERENCES

- [1] OLANDER, A. (1932): An electrochemical investigation of solid cadmium-gold alloys. *J. Am. Chem. Soc.*; Vol. 54, No. 3819-3833.
- [2] GRENINGER, A.B., MOORADIAN, V.G. (1938): Strain transformation in metastable beta copper-zinc and beta copper-tin alloys. *AIME.*; Vol. 128, pp. 337-368.
- [3] CHANG, L.C., READ, T.A. (1951): Plastic deformation and diffusionless phase changes in metals-the gold-cadmium beta phase. *Am. Inst. Min. Metall. Eng., J. Met.*; Vol. 191/1, pp. 47-52.
- [4] BUEHLER, W.J., WANG, F.E. (1967): A summary of recent research on the Nitinol alloys and their potential application in ocean engineering. *Journal of Ocean Engineering.*; Vol. 1, pp. 105-108.
- [5] WAYMAN, C.M. (1964): *Introduction to the crystallography of martensitic transformations*. The Macmillan Company.
- [6] OTSUKA, K., WAYMAN, C.M. (1998): *Shape memory materials*. Cambridge University Press.
- [7] WECHSLER, M.S., LIBERMAN, D.S., READ, T.A. (1953): On the theory of the formation of martensite. *Trans. AIME.*; Vol. 197, pp. 1503-1515.
- [8] BOWLES, J.S., MACKENZIE, J.K. (1954): The crystallography of martensite transformations I. *Acta Metallurgica.*; Vol. 2, pp. 129-137.
- [9] SABURI, T., WAYMAN, C.M. (1979): Crystallographic similarities in shape memory martensites. *Acta Metallurgica.*; Vol. 27/6, pp. 979-995.

- [10] ADACHI, K., PERKINS, J., WAYMAN, C.M. (1986): Type II twins in self-accommodating martensite plate variants in a Cu-Zn-Al shape memory alloy. *Acta Metallurgica.*; Vol. 34/12, pp. 2471-2485.
- [11] JAMES, R.D., HANE, K.F. (2000): Martensitic transformations and shape-memory materials. *Acta Materialia.*; Vol. 48/1, pp. 197-222.
- [12] KRISHNAN, M. (1998): The self accommodating martensitic microstructure of Ni-Ti shape memory alloys. *Acta Materialia.*; Vol. 46/4, pp. 1439-1457.
- [13] INAMURA, T., KINOSHITA, Y., KIM, J.I., KIM, H.Y., HOSODA, H., WAKASHIMA, K., MIYAZAKI, S. (2006): Effect of $\{0\ 0\ 1\} <1\ 1\ 0>$ texture on superelastic strain of Ti-Nb-Al biomedical shape memory alloys. *Materials Science and Engineering A.*; Vol. 438-440, pp. 865-869.
- [14] BHATTACHARYA, K. (2003): *Microstructure of martensite: why it forms and how it gives rise to the shape-memory effect.* Oxford Series on Materials Modelling, 1st Ed., Oxford University Press, Oxford.
- [15] STALMANS, R., DELAEY, L., VAN HUMBEECK, J. (1997): Generation of recovery stresses: thermodynamic modelling and experimental verification. *J. de Phys. IV.*; Vol. 7, pp. 47-52.
- [16] BARSCH, G.R., KRUMHANSL, J.A. (1984): Twin boundaries in ferroelastic media without interface dislocations. *Phys. Rev. Lett.*; Vol. 53/11, pp. 1069-1072.
- [17] FALK, F. (1980): Model free energy, mechanics, and thermodynamics of shape memory alloys. *Acta Metall.*; Vol. 28, pp. 1773-1780.
- [18] MAUGIN, G.A., CADET, S. (1991): Existence of solitary waves in martensitic alloys. *Int. J. Eng. Sci.*; Vol. 29/2, pp. 243-258.
- [19] BRINSON, L.C., LAMMERING, R. (1993): Finite element analysis of the behavior of shape memory alloys and their applications. *Int. J. Solids and Struct.*; Vol. 30/23, pp. 3261-3280.
- [20] IVSHIN, Y., PENCE, T.J. (1993): A thermomechanical model for a one variant shape memory material. *J. Intell. Mat. Syst. and Struct.*; Vol. 5/7, pp. 455-473.
- [21] LIANG, C., ROGERS, C.A. (1990): One-dimensional thermomechanical constitutive relations for shape memory materials. *J. Intell. Mater. Syst. and Struct.*; Vol. 1/2, pp. 207-234.
- [22] BOYD, J.G., LAGOUDAS, D.C. (1994): Thermomechanical response of shape memory composites. *J. Intell. Mater. Syst. and Struct.*; Vol. 5, pp. 333-346.
- [23] TANAKA, K. (1986): A thermomechanical sketch of shape memory effect: One-dimensional tensile behaviour. *Res Mech.*; Vol. 18, pp. 251-263.
- [24] BRINSON, L.C. (1993): One-dimensional constitutive behavior of shape memory alloys: thermomechanical derivation with non-constant material functions and redefined martensite internal variable. *J. Intell. Mater. Syst. and Struct.*; Vol. 4, pp. 229-242.
- [25] LUBLINER, J.F., AURICCHIO, F. (1996): Generalized plasticity and shape-memory alloys. *Int. J. Solids and Structures.*; Vol. 33/7, pp. 991-1003.
- [26] PANOSKALTSIS, V.P., BAHUGUNA, S., SOLDATOS, D. (2004): On the thermomechanical modeling of shape memory alloys. *Int. J. Non-Linear Mech.*; Vol. 39/5, pp. 709-722.

- [27] SUN, Q.P., HWANG, K.C. (1994): Micro-mechanics constitutive description of thermoelastic martensitic transformations. *Advances in Applied Mechanics*.; Vol. 31, pp. 249-298.
- [28] KOSEL, F., VIDENIC, T. (2007): Generalized plasticity and uniaxial constrained recovery in shape memory alloys. *Mech. Adv. Mater. Struc.*; Vol. 14/1, pp. 3-12.
- [29] DENKHAUS, E., SALNIKOW, K. (2002): Nickel essentiality, toxicity, and carcinogenicity. *Critical Reviews in Oncology/Hematology*.; Vol. 42, pp. 35-56.
- [30] NIEBOER, E., TOM, R.T., SANFORD, W.E. (1988): *Nickel metabolism in man and animals* (In: Nickel and Its Role in Biology: Metal Ions in Biological Systems), Vol. 23 (Sigel H, ed). New York: Marcel Dekker, pp. 91-121.
- [31] FLETCHER, G.G., ROSSETTO, F.E., TURNBULL, J.D., NIEBOER, E. (1994): Toxicity, Uptake, and Mutagenicity of Particulate and Soluble Nickel Compounds. *Environ Health Perspect.*; Vol. 102 (Suppl 3), pp. 69-79.
- [32] YAMAMOTO, A., HONMA, R., SUMITA, M. (1998): Cytotoxicity evaluation of 43 metal salts using murine fibroblasts and osteoblastic cells. *Journal of Biomedical Materials Research*.; Vol. 39, pp. 331-340.
- [33] COMBES, C., REY, C., FRECHE, M. (1998): XPS and IR study of dicalcium phosphate dihydrate nucleation on titanium surfaces. *Colloids and Surfaces B: Biointerfaces*.; Vol. 11/1-2, pp. 15-27.
- [34] SHIH, C., LIN, S., CHUNG, K., CHEN, Y., SU, Y., LAI, S., WU, G., KWOK, C., CHUNG, K. (2000): The cytotoxicity of corrosion products of Nitinol stent wires on cultured smooth muscle cells. *J. Biomed. Mater. Res.*; Vol. 52, pp. 395-403.
- [35] WEVER, D.J., VELDHIJZEN, A.G., SANDERS, M.M., SCHAKENRAAD, J.M., HORN, J.R. (1997): Cytotoxic, allergic and genotoxic activity of a nickel-titanium alloy. *Biomaterials*.; Vol. 18, pp. 1115-1120.
- [36] WATAHA, I.C., LOCKWOOD, P.E., MAREK, M., GHAZI, M. (1999): Ability of Ni-containing biomedical alloys to activate monocytes and endothelial cells in vitro. *J Biomed Mat Res.*; Vol. 45, pp. 251-257.
- [37] RYHÄNEN, J., NIEMI, E., SERLO, W., NIEMELÄ, E., SANDVIK, P., PERNU, H., SALO, T. (1997): Biocompatibility of nickel-titanium shape memory metal and its corrosion behavior in human cell cultures. *J Biomed Mat Res.*; Vol. 35, pp. 451-457.
- [38] WIRTH, C., COMTE, V., LAGNEAU, C., EXBRAYAT, P., LISSAC, M., JAFFREZIC-RENAULT, N., PONSONNET, L. (2005): Nitinol surface roughness modulates in vitro cell response: a comparison between fibroblasts and osteoblasts. *Materials Science and Engineering: C*.; Vol. 25, pp. 51-60.
- [39] TREPANIER, C., LEUNG, T., TABRIZIAN, M., YAHIA, L'H., BIENVENU, J., TANGUAY, J., PIRON, D., BILODEAU, L. (1999): Preliminary investigation of the effect of surface treatment on biological response to shape memory NiTi stents. *J. Biomed. Mater. Res.*; Vol. 48, pp. 165-171.

- [40] SHABALOVSKAYA, S.A. (2002): Surface, corrosion and biocompatibility aspects of Nitinol as an implant material. *Biomed. Mater. Eng.*; Vol. 12, pp. 69-109.
- [41] SHABALOVSKAYA, S.A. (1996): On the nature of the biocompatibility and on medical applications of NiTi shape memory and superelastic alloys. *Biomed. Mater. Eng.*; Vol. 6, pp. 267-289.
- [42] FRAUCHIGER, V.M., SCHLOTTIG, F., GASSER, B., TEXTOR, M. (2004): Anodic plasma-chemical treatment of CP titanium surfaces for biomedical applications. *Biomaterials.*; Vol. 25, pp. 593-606.
- [43] LU, X., ZHAO, Z., LENG, Y. (2006): Biomimetic calcium phosphate coatings on nitric-acid-treated titanium surfaces. *Materials Science and Engineering: C.*; Vol. 27/4, pp. 700-708.
- [44] PARK, J., KIM, D.J., KIM, Y.K., LEE, K.H., LEE, H., AHN, S. (2003): Improvement of the biocompatibility and mechanical properties of surgical tools with TiN coating by PACVD. *Thin Solid Films.*; Vol. 435/1-2, pp. 102-107.
- [45] SHEVCHENKO, N., PHAM, M.T., MAITZ, M.F. (2004): Studies of surface modified NiTi alloy. *Applied Surface Science.*; Vol. 235, pp. 126-131.
- [46] ENDO, K. (1995): Chemical modification of metallic implant surfaces with bio-functional proteins (Part 1). Molecular structure and biological activity of a modified NiTi alloy surface. *Dent. Mater. J.*; Vol. 14, pp. 185-198.
- [47] LIU, F., WANG, F., SHIMIZU, T., IGARASHI, K., ZHAO, L. (2006): Hydroxyapatite formation on oxide films containing Ca and P by hydrothermal treatment. *Ceramics International.*; Vol. 32/5, pp. 527-531.
- [48] SCHILLINGER, M., SABETI, S., LOEWE, C. (2006): Balloon angioplasty versus implantation of nitinol stents in the superficial femoral artery. *Journal of Vascular Surgery.*; Vol. 44/3, pp. 684.
- [49] RAPP, B. (2004): Nitinol for stents. *Materials Today.*; Vol. 7/5, pp. 13.
- [50] TYAGI, S., SINGH, S., MUKHOPADHYAY, S., KAUL, U.A. (2003): Self- and balloon-expandable stent implantation for severe native coarctation of aorta in adults. *American Heart Journal.*, Vol. 146/5, pp. 920-928.
- [51] SIMON, M., KAPLOW, R., SALZMAN, E., FREEMAN, D. (1977): A vena cava filter using thermal shape memory alloy Experimental aspects. *Radiology.*; Vol. 125, pp. 87-94.
- [52] DUERIG, T., PELTON, A., STÖCKEL, D. (1999): An overview of nitinol medical applications. *Materials Science and Engineering: A.*; Vol. 273-275, pp. 149-160.
- [53] FISCHER, H., VOGEL, B., GRÜNHAGEN, A., BRHEL, K.P., KAISER, M. (2002): Applications of Shape-Memory Alloys in Medical Instruments. *Materials Science Forum.*; Vol. 394-395, pp. 9-16.
- [54] PELTON, A.R., STÖCKEL, D., DUERIG, T.W. (2000): Medical Uses of Nitinol. *Materials Science Forum.*; Vol. 327-328, pp. 63-70.
- [55] DAI, K., WU, X., ZU, X. (2002): An Investigation of the Selective Stress-Shielding Effect of Shape-Memory Sawtooth-Arm Embracing Fixator. *Materials Science Forum.*; Vol. 394-395, pp. 17-24.

- [56] ZHANG, C., XU, S., WANG, J., YU, B., ZHANG, Q. (2002): Design and Clinical Applications of Swan-Like Memory-Compressive Connector for Upper-Limb Diaphysis. *Materials Science Forum.*; Vol. 394-395, pp. 33-36.
- [57] DA, G., WANG, T., LIU, Y., WANG, C. (2002): Surgical Treatment of Tibial and Femoral Fractures with TiNi Shape-Memory Alloy Interlocking Intramedullary Nails. *Materials Science Forum.*; Vol. 394-395, pp. 37-40.
- [58] SONG, C., FRANK, T.G., CAMPBELL, P.A., CUSCHIERI, A. (2002): Thermal Modeling of Shape-Memory Alloy Fixator for Minimal-Access Surgery. *Materials Science Forum.*; Vol. 394-395, pp. 53-56.
- [59] XU, S., ZHANG, C., LI, S., SU, J., WANG, J. (2002): Three-Dimensional Finite Element Analysis of Nitinol Patellar Concentrator. *Materials Science Forum.*; Vol. 394-395, pp. 45-48.
- [60] CHU, Y., DAI, K., ZHU, M., MI, X. (2000): Medical Application of NiTi Shape Memory Alloy in China. *Materials Science Forum.*; Vol. 327-328, pp. 55-62.

Artificial tooth and polymer-base bond in removable dentures: the influence of pre-treatment on technological parameters to the bond's strength

Vez med umetnim zobom in polimerno osnovo v snemljivi zobni protezi: vpliv tehnoloških parametrov pred-obdelave na trdnost nastale vezi

MARTIN PAVLIN¹, REBEKA RUDOLF², VJEKOSLAV JEROLIMOV³

¹Private dental practice, Turnerjeva ulica 33, SI-2000, Maribor, Slovenia;
E-mail: martin.pavlin@triera.net

²University of Maribor, Faculty of Mechanical Engineering, Smetanova ulica 17, SI-2000 Maribor, Slovenia; E-mail: rebeka.rudolf@uni-mb.si

³University of Zagreb, School of Dental Medicine, Department of Prosthodontics, Gunduličeva 5, HR-10000 Zagreb, Croatia; E-mail: jerolimov@sfdzg.hr

Received: November 9, 2007

Accepted: May 18, 2008

Abstract: The aim of this study was to evaluate the artificial tooth and polymer-base bond, and to measure any formed gaps between tooth and base. Acrylic models were classified into four groups depending on the type of surface pre-treatment. A pre-treatment of the surface combining mechanical and chemical procedures led to the highest bond strength between the acrylic tooth and the denture-base. The fore-mentioned pre-treatment had a significant influence on gap formation with an average value of 68.250 μm , which is 70 % of the gap for the untreated samples. Furthermore, the measured compressive strength was above 6000 N/mm^2 , yet only 3200 N/mm^2 on the untreated samples.

Izvleček: Študija predstavlja raziskavo nastale vezi med umetnim zobom in polimerno osnovo z meritvijo nastale špranje med zobom in osnovo. Za ta namen so bili pripravljene akrilatni modeli, ki smo jih uvrstili v štiri skupine in sicer v odvisnosti od vrste površinske pred-obdelave. Površinska pred-obdelava, ki je predstavljala kombinacijo mehanske in kemijske, omogoča nastanek trdne vezi med akrilnim zobom in polimerno osnovo. Takšna pred-obdelava ima velik vpliv na nastanek špranje s povprečno vrednostjo 68,250 μm , kar predstavlja le 70 % velikosti špranje, ki je nastala pri neobdelanem vzorcu. Še več, rezultati meritev tlačne trdnosti za vzorce s pred-obdelavo kažejo vrednosti nad 6000 N/mm^2 , medtem ko smo pri neobdelanih vzorcih izmerili le 3200 N/mm^2 .

Key words: bond, acrylic tooth, polymer base, technological parameters

Ključne besede: vez, akrilni zob, polimerna osnova, tehnološki parametri

INTRODUCTION

The acrylic resin is the most commonly used artificial resin in dentistry. Most mobile dentures over the last 60 years had been created by conventional polymerization. Acrylic materials and the process of polymerization have been modified in the last 10 years, which has consequently resulted in better physical-chemical properties^[1]. This has been achieved by adding certain chemical substances, and changing the process of polymerization by adding light and microtalmic energy^[2]. Significant research work has shown that almost 30 % of all repairs are due to mistakes during tooth-denture base bonding^[3,4]. Consequently, this study focused on the evaluation of various treatments' influences on bonding quality between the denture-base and the artificial tooth, the measurement of gaps between the acrylic tooth and the denture base using an optical or electronic microscope, and the determination of mechanical properties by compressive testing.

MATERIALS AND METHODS

Four groups containing 12 acrylic models with the same dimensions were formed for evaluating the bonds between acrylic teeth and a denture-base (Gnathostar, Pro Base HOT, Ivoclar-Vivadent). The base surfaces of the acrylic teeth were prepared in four different ways as described later. The models were inserted in a brazen mould filled with gypsum. The mould was closed and placed into boiling water after the gypsum had hardened, in order to melt the wax. Then the mould was opened, the

elastomer-base removed, and the remains of the wax cleaned.

Finally, 12 special acrylic models (3 for each group) were created for compressive testing with internal dimensions of 20 mm × 9 mm.

Surface Conditioning Methods

Sample A, the surface was untreated and cleaned with 70 % ethyl alcohol (10 seconds), degreased and placed above boiling water (10 seconds). The cleaned tooth was placed on an elastomer-base.

Sample B, the surface coming into contact with the acrylic base was mechanically prepared using a 3M-8691C paper grinder (3M Dental, Pithiviers, France). This paper grinder was pulled over the contact surface twice.

Sample C, the surface was cleaned and moistened using monomer. The model was then left to dry at room temperature. The procedure was repeated after drying.

Sample D, the surface coming into contact with the acrylic base was mechanically prepared, cleaned and moistened using monomer (20 seconds). The model was then left to dry at room temperature. The procedure was repeated after drying.

A heat-polymerized cyclic resin (Pro Base HOT, Ivoclar-Vivadent, Schaan, Liechtenstein) was prepared and polymerized according to the manufacturer's instructions. The mixed acrilate mixture was left in a closed container at room temperature (23 °C) for 8-10 minutes, and then applied in the mould. The mould was then exposed to a pressure of 2×10^7 Pa (200 bar). The samples were thermally polymerized (at 65-70

°C for the first 45 minutes and at 100 °C for the next 45 minutes). The mould was left for 30 minutes at room temperature and was then completely cooled in cold water. The completely cooled mould was opened and the models extracted, cleaned and polished.

Specimens' preparation

The specimens (Figure 1) for microscopic analysis were prepared using an *ISOMET slow rotation saw*, abrasive diamond paste (3-9 µm), and special paper grinders. Alcohol and ultrasound were then used for cleaning. The prepared models were analysed using a light-inverse *NIKON Epiphot 300 microscope*. The selected models were also analysed with a (SEM) – *Sirion 400 NC scanning microscope* for visualisation of the microstructure. The size of each gap was measured on six different spots.

Compressive testing

Pressure testing was performed on a *Zwick/Roell Z010* pressure machine. The compressive tests were supposed to establish any influence of the surface preparation procedure and resulting border surface on the point tooth – denture-base regarding

pressure from chewing forces that dental prostheses pass-on to the jaw segment during their function in the oral cavity. The problem in this case was specific, since molar teeth were chosen for testing, which are only subjected to direct pressure forces. Special supports were created so that the models could be fixed into the machine, and the supports were placed in such a way as to simulate the occlusal relationship between the upper and the lower teeth in the mouth (Figure 2).

RESULTS

Gap-width and compressive strength depend on the type of mechanical-chemical pre-treatment. The results for measured gap width (Figure 3) show (A (x = 88-105 µm) > B = C (x = 68-86 µm) > D (39-66 µm)) justify the hypothesis on homogenous variances (Test of Homogeneity of Variances, ANOVA) (Table 1 and 2). It confirms that there are statistically significant differences between all four sample groups. In addition, the compressive test results show differences between samples A(3200 N/mm²)<C(5800 N/mm²)<B(6000 N/mm²)<D(6050 N/mm²).



Figure 1. Acrylic model after its removal from the mould, prepared for microscoping

Slika 1. Akrični model po odlitju, pripravljen za mikroskopijo

CONCLUSIONS

It can be concluded from the acquired results that the thickness and width of the gap depend on the type and mechanical pre-treatment of the tooth's surface. Microscopic examinations show that there is no statistically significant difference between roughened models and those wetted with a monomer, but there is one between rough-

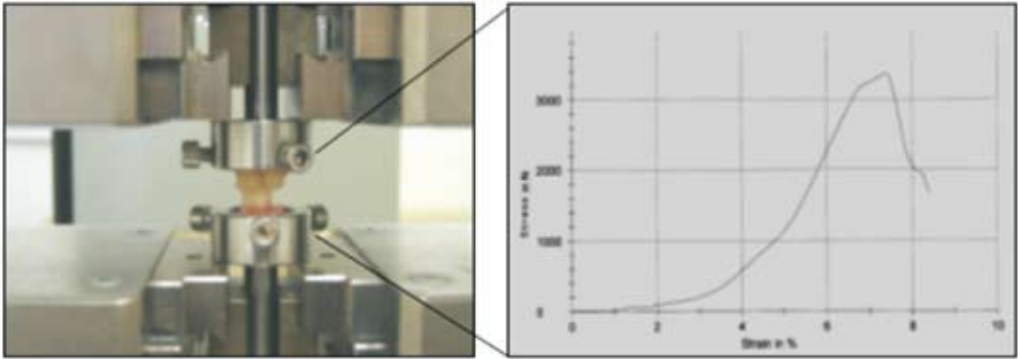


Figure 2. Compressive testing and typical σ - ε diagram for sample A
Slika 2. Tlačni preizkus in tipični σ - ε diagram za vzorec A

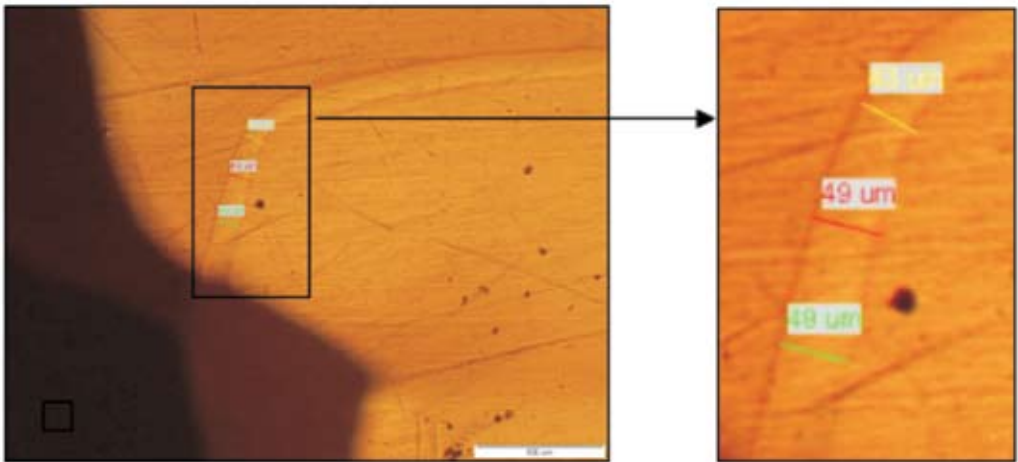


Figure 3. Schematic survey of measuring points at a micro-level
Slika 3. Shematski prikaz meritvenih točk na mikro-nivoju

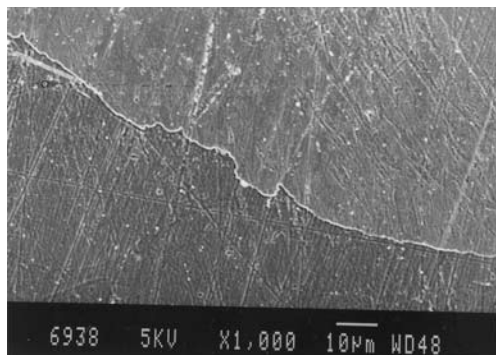


Figure 4. SEM picture of the sample D
Slika 4. SEM fotografija vzorca D

Table 1. Test of Homogeneity of Variances**Tabela 1.** Test homogenosti varianc

Test of Homogeneity of Variances

	Levene Statistic	df1	df2	Sig.
v_edge	1,550	3	44	,215
v_200	,044	3	44	,988
v_curve	3,210	3	44	,032
v_centre	2,930	3	44	,044
v_max	,563	3	44	,642
v_min	4,660	3	44	,006

Table 2. Two-way ANOVA of gap dimensions**Tabela 2.** Dvo-smerna ANOVA za dimenzije špranje

ANOVA

		Sum of Squares	df	Mean Square	F	Sig.
v_edge	Between Groups	7580,333	3	2526,778	68,110	,000
	Within Groups	1632,333	44	37,098		
	Total	9212,667	47			
v_200	Between Groups	8947,083	3	2982,361	64,679	,000
	Within Groups	2028,833	44	46,110		
	Total	10975,917	47			
v_curve	Between Groups	9813,729	3	3271,243	167,935	,000
	Within Groups	857,083	44	19,479		
	Total	10670,813	47			
v_centre	Between Groups	6634,833	3	2211,611	32,697	,000
	Within Groups	2976,167	44	67,640		
	Total	9611,000	47			
v_max	Between Groups	8575,729	3	2858,576	28,510	,000
	Within Groups	4411,750	44	100,267		
	Total	12987,479	47			
v_min	Between Groups	9950,396	3	3316,799	137,086	,000
	Within Groups	1064,583	44	24,195		
	Total	11014,979	47			

ened and monomer wetted models, and untreated models. Those models prepared by roughening and wetting with a monomer had the most homogenous structure and the smallest gap (Figure 4). Border surfaces showed that untreated samples often have faults, such as porosity, and discord between border surfaces, which then have a strong influence on the quality of any bond between an artificial tooth and denture-base.

Consequently, gap thickness has an influence on the mechanical characteristics of a sample, there are namely they are inversely connected, the higher the gap-width, the lower the compressive strength of the artificial tooth and the polymer-base model.

Acknowledgments

This paper is a part of the Slovenian Applied Project no. L2-7096, Bilateral Project SLO/SR BI-CS/06-07-031 and EUREKA Programme E!3555 DEN-MAT. The authors gratefully acknowledge the Ministry of Higher Education, Science and Technology, and the Slovenian Research Agency.

POVZETEK

Vez med umetnim zobom in polimerno osnovo v snemljivi zobni protezi: vpliv tehnoloških parametrov pred-obdelave na trdnost nastale vezi

Vez med umetnim zobom in polimerno osnovo v snemljivi zobni protezi je eden od glavnih dejavnikov, ki vpliva na kvaliteto in funkcijo končnega izdelka ter ima tudi pomembno klinično vlogo.

V predstavljeni *in vitro* raziskavi je bila merjena in primerjana špranja, ki nastaja na mestu vezi med umetnim zobom in polimerno osnovo v snemljivi zobni protezi. Raziskava je zajemala vzorce, ki so bili izdelani na štiri različne načine.

Rezultati raziskav so pokazali, da je najmanjša izmerjena špranja na tistih modelih, kjer je bila kontaktna površina mehansko obdelana in navlažena z monomerom. Statistična obdelava dobljenih rezultatov je pokazala, da so meritve pri obdelanih površinah statistično nižje kot pri neobdelanih. Posledica le teh je večja špranja in oslABLJENA vez na kontaktni točki, kar je seveda pomemben statistični pokazatelj.

Na podlagi navedenega lahko zaključimo, da je potrebno kontaktne površine med umetnim zobom in polimerno osnovo mehansko in kemično obdelati, kljub splošno znanim izkušnjam iz stomatološke prakse, ki zagovarjajo le nujnost mehanske obdelave (retencije).

REFERENCES

- [1] VERGANI, CE., MACHADO, AL., GIAMPAOLO, ET., PAVARINA, AC. (2000): Effect of surface treatments on the bond strength between composite resin and acrylic resin denture teeth. *Int J Prosthodont.*; Vol. 13, pp. 383-6.
- [2] VALLITTU, PK. (1995): Bonding of resin teeth to the polymethyl metacrylate denture base material. *Acta Odontol Scand.*; Vol 53, pp. 99-104.
- [3] DARBAR, UR., HUGGETT, R., HARRISON, A., WILLIAMS, K. (1995): Finite element analysis of stress distribution at the tooth-denture base interface of acrylic resin teeth debonding from the denture base. *J Prosthet Dent.*; Vol. 74, pp. 591-4.
- [4] CUNNINGHAM, JL., BENINGTON, IC. (1999): An investigation of the variables which may affect the bond between plastic teeth and denture base resin. *J Dent.*; Vol. 27, pp. 129-35.

The onset of Maastrichtian basinal sedimentation on Mt. Matajur, NW Slovenia

Začetek maastrichtijske bazenske sedimentacije na Matajurju, SZ Slovenija

BLAŽ MIKLAVIČ¹, BOŠTJAN ROŽIČ²

¹Jožef Stefan Institute, Jamova cesta 39, SI-1000 Ljubljana, Slovenia;
E-mail: blaz.miklavic@gmail.com

²University of Ljubljana, Faculty of Natural Sciences and Engineering,
Department of Geology, Aškerčeva cesta 12, SI-1000 Ljubljana, Slovenia;
E-mail: bostjan.rozic@ntf.uni-lj.si

Received: October 28, 2007

Accepted: May 26, 2008

Abstract: Maastrichtian limestone breccia with varying thickness was deposited with angular discordance on Jurassic and Cretaceous platform limestones on the northern part of Mt. Matajur, Slovenia. The whole area was later overlaid by finer siliciclastic rocks with intra layers of limestone breccia, which changes the frequency of its appearance. We interpreted the resulting situation as a consequence of the sedimentation environment at the margin of the retrograding Dinaric Carbonate Platform in the late Cretaceous.

Izveleček: Na severni strani Matajurja je bila na jurske in kredne platformske apnenice s kotno diskordanco odložena maastrichtijska apnenčeva breča različne debeline. Celotno območje je bilo kasneje prekrito s finejšimi siliciklastičnimi kamninami z vmesnimi plastmi apnenčeve breče z različno pogostnostjo pojavljanja. Nastalo situacijo smo interpretirali kot posledico sedimentacijskega okolja na robu retrogradirajoče Dinarske karbonatne platforme v pozni kredi.

Keywords: Maastrichtian, Dinaric Carbonate Platform, Mt. Matajur, flysch, limestone breccia

Ključne besede: maastrichtij, Dinarska karbonatna platforma, Matajur, fliš, apnenčeva breča

INTRODUCTION

The area of Mt. Matajur is located in the Julian Prealps, NW Slovenia. In the Late Triassic, Jurassic and early Cretaceous it was located in the northern margin of the Dinaric Carbonate Platform. In the late Campanian and Maastrichtian the area experienced accelerated subsidence, related to the tectonically induced southward-retrograding platform. The area was firstly a part of a fault-dissected slope that experienced erosion. Subsequently, due to continuing back-stepping of the platform, the area gradually subsided and the deposition started. Sedimentation was firstly characterized by limestone breccias that originated from the collapse of the platform margin. Later it was reached by the southwards prograding flysch basin (BUSER & PAVŠIČ, 1978) that was marked by flysch deposits originating from the rising Alpine orogen in the north, alternating with limestone gravity-flow deposits originating from the south-retreating Dinaric Carbonate Platform. The depositional setting fits well with the collisional foredeep basin model of BRADLEY and KIDD (1991). The model is additionally supported by the corresponding south-shifting forebulge of the same period that was recognized in the inner parts of the Dinaric Carbonate Platform (OTONIČAR, 2007).

Although the late Cenomanian/Maastrichtian sedimentary evolution of western Slovenia is generally well resolved, no smaller-scale sedimentological studies were made on the northern margin of the Dinaric Carbonate Platform. The present paper presents such a study from the Mt. Matajur area. It compiles older stratigraphic

observations and new data obtained by detailed mapping on a scale of 1:5000, which gave a new insight and interpretation of the sedimentation regime in Maastrichtian for the area concerned. The study focuses on limestone breccia bodies, i.e., their shape, lateral continuity and, the vertical as well as horizontal relationship with the underlying carbonates and the surrounding flysch deposits.

GEOLOGICAL SETTINGS

The Mt. Matajur area structurally belongs to the External Dinarides (BUSER, 1986), characterized by SW-verging thrust displacements. It lies within the uppermost Trnovo Nappe in its north-western part (PLACER, 1981; BUSER, 1987). On a smaller scale, the succession forms the Mija–Matajur Anticline, where the Mt. Matajur area is situated in its southern hinge, where the beds generally dip towards the south (WINKLER, 1921; COUSIN, 1981; PIRINI RADRIZZANI et al., 1986; BUSER, 1986). Another important structural feature marks the investigated area; it lies at the boundary with the Southern Alps, a macrotectonic unit that consists of the Tolmin Basin and the Julian Carbonate Platform successions (BUSER, 1989, 1996; PLACER, 1999; ŠMUC, 2005; ROŽIČ, 2005; ROŽIČ and POPIT, 2006). The Southern Alps are characterized by younger (Miocene) south-verging thrust displacements (PLACER, 1999; VRABEC and FODOR, 2006). Although western Slovenia is dissected by intense NW-SE strike-slip neotectonics, the investigated area is not deformed, which leaves the primary facies relationships undisturbed.

In the Mt. Matajur area one of the northernmost Dinaric Carbonate Platform successions is preserved. It is generally marked by continuous shallow-water sedimentation during the Jurassic, succeeded by a more complex depositional pattern of the tectonically forced, retrograding platform margin. Therefore, the succession that overlies the platform limestones is characteristic for the slope depositional setting, experiencing long periods of non-deposition or erosion, i.e., stratigraphic gaps and occasional condensed carbonate sedimentation. The late Cretaceous is marked by further subsidence in the area and the reoccurrence of continuous sedimentation, this time in the basinal setting. It begins with the base-of-slope deposits, i.e., basal limestone breccias, and is overlain by flysch deposits, occasionally interrupted by abundant carbonate breccias. The composition of the clasts of the breccia indicates that the material must have originated from the collapsing slope of the south-retreating Dinaric Carbonate Platform (BUSER & PAVŠIČ, 1978; BUSER, 1986). The siliciclastic material of the flysch, on the other hand, must have had a different origin, which may also be concluded from the paleo-current marks observed in the nearby area by KUŠČER et al. (1974). The shown SE direction, corrected by the anti-clockwise rotation of the region (30° in the post-Eocene times, MARTON & VEJOVIĆ, 1983), point to north-deriving turbidites.

STRATIGRAPHIC UNITS

The territory of our interest on the northern part of Mt. Matajur has been the subject of some previous general geological surveys

(WINKLER, 1921; COUSIN, 1981; BUSER, 1986). A more detailed stratigraphic research was made in a nearby area in the Italian territory (PIRINI RADRIZZANI et al., 1986). We present a compilation of these studies and our own work.

Platform limestones – Jurassic

Platform limestones succession forms the northern slopes of the Mt. Matajur range. It begins with Upper Triassic Dachstein Limestone, with typical lofer sequences, and passes upwards into Jurassic limestone. In the investigated area only the topmost Jurassic part of the succession was included in the study. The Jurassic platform limestone typically occurs in layers 0.2 to 1.5 m thick and mostly consists of micrite with stromatolite horizons and frequent desiccation cracks. Bivalves from macrofossils are most abundant (Plate 1, Figure 1). In the western part of the area these beds are overlain by ooidal limestone with interlayers of intraformational limestone breccia.

Close to the mapped area at the Svinja planina, BUSER (1986) found Lithiotis bivalves and assigned the overall limestone succession above the Dachstein Limestone to the Lower Jurassic. The Middle Jurassic succession of the Dinaric Carbonate Platform is characterized by abundant ooides (BUSER, 1989, 1996), and the ooidal limestone with intraformational breccias that ends the platform limestone succession on the observed territory could be Middle Jurassic in age. Upper Jurassic is probably not preserved in the investigated area. In contrast, a more complete Jurassic succession is reported from the northern hinge of the Mija-Matajur Anticline (BUSER, 1987)

as well as westward from across the state border (COUSIN, 1981; PIRINI RADRIZZANI et al., 1986).

Nodular limestone and calcarenite with chert – Uppermost Jurassic and Lower Cretaceous

On the western part of the mapped area the Jurassic platform limestones are overlain with layers of nodular-bedded micritic limestone intercalated by even-bedded calcarenite (Plate 1, Figure 2). Both facies are replaced with chert nodules and sheets. They have a similar dip to the underlying platform limestone and their total thickness gradually increases towards the west of the mapped area where it reaches 60 m.

The stratigraphic ordering of these limestones varies a great deal from author to author. WINKLER (1921) assigned them to the Lower Jurassic, COUSINE (1981) classifies the same layers observed in the nearby territory to the Upper Jurassic, whereas BUSER (1985, 1987) considers them as Coniacian to Lower Maastrichtian Volče Limestone Formation. PIRINI RADRIZZANI et al. (1986) classify similar layers across the state border to the upper Tithonian to Albian (Soccher limestone). Because they made the most detailed survey of these beds their conclusion is likely to be the most accurate.

Upper Flyschoid Formation – Maastrichtian

The Upper Flyschoid Formation characterizes the Maastrichtian sedimentation of the Slovenian Basin (COUSIN 1970, 1981; CARON and COUSIN, 1972). It usually begins with a rather thick horizon of basal limestone breccia and is upwards replaced

by flyschoid development; i.e., marls and shales alternating with siliciclastic and carbonate turbidites (later in the text the term flysch is used only for the siliciclastic portion of the flyschoid deposits). A very similar facies association is also observed in the Mt. Matajur area, but thick limestone breccias also occur within flyschoid development.

Basal limestone breccia

The basal limestone breccia is thickest on the eastern part of the territory where it reaches 130 m and gradually wedges out toward the west. It consists of several horizons with differing levels of sorting. Clasts are typically 2-5 cm in size with occasional blocks that exceed 1 m in diameter. The roundness varies significantly and these facies would often be better classified as conglomerate. Nevertheless, due to generalization the term breccia is used in the paper. Their composition varies considerably: macroscopically rudist, reef, micritic, and ooidal limestone have been identified. Less common were clasts of Dachstein limestone and chert. The layering is poorly visible with beds above 1 m thick. The matrix is mostly calcarenite, but rarely the marly matrix is also present. Upwards the unit tends to end with calcarenite/limestone sandstone. On the eastern part the limestone breccia is channelized into Jurassic limestones with an angle discordance. Westwards, in the middle part of the mapped area, where it gradually wedges out, it appears only in the form of small pockets on the Jurassic ooidal limestone (Plate 1, Figure 3). On the westernmost part it reappears on the Cretaceous nodular limestone with chert. These layers are most probably younger than the basal limestone

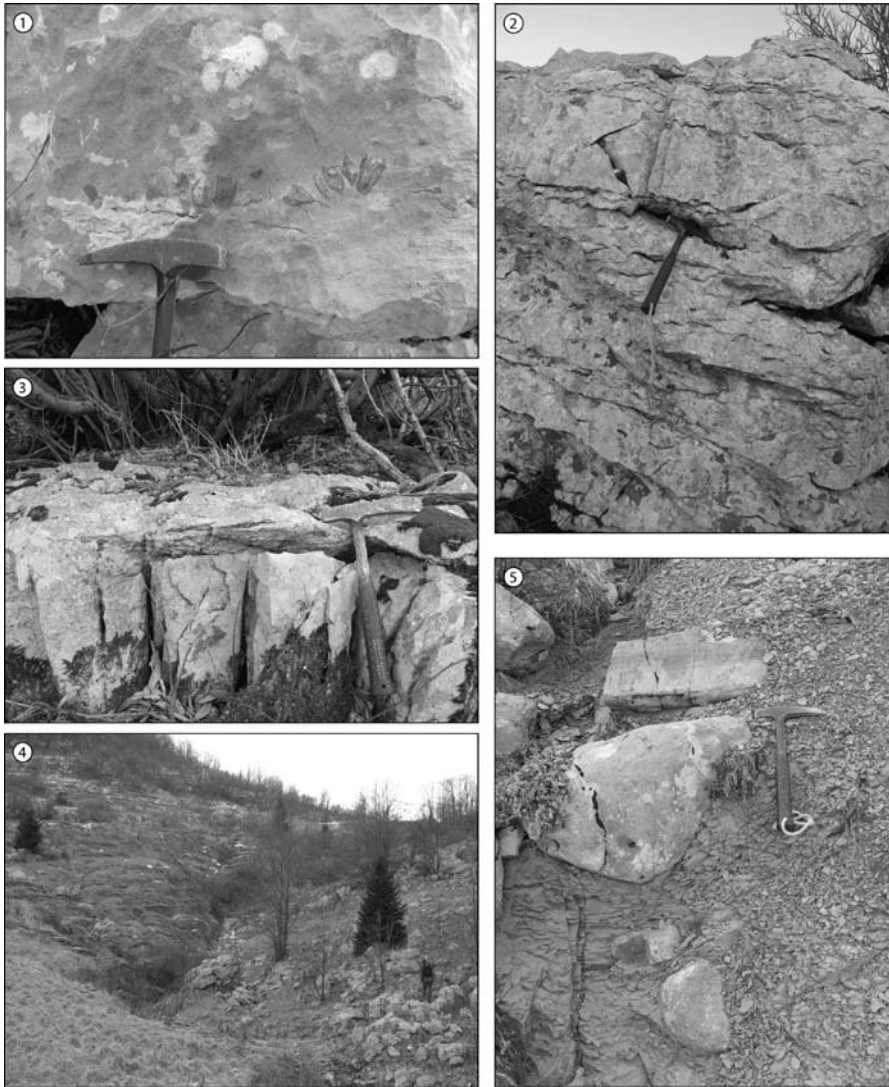


Plate 1. Fig. 1: Jurassic platform limestones with bivalves in the living position, Fig. 2: Lower Cretaceous nodular-bedded limestone and even-bedded calcarenite (above hammer), Fig. 3: Contact between Jurassic ooidal limestone and overlying basal limestone breccia in the central part of the mapped area, Fig. 4: On-lapping of the flyschoid sediments (left) on the paleo-slope composed of Jurassic platform limestones, Fig. 5: Chaotic breccia with limestone and chert clasts outcropping near the 'paleo'-slope

Tabla 1. Sl. 1: Jurski platformni apneneci s školjkami v življenjskem položaju, Sl. 2: Spodnjekredni gomoljastoplastnati apnenec in ravnoplastnati kalkarenit (nad kladivom), Sl. 3: Stik med jurskim ooidnim apnencem in višje ležečo bazalno apnenčevo brečo v centralnem delu raziskanega območja, Sl. 4: Naleganje flišoidnega zaporedja (levo) na »paleopobočja«, ki ga sestavljajo jurski platformski apneneci (desno), Sl. 5: Kaotična breča z apnenčevimi in roženčevimi klasti, ki izdanja v bližini »paleopobočja«

breccias in the eastern part of the mapped area. They thicken westwards, like the underlying limestone with chert (Figure 1).

Flyschoid development with layers of limestone breccia

Flyschoid sediments overlie all the previously described stratigraphic units throughout the Mt. Matajur area. On the extreme eastern and western parts they cover the Maastirchtian limestone breccia, whereas in the middle part they lie over the Jurassic and lower Cretaceous limestones. They mainly consist of reddish, laminated to thin-bedded claystone and marl or brown sandy claystone or marl, rarely exhibiting an incomplete Bauma sequence. Frequently, there are very thin, normally graded siliciclastic sandstone beds. In the central part of the area the several-meters-thick, gray claystone occurs just above the contact with limestone breccia. The X-ray diffraction analysis of this claystone showed a simple mineral composition of the rock containing just filosilicates (chlorite and illite/muscovite), whereas quartz was detected in only a few samples (MIKLAVIČ, 2007). Mud-supported (chaotic) breccias occur in the central part of the terrain near the paleotopographic slope (Plate 1, Figures 4,5) (for details see the following section). The clasts in this bed are shallow-water carbonates as well as rare angular cherts (Plate 1, Figure 5). Westward of this paleo-slope, lower Cretaceous nodular limestone is preserved, whereas eastward it was eroded.

Typical for this stratigraphic unit are the 0.1 to 1.5 m thick layers of channelled limestone breccia and calcarenite, which start to occur 10 m above the basal limestone

breccias/flyschoid border and stretch laterally over a couple of hundred meters. Normal gradation was observed, especially in the calcarenites. Higher up the stratigraphic sequence the layers of the limestone breccia and calcarenite get thicker and more frequent, thus forming limestone-dominated intervals that are several tens of metres thick. Within the limestone beds interlayers of flysch sediments are still present, being up to 3 m thick. Two such thick intervals are observed on the northern slope of Mt. Matajur. The first characterizes the eastern part of the territory, where it forms the present-day topographic range eastward of Mt. Matajur above the Tršča spring and continues to the peak of Mt. Mrzli vrh. Westward it becomes thinner and finally wedges out above the paleotopographic slope in the western part of the mapped area (Figure 1). The thickness of the flyschoid sediments between the first interval and the basal breccia is generally around 60 meters. It quickly thins above the paleotopographic slope to only 15 meters. In this part of the territory no basal breccia horizons are deposited and the flyschoid sediments directly overlie the lower Cretaceous nodular limestone. A second interval is observed in the western part of the territory, and this forms the top of Mt. Matajur. The thickness of the flyschoid sediments between the second interval and the basal breccia or nodular limestone is relatively uniform and is around 70 meters.

DISCUSSION

In the late Triassic and Jurassic, Mt. Matajur was located on the northern margin of the Dinaric Carbonate Platform. Although

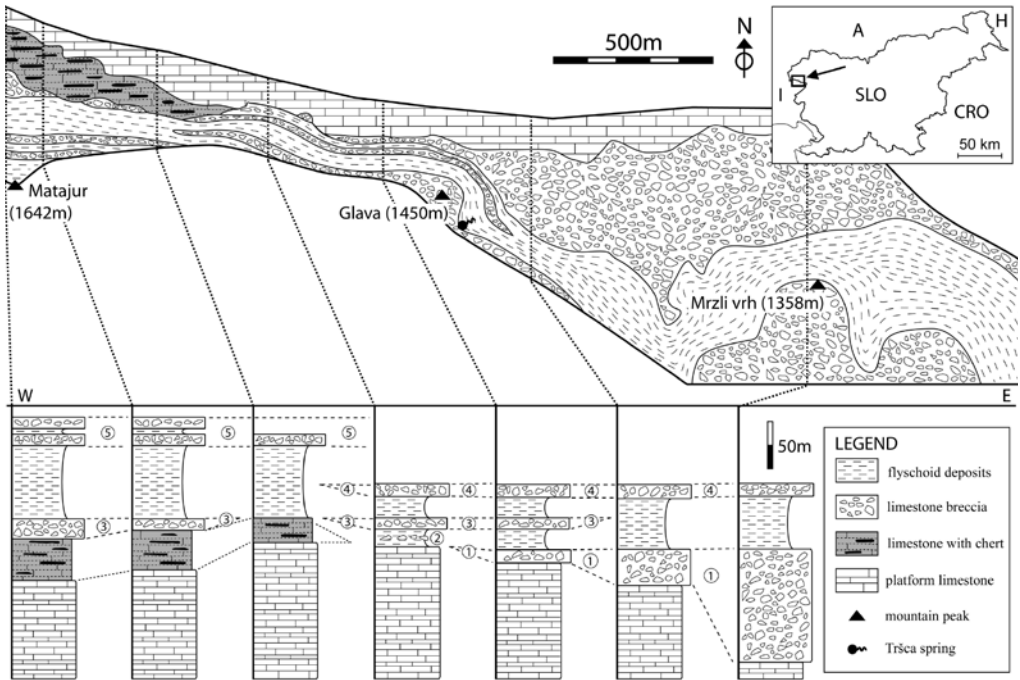


Figure 1. Location (upper-right corner) and geological map of the Mt. Matajur area with simplified stratigraphic sections. Numbering of limestone breccia horizons: 1-basal limestone breccia, 2-mud-supported (chaotic) breccia with limestone and chert clasts, 3-»western« basal limestone breccia, 4-first interval dominated by limestone breccia and calcarenite, 5-second interval dominated by limestone breccia and calcarenite.

Slika 1. Lokacija (zgornji desni kot) in geološka karta območja Matajurja s poenostavljenimi stratigrafskimi stolpci. Oštevilčenje horizontov apnenčevih breč: 1-bazalne apnenčeve breče, 2-kaotične breče s klasti apnencev in rožencev, 3-»zahodne« bazalne apnenčeve breče, 4-prvi interval s prevladujočimi apnenčevimi brečami in kalkareniti, 5-drugi interval s prevladujočimi apnenčevimi brečami in kalkareniti.

Upper Jurassic limestones are probably not preserved in the Mt. Matajur area, the shallow-water sedimentation in the wider area persisted until the late Jurassic, because the Upper Jurassic shallow-water limestones are reported from the northern part of the Mija-Matajur Anticline (BUSER, 1989) and also westward in the nearby Italian territory (PIRINI RADRIZZANI et al., 1986).

The Jurassic platform limestones are overlain by upper Tithonian to Albian nodular

micritic limestone with chert nodules and calcarenite interbeds. The facies association indicates a deposition in a deeper-water sedimentary environment. Furthermore, nodular bedding of the micritic limestone elucidates a rather condensed carbonate sedimentation (e.g., MARTIRE, 1996), thus the sedimentation of these beds in the slope seams most convenient. The end Jurassic/early Cretaceous subsidence of the Dinaric Carbonate Platform margin coincides with the initial phases of

the compressive tectonic regime in the internal domains of the Dinarides (CHANNELL et al., 1979; DIMITRIJEVIĆ, 1982; KARAMATA, 1988) and with the onset of thrusting in the Northern Calcareous Alps (GAWLICK et al., 1999). According to PIRINI RADRIZZANI et al. (1986) the sedimentation of this unit ends in the Albian. The termination coincides with the onset of the sedimentation of the Lower Flyschoid Formation in the Tolmin Basin, characterized in the areas proximal to the Dinaric Carbonate platform by thick basal limestone breccias (CARON and COUSIN, 1972; BUSER, 1987; SAMIEE, 1999; ROŽIČ, 2005). These breccias indicate a new pulse of increased subsidence and the reorganisation of the depositional setting. Namely, the slope became dissected by normal faults, which increased the overall angle and resulted in erosion or at least the non-deposition in the slope, as evidenced by the Albian–Campanian stratigraphic gap in the Mt. Matajur area.

In the Late Campanian/early Maastrichtian a new pulse of accelerated subsidence (the Laramian tectonic phase in BUSER, 1989, 1996) led to the reorganisation of the sedimentary environment in the Mt. Matajur area. Firstly, during subsidence a tectonic block of Mt. Matajur tilted towards the west (Figure 2). This can be deduced from the increasing thickness towards the west of the lower Cretaceous limestones, together with the overlying basal limestone breccia of the Maastrichtian Upper Flyschoid Formation. Further subsidence resulted in the onset of the base-of-slope deposits, i.e., of the basal limestone breccia. The composition records the erosion of older platform limestones, which were exposed in the fault-dissected slope. The

deposition of these breccias was at the beginning limited to the eastern part of the examined area (Figure 3). It is either the consequence of (1) erosion of those gravity currents that were directed by the feeder channel, predominantly in the eastern part of the area, or (2) gravity currents filled pre-existing paleotopographic low in the eastern part. Simultaneously, the western part of the area formed paleotopographic high, which was by-passed by gravity currents (Figure 3). In second scenario the paleorelief was moderately increasing towards the west. The exception was the steeper paleo-slope in the western part of the area that was several tens of meters high and extended probably in the N-W direction (Figure 2). At the top of this slope the lower Cretaceous limestone starts to occur. It could indicate that this formation was relatively more erosion-resistant, thus forming the paleotopographic high.

The sedimentation of the basal limestone breccias ceased due to the further retrogradation of the Dinaric Carbonate Platform. Subsequent sedimentation is characterized by hemipelagic deposits, as evidenced by the relatively simple mineral composition of the overlying claystones and by the distal flysch deposits marked by incomplete Bouma sequences. This relatively quiet sedimentation period was only occasionally interrupted by carbonate gravity flows originating from the south-retreating platform and the slope. Conspicuous sediments, i.e., debris flow deposits, occur within the flysch near the previously described paleotopographic slope. These chaotic breccias with a marly matrix contain limestone as well as chert clasts and most probably originated by tectonically

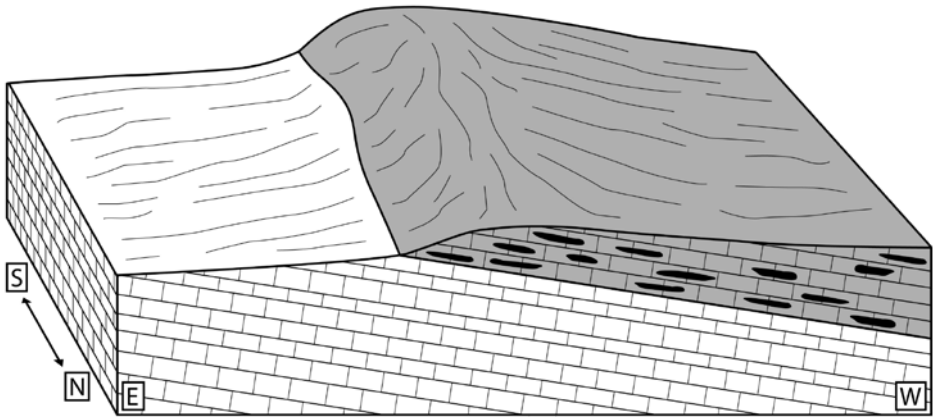


Figure 2. Schematic reconstruction prior to the deposition of the Upper Flyshoid Formation: the succession is tilted toward the west and the paleotopography is gently rising towards the west with a steeper paleo-slope in the central part (for Figures 2 to 7 take into consideration: a) for legend see Figure 1; b) view is from north-east; c) the eastern part of the area is shortened due to more representative reconstruction; d) facts are presented in the front wall, whereas the rest of the reconstruction is an assumption)

Slika 2. Shematska rekonstrukcija stanja pred odlaganjem zgornje flišoidne formacije: zaporedje kamnin je nagnjeno proti zahodu in paleotopografija se blago viša proti zahodu s strmejšim »paleopobočjem« v srednjem delu območja (na slikah 2 do 7 naj bralec upošteva: a) litostratigrafske oznake so enake kot na sliki 1, b) pogled je s severovzhoda, c) vzhodni del območja je skrajšan zaradi preglednejše rekonstrukcije, d) dejstva so predstavljena na sprednjem delu skice, medtem, ko je ostali del rekonstrukcije domneven)

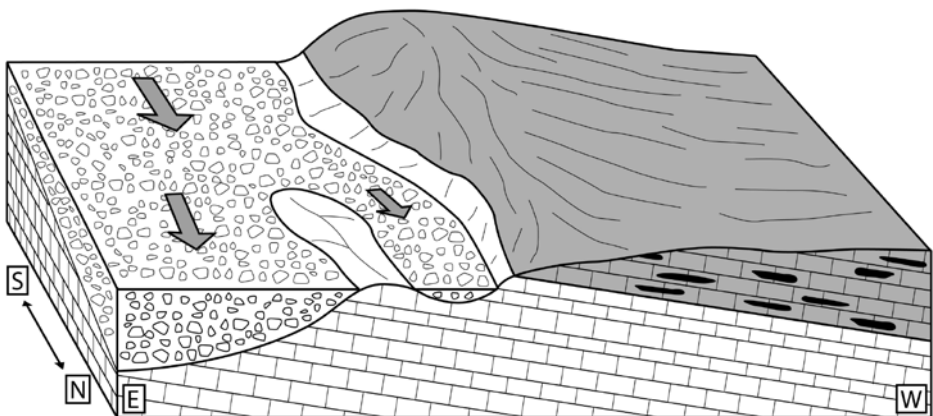


Figure 3. Schematic reconstruction of the basal limestone breccia deposition (for details of the reconstruction see the text for Figure 2)

Slika 3. Shematska rekonstrukcija sedimentacije bazalne apnenčeve breče (podrobnosti rekonstrukcije so obrazložene v besedilu pri sliki 2)

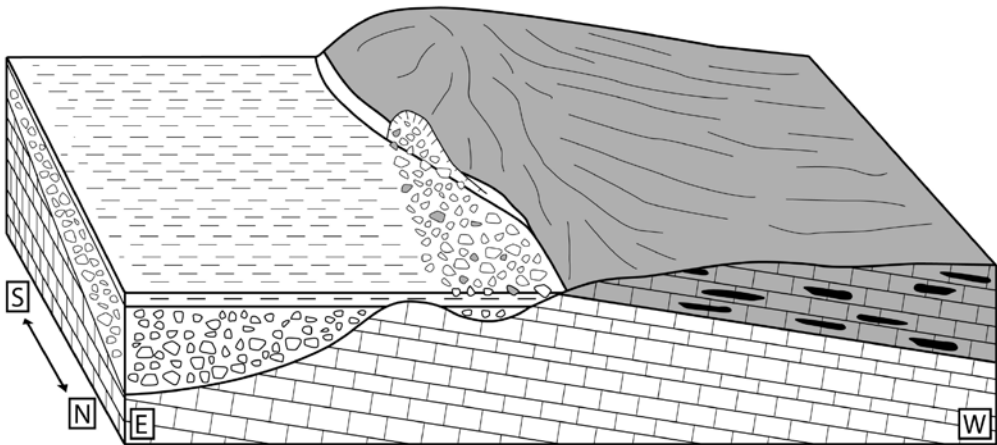


Figure 4. On-lapping of the flyshoid sediments (left) on the paleo-slope composed of Jurassic platform limestones (right)

Slika 4. Shematska rekonstrukcija sedimentacije kaotične breče, ki je nastala s poružitvijo »paleopobočja« v srednjem delu območja (podrobnosti rekonstrukcije so obrazložene v besedilu pri sliki 2)

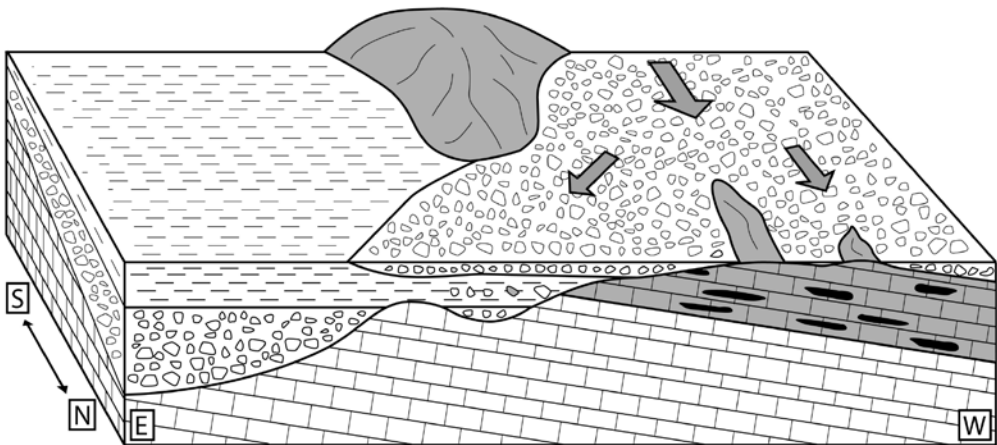


Figure 5. Schematic reconstruction of the »western basal limestone breccia« deposition (for details of reconstruction see the text for Figure 2)

Slika 5. Shematska rekonstrukcija sedimentacije »zahodne« bazalne apnenčeve breče (podrobnosti rekonstrukcije so obrazložene v besedilu pri sliki 2)

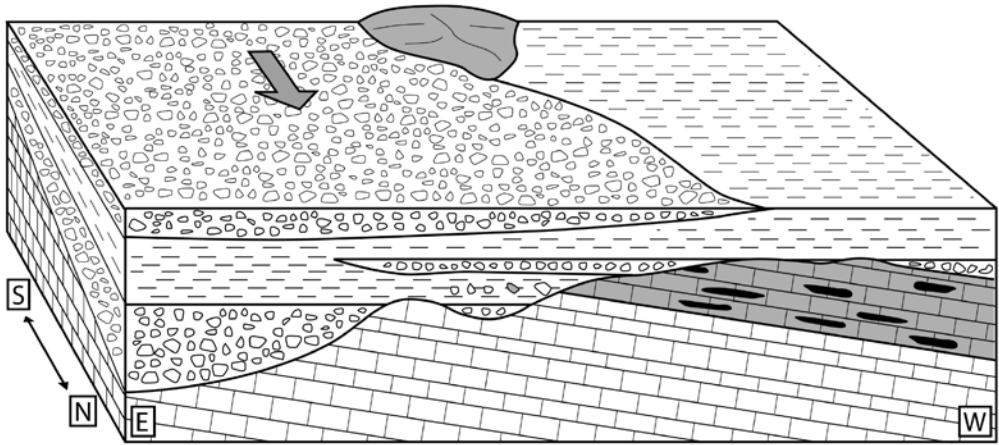


Figure 6. Schematic reconstruction of the deposition during the first interval dominated by limestone breccia and calcarenite (for details of the reconstruction see the text for Figure 2)

Slika 6. Shematska rekonstrukcija sedimentacije prvega intervala s prevladujočimi apnenčevimi brečami in kalkareniti (podrobnosti rekonstrukcije so obrazložene v besedilu pri sliki 2)

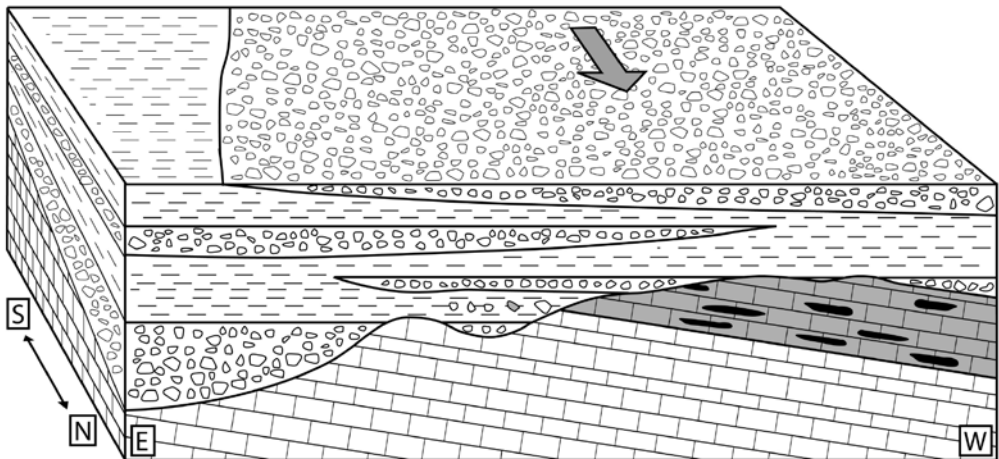


Figure 7. Schematic reconstruction of the deposition during the second interval dominated by limestone breccia and calcarenite (for details of the reconstruction see the text for Figure 2)

Slika 7. Shematska rekonstrukcija sedimentacije drugega intervala s prevladujočimi apnenčevimi brečami in kalkareniti (podrobnosti rekonstrukcije so obrazložene v besedilu pri sliki 2)

triggered collapses of the previously mentioned slope (Figure 4).

The deposition of limestone breccia that overlies the lower Cretaceous limestone in the western part of the studied area (»western basal limestone breccia«) started when the eastern paleotopographic low was almost filled with distal flysch deposits and minor carbonate resediments (Figure 5). This breccia is thickest on the west; towards the east it thins out and is occasionally discontinued. The widest lateral discontinuity appears above the paleo-slope (Figure 5). Eastward, near the top of this slope, a rather thick limestone breccia bed is situated within the flyschoid deposits and probably represents the eastern continuation of the »western basal limestone breccia«. This bed gradually wedges out further east.

The following distal flysch deposits blanketed the entire paleorelief existing in the examined area. These deposits are interrupted by two thick intervals of limestone breccia and calcarenite, probably originating in periods of increased tectonic activity. The lower interval is deposited predominantly in the eastern part of the mapped area; it still occurs above the paleotopographic slope and finally wedges out towards the west (Figure 6). The upper interval forms the top of Mt. Matajur, which is located in the western part of the area (Figure 7). Although the eastern continuation of the upper interval was not studied, the described distribution of the two horizons probably indicates a westward migration of the limestone breccias supply channel.

SUMMARY

The compilation of the detailed mapping and the older stratigraphic research of the Mt. Matajur area leads to the following conclusions:

- A. In the Mt. Matajur area the shallow-water carbonate sedimentation probably persisted almost all through the Jurassic and was only in the latest Jurassic replaced by slope deposits, characterized by nodular micritic limestone with chert nodules and interbedded calcarenites.
- B. At the end of Albian the tectonic phase dissected the slope with normal faults, which resulted in an increased slope angle and a subsequent long period of erosion or at least non-deposition.
- C. In the late Campanian/early Maastrichtian a new tectonic pulse caused further subsidence of the Mt. Matajur area. Before the deposition reoccurred, the tectonic block was tilted towards the west and an uneven paleorelief existed. The paleorelief was gentle with the exception of a steeper slope in the centre of the mapped area that separated the eastern paleotopographical low and the western paleotopographical high.
- D. In the Maastrichtian the Upper Flyschoid Formation deposited. It is characterized by alternating south-derived limestone breccias originating from platform collapsing, hemipelagic deposits and north-derived distal flysch deposits. The following depositional stages were recognized: 1. Basal limestone breccias probably additionally eroded and subsequently filled the eastern paleotopographic low. 2. When the deposition of these beds ceased the western paleotopographic high still existed. 3. The remain-

ing depression was filled predominantly by hemipelagic and distal flysch deposits. The collapses of the paleotopographic slope of the area resulted in the formation of debris flow deposits (chaotic breccias) that occur near the slope within the distal flysch deposits. 4. Just before the paleorelief was levelled the new horizon of limestone breccias deposited predominantly in the western part of the area. 5. The following sedimentation of distal flyschoid deposits finally blanketed the paleorelief. 6. The flyschoid sedimentation was interrupted by two thicker intervals composed predominantly of limestone breccia and calcarenite. The lower interval deposited predominantly in the eastern part, whereas the upper was observed only in the western part of the area. Such a distribution presumably resulted from the westward migration of the supply channel for these deposits.

POVZETEK

Začetek maastrichtijske bazenske sedimentacije na Matajurju, SZ Slovenija

Z izsledki detajlnega kartiranja in starejših stratigrafskih raziskav na Matajurju smo prišli do naslednjih zaključkov:

- A. Na območju Matajurja je plitvodna karbonatna sedimentacija najverjetneje trajala večji del jure in je bila šele v pozni juri nadomeščena s pobočno sedimentacijo, pri kateri je bil odložen gomoljasti mikritni apnenec z gomolji roženca in vmesnimi kalkareniti.
- B. Na koncu albija je tektonska faza povzročila razkosanje pobočja z normalni-

mi prelomi, zaradi česar je prišlo do povečanega nagiba pobočja in posledične erozije oz. prekinitev sedimentacije.

- C. V poznem campaniju/zgodnjem maastrichtiju je nova tektonska aktivnost povzročila dodatno tonjenje območja Matajurja. Pred ponovno sedimentacijo je prišlo do nagiba tektonskega bloka proti zahodu in obstoja neravnega paleoreliefa. Paleorelief je bil položen z izjemo osrednjega dela kartiranega območja, kjer je strmejši del ločeval vzhodni (paleotopografski) nižji predel od zahodnega višjega predela.
- D. V maastrichtiju so se odlagali sedimenti zgornje flišoidne formacije. Zanjso značilne izmenjujoče se plasti apnenčeve breče, hemipelagičnih in flišnih sedimentov. Material apnenčevih breč je izviral iz rušeče se karbonatne platforme na jugu, medtem ko so flišni sedimenti prihajali s severa. Prepoznane so bile sledeče faze odlaganja: 1. Bazalne apnenčeve breče, ki so dodatno erodirale in zatem zapolnile paleotopografski nižji predel. 2. Ko se je odlaganje teh plasti zaključilo, je zahodni paleotopografski višji predel še vedno obstajal. 3. Preostala depresija je bila v glavnem zapolnjena s hemipelagičnimi in distalnim flišnimi sedimenti. Posledica rušenja paleotopografskega pobočja so sedimenti debritnih tokov (kaotična breča), ki se odložili znotraj distalnih flišnih sedimentov. 4. Tik pred izravnavo paleoreliefa se je pretežno na zahodnem delu območja odložil nov horizont apnenčeve breče. 5. Kasneje odloženi distalni flišoidni sedimenti so dokončno prekrili paleorelief. 6. Flišoidna sedimentacija je bila prekinjena z odložitvijo dveh debelejših intervalov sestavljenih pretežno

iz apnenčevih breč in kalkarenita. Spodnji interval je bil odložen v glavnem na vzhodnem delu, medtem ko najdemo zgornjega samo na zahodnem delu območja. Takšna porazdelitev je najbrž posledica migracije dovodnega kanala proti zahodu.

Acknowledgements

We would like to thank the lectors, Dr. Paul McGuinness (English part of the text), and Dr. Matej Šekli (Slovenian part of the text), and the reviser, Dr. Dragomir Skaberne, for their corrections.

REFERENCES

- BRADLEY, D.C., KIDD, W.S.F. (1991): Flexural extension of the upper continental crust in collisional orogens. *Geological Society of America Bulletin.*; Vol. 103, pp. 1416-1438.
- BUSER, S. (1985): *Rokopisna delovna karta merila 1:25.000 izdelana za Osnovno geološko karto SFRJ 1:100.000, list Tolmin in Videm (Udine)*. Geološki zavod Ljubljana, Ljubljana.
- BUSER, S. (1986): *Osnovna geološka karta SFRJ, Tolmač listov Tolmin in Videm (Udine)*. Zvezni geološki zavod, Beograd, 103 p.
- BUSER, S. (1987): *Osnovna geološka karta SFRJ 1:100 000, list Tolmin*. Zvezni geološki zavod, Beograd.
- BUSER, S. (1989): Development of the Dinaric and Julian carbonate platforms and the intermediate Slovenian basin (NW-Yugoslavia). In: Carulli, GB., Cucchi, F., Radizzani, CP. (eds.): *Evolution of the Karstic carbonate platform: relation with other periadriatic carbonate platforms. Mem. Soc. Geol. Ital.*; Vol. 40, pp. 313-320.
- BUSER, S. (1996): Geology of Western Slovenia and its paleogeographic evolution. In: Drobne, K. et al. (ed.): *The role of impact processes in the geological and biological evolution of planet Earth*. International workshop, September 27 – October 2, 1996, Postojna/Slovenia, pp. 111–123.
- BUSER, S., PAVŠIČ, J. (1978): Pomikanje zgornjekrednega in paleogenskega flišnega bazena v zahodni Sloveniji. *Zbornik radova 9. kongresa geologa Jugoslavije, Sarajevo 1978.*; pp. 399-419.
- CARON, M., COUSIN, M. (1972): Le sillon slovène: les formations terrigènes crétacées des unités externes au Nord-Est de Tolmin (Slovénie occidentale). *Bull. Soc. Géol. France.*; Vol. 14, pp. 34-45.
- CHANNELL, J.E.T., D'ARGENIO, B., HORVATH, F. (1979): Adria, the African Promontory, in Mesozoic Mediterranean Paleogeography. *Earth-Science Reviews.*; Vol. 15, pp. 213-292.
- COUSIN, M. (1970): Esquisse géologique des confins italo-yougoslaves: leur place dans les Dinarides et les Alpes méridionales. *Bull. Soc. Géol. France.*; Vol. 7 (XII), pp. 1034-1047.

- COUSIN, M. (1981): Les repports Alpes – Dinarides. Les confins de l' Italie et dela Yougoslavie. *Società Geologica du Nord.*; Publi. 5, Vol. 2 – Annexe, 521 p., Villeneuve.
- DIMITRIJEVIĆ, M.D. (1982): Dinarides: An Outline of the Tectonics. *Earth Evolution Sciences.*; Vol. 2, pp. 4-23.
- GAWLICK, H.J., FRISCH, W., VESCEI, A., STEIGER, T., BOHM, F. (1999): The change from rifting to thrusting in the Northern Calcareous Alps as recorded in Jurassic sediments. *Geologische Rundschau.*; Vol. 87, pp. 644-657.
- KARAMATA, S. (1988): ``The Diabase-Chert Formation`` some generic aspects. *Bulletin de l'Academis Serbe des Sciences et des Arts, Clase des Sciences naturelled et mathematiques.*; Vol. 95, pp. 1-11.
- KUŠČER, D., GRAD, K., NOSAN, A., OGORELEC, B. (1974): Geološke raziskave soške doline med Bovcem in Kobaridom. *Geologija.*; Vol. 17, pp. 426-476.
- MARTIRE, L. (1996): Stratigraphy, Facies and Synsedimentary Tectonics in the Jurassic Rosso Ammonitico Veronese (Altopiano di Asiago, NE Italy). *Facies.*; Vol. 35, pp. 209-236.
- MARTON, E., VELJOVIĆ, D. (1983): Paleomagnetism of the Istria Peninsula, Yugoslavia. *Tectonophysics.*; Vol. 91, pp 73-87, Amsterdam.
- MIKLAVIČ, B. (2007): *Pogoji nastanka piritnih in markazitnih konkretij na Matajurju*. Undergraduate thesis, Univerza v Ljubljani, Naravoslovnotehniška fakulteta, Oddelek za geologijo. 63 p., Ljubljana.
- PIRINI RADRIZZANI, C., TUNIS, G., VENTURINI, S. (1986): Biostratigrafia e paleogeografia dell' area sud-occidentale dell' anticlinale M. Mia – M. Matajur (Prealpi Giulie). *Riv. It. Paleont. Strat.*; Vol. 92/3, pp. 327-382, Milano.
- OTONIČAR, B. (2007): Upper Cretaceous to Paleogene forbulge unconformity associated with foreland basin evolution (Kras, Matarsko podolje and Istria; SW Slovenia and NW Croatia). *Acta Carsologica.*; Vol. 36/1, pp. 101-120, Postojna.
- PLACER, L. (1981): Geološka zgradba JZ Slovenije. *Geologija.*; Vol. 24/1, pp. 27-60, Ljubljana.
- PLACER, L. (1999): Contribution to the macrotectonic subdivision of the border region between Southern Alps and External Dinarides, Prispevek k makrotektonski rajonizaciji mejnega ozemlja med Južnimi Alpami in Zunanjimi Dinaridi. *Geologija.*; Vol 41, pp. 223-255.
- ROŽIČ, B. (2005): Albian - Cenomanian resedimented limestone in the Lower flyschoid formation of the Mt. Mrzli Vrh Area (Tolmin region, NW Slovenia). *Geologija.*; Vol. 48/2, pp. 193-210, Ljubljana.
- ROŽIČ, B., POPIT, T. (2006): Resedimented Limestones in Middle and Upper Jurassic Succession of the Slovenian Basin. *Geologija.*; Vol. 49, pp. 219-234.
- SAMIEE, R. (1999): *Fazielle und diagenetische Entwicklung von Plattform-Becken-Übergängen in der Unterkreide Sloweniens - PhD Thesis*. University of Erlangen, 185pp.

- ŠMUC, A. (2005): *Jurassic and Cretaceous Stratigraphy and Sedimentary Evolution of the Julian Alps, NW Slovenia*. Založba ZRC, 98 pp., Ljubljana.
- VRABEC, M., FODOR, L. (2006): Late Cenozoic tectonics of Slovenia: structural styles at the Northeastern corner of the Adriatic microplate. In: Pinter, N., Grenerczy, G., Weber, J., Stein, S. & Medak, D., Eds., *The Adria microplate: GPS geodesy, tectonics and hazards. NATO Science Series, IV, Earth and Environmental Sciences.*; Vol. 61, pp. 151-168.
- WINKLER, A. (1921): *Das mittlere Isonzgebiet*. Jb. Geol. B.A., Wien.

Analitical surface water forecasting system for Republic of Slovenia

Analitičen sistem napovedovanja pretokov površinskih vod v Republiki Sloveniji

GORAN VIŽINTIN¹, SANDI VIRŠEK²

¹University of Ljubljana, Faculty of Natural Sciences and Engineering, Aškerčeva cesta 12, SI-1000 Ljubljana, Slovenia; E-mail: goran.vizintin@ntf.uni-lj.si

²Agency for Radioactive Waste Management, Parmova ulica 53, SI-1000 Ljubljana, Slovenia; E-mail: sandi.virsek@gov.si

Received: September 21, 2007

Accepted: April 14, 2008

Abstract: River management is one of the key factors of environmental management.

On the territory of the Republic of Slovenia there are four main rivers (Mura, Drava, Sava and Soča) which drain water from the Alpine region in the north of the country and from a typically Karstic part in the south. It is a well known fact that all main Slovenian river flows can take a disastrous proportion in case of strong rain precipitation in their recharge area. For this reason the Environmental Agency of Republic of Slovenia (ARSO) put the hydrological monitoring system and data analysis in a common system known as HIDPRO. HIDPRO is a Slovenian acronym for Hydrological prognostic system. The main aim of Hydrological prognostic system is to analyze the collected data in an oracle database to make flow forecasts and take precaution measures against possible flooding whenever a worst case scenario is predicted.

Izvleček: Upravljanje z vodami je eden od ključnih faktorjev upravljanja okolja.

Na območju Republike Slovenije so štiri glavne reke (Mura, Drava, Sava in Soča), ki drenirajo vodo iz alpskega sveta na severu države in kraškega sveta na jugu. Znano je, da v primeru obilnega deževja na zbirnem območju, pretoki rek dosežejo vrednosti, ki lahko povzročijo katastrofalne hidrološke razmere. Zaradi tega je Agencija Republike Slovenije za okolje združila monitoring in obdelavo podatkov v skupni sistem imenovan HIDPRO. HIDPRO je slovenski akronim za Hidrološki prognostični sistem. Glavna naloga hidrološkega prognostičnega sistema je analiza zbranih podatkov v Oraclovi bazi in izdelava prognoze pretokov rek ter v primeru poslabšanja poplavne varnosti opozarjanje prebivalstva.

Key words: river prognostic system, database analysis, client server DSS, data classification, river flow forecasting

Ključne besede: rečni prognostični sistem, klient – server ekspertni sistem, klasifikacija podatkov, napovedovanje pretokov rek

INTRODUCTION

During the 1980s and 1990s a series of programmes for river data collection and analysis were being built in the former Hydrometeorological Institute of Slovenia. During that time data were being collected in an Oracle database. A collection of data measurements has been partly done by the observers on the field and partly by automatic gauging stations, which is also the case nowadays. The data collected in database were first stored inside the so-called rough database and after the validation process the data were transferred into a database and opened to the public. As the process of hydrology forecasting has to be done in real time, a series of FORTRAN programmes have been made. The operating system for FORTRAN made software was VAX. A great job was done by programming those FORTRAN programmes. But the main not-yet-solved difficulty was that the programmes were not directly linked to the Oracle database; even more – the data needed for hydrological records coming from weather forecasting super computer had to be put inside the FORTRAN made programmes manually. In addition the reports of final products were sent to the user partly electronically and partly manually. The FORTRAN programmes for hydrological forecasting were used until the end of the previous century. At the end of the last century a decision was made to form a new Hydrological forecasting and decision support system. The main aim was to make a programme system in Windows 2000/XP which would allow hydrologists to use the incoming data in real time and would also help them make a validation process before hydrological forecasting. The Hydro-

logical prognostic system (HIDPRO) was built during a period between years 2000 and 2002. The system was built in the Windows 2000/XP platform and the database Oracle was selected again. The system became operational in the year 2002 and is now the main forecasting and decision support system for hydrology in Slovenia.

REQUIREMENTS FOR THE HIDPRO SYSTEM

- For a new system replacement a series of demands were put together.
- Data have to be stored inside Oracle database.
- All data coming from different sources have to be transferred in the system automatically.
- Validation of data has to be done during the process of data transfer from the measurements stations to the Oracle database.
- The hydrologist has to have the possibility to check and change the data during the entire process of forecasting.
- The system has to provide a series of automatic reports for different users (government's offices, newspaper, TV, radio etc.).

On the basis of demands shown above and operating systems used in the government's offices a client server application (Figure 1) was selected for the Hydrological Prognostic System (HIDPRO). This firstly means that data are stored inside the oracle database and secondly that programmes for the data management are made with MS Access XP development programme Visual basic for the Application. The decision to adopt MS Access XP was also made on the basis that people working in hydrology

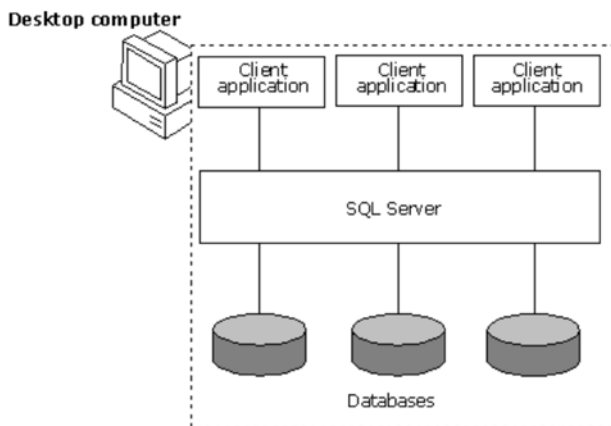


Figure 1. Diagram of HIDPRO client server architecture
Slika 1. Diagram HIDPRO server – klient arhitekture

prognosis are very well acquainted with MS Access and MS Excel.

DATA FLOW AND ANALYSIS

For a smooth flow of data between different sources and real time validation one has to know a data flow diagram very well. Figure 2 presents a data flow diagram with all check points of automatic validation and phases of hydrology forecasting and decision support system. The detailed look at the data flow diagram (Figure 2) can show there are two very important steps: the first step is the automatic analysis of data coming from automatic gauging station. The analysis in use for this step is only to control the data; if the data are erroneous on a large scale, they are not to be transferred to the rough data of AMP database. The data

coming from the gauging stations are the observed river level in centimetres and the river water temperature.

A quick check of data can show if the measurements are inside the logically expected values or not. In case of error detection a numerical value for a type of error is transferred into the database instead of the erroneous value. If the data pass the first check, the river level values are transferred in the rough database of automatic measurements (AMP database). For the hydrology forecasting a data transformation is needed; therefore the water river level data are transformed in the river flow data (Figure 2). The process is done inside the rough AMP database. The data are transformed on the basis of step polynomial functions of high order (Equation 1) which coefficients are obtained by the regression.

$$q = \left\{ \begin{array}{l} 96cm \leq h < 110cm \Rightarrow 0.103370E - 04 + h 0.866970E - 03 + h^2 0.225364E - 07 + h^3 0.504223E + 01 \\ 110cm \leq h < 180cm \Rightarrow 0.140766E - 04 + h 0.200405E - 02 - h^2 0.148332E - 05 - h^3 0.139660E + 02 \\ 180cm \leq h < 290cm \Rightarrow 0.639307E - 05 + h 0.392923E - 02 + h^2 0.518343E - 06 - h^3 0.314814E + 02 \\ 290cm < h < 450cm \Rightarrow -0.853863E - 05 + h 0.100931E - 01 - h^2 0.144057E - 05 - h^3 0.186105E + 03 \\ 450cm < h < 540cm \Rightarrow -0.714420E - 05 + h 0.879800E - 02 + h^2 0.500243E - 06 - h^3 0.500243E - 06 \end{array} \right. \quad (1)$$

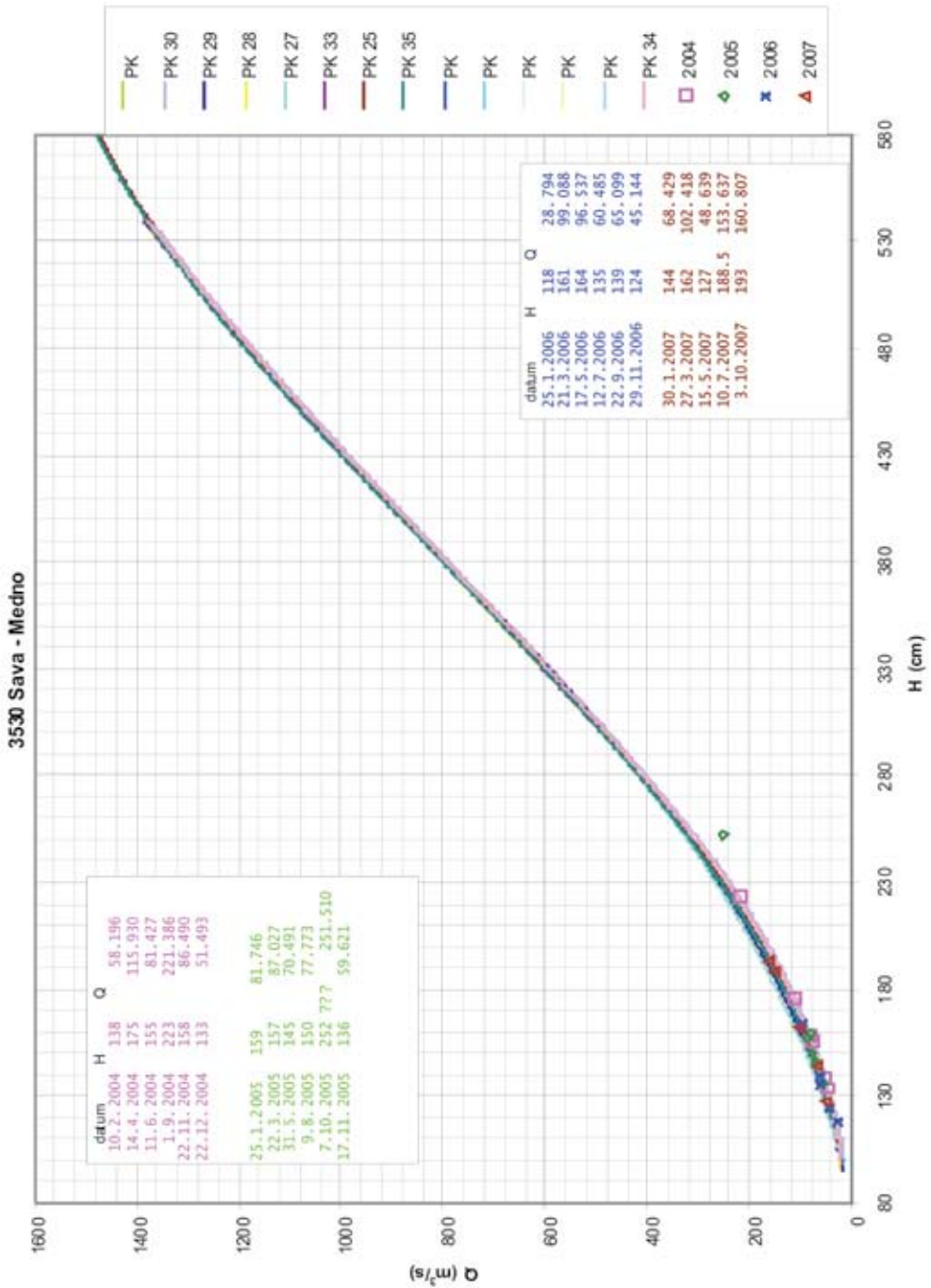


Figure 2. Typical H-Q curve fitted using step polynomial equations
Slika 2. Tipična H-Q krivulja določena z množico polinomskih funkcij

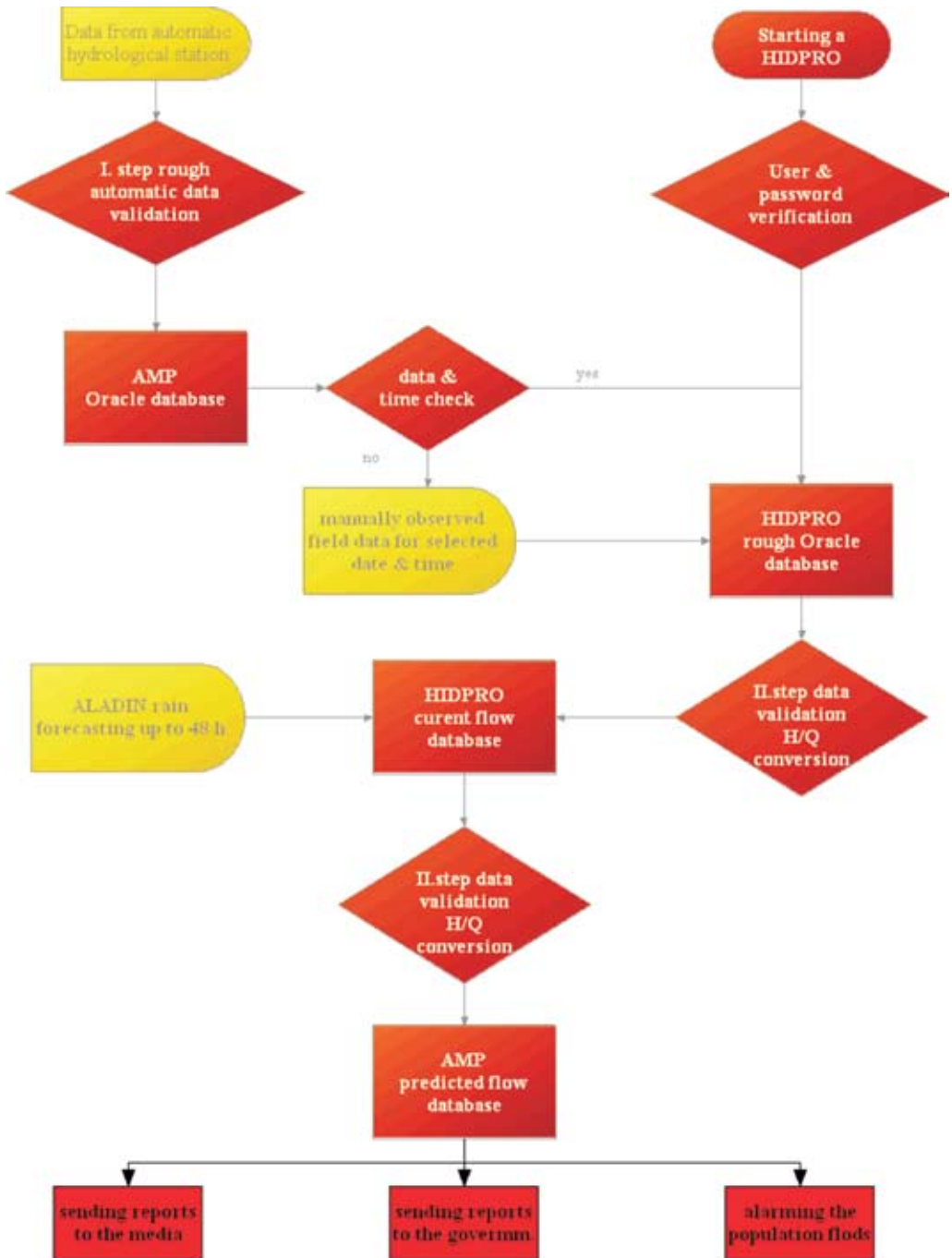


Figure 3. Data flow diagram of HIDPRO
Slika 3. Diagram toka podatkov v HIDPRO-ju

For this, transformation calibration measurements are needed on the river. Due to erosion and sedimentation inside the rivers, this is an ongoing process which means that the calibration can not be done once but has to be repeated in certain time intervals. Thus the time intervals for transformation function are an important key in flow calculations. The function duration is checked during the flow calculation and in case of finding the function out of date, a typical numerical value is shown. This means that the hydrologist himself is able to see the values and on its basis he can inform a technical support team about the problem with the water level – water flow conversion. The out-of-date check process is impeding erroneous calculations of flow from river's water levels, which can be a result of natural changes in river.

As it can be seen on the data flow chart (Figure 3), some measurements are coming from the field observation made manually. There are still series of gauging station which are not equipped with the automatic water level and temperature measurements devices. There are also some controlling measurements on the automatic gauging station which are performed by people under contract. If data sets from the stations are erroneous, data from manual measurements can be used. A special situation occurs when the automatic station is making good measurements but data are not shown for a certain period of time; in such a case a station has to be moved from the automatic station set to a manual station set. The time limit is set up to 2 hours from the time of making a prediction (Figure 4).

There are three important buttons shown on Figure 4:

- Klicane (Calling)
- Zlitja (Conjunction)
- Napoved (Forecast)

The “Klicane” button allows access to the manually measured hydrological station and the automatic gauging stations with 2 hours data missing gap. Button “Zlitje” has to be pressed after entering manual data, thus connecting it with automatic data (Figure 5).

Different coloured cells show unusual condition: if the flow is too low, a green colour is used and if the flow is statistically too high, a red colour is shown. On the basis of colours the hydrologist has the first information of the hydrological situation in the country. A tendency of river flow is also tested: if a river flow tendency is increasing, the sign + is selected; for decreasing, the sign – is selected; and for steady hydrological situation on the gauging station, the sign 0 is shown. The estimation of river flow tendency is possible only in the automatic stations. A statistical approach was selected to classify the two hydrological parameters mentioned before. This means that a statistical table of hydrology seasons characteristics values was made and put in the database for river flow classification. The current calculated flow is compared with the values stored for specific stations in the table mentioned before and if needed, a colour is used to show the actual hydrological situation. The hydrological season's table stores data from statistical analysis of every station and a

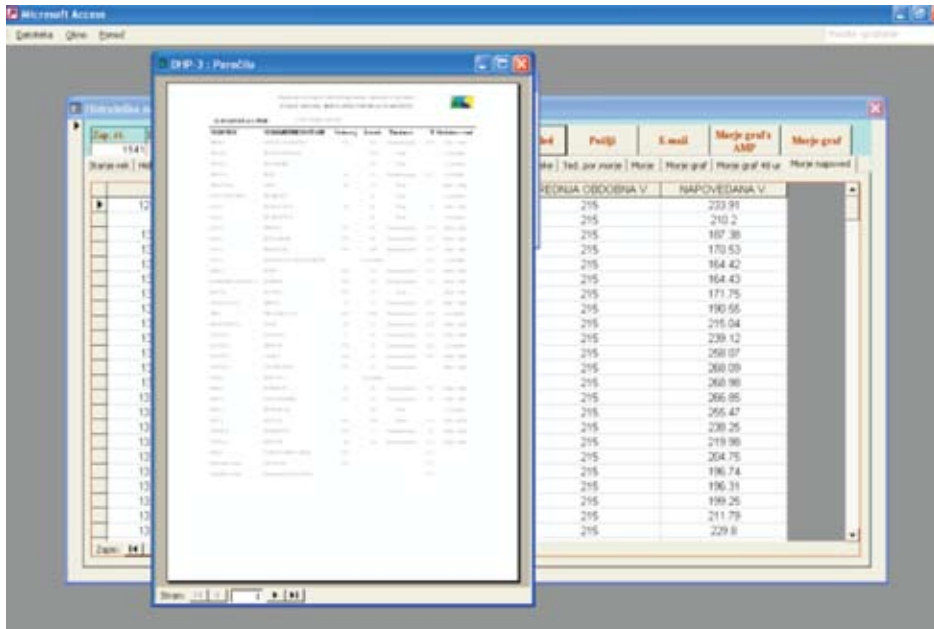


Figure 6. The last forecasting form with all data necessary for hydrological forecasting
Slika 6. Zadnji napovedni obrazec z vsemi potrebnimi podatki za hidrološko napoved

long time data sets are usually used for statistical data calculations. The tendency is to only check if the values in the last half hour have changed; this is made by using a simple mathematical equation where the average value of last half hour is compared with the actual value. If a positive or negative change greater of 10 percent is detected, then a sign of + or – is selected for presentation. If the changes are less than 10 percent a 0 sign is used.

After all hydrological data are available, the last step can take place. By pressing button “Napoved” (see Figure 4), all data are transferred to the forecasting table (Figure 6). During this process data from weather forecasting are put inside the hydrology forecasting table. Two forecast precipitations data are available. They are the 24 and the 48 hour rain precipitations.

The data are calculated for the rain fall precipitation’s stations, by using the analytical model of hydrological prediction to calculate the flow for the next 24 or 48 hours. The calculated values are compared to the hydrological season’s characteristic values; on the basis of this the warnings to the water authority are dispatched.

The river flow prediction is made on the basis of predicted rainfalls for a certain rain measuring station and correlation between the rain and hydrology stations. The correlation or better dependency of river flow on the hydrological station is mainly described with the elementary mathematical functions. In some cases the dependency is described with the mathematical function with predicted precipitations values from the program ALADIN only for the first station in a set of stations on the same

river. For all other stations of the same set the prediction is made on the basis of correlation between the river flow on the predicted station and the river flow on the previous station.

CONCLUSIONS

The HIDPRO system became fully operational in 2003. Since then, all the hydrological forecasting operations and warnings for high or low river flow have been made on it. The biggest progress is that all data coming from different sources are stored in the same database and logical operations are available for quick data checking; a hydrologist can also check the data after the automatic data checking. The main data flow occurs inside the Oracle database and data from some operational stages are always available to the registered users. A lot of work has been done by transferring the ASCII stored data with Visual Basic procedures to the ARSO net. The main problem was that data structured in ASCII formats was quite difficult to understand, thus there had to be a lot of cooperation between the programmers and developers on one side and the hydrologist and meteorologist on the other side. The problems with data gap, which can occur due to specific meteorological or hydrological conditions, were solved with the procedure of the 2-hour data check. There are also some visual data presentations for hydrologist available and the possibility of human data checking and repairing the erroneous data is always possible. The three step data analysis and checking reports are available to the media and governments offices. In a case of high river flow, the government service respon-

sible for flood alarming is called. Further developments will try to make a connection between numerical river flow prediction modelling and data stored inside the database, thus gradually replacing analytical modelling with the numerical one.

Acknowledgments

The authors are indebted to Mira Kobolt, Mojca Sušnik, Janez Polajnar and Jože Guši Miklavčič for their help in explanations of the hydrological formulas and models.

POVZETEK

Analitičen sistem napovedovanja pretokov površinskih vod v Republiki Sloveniji

Na območju Republike Slovenije so štiri glavne reke (Mura, Drava, Sava in Soča), ki drenirajo vodo iz alpskega sveta na severu države in kraškega sveta na jugu. Znano je, da v primeru obilnega deževja na zbirnem območju, pretoki rek dosežejo vrednosti, ki lahko povzročijo katastrofalne hidrološke razmere. Zaradi tega je Agencija Republike Slovenije za okolje združila monitoring in obdelavo podatkov v skupni sistem imenovan HIDPRO. HIDPRO je slovenski akronim za Hidrološki prognostični sistem. Glavna naloga hidrološkega prognostičnega sistema je analiza zbranih podatkov v Oraclovi bazi in izdelava prognoze pretokov rek ter v primeru poslabšanja poplavne varnosti opozarjanje prebivalstva. Med letoma 1980 in 1990 je bila na nekdanjem Hidrometerološkem za-

vodu Republike Slovenije izdelana serija programov za zbiranje in obdelavo hidroloških podatkov. V tem času so se zbrani podatki hranili v Oraclovi bazi. Podatke so že takrat zbirali z opazovalci na terenu in z avtomatskimi hidrološkimi merilnimi postajami. Tako zbrani podatki so se hranili v bazi neobdelanih podatkov, po pregledu oz. obdelavi podatkov so bili podatki preneseni v bazo podatkov in s tem dostopni širši javnosti.

Ker je za napovedovanje hidrološkega stanja potrebna obdelava v realnem času, je bila izdelana serija programov v FORTRAN-u. Za osnovni operacijski sistem je bil izbran VAX. Glede na obseg dela, ki ga je tako programiranje zahtevalo, lahko sklepamo, da so takratni programerji opravili zahtevno delo. Kljub temu je glavni problem ostal nerešen, saj podatki med FORTRAN-novimi programi in ORACLOM niso bili povezani in celo vremenske podatke izračunane na super računalniku je bilo potrebno ročno prenašati najprej v ORACL in nato še v FORTRAN-ove programe. Zaradi tega je bil med letoma 2000 in 2003 izdelan nov hidrološki prognostični sistem. Sistem je bil izdelan na Windows2000/XP platformi, hramba podatkov pa je bila spet zaupana ORACLU. Sistem je postal operativen v letu 2003 in ja ta trenutek edini prognostični hidrološki sistem z elementi ekspertnega sistema podpore odločanja na območju Republike Slovenije. Največji napredek je, da so vsi podatki, ki prihajajo iz različnih virov, sedaj hranjeni na istem mestu. V sistemu je vgrajena serija logičnih funkcij, ki omogočajo avtomatsko kontrolo podatkov in so po potrebi lahko tudi še neodvisno kontrolirani s strani ekspertov prognostikov.

Glavni pretok in obdelava podatkov se dogaja znotraj ORACLA, ki hkrati omogoča dostop do obdelanih podatkov prijavljenim uporabnikom. Veliko dela je bilo opravljeno za izdelavo procedur v Visual Basicu za prenos podatkov iz ASCII datotek na ARSO omrežje. Glavna težava je bila, da je bila struktura ASCII formatov relativno zapletena, zaradi česar je bila potrebna dobra sodelava med razvijalci sistema in hidrologi prognostiki. Problem izpada podatkov, ki se lahko pripeti med neugodnimi vremenski pogoji, je bil rešen z izdelavo posebnih programskih kontrolnih procedur. Obenem pa so hidrologom na razpolago številna orodja za vizualno prezentacijo in možnosti številnih kontrol in popravljanj obdelanih podatkov.

REFERENCES

- [1] JERKE, N. (2003): *Microsoft Office Access 2003 Professional Results*. Mcgraw-Hill Osborne Media, 400p.
- [2] KYTE, T. (2005): *Expert Oracle Database Architecture: 9i and 10g Programming Techniques and Solutions*. Apress, 768p.
- [3] NAZARETH, J. L (2001): *DLP and Extensions: An Optimization Model and Decision Support System*. Springer, 207p.
- [4] POWER, J.D (2004): *Decision Support Systems: Frequently Asked Questions*. iUniverse, Inc., 252p.
- [5] SAUTER, L. (1996): *Decision Support Systems: An Applied Managerial Approach*. Wiley, 408p.
- [6] TURBAN, E. (2004): *Decision Support Systems and Intelligent Systems*. Prentice Hall, 960p.

Rodoretto talc mine (To, Italy): studies for the optimization of the cemented backfilling

DANIELE PEILA^{1,2}, CLAUDIO OGGERI¹, PIERPAOLO ORESTE¹, SEBASTIANO POLIZZA¹,
FRANCO MONTICELLI³

¹DITAG-Politecnico di Torino, Italy; E-mail: daniele.peila@polito.it,
claudio.oggeri@polito.it, pierpaolo.oreste@polito.it, sebastiano.pelizza@polito.it

²IGAG, CNR (National Research Council of Italy), Torino, Italy;

E-mail: daniele.peila@polito.it

³Rio Tinto Minerals-Luzenac Val Chisone, Porte, Italy;

E-mail: franco.monticelli@riotinto.com

Received: November 14, 2007

Accepted: April 8, 2008

Abstract: The underground talc mine of Fontane (Prali, near Torino, North West of Italy) has been exploited for decades by conventional cut and fill method using loose fill and, in the last 30 years, using cemented backfill and exploiting the orebody downwards. With this exploitation approach, the orebody recovery and the safety of the mining operations have been greatly improved. In the new mine section, located in Rodoretto, a detailed numerical modelling has been carried out to simulate the various geometrical and mining conditions and the fill properties. In the meantime an experimental research carried out to check the possibility of using the waste rock for the fill mix have been carried out in order to establish a procedure able to reduce the filling costs.

Key words: mining, stability, backfill, numerical modelling, rock mechanics

INTRODUCTION

The underground talc mine in Fontane (Prali, near Torino, North West of Italy) has been exploited for decades by conventional cut and fill method using loose fill and, in the last 30 years, using cemented backfill and exploiting the orebody downwards (DEL GRECO & POLIZZA, 1984; DEL GRECO et al., 1976, 1989; POLIZZA et al., 1990). With this exploitation method the orebody recovery and the safety of the mining operations have been improved.

The Rodoretto section of Fontane mine is the only one that is at present active in the area and in the Southern zone it is made of a talc mass which is located at a depth of about 400 m. The orebody is exploited on subhorizontal levels about 4 m high moving downwards and each level is mined with the excavation of sub-parallel drifts (ranging from 3.5×3.5 m to 4×4 m) excavated from the footwall to the hanging wall of the orebody, and only backfilled with cemented fill before the lower slice is started to be exploited (Figure 1). The



Figure 1. View of a drift supported by timber sets and hydraulic (arrows) and mechanical props

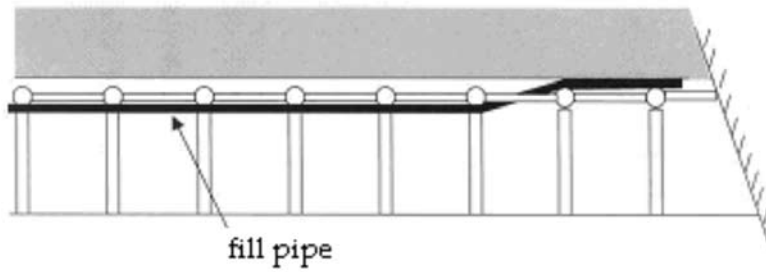


Figure 2. Scheme of the filling of a drift and photograph of a drift ready to be filled, where an impervious membrane has been installed to protect the not yet mined talc against pollution

used cemented fill is a concrete with a low compressive strength, but high workability. Due to the orebody geometry and the rock mass properties it is necessary that the cemented fill has mechanical properties that are able to control the deformation of the talc and of the embedding rock and to guarantee that the drift roof is stable in order to reduce the supports and to enlarge to the drift size, thus reducing the excavation costs and improving the profitability of the mining activity. The backfill is put in place through a HDPE pipe installed on the top of the drift using a standard concrete pump and it is carried by a mixer or from a centralized pumping station, with a pipe line that reaches the drifts of each level through the ramp and some especially excavated shafts (Figure 2).

In order to achieve these goals, the stresses induced in the embedding rock masses, in the talc and in the cemented fill, while the exploitation proceeds, were studied through numerical modelling. The possibility of using the mine waste rock as cemented fill aggregates was also examined through laboratory tests.

During excavation, the drifts are supported with timber sets (Figure 1) when there are relevant loads (for example in the first level or when the excavation in the drift is out of the backfilled area due to the orebody geometry) or with mechanical or hydraulic props when the roof is more stable, that is, below the cemented fill.

A correct study for the optimization of the fill properties must take into account both the global stability of the whole mine panel and the stability of the drift roof when the

excavation is carried out in the lower level and this was carried out with a numerical model that is able to simulate the development of the exploitation of the whole mine.

GEOLOGICAL ENVIRONMENT

The geological environment of the Germanasca Valley records the complex structural history of a portion of the paleo-european continental margin, composed of a metamorphic Paleozoic basement covered by both continental and shallow water marine deposits. The Alpine orogenesis disrupted and relocated the original environments by creating a complex nappe structure with a wide variety of structural and petrological features.

The Germanasca Valley extends for an important part of its length along the contact between the Ophiolitic oceanic complex, better known as “Calcescisti (or Piemontese) nappe” and the continental domain known as “Dora Maira massif”.

Most of the existing and exhausted talc mines are distributed along this tectonic contact, hosted in the silicatic metamorphic rocks belonging to the upper part of the Dora Maira massif. According to the traditional geological approach, the geologic framework can be subdivided into two main units, from East to West:

- Brianzonese Unit (Permo-Carboniferous) composed of two distinct complexes:
 - Faetto and Pinerolo Complex: fine gneisses and micaschistes of detritic

sedimentary origin frequently graphite rich, with quartzite and metabasites inter-layers;

- Freidou Complex: augen-gneiss, probably representing the bedrock of the previous complex, outcropping inside the former as folded layers.
- Piemontese Unit (Mesozoic) also composed of two distinct complexes:
 - Dora-Maira Unit: garnet-chloritoid micaschistes, with gneiss, white banded marble and metabasites;
 - Calceschists and ophiolite nappe: calceschists with interlayered marble and metabasites (ophiolites).

All the previously mentioned units are visible along the Germanasca Valley, from the junction with the Chisone Valley going back up to higher elevations. The mine sites are hosted in the garnet micaschistes of the Dora-Maira unit. Several mines were exploited in the past and just one, the Fontana mine in the Rodoretto section is still active. As a general features, the white talcschist which constitutes the most part of the orebodies, shows an evident field association with the banded marble and the gneisses. The structural history and the origin of the talc is still a matter of debate and would seem to extend back in time even before the alpine orogenesis. The recent metamorphism, ductile folding and shear events associated with the formation of the Alps have overprinted the older phases and are responsible for the present structural environment where the talc can be found. The different mine (and orebody) geometries show that the economic resource concentrations are closely linked to the folding phases which created the conditions for the talc redistribution in

the space and its accumulation in defined masses. In the past, thin layers were also exploited and the mining records show that panels of a thickness of less than one meter were extensively mined but recently most of the exploitation was progressively been relocated to the thicker masses, for economic and productive reasons, as is the case of the Rodoretto section.

NUMERICAL MODELLING AND GEOMECHANICAL CHARACTERIZATION

Introduction

Starting from the study of the geomechanical properties of the rock mass (talc and embedding rock) many different numerical models were developed with the finite difference code FLAC^{2D} (ver. 4.0, Itasca). The numerical models were set up with the purpose of simulating the exploitation of the whole panel made of seven levels in the south-Rodoretto mine (Figure 3). The influence of various fill conditions: mechanical properties and complete or incomplete backfilling of the drifts and of different natural stress conditions were also investigated.

Modelling strategy and input data

The adopted modelling sequence (DEL GRECO et al., 1990; PEILA et al., 1994; POLIZZA et al., 2000) consists of the following steps:

- [1] excavation of the ramp tunnels;
- [2] exploitation of the first level by modelling the excavation of the various drifts (which cross the model in a transversal direction), the supporting of the drifts with timber sets, and backfilling after the excavation of the adjacent drift;

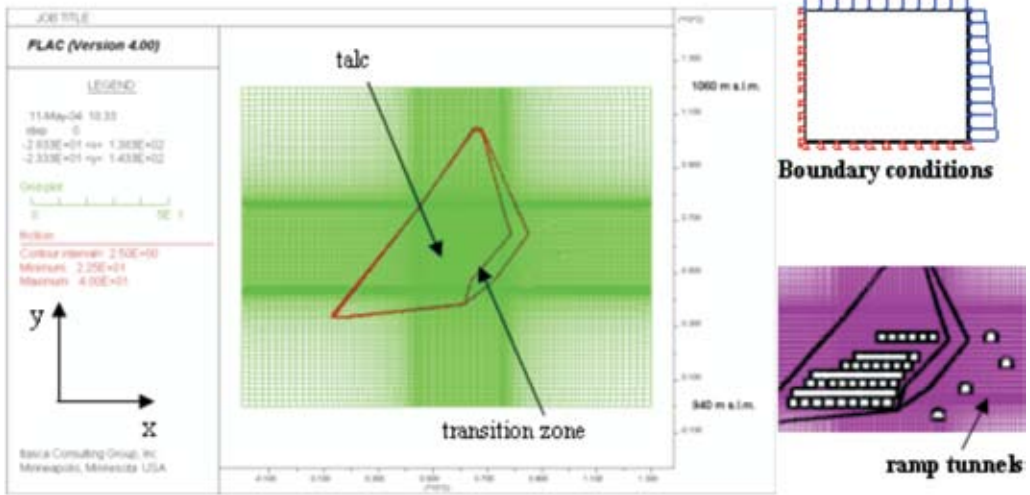


Figure 3. Global view of the geometry of the Rodoretto orebody and the numerical model (the red lines indicate the boundary of the various materials) the applied forces and the exploited levels. The transition zone represent a weak geomechanical section which consists of chaotic rock mass with talc veins, gneiss and marble. The model is 150 m wide and 120 m high.

- [3] exploitation of the second level by modelling the excavation of the drift which crosses the model in a longitudinal direction, the supporting of the drift with timber sets and backfilling at the end of the excavation;
- [4] repetition of points [2] and [3] till the end of the exploitation of the 7th level.

The research was developed in three different steps:

- [1] development of a set of preliminary models which were set up to define the minimum acceptable strength of the fill, taking into account the complete backfilling of the drifts;
- [2] development of more refined models which were set up to study the mine condition when the drifts are not completely backfilled, as frequently occurs in the mine, but taking into account

the fill strength defined in the first set of models. A value of 20 % of contact zones was considered;

- [3] an analytical analysis of the stability of the drift roof, taking into account the loads which were computed in the numerical modeling and using simplified analytical approaches such as a cantilever beam or the arch model (OBERT & DUVALL, 1967) to verify whether the stability of the fill is ensured by the strength of the fill. In order to simulate the drift excavation advancement, an internal fictitious pressure was applied to the excavation boundary nodes and this pressure was reduced to 70 % before the supports were installed (ORESTE, 1999) and reduced to zero to simulate the final excavation of the drift. Another relevant problem for a correct modelling was the definition

of the natural state of stress in the orebody, due to the geometrical and geomechanical complexity of the talc orebody and of the embedding rock and of the embedding rock and to the absence of measured data. For this reason, in the first step of numerical modeling, k_0 (the ratio between the vertical and horizontal natural state of stress) was assumed to be equal 1, while in the second step of the modelling, the stress redistribution due to the difference in deformability between the talc and the embedding rock was taken into account, as suggested by JEREMIC (1987) and by AMADEI & STEPHANSSON (1997). This computation made it pos-

sible to see that an important arch effect had developed in the embedding rock (more rigid) and a reduction in the stresses in the talc was observed (Figure 3).

Geomechanical characterization

The geomechanical properties assumed in the model (Table 1) were evaluated through a series of laboratory tests and from the rock mass characterization in the mine drifts and mine tunnels, which allowed a RMR of 60 to be obtained for the embedding rock (micaschistes and gneiss) and a RMR of 35 for the talc mass.

From this characterization, the geomechanical properties were defined (BIENIAWSKI, 1989; BRADY & BROWN, 1985; HOEK, 2000; HOEK, CARRANZA-TORRES & CORKUM, 2002). The stress-strain law was an elastic ideally plastic law and the yielding criterion was the Mohr-Coulomb one. The fill properties used in the models was defined starting from the admissible uniaxial compressive strength which is the parameter that can be easily controlled in the mine. Two different values were considered in the first set of the models: 10 MPa (type 1) and 6 MPa (type 2). Only the type 1 was applied in the second set.

Numerical modelling results

The results obtained with the first set of numerical models show that the type 1 fill allowed a stable condition of the mine and the embedding rock mass to be obtained, even though, a wide plasticization of the orebody mass was present after the exploitation of the seven levels and high stress values are located around the ramp tunnels

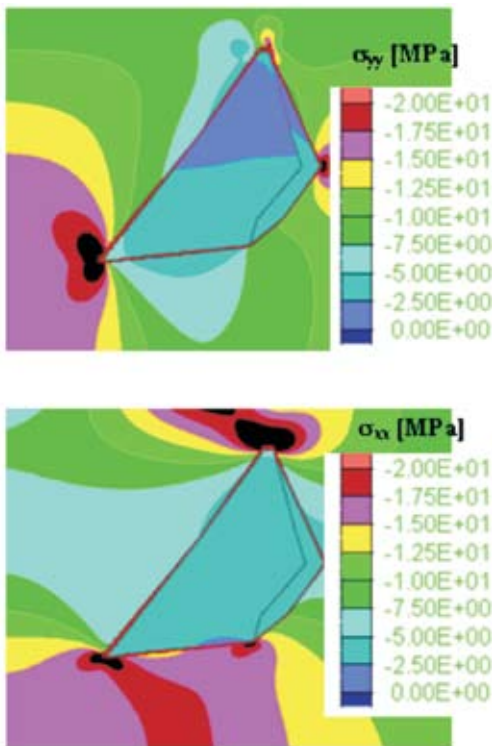


Figure 4. Computed undisturbed stresses taking into account the deformability of the talc and of the embedding rock

Table 1. Geomechanical parameters of the rock mass used in the model

Geomechanical property	Embedding Rock mass	Talc	Transition zone
Density [kg/dm ³]	2.6	2.75	2.6
Deformability modulus [MPa]	13300	860	670
Poisson ratio [/]	0.28	0.25	0.4
Peak cohesion [MPa]	4	0.18	0.2
Peak friction angle [°]	48.5	16	25
Dilatance [°]	0	16	25

and in the hanging wall near the 6th and 7th levels. In these models, the fill is mainly under compressive stresses. The type 1 fill is elastic throughout while the type 2 fill induces plastic zones in the 1st-5th levels and this can be an index of local stability problems during exploitation. The computed vertical displacements in the 1st and 2nd levels were larger than 1 m and these values are larger than those observed in other mine sectors.

This result allows to say that the chosen natural stress:

$$\sigma_v = \gamma \cdot h \text{ and } k_0 = 1$$

was probably too high to correctly model the Rodoretto mine. Therefore of models was developed to take into account the influence of the embedding rock mass and talc deformability on the natural stresses and the incomplete backfilling of the drifts. In the second set of models, the computed vertical displacements of the first level were 30-50 cm, at the end of the exploitation (Figure 6) and were consistent with the in situ observations in the other sections of the mine where the vertical displacements of the drifts during the development of the

mine was never larger than 50 cm. To verify this data a sub-horizontal assestometric device (29 m long) was installed in a drift at the 5th level. During the passage of the first drifts at the lower level a deflection of 15 cm has been measured in the middle of the drift.

This model was, therefore, chosen as the reference one and it was used to define the stresses acting in the fill and around the mine infrastructures:

The maximum vertical stresses acting in the contact points of the fill between the levels at the end of the exploitation were: 1st level: 3.0 MPa; 3rd level: 2.8 MPa; 5th level: 2.5 MPa; 7th level: 1.6 MPa. These values are lower that the admissible fill strength;

- the plastic zones in the fill and around the mine ramp are very small. The plasticity could only be critical around the lowest part of the ramp where it could easily be controlled by tunnel supports, such as bolts and/or steel arches;
- the stresses acting in the hanging wall and around the mine ramp did not induce critical conditions except for a vertical stress concentration between the upper portion of the ramp and the orebody.

Analytical model of the fill

The analytical models which were adopted to verify the local stability of the fill when mining a drift below a filled drifts were developed with the hypothesis that:

- the filled drift work as a loaded thick cantilever beam or as an arch of independent elements (OBERT & DUVAL, 1957), (Figure 7);
- the load computed with the second set of numerical models, was applied onto the beam: 1 MPa when the upper 3 levels are considered and 0.5 MPa for the other levels.

It was possible to verify that for a uniaxial compressive strength of 10 MPa for the fill, the drift could be 6.5 m large with a load of 1 MPa and 9 m large with a load of 0.5 MPa.

CONCLUSIONS

The Fontane mine (Prali, near Torino in the North-West of Italy) has used a cut and fill descending slices with the cemented fill since 1974. When the new Rodoretto orebody was started to be exploited, a detailed numerical study was focused on the definition of the minimum acceptable strength of the fill and a laboratory test campaign was conducted to verify the possibility of using the mine wastes. The analytical and numerical modelling results suggested that, to guarantee the stability of the filled drifts, when excavating downwards and to maintain adequate stability conditions of the whole orebody and mine infrastructures, the compressive strength of the fill should be no less than 9-10 MPa and that the length of the unsupported filled drift

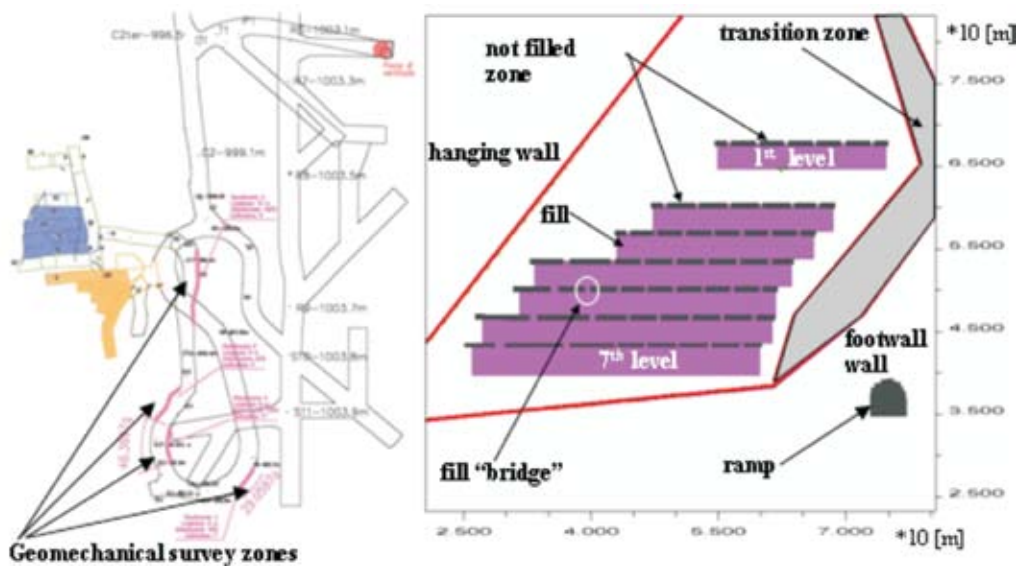


Figure 5. Plan of the south Rodoretto mine with indication of the filled drifts (1st and 2nd levels) in May 2003 and with the position of the geomechanical survey along the mine ramp (on the left) and the scheme of the partial filling of the mine adopted in the second set of numerical models (on the right)

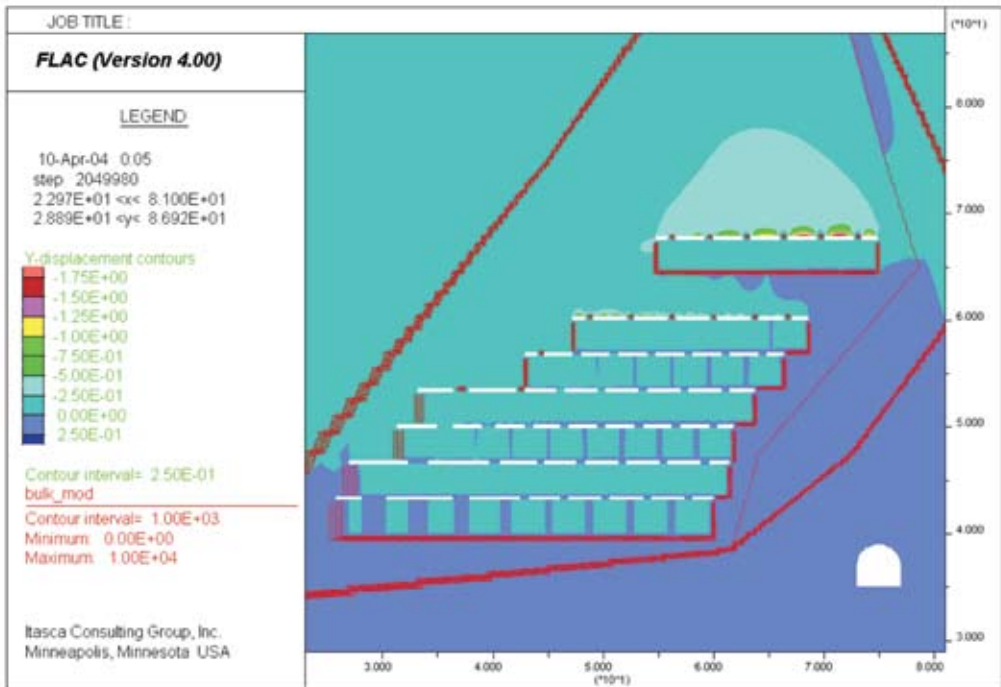


Figure 6. Vertical displacements at the end of the exploitation in the second set of models with a type 1 fill. Vertical displacement of the alignment AA at different distances (d) from the roof of the 1st level – the positive displacement (δ_{yy}) are in the direction of the arrow.

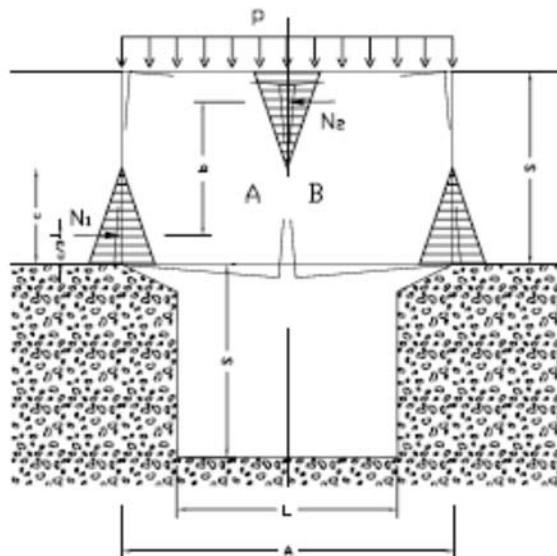


Figure 7. Analytical scheme of the arch made up of independent elements

below the backfilled drifts should be no longer than 6 m.

The stability of the levels was also checked by some topographical measurements and the monitoring of a cemented drift by an assestimetrical device which gave results in good agreement with the numerical modelling.

REFERENCES

- AMADEI, B., STEPHANSSON, O. (1997): *Rock Stress and its measurements*. London, Chapman & Hall.
- BIENIAWSKI, Z. T. (1989): *Engineering Rock Mass Classification*. New York, Wiley.
- BRADY, B., BROWN, E. (1985): *Rock Mechanics for Underground Mining*. London, George Allen & Unwin.
- DEL GRECO, O., POLIZZA, S., SARTORIO, P., STRAGIOTTI, L. (1976): Coltivazione con ripiena cementata nella miniera di talco di Fontane. *Bollettino dell'Associazione Mineraria Subalpina.*; Vol. XIII, Torino, GEAM (in Italian).
- DEL GRECO, O., POLIZZA, S. (1984): The underground Fontane Talc Mine: main characteristics of the deposit and exploitation methods. *Bollettino dell'Associazione Mineraria Subalpina.*; Vol. XXI, Torino, GEAM, pp. 85-92.
- DEL GRECO, O., PATRUCCO, M., POLIZZA, S. (1989): La miniera in sotterraneo di talco di Fontane: caratteristiche del giacimento, metodi di coltivazione, impiantistica. *Bollettino dell'Associazione Mineraria Subalpina.*; Vol. XXVI, Torino, GEAM, pp. 415-430 (in Italian).
- DEL GRECO, O., GIANI, G.P., PEILA, D., STRAGIOTTI, L. (1990): Analysis of three mining methods for the exploitation of a vein in a deep mine. *Mineral Resources Engineering.*; Vol. 3, No. 4, London, Taylor & Francis, pp. 267-280.
- HOEK, E. (2000): *Practical Rock Engineering*. Available on www.rocscience.com.
- HOEK, E., CARRANZA-TORRES, C., CORKUM, B. (2002): *Hoek-Brown criterion, 2002 edition*. Proc. NARMS-TAC Conference, Toronto.
- JEREMIC, M. L. (1987): *Ground mechanics in hard rock mining*. Rotterdam, Balkema.
- OBERT, L., DUVAL, W. (1967): *Rock mechanics and the design of structures in rock*. New York, Wiley.
- ORESTE, P.P. (1999): *Aspetti notevoli dell'analisi di dimensionamento dei sostegni delle gallerie attraverso i metodi di calcolo numerici*. Gallerie e grandi opere sotterranee, Bologna, Patron 57.
- POLIZZA, S., FERRERO, A.M., CAROSSO, G., PEILA, D. (1990): Improvement of exploitation methods in two Italian talc mines. *III Congresso Suramericano de Mecanica de Rocas*. Caracas, pp. 575-585.
- PEILA, D., ORESTE, P.P., POLIZZA, S. (1994): Analysis of mine exploitation using partial cemented-fill methods in a sub-horizontal layer. *EMC'94*. Dresden, pp. 93-104.

Determination of environmental criteria for estimation of land development using GIS

Uporaba GIS-a za določitev naravnih kriterijev možnosti okoljskega razvoja

GORAN VIŽINTIN¹, LIDIJA STEVANOVIC¹, ŽELJKO VUKELIČ¹

¹University of Ljubljana, Faculty of Natural Sciences and Engineering, Aškerčeva cesta 12, SI-1000 Ljubljana, Slovenia; E-mail: goran.vizintin@ntf.uni-lj.si, lidijas@gmail.com, zeljko.vukelic@ntf.uni-lj.si

Received: October 12, 2007

Accepted: June 9, 2008

Abstract: It is well known that GIS techniques are very useful in the environmental control and planning operation. According to actual environmental law in Slovenia all main human impacts on the environment have to be revised and independently checked. The processes of revising and checking are mainly made by hand review and subjected to the subjective evaluation. In many cases the revisers are subjected to criticism that their decisions were not strict and correct enough. For these reasons it is necessary to use independent tools. GIS techniques are one of the possibilities, which can make the decisions and evaluations of the verified human impact on the environment much faster and not as subjectively evaluated by revisers. For using the GIS techniques the data needs to be stored in GIS formats. Even though this does not present a huge problem any more, the data organization and data description can be. Especially, if taken into consideration that some GIS analysis can be performed only if the data stored in GIS have the inputs we need in further analysis process. We will show that the data, nowadays available, can be analysed using low cost GIS software and that environmental impacts can be verified and evaluated using elementary GIS analysis techniques. We will also show that in order to be able to use GIS techniques in the revising phase, the project designers have to take into account that their work will be analysed using GIS techniques; if this is not the case, then the GIS techniques can not be used straight away and some additional work has to be done on the data description and especially on the topology. For the case study site the “third development axis” was selected. The third development axis is a future highway which will stretch from the northern border of the Republic of Austria via Koroška and Savinjska region to the motorway A1 Koper-Šentilj.

Izvleček: Zelo dobro je poznano, da so GIS orodja zelo uporabna pri planiranju in nadzoru stanja v okolju. V skladu z okoljsko zakonodajo morajo biti vsi

večji posegi v prostor pregledani in ocenjeni. Večinoma so postopki revizije in pregledovanja izvedeni ročno in zato podvrženi subjektivni oceni. V veliko primerov so revidenti podvrženi kritikam, češ da niso bili dovolj strokovni in natančni. Zaradi tega je nujna uporaba orodij odločanja, ki so čim bolj neodvisna. Med njimi so gotovo GIS orodja, ki omogočajo relativno neodvisno in hitro izdelavo ocen vplivov posegov v prostor. Za uporabo GIS orodij pa morajo biti podatki shranjeni v GIS zapisih. Kljub temu, da danes to ni več problem, pa lahko problem predstavljata organiziranost in opis podatkov. Posebej to velja, če vemo, da je za določene GIS analize potrebna predhodna organiziranost podatkov. Pokazali bomo, da podatki, ki so nam ta čas na voljo, že zadostujejo za izvedbo osnovnih analiz s poceni GIS orodji z uporabo osnovnih GIS tehnik. Prav tako bomo pokazali kako pomembno je, da projektanti že v fazi projektiranja pripravijo dokumentacijo na tak način, da je ta pripravljena za uporabo znotraj GIS orodij; če temu ni tako, direktna uporaba GIS-a ni možna in zahteva dodatno obdelavo opisa podatkov zlasti pa topologije prikazov. Za primer uporabe je bila izbrana tretja razvojna os. Ta bodoča avtocestna povezava bo povezovala Avstrijo preko Koroške in Savinjsko dolino z avtocestno povezavo A1 Koper-Šentilj.

Key words: GIS, data models, third development axis, environmental report, limiting factors, GIS analysis

Ključne besede: GIS, podatkovni modeli, tretja razvojna os, okoljsko poročilo, omejitveni faktorji, GIS analiza

INTRODUCTION

The aim of this paper is to show the possibilities GIS offers when making an environmental report. The first part of the paper comprises some general information about GIS, followed by a general overview of data that can be used in GIS environment. We also presented data models, which can be used to process data. The second part of the paper demonstrated the use of a GIS tool in form of an aid in making an environmental report. We also listed the methodology used and analysed the limiting factors that we took into consideration when calculating the optimal result of an environment assessment.

GEOINFORMATION SYSTEM (GIS)

GIS is an information system, designed to work with data referenced by geographic coordinates. In other words, GIS is a database system with specific capabilities for spatially-referenced data, as well as a set of operations for working [analysis] with the data. We could also refer to it as a system for capturing, storing, checking, integrating, manipulating, analyzing and displaying spatially referenced data. It is a system of hardware, software, and procedures designed to support the capture, management, manipulation, analysis, modelling and display of spatially-referenced data for solving complex planning and manage-

ment problems. Data is a representation of a fact in a formalised manner suitable for communication, interpretation, or processing. Data are joined in data tables; the system that defines the connection between data and determines the manner of processing is called a database. It is a collection of data on a certain subject, organised in a way that a user can add, change and review data. Databases are used to store data. They are easy to review and data is therefore easy to manage. The advantages lie in a large quantity of data, quick and precise transfer of data through computer programmes and quick data processing. GIS depends on real world data and the decisions, based on which a human intervenes into the real world, depend on data from GIS. GIS database contains spacial (graphic) and descriptive (attributive) data. Spacial data, which determine the location, form and relations between space elements, are stored in the spacial database and descriptive data in the relational database. Spacial database differ from other types of data by being georeferentiated (placed on the Earth's surface). The reference may be implicit or explicit. An implicit reference refers to object with a known geographic location, while explicit reference refers to geographic co-ordinates. Both types of spacial reference determine the position of data and events on the Earth's surface and enable the study any analysis of the occurrences, described by data (RIBIČIČ, 2002).

GEOINFORMATION DATA TYPES

Geoinformation data types depend on the structure of reality data and reflect the for-

mal equivalent of the conceptual model, built to understand geographically dependent events. It is used to formalize the discretisation of space into parts, suitable for an analysis, to re-establish the correlation between individual parts and establish a clear identification of events within them. The data can be acquired in different ways; it is important to know the method of acquisition and the resolution upon entry. Before deciding on a certain type of data we need to know how data functions in space. The data on surface geology, geology of rivers, winning areas, wells and almost all data on anthropogenic factors (residences, roads, agricultural land etc.) can be presented in space as points (wells, wining areas, run-offs etc.), lines (rivers – the boundaries of feeding or draining of water from aquifer, traffic routes etc.) or concluded polygons (agricultural land, forests, different areas for calculation of evapotranspiration etc.). Other data are continuous and smooth – they do not have large leaps and therefore it is not possible or reasonable to limit them to one of the before mentioned forms. Such data are data on the distribution of substances in the terrain, height above sea-level, temperature etc. It is much more appropriate to present these types of data in a continuous form by giving the values in points, where the measures have been taken, and do an interpolation with a mathematic function in the rest of the space. According to the occurrence of data in the real environment and the possibilities of presenting them in the virtual environment the data is divided into two groups (BURROUGH and McDONNELL, 1998):

- vector data and
- raster data

Vector data

Geographic data structure, which uses points, lines or polygons to describe geolocated events in space, is known as vector data structure. To present the data with vector units they have to have a well-known geographic location, they have to be independent and clearly defined. The deviation between data within the vector units may be zero or very small, considered from the viewpoint of the problem that is being analyzed. The position in space is defined by geographic location and suitable quality and/or qualitative descriptions. A well can be presented as a point with (x,y) coordinates with additional corresponding descriptions (name, angle, depth etc.). A river segment is presented as a line with all other required description (the quantity of feeding or draining of water from aquifer per unit of length). Geological layer on the surface is presented by a polygon and descriptions of name, age, lithology etc. The simple elements of vector data base enable more demanding ones. For example, subsidiary streams of rivers form a river grid across defined points, called hubs. The hubs also define the relations between contiguous vector elements.

Raster data

If the data is presented in a regular square grid, the type of data is a raster data type. The main difference between raster and vector data is that the units of raster are grid cells. Cells differ from each other according to different indicators, contrary to different vector data, which differ according to data base indicators. As the data available rarely matches the number of cells in a raster grid, the values of the unknown cells need to be determined by an interpolation.

The choice between vector and raster data

The choice of the type of spacial data depends on the following factors:

- quantity of data (raster data take up more space in the computer);
- topology and spacial analysis (the search for data in the raster data base is easier and more efficient, spacial and topological analysis are simpler);
- characteristics of the problem – generalisation of data differs according to the user (clarity, accuracy, detail). Vector data are easier to generalize as raster data;
- analytic possibilities and needs;
- accuracy of the data source.

Vector format is usually based on maps. Reliability depends on their origin and accuracy. Raster data are usually gained by converting vector data or from images, captured by satellite and aircraft. These images are captured in different seasons and provide additional information on the chronological sequence of an event. The results of overlay in raster data are questionable, as the interpolations between point data bring a certain level of an error (RIBIČIĆ, 2002).

Database

Data are the description of the real world and present a fact in an agreed way, which is suitable for communication, interpretation and further processing. Data are joined in data tables. The system that defines the correlation between them and determines the way the data are worked with is called a database (WORBOYS, 1995; HERRING, 1992; ARCTUR and WOODSFORD, 1996).

Table 1. Advantages and disadvantages of vector data**Tabela 1.** Prednosti in slabosti vektorskih podatkov

Advantages (+)	Disadvantages (-)
<ul style="list-style-type: none"> • good data presentation, • compact data structure, • explicit presentation of topology, • the transformation of coordinates is simple and inexpensive, • the sharpness of the graphic presentation is not dependent from the scale of the presentation, • simple generalization. 	<ul style="list-style-type: none"> • complexity of data model, • the combination of multiple polygon grids and lines is time consuming and demanding, • the outline of the graphic is time consuming, • special analysis within the polygons is very demanding, • modelling according to the vector data is more demanding than according to the raster data.

Table 2. Advantages and disadvantages of raster data**Tabela 2.** Prednosti in slabosti rasterskih podatkov

Advantages (+)	Disadvantages (-)
<ul style="list-style-type: none"> • simple structure, • simple processing, • simple mathematic modelling, • simple filtration, • inexpensive technology. 	<ul style="list-style-type: none"> • large quantity of data, • large cells mean worse resolution, • the sharpness of the graphic presentation is dependent from the scale of the presentation, • the transformation of coordinates is slow and information may be lost in the process.

There are more definitions of database:

- it is a model of the environment, which is presenting the basis for decision-making and performing actions;
- it is number of interrelated data, saved in a computer system; the access is centralised and enabled with the database management system (DBMS);
- mechanised, for more users, formally

defined and centrally monitored collection of data.

Database management

Data are the foundation of a whole organisation; therefore their management, as with other organisation means needs to be sensible:

- provision of data availability;
- supervision of data use.

Table 3. Differences between raster and vector data structure**Tabela 3.** Razlika med rastersko in vektorsko podatkovno strukturo

Raster data structure	Vector data structure
Simple data structure	More complex data structure
Efficient overlay of individual layers	Overlay of individual layers is more difficult
Space is presented with matrix, every cell represents a value for a square of analysed area and has only one attribute value	Locations, lengths, distances and areas of object are clearly shown with consideration of geometric laws
Simpler and more effective spacial analysis, search for data is easier	Spacial data and search for data are not as simple as with raster structures
Accuracy of the description is defined by the size of the cell and demands a lot of memory	The accuracy depends on the measure or source of the map, where the vector data is gained from
Graphic presentation is not as good; we get »toothed« lines, which can be avoided with a large number of cells, but the file is larger	More suitable for a graphic presentation (map outlines)

The data part of a data base consists of:

- physical database (PDB), it comprises the value of data elements;
- meta database (MDB), it comprises the description of physical data, storage, meaning, their accessibility.

Meta database has a three-level composition:

1. Outer scheme: users point of view, the model of an individual user's surroundings;
2. Conceptual scheme: global model of the

environment;

3. Inner scheme: the collection of logical records.

Data model types

Large quantity of data which can be used when analysing the position in space need to be stored in databases. The most fundamental element in a database is the record of the most fundamental information about the position of an individual entity. Entity is something that exists in the real world, whether an object, subject or a notion.

Their interaction, purpose and practicability dictate the type of the data model. The basic demand of every database system is that it enables a quick access to data and interoperability. The computer program intended for data management is called DBMS (**D**atabase **M**anagement **S**ystem).

Data model: consecutive sequence files

The most basic data system is a consecutive record of data, which are not arranged by any rules. The advantage of this system is the adding of data, which is very simple. Everyone who has ever worked with data saved in this way knows that searching through such a structure can be very demanding. Also, in such a structure data is not gathered according to the content of information.

Data model: organising sequence files

When describing consecutive sequence files, we can compare them to a phone book. The data is organised in a logical way and the system needs more time to record the data. Its advantage is the algorithm, based on the manner of searching – it starts in the middle of all data in the database, verifies, whether the data searched for according to its bit value is in front or behind its position and moves to a new centre of a newly chosen data group. Such manner of searching is approximately four hundred times faster than searching in the previous data model.

Data model: indexed files

Data models explained above do not solve the problem of recording data, which has additional information, as for example data on a well. The name of the well is the basic data, with additional data on depth, x,y,z

angles etc. Searching in such a data model is the quickest if we set up an index. We could say that index is as a page in a book, which comprises certain information. If indexation and searching is based on the main data, the file is a directly indexed file, and if indexation is based on a field, added for this purpose, we speak of an inversely indexed file.

Data model: hierarchic data base

When speaking of a relation model type one against many, the data system is of hierarchic type. These are used mainly in environmental sciences, as they can be used to classify the soil, vegetal and animal taxonomy etc. Such models can be used, if the data fills two criteria:

- a good correlation between the main and other attributes;
- it is possible to set a number of discriminatory criteria, which define the hierarchic structure.

The main advantage is a simple access to the data through the structure defining criteria. The structure is simple and easy to comprehend (the data can be easily filled in), and the data can be added easily. Even though the advantage is access to data, which is simple, the problem arises when searching for bound data, where the structure is set up in advance. Such data structure can be used only if the filters are set in advance. The main weakness of this system is that it is not flexible and does not enable the search for bound data, if that was not already foreseen in the structure.

Data model: Net database (vertical and horizontal interoperability)

It is a version of the hierarchic model

above. The data structure is more open and enables connections within same and/or different levels. The search for bound data is simpler, however the structure, set up beforehand, demands that filters are set up in advance. The main advantage is the option of setting filters between same and different levels, while the weakness is the form of the filters, which is determined in advance and according to the data model. The relation between data is based on indicators, which are a special part in the database (after every correction of the base the indicators need to be “refreshed”, as the quantity of indicators presents the majority of the quantity of data) and can take up a lot of memory in very extensive databases.

Data model: relational database

Relational database is the simplest data structure, where there is no hierarchy between data groups. The data is saved as a record, representing a number of fields. They join together in two-dimensional tables called relations. Indicators from the net data models and keys from the hierarchic data models are replaced by redundancy data in form of single key identifiers. Relational data bases have a great advantage in comparison with other data models - they are very flexible and enable us to use any filters, based on Boole’s logic and mathematical operators. As the relational databases function on the basis of redundancy, it is very important to allow only the most necessary redundancies, needed for proper functioning of the database. Too many redundancies reflect in slow performance and accumulation of unnecessary data within the base, which results in a greater use of memory.

Data model: object-orientated database

This is the latest development in the field of data structures. It was made on the basis of a wish to join all the advantages and reduce the weaknesses of above mentioned data models. The phrase “object-orientated” derives from the Simul (DAHL and NYGAARD, 1966) and Smalltalk¹ (GOLDBERG and ROBSON, 1983) programme language, which were the first to work with objects in the programming field. The advantage is that everyone, who can programme, can make an object with specific characteristics. An object can be made of already pre-programmed objects and the new object “inherits” the characteristics of object(s), from which it is made of. In the relational data structure every entity is determined by the recorded data and relations, determining the relation between individual data. In the object-orientated bases the data with certain common characteristics are joined in an object and objects are joined in classes. The relations between different objects and classes are set with explicit connections. The characteristics of objects are determined by the state of the objects and functions, determining their form. This way the data are joined in an object, which has a determined form within the database. It does not change, even if the values that determine the characteristics of the object change - as an object, whose structure and usage changes with time, but its label remains the same. In the relational data model the data tables are connected through certain data in the tables. In object-orientated data structures the tables become objects with relations

¹ Smalltalk is a programme language, the predecessor of C++ language, which is the foundation for most of today’s software.

as “is as follows”. Once the data are integrated into objects, the performance of pre-programmed functions is the only way to change the data or choose it according to a certain condition. A choice according to a condition depends on operations, used for definition of an object. The response of an object to a “demand” depends on the state of the object, which means, the responses to a same “demand” will be different. That is called polymorphism. The data in object-orientated data structures have to be clearly structured. It is possible to use them especially where the data is gathered according to different hierarchy principles. Setting up an object is a demanding operation, which takes up a lot of time, but, in the end, offers optimal options of search according to an object. Despite this the relational data structures have the advantage when searching according to value attributes.

As already mentioned, we can choose between four different data models:

- hierarchic data model;
- net data model;
- relational data model;
- object-orientated data model.

Hierarchic data model enables a simple division of large quantities of data into tables, which are easy to manage, but do not enable associational relations between different levels due to the vertical hierarchy. That influences the quantity of multiplied data, as it can not be taken from other tables. The net model reduces the quantity of multiplied data and has quick access times due to pre-programmed searches. Object-orientated data models enable a great flexibility and optional relation dependency, which can change according to the demands of

the user, but demand a great programming knowledge and a lot of programming in order to set them up. Relational models are also very flexible and can adapt to different data reviews, but are often too occupied by repeating data, the basis of relation, which reflects in longer search times in the data base (VIŽINTIN, 1999).

Database management system (DBMS)

DBMS stands for a computer programme, intended for organisation and management of data. The basic aims of DMBS are: a quick and easy access to data, stored in the base, preservation of the integrity of the base, protection of data from deletion and abuse, and a simple way of adding and removing data. It can be build on the basis of data models, introduced above, or as a combination of the models. For the DBMS to be successful, Frank (FRANK, 1988) introduced the following demands:

1. It enables saving and entering of data and the choice of data according to one or more attributives or relations.
2. It enables a standardised access to data, which separates the data, used in different computer programmes.
3. It enables an interface between the user programmes and the data base on logical data descriptions, without any necessary knowledge of saving data in a physical way.
4. It enables user programmes to be independent from saving data in a physical way.
5. It enables access to data to more users.
6. It disables unauthorised access to the base.
7. It disables illogical entering of data into the database and has a control and warning system built in for such purposes.

The majority of DBMS programmes enable access to data by a high-level programme language, as for example SQL (Structured Query Language), which is mostly used in the relational databases with a large quantity of data. A good DBMS programme enables saving of data to a physical medium in such way that they take up the least possible amount of space and have very short access times (VIŽINTIN, 1999).

For analysis of practicability of GIS tools we anticipated a GIS system which enables working with relational data bases. At present there are numerous GIS programs on the market which enable the analysis needed for making of environmental reports. A particularly useful tool seems to be Manifold, which operates on the basis of operational system Windows XP and is highly compatible with Microsoft products. When choosing a program, it does not really matter who software belongs to, the most important factor is its ability to perform the tasks needed. We found that Manifold combines the GIS environment with relational bases into a robust integrity and enables performance of basic topological operations needed for evaluation of an individual area for a relatively low price. We used Manifold to test the methodology on the proposed alignments of the future transport infrastructure. Because the whole area would be too extensive, we concentrated on the part of the alignment that is going to link Koroška to the central Slovenia.

CASE STUDY

For case study we selected to make the environmental report for the third development axis and made an environmental impact assessment according to the future motorway alignment with the help of limiting factors. The third development motorway axis is an important project of the future and therefore it is of outmost importance to do the research needed and find the most optimal alignment of the axis without doing too much harm to the environment. That is one of the reasons we chose this project and analysed, with the help of GIS tools, how different the impact of the limiting factors is on the environment, which gave us the most optimal motorway alignment. The purpose of this project is to explain construction, modernization and renovation of the state road network on the prioritised third development axis. The project of the third development axis is to insure public good in form of road infrastructure, one of the necessary conditions for achieving the objectives of an integrated and sustainable society development. The project contributes to achieving competitiveness, a more coherent regional development and a more balanced space policy. That will enhance the regional potential for development, which will enable the development of the economy and a quality living environment for people in the regions. Modernisation of road links and partially construction of new ones already figure in a number of national implementation

programmes. It is necessary to improve the capacity in the alignment by elimination of bottlenecks on the state road network. In the development of the project the emphasis is on the large contents of environmental report development and adoption of the infrastructure to the needs and the benefits. In order to achieve set goals, according to Slovenian legislation, an environmental report is required; it introduces an expert impact assessment of the third development axis on the environment. Due to the before mentioned requirement the goal of this project was primarily to determine the factors that have a restricting effect on the construction of the third development axis.

- For the chosen motorway alignment an environmental report is made; on the basis of required information the report determines, along with the monitoring during the construction and operation, all necessary parameters, which are considered in the outline scheme. The environmental report is a constituent part of the detailed motorway plan.
- Specific researches, aimed at the construction of motorways, are carried out at the earliest possible stages of planning, during the construction and once the motorway is opened to traffic.

The third development axis stretches from the northern border of the Republic of Austria via Koroška and Savinjska region to the motorway A1 Koper - Šentilj, continues to Novo mesto and through Dolenjska and Bela Krajina regions to the border of the Repub-

lic of Croatia. The northern part of the axis, which this project analyses more precisely, stretches through the Koroška and Savinjska regions, mostly on the existing transport corridors. The middle part between motorways A1 and A2 is the most demanding as it stretches over the ridges of the hills, lying in the transverse direction.

For the purpose of our research we chose only one part (Part F) of the alignment – the constituent part of the Koroška - central Slovenia connection (Figure 6). This decision is based on the inconsistency of the project documentation topology and data descriptions.

METHODOLOGY

For testing the GIS approach, we chose the method of elimination factors. Every used parameter has a different effect on space and it is the latter that gives us an assessment on environment. To get an optimal assessment we have evaluated the individual factors and given the equation for calculation of a more or less optimal impact assessment. In the foreseen project three variants of alignments of the future motorway alignment were proposed. The most optimal solution takes account of the environmental impact assessment. The environmental report was carried out with the help of the GIS system. To achieve the most optimal results the use of informational layers needs to be well thought-out. With our work the following limiting factors have been used:

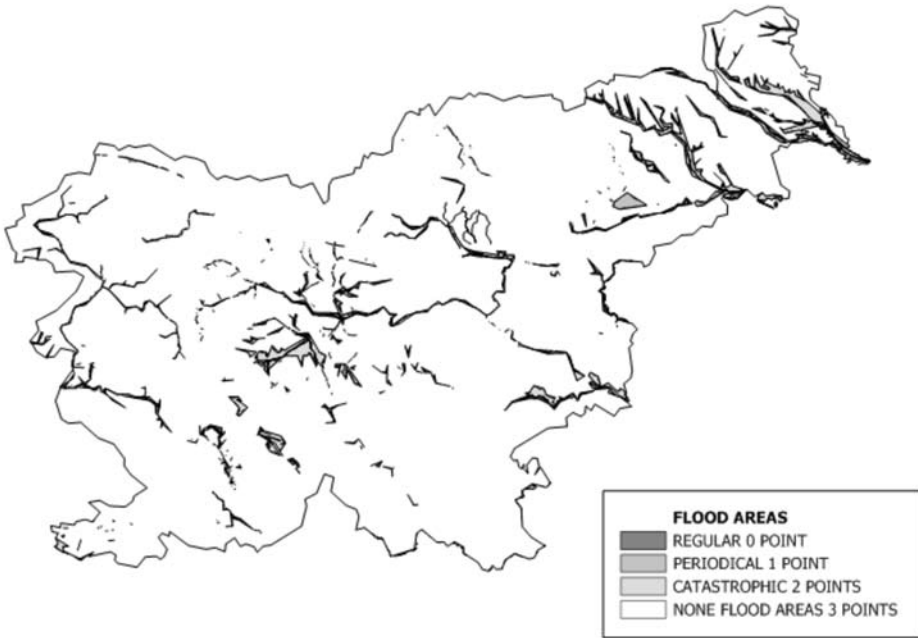


Figure 1. Map of Flood Areas in Republic of Slovenia
Slika 1. Karta poplav v Republiki Sloveniji

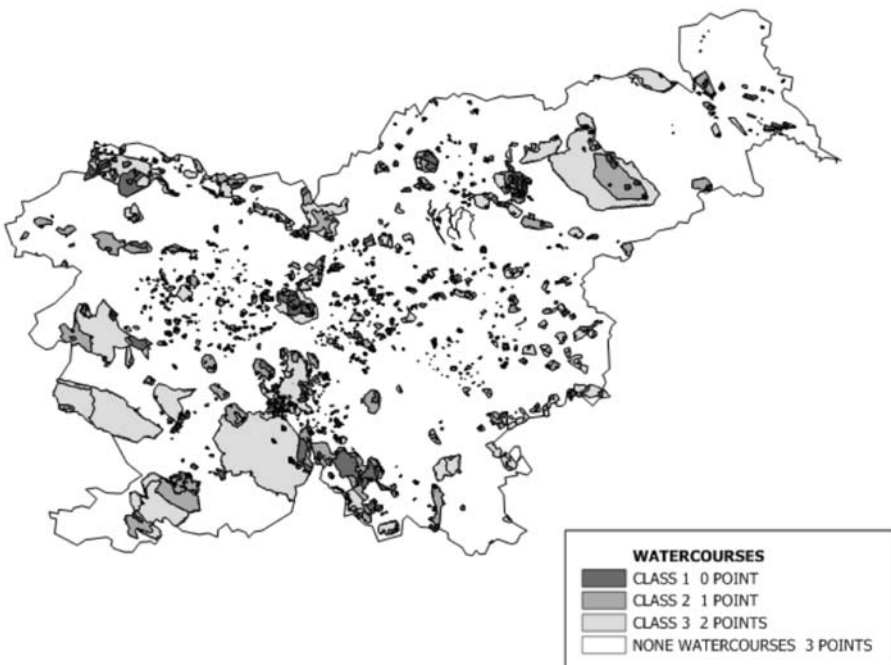


Figure 2. Map of Water protection zones in Republic of Slovenia
Slika 2. Karta vodovarstvenih območij v Republiki Sloveniji

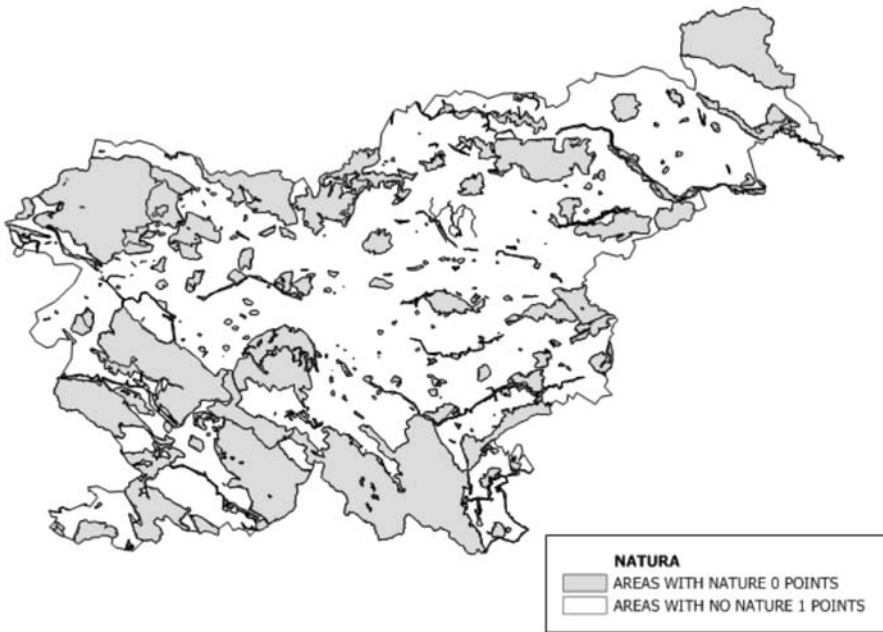


Figure 3. Map of “Natura 2000” in Republic of Slovenia
Slika 3. Karta “Nature 2000” v Republiki Sloveniji

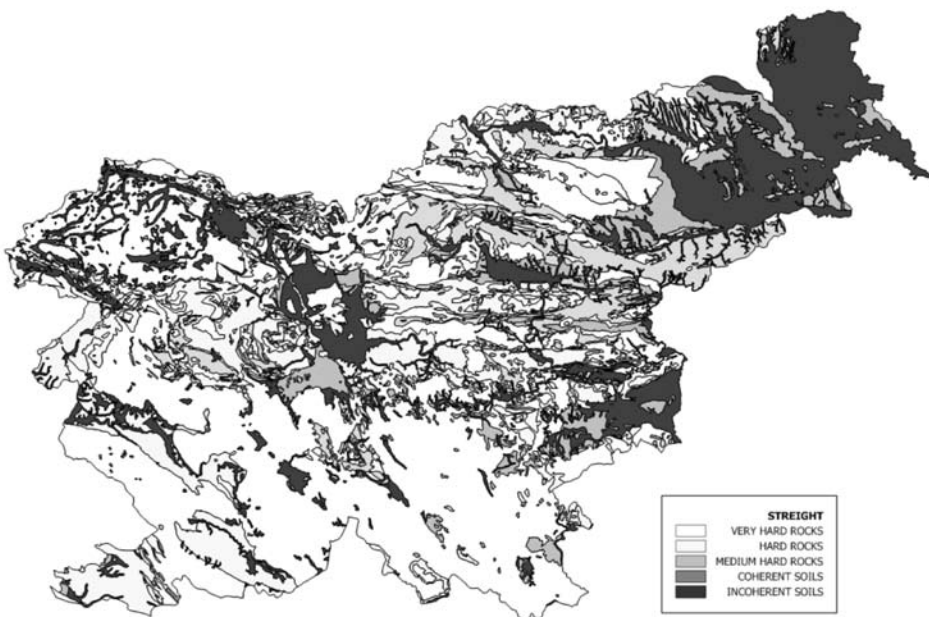


Figure 4. Map of rock straight in Republic of Slovenia
Slika 4. Karta trdnosti kamnin v Republiki Sloveniji

1. Flooding areas;
2. Map of water protection zones;
3. Map of “Natura 2000” protection zones;
4. Variants of (motorway) alignments;
5. Strength of terrain (derived from geology information);
6. Stability of terrain (derived from geology information).

The limiting factors we considered when making this report will be presented in a greater detail at the end of the report.

Flood map

The flood map was made by Institute for Water of the Republic of Slovenia; the scale is 1:25.000 (Figure 1).

Flood areas are divided into three classes:

1. Regular flood areas
2. Frequent flood areas
3. Catastrophic flood areas

Map of water protection zones

The map of water protection zones was made by the Geological Survey of Slovenia. The water protection zones are divided into three different areas according to valid criteria set by an institution (Figure 2).

Map of “Natura 2000” protection zones

The map “Natura 2000” presents areas, protected in accordance with the EU directives. Any activities on such areas are forbidden and construction may be done only with the consensus of EU (Figure 3).

Map of rock strength

Map of rock strength is a map, based on a geological map. It presents the structure of the area according to rock stability. It divides rocks into five classes (Figure 4).

Map of rock stability

Map of rock stability is a map, based on geological map. It presents the areas of stability (Figure 5).

Review of six variants of motorway alignment

Table 4 below presents the evaluation of individual limiting factors. According to the set calculation we received the numeric value of a more or less optimal result, depending from the evaluation of an individual information layer. It can be seen that only flood areas, “Natura 2000” and water protection zones are also the elimination factors, but the parameters deriving from geology are not. This can be seen as an erroneous conclusion but in our cases this was made because the scale on geological map used for GIS analyses were too small for showing the geological risk hazard in a proper way.

Despite this it has to be noted that the authors are aware that the geological structure of an area is the cause for a disaster on many occasions. For such analyses a really exact geological mapping is needed, and it has to be presented with large ratio maps. When this analysis was taking place we did not have access to such information and that is why we did not eliminate the condition valued 0 to the adequacy parameters. When doing the evaluation, we used only a part of the segments of anticipated variations and performed their evaluation according to the methodology, presented below (Figure 6).

The equation for a common estimate of an individual alignment is:

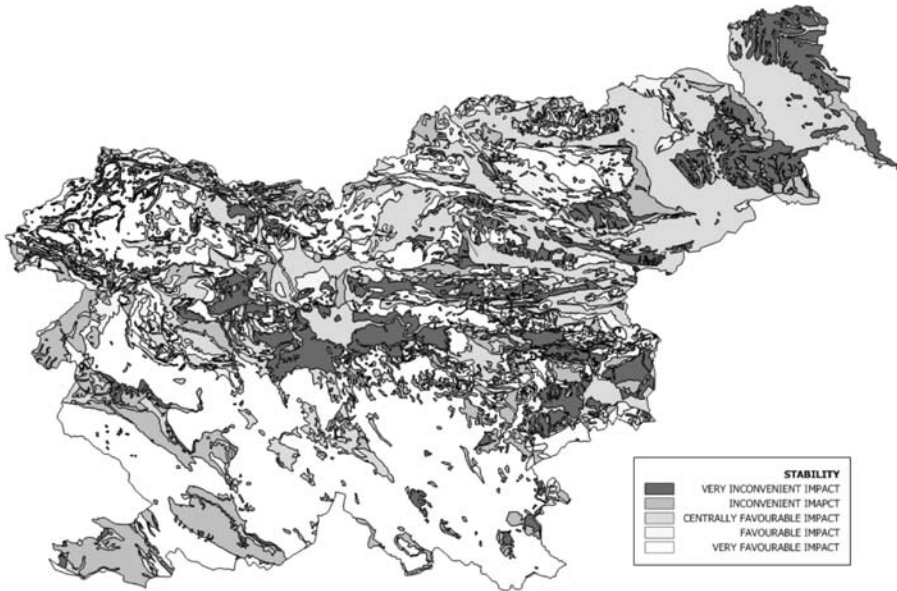


Figure 5. Map of rock stability in Republic of Slovenia
Slika 5. Karta stabilnosti kamnin v Republiki Sloveniji

$$P = P(f) \cdot P(n) \cdot P(wp) \cdot P(str) \cdot P(s) \quad (1)$$

$P(str)$ mean value of strength and $P(s)$ mean value of stability.

Individual parts of the equation are calculated according to the following equations (when one part of the amounts is 0, the collective values of sum have to be 0):

$$P(f) = \sum y_f \cdot x_{fi} / \sum x_{fi} \quad (2)$$

$$P(n) = \sum y_n \cdot x_{ni} / \sum x_{ni} \quad (3)$$

$$P(wp) = \sum y_{wp} \cdot x_{wpi} / \sum x_{wpi} \quad (4)$$

$$P(str) = \sum y_{str} \cdot x_{stri} / \sum x_{stri} \quad (5)$$

$$P(s) = y_s \cdot x_{si} / x_{si} \quad (6)$$

The parameters are: $P(f)$ mean value of flood area, $P(n)$ mean value of natura, $P(wp)$ it is value of water protection zone,

Y is the evaluation of an individual factor; x_i is the length of value of a certain factor of the alignment. Equations above are pondered values of estimations for an individual factor in subordination to the length of the alignment.

TOPOLOGICAL OPERATIONS AND ANALYSIES

As we said before a GIS package is different than an “atlas” package products that can display only one, built-in, read-only map. A GIS can work with many different maps and can be used to create new maps, to edit maps and to combine maps with database information. It is also a “database

Table 4. Marks used for individual parameters of the analysis**Tabela 4.** V analizi uporabljene ocene za posamezne parametre

FLOOD AREAS	P
REGULAR	0
PERIODICAL	1
CATASTROPHIC	2
NONE	3
“NATURA 2000”	
YES	0
NO	1
WATER PROTECTION ZONES	
NONE	3
WATER PROTECTION ZONE 3	2
WATER PROTECTION ZONE 2	1
WATER PROTECTION ZONE 1	0
STRENGTH	
INCOHERENT SOILS	1
COHERENT SOILS	2
SOFT ROCK	3
MEDIUM ROCK	4
SOLID ROCKS	5
STABILITY	
VERY INCONVENIENT IMPACT	1
INCONVENIENT IMPACT	2
CENTRALLY INCONVENIENT IMPACT	3
FAVOURABLE IMPACT	4
VERY FAVOURABLE IMPACT	5

system for maps” that will allow us to embed database information into a map so that the map can be used as a visual interface into the data. One of the most important features of every GIS is topology overlay. It is used for making the GIS analysis and transferring data between vector data types which pass the topological analysis. The below descriptions is based on the Manifold User Manual.

Topology Overlay

The Topology Overlay dialog modifies drawings using Identity, Intersect, Union and Update overlay functions. These functions may also be performed by a sequence of transform toolbar operators. The Topology Overlay tool provides one-step functionality to make it easy to perform these common functions. Overlays simultaneously modify objects and also manipulate

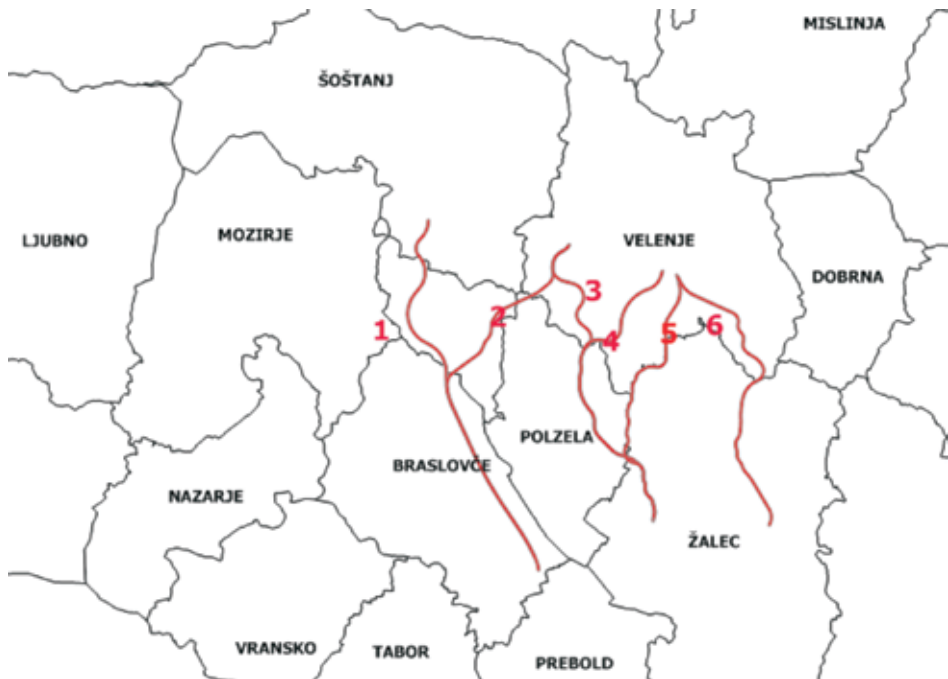


Figure 6. The estimated segments of variants
Slika 6. Ocenjevani odseki variant

data columns as necessary. Overlay functions are also referred to simply as overlays. All overlays in Manifold require two drawings: a target drawing that may contain areas, lines and points and a source drawing that must contain areas. The areas in the source drawing guide the overlay function used. The result is either to modify the target drawing or to create a new result drawing (the default). When creating a new result drawing, the result drawing will inherit all columns from both the source drawing and the target drawing. When modifying the target drawing, the source drawing will retain its own columns and will also acquire all columns from the target drawing. There is no mapping between the columns in the source drawing and the target drawing. Each resulting object in-

herits all data from the source and target objects it has been produced from, according to the transfer rules specified for those columns. Update intersects all areas, lines and points in the target drawing with areas in the source drawing and first places each part of the original target object that does not lie in any source area into the result drawing, then second placing each source area into the result drawing. The above overlays are similar to those in various legacy GIS systems. However, because legacy GIS systems typically cannot handle drawings with overlapping areas and Manifold can, the overlays are defined in a slightly different manner than their equivalents in other GIS products. If neither the target nor the source drawing contains overlapping areas, the outcome of the overlays is

identical to that produced by similar tools in other GIS products. If either the source or target drawing contains overlapping areas, the outcome of the Intersect and Union overlays will be asymmetric. That is, the result will depend upon which drawing is chosen as the source and which as the target drawing. Because of the potential of the outcome to be asymmetric if either drawing contains overlapping areas, launching Intersect or Union overlays with drawings that do not contain overlapping areas within themselves yet contain vastly different numbers of objects has the potential of being much faster if the drawing that contains the higher number of objects is used as the source drawing. Using the topology overlay a transfer rules are of essential importance.

Transfer rules

Transfer rules come into play when the transform commands transfer fields between objects. A transfer rule may be set for each column (field) in the table that specifies how that field will be transferred to any new objects created by various transform operators. By default, all fields in a table are copied to the new record created for the new object. The transfer rules specified for each field will be used whenever a transform operator creates a new object. There are two types of transform operators that create new objects: One to Many (1 to N) Operators - For each original object these operators create one or more new objects. The task for transfer rules for such operators is to specify how one value from the original object should be apportioned

to the possibly many new objects created. Many to One (N to 1) Operators - These operators create a single new object from many original objects.

Buffers

Before we started with the analysis we needed first to transform the axis of motorways in closed regions which are presenting the influence perimeter of different variants of motorways. For doing this the buffer command was used. We use an option to make a buffer for all variants of motorway alignment. Exactly the same procedure as is here describes but with a different choice of transform operator is used to create inner buffers or other buffer zones. For our analysis we created a border buffer zone extending 50 m outward from the boundary. To check what units of measure are in use, we use the tracker tool to measure a distance near the areas. The result was a newly created area in the shape of the border buffer that appears in the drawing. The newly created areas presenting the variants of motorways were the basics GIS table used in the analysis process.

In the process of analysis we used buffered motorways axes and put them through separated topology overlays operations. As a transfer rule for one to many relations we always selected a copy and for many to one an average transfer rule. Using this procedure we get divided axes according to the areas they were cutting. The results are presented in the Table 5.

Table 5. Individual marks of suggested variants of motorways**Tabela 5.** Ocene posameznih predlaganih variant

Variant	Strength	Stability	Flood	WPZ	“Natura 2000”	Altogether mark
1	1.94347987	2.9184488	2.9881478	3	0	0
2	2.02245731	2.7401818	2.9888004	3	0	0
3	3.37622426	2.9193593	3	3	1	88.70770524
4	3.36373513	3.0746551	3	3	1	93.42652497
5	3.64852875	3.4898871	3	3	1	114.5965803
6	3.53021057	2.9769197	3	3	1	94.58237946

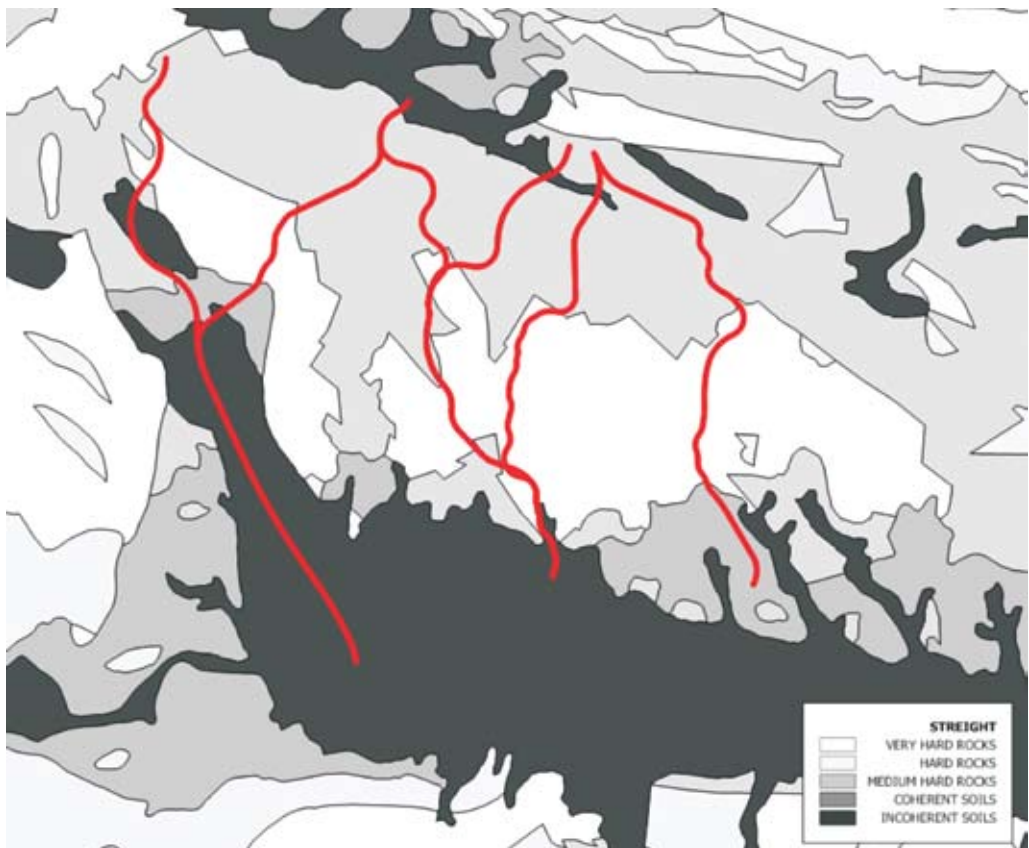


Figure 7. Alignment crossing areas with different rock stabilities
Slika 7. Primer prečkanja tras različnih območij trdnosti kamnin

RESULTS OF ANALYSIS

The results were extracted to Excel, where we were able to finish the evaluation based on equations 1 to 6. As it can be seen from Table 5 there are two alignments, variant 1 and 2, with evaluation 0 – meaning, they run through areas that do not allow any construction, or it is highly undesirable. The individual evaluations were not evaluated according to the meaning of an individual factor. We believe that that would demand a special economic-social analysis, which can be done within GIS programme environment, but it is highly demanding, as it bases on knowledge of expenses evaluation according to parameters of areas.

All values which are not whole numbers are due to the fact that individual alignments cross two or more differently evaluated areas of an individual factor (Figure 7). Alignments 1 and 2 have evaluation 0 at “Natura 2000” factor due to the fact that they cross (partly or in whole) the “Natura 2000” area (Figure 8).

From the Table 5, a variant number 5 has the highest number, so according to our methodology it should be select. But we have to take into account also that we did the evaluation purely on the natural depended factors and that we didn't take into account the socio-economic factors, which in some cases can completely different the choice.

CONCLUSIONS

The evaluation was made on the basis of already existing data, describing certain natural factors as geological-geomechanical

factors, protected areas “Natura 2000”, flooding areas and water protection zones of underground water. As shown, we have selected the alignment in a transparent and repeatable manner using GIS tools. A part of a subjective evaluation lies in the composition of map of strength and stability of rocks, made on the basis of geological map, as well as on the protected zones and flood lines maps. The advantage of GIS is that it enables verification on every step of the analysis. As shown in Table 5 variant 5 was chosen as the best one. Its evaluation is based solely on the parameters from this article. Realistic evaluation should comprise a larger spectrum of parameters. Two of the proposed alignments run through protected areas and are as such automatically eliminated (Figure 8). When doing the evaluation the biggest problem presented GIS documentation, which was made on the basis of the project. The most problematic are the errors in topology; so we had to use only the axes and expand them for 50 m to gain a “buffer” zone. That is how we were able to determine the influence of future motorways on the environment. We did not analyse the quality of data in the article. Despite this we believe that such an analysis is useful for a quick overview, but acknowledge that for a more detailed evaluation verification on the spot is a necessary factor. We also did not do an evaluation of the influence of an individual factor on the field, as it requires an economical and sociological analysis of an individual intervention.

Based on the analysis done we can see that the use of GIS tools for transparent and repeatable analysis of evaluations of different environmental impact is possible. On the other hand the biggest problem presents the data, which is often not processed enough



Figure 8. Variants 1 and 2 cross “Natura 2000” and are excluded according to our methodology

Slika 8. Varianti 1 in 2 prečkata območje “Nature 2000” in sta zato v skladu z našo metodologijo ocenjevanja izključeni

and do not contain the information, needed to make the estimations of the impact the infrastructure would have on the environment. Whatever the case – we have to know that the quality of gained values depends on the quality of input data.

POVZETEK

Uporaba GIS-a za določitev naravnih kriterijev možnosti okoljskega razvoja

Izdelava okoljskih poročil je določena z okoljsko zakonodajo. Glavni namen okoljskih poročil je, da se v času odločanja za posamezno varianto posega v prostor izbere tista, ki je s stališča naravovarstvenih kriterijev najugodnejša. V času izdelave okoljskega poročila se zato, za potrebe presoje in njegove izdelave, zbirajo različni prostorsko vpeti podatki. Njihova ocena je zmeraj podvržena subjektivnemu ocenjevanju presojevalcev, ki so sicer specialisti za področje, ki ga presojujejo.

Največji problem pri presojanju pa predstavljajo številni kriteriji in prostorski pogoji, ki se med seboj prepletajo in velikokrat izključujejo. Veliko primerov ocen je postavljenih pod vprašaj tudi zaradi nepreglednosti uporabljene metodologije. Prav uporaba orodij, ki temeljijo na GIS tehnologiji je tisti pristop, ki naredi metodologijo ocenjevanja bolj transparentno. Hkrati pa poskrbi, da so vse prostorske danosti, omejitve in specifičnosti istočasno ocenjevane in pregledane. Poleg tega pa GIS omogoča tudi oceno socioekonomskih parametrov, ki včasih zaradi razumevanja razvoja premagajo parametre naravnega izvora.

Kot primer ocenjevanja smo izbrali tretjo razvojno os, ki bo povezala Koroško z osrednjo Slovenijo in Dolenjsko. Zaradi problemov v tehnični dokumentaciji smo obdelali le odsek F, ki je bil razdeljen na šest variant. Ocenjevali smo le naravne danosti, kot so vodovarstvena območja, pojavljanje poplav, geološko-geomehanski pogoji gradnje itd. Na začetku ocenjevanja smo izdelali metodologijo in izbrali računski model. Na osnovi izdelane metodologije smo naredili oceno posamezne trase, kot je razvidno iz ocen v tabeli 5 je najbolj optimalna varianta 5. Pri ocenjevanju je treba vedeti, da smo ocenjevali le odsek F brez ostalih in tudi socioekonomskih faktorjev. Zato je oceno variante treba jemati z rezervno. Hkrati pa je v članku lepo pokazan primer in zmožnosti, ki jih GIS tehnologija omogoča pri izdelavi okoljskih poročil in študij vplivov na okolje.

REFERENCES

- ARCTUR, D. and WOODSFORD, P. (1996): *Introduction to Object-Oriented GIS Technology Workshop Outline*. Laser-Scan, Cambridge, 202 p.
- BURROUGH, P. and McDONNELL, R. (1998): *Principles of Geographical Information Systems*. Oxford University Press, pp. 52-60.
- DAHL, O.J. and NYGAARD, K. (1966): *SIMULA – an algobased simulation language*. Communications of the ACM, pp. 671-678.
- FRANK, A.U. (1988): Requirements for a database management system for a GIS. *Photogrammetric Engineering and Remote Sensing*; Vol. 54, pp. 1557-1564.
- GOLDBERG, A. and ROBSON, D. (1983): »Small-talk-80: The Language and its Implementation«. Addison-Wesley, Reading.
- HERRING, J.R. (1992): TIGRIS: a data model for an object-oriented geographic information system. *Computers and Geosciences*; Vol. 18, No. 4, pp. 443-448.
- Internet address: www.arso.gov.si/metapodatki
- RIBIČIČ, M. (2002): *Engineering geology 1*. Faculty of Natural Sciences and Engineering, Department of Geology, Ljubljana.
- VIŽINTIN, G. (1999): *Use GIS tool at modeling of holster of ground water: Master's degree*. Ljubljana, 120 p.
- WORBOYS, M. F. (1995): *GIS-a Computing Perspective*. Taylor & Francis, London.

Construction of the Šentvid tunnel

Gradnja predora Šentvid

ANDREJA POPIT¹, JOŽE RANT²

¹SCT d.d., Vošnjakova ulica 8a, SI-1000 Ljubljana, Slovenia; E-mail: andreja.popit@sct.si

²SCT d.d., Slovenska cesta 56, SI-1000 Ljubljana, Slovenia; E-mail: joze.rant@sct.si

Received: March 6, 2007

Accepted: May 8, 2008

Abstract: Construction of the Šentvid Tunnel is one of the toughest tasks on the 5.5 km long motorway from Šentvid to Koseze that will connect the north-western motorway with the Ljubljana ring which links the motorway between the Northeast to Southwest and Northwest to Southeast of Slovenia. The tunnel connects Šentvid with Pržanj and consists of two tubes of 1030 m (left) and 1060 m (right). The contract for its construction was signed on November 4, 2004 between DARS and SCT d.d. Ljubljana (the leading partner) and Primorje Ajdovščina. Construction of the three-lane tunnel with connecting caverns and ramp tunnels is a major challenge for SCT d.d. engineers, both in terms of building such an unique object and excavating it in highly tectonized Permo-Carboniferous rocks. Constant adjustments in construction technology had to be made, due to complex geological conditions in the rock mass. It was necessary to proceed the excavation with reinforced forepoling and pipe roof, as well as to systematically stabilize the working face by a great number of rock bolts, even under a pipe roof. The number of excavation sequences in the top heading was increased, round lengths were shortened, as well as lengths between the top-heading and the invert. The support elements designed in the tunnel profiles needed reinforcing during execution of the works.

Izvleček: Predor Šentvid je najzahtevnejši objekt na 5,5 kilometra dolgem avtocestnem odseku Šentvid-Koseze, ki bo povezal gorenjsko avtocesto z ljubljanskim avtocestnim obročem in s tem sklenil avtocestni križ na območju Ljubljane. Predorski cevi potekata med Šentvidom in Pržanjem v dolžini 1030 m (leva cev) in 1060 m (desna cev). Pogodbo za gradnjo predora je DARS 4. novembra 2004 sklenil z izvajalcema SCT d.d. Ljubljana (vodilni partner) in Primorje Ajdovščina. Za predorske strokovnjake SCT d.d. je gradnja tropasovnega predora s kaverno in polnim priključkom na Celovško cesto že od vsega začetka velik izziv, ne le zaradi tako edinstvenega objekta, ampak predvsem zaradi zahtevnosti gradnje v močno tektoniziranih permokarbonskih kamninah. Prav zaradi kompleksnih geoloških razmer je bilo treba stalno prilagajati tehnologijo gradnje predora. Za napredovanje izkopa je bilo potrebno ojačevanje stropa in bokov predora z vgradnjo sulic

ali cevnega ščita in sistematično varovanje izkopnega čela z vgradnjo sider. Izkop smo izvajali v bistveno več fazah, podaljšali smo odseke z začasnim talnim obokom, skrajšali korake napredovanja v kaloti, stopnici in talnem oboku ter skrajšali razdaljo kalota – talni obok in primarno podgradnjo ojačevali z dodatnimi sidri.

Key words: three lane tunnel, cavern, phase excavation, tectonized rocks, geological overbreaks, adjustment of support measures

Ključne besede: tripasovni predor, kaverna, fazni izkop, tektonizirane kamnine, geološki zruški, prilagajanje podpornih ukrepov

INTRODUCTION

Preliminary geological-geotechnical research for the Šentvid Tunnel was carried out between 1991 and 2003. Geological and hydrogeological mapping, drilling, in situ analyses of the exploration wells (i.e. pressiometric and water level measurements), geophysical measurements (seismicity and electricity) and laboratory analyses of rock samples were all included in these studies^[1,2]. Estimated values of the geomechanical parameters of the rock mass were the basis for the tunnel design and for selecting the appropriate excavation method. The important characteristics for designing a tunnel in fault zones are: rock mass strength, deformation characteristics of the rocks, and primary stress conditions in the rock mass^[3].

In the tender documents, double two-lane tubes were planned or, in the case of favourable geological and geomechanical conditions, the left tube as a two-lane tube and the right one as a three-lane tube with cavern and ramp tunnel^[4]. SCT d.d. Ljubljana, as the leading partner, and Primorje Ajdovščina signed the contract with DARS on November 4, 2004. In the tender docu-

ments it was determined that the investor will decide on the final design of the tunnel during its construction. The investor ordered additional geological-geomechanical investigations to study the feasibility of the caverns and to select their most favourable locations. SCT d.d. started excavating the exploration gallery in April 2004 and finished it in December 2004; final reports on this investigation were published in January and March 2005. SCT started with the excavation of the two-lane tunnel from the Šentvid direction in November 2004. Additional studies of the traffic in this location, as well as results of geological, geomechanical and hydrogeological conditions obtained from the exploration gallery, were the main reason for the investor's decision that both tubes would be three-lane with cavern and the ramp tunnels. SCT d.d. started with excavation of both three-lane tubes from the Pržanj direction in June 2005.

Šentvid Tunnel is constructed according to the New Austrian Tunnelling Method (NATM). Continuous monitoring of deformation of the primary tunnel lining and deformation of the rock mass around the tunnel is performed to check the sta-

bility of the primary tunnel lining. Study of the secondary stress and deformation field around the primary tunnel lining enables timely and adequate adjustments of the support measures and the excavation method. Using this method the most stable and economical tunnel lining is achieved.

GEOLOGICAL STRUCTURE OF ROCKS IN THE TUNNEL ALIGNMENT

Geological structure in the tunnel alignment was interpreted in the tender documents (PZR) as a synclinal fold of Permian-Carboniferous layers, deformed by the thrusting of three tectonic units and by movements along subvertical faults of NW-SE, NE-SW and N-S direction^[4]. Mudstone and clayey slate (mu-gs CP), alternation of clayey slate and clayey siltstone (cm-dm) with sandstone (pem CP), and tectonic clay were foreseen in the tunnel alignment^[1,2,4].

The fact that the geotectonic composition of the Šentvid hill is much more complex than foreseen in the tender documents was already known at the time of excavation of the exploration gallery, which was excavated to study the feasibility of the caverns and to find the most suitable location according to geological composition of the rock mass. The first results of this research were published in January 2005^[5], although SCT d.d. had already been introduced into the excavation works in November 2004. Tectonized rocks were excavated very frequently in both main tubes. Many faults and thrusts cross the tunnel alignment, with cracked and crushed rocks. The main tubes were frequently excavated in the ma-

ior fault or thrust zones, where rocks were changed into tectonic clay with the worst mechanical characteristics^[6]. Additional obstacles were minor water inflows, which made the geomechanical characteristics of tectonized rocks even worse.

Part of the longitudinal geological profile of the left tube from the chainage between 1090 and 1340 m is shown in Figure 1^[4]. On the section between 1150 and 1200 m are layers of mudstone and clayey slate with the direction of the schistosity, and layers of 140-170°/20-30°. The actual geological composition in section A (Figure 1) in the smaller scale is shown in the rectangle below the longitudinal profile. In the top-heading along the whole section A there is a thrust zone parallel to the tunnel axis, filled with tectonic clay (winding, interrupted lines), while rocks in the vicinity of the thrust zone are crushed (small black crosses). Between 1150 and 1161 m there are layers of shaly siltstone with subordinated layers of clayey slate and sandstone with a direction of 100-180°/10-30° and with two systems of cracks 210°/85° and 300°/80°^[6]. Between 1161 and 1176 m there is a steep fault zone directed to the south, filled with tectonic clay, cracked rocks and folded layers of shaly siltstone and clayey slate. Between 1176 and 1200 m sub-horizontal layers of shaly siltstone and clayey slate predominate over thin layers of sandstone. In this section there are many faults parallel to the layers (thrusts). At 1194 m there is a fault transverse to the layers, along which rocks are crushed (small black crosses)^[6].

In the left tube at the chainage 1161 m one of the biggest (100 m³) overbreaks oc-

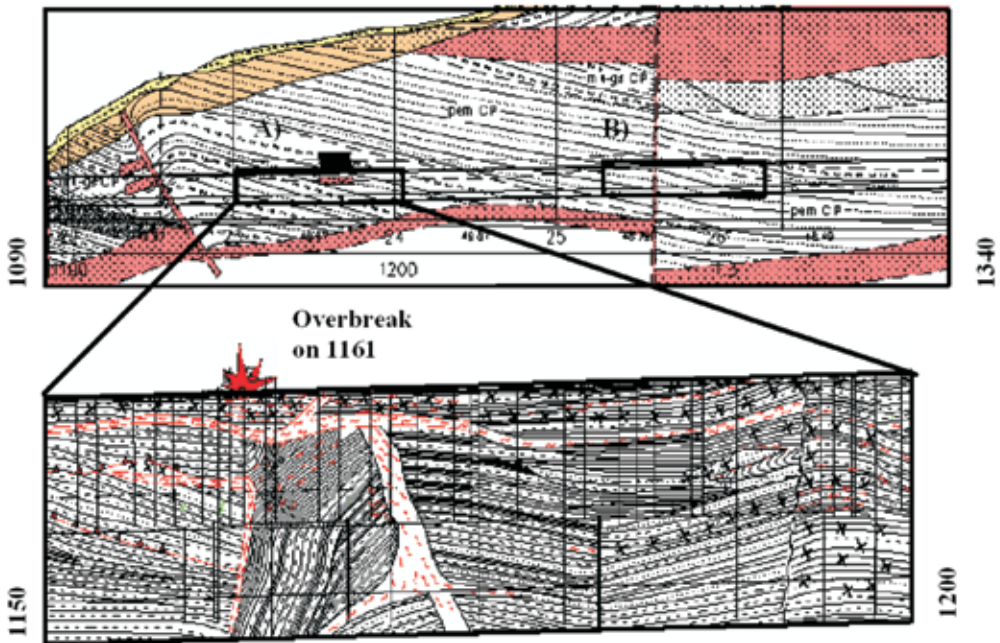


Figure 1. Longitudinal geological profile^[4] of the left tube between 1090 and 1340 m that as foreseen in the tender documents (above) and the actual geological composition of the section A between 1150 and 1200 m (below)

Slika 1. Zgoraj je predviden vzdolžni geološki profil^[4] za levo cev na stacionažah med 1090 in 1340, spodaj (A) pa dejanska geološka zgradba na stacionažah med 1150 in 1200

curred on February 22nd, 2005. Instability of the top-heading occurred in the region of tectonic zone, with the water inflow of up to 48 L/min. Overbreak occurred despite that excavation face was protected with a great number of rock bolts (on the average 6 IBO rock bolts of $l = 12$ m per 7 m), despite that excavation was proceeded with reinforced forepoling (average 30 pc SN, $l = 3$ m per 1 m) and despite that excavation works in the top-heading were proceeded on the average in 7 phases. Excavation works were stopped for 8 days.

In section B (1260-1310 m), between 1260 and 1274 m, layers of sandstone and silt-

stone with direction of $140-170^{\circ}/20-30^{\circ}$ were foreseen. Between 1274 and 1284 m a sub-vertical fault zone was foreseen, between 1284 and 1289 m alternation of clayey slate and shaly siltstone (cm-dm) with sandstone (pem CP), while between 1289 and 1310, layers of clayey slate between the layers of sandstone and siltstone with direction $150^{\circ}/10-15^{\circ}$ were foreseen (Figure 1). Actually, in the top-heading between 1260 and 1284 m is tectonic clay, crashed clayey slate and shaly siltstone with thin layers of sandstone. In this section there are a fault zone with direction $300-320^{\circ}/60^{\circ}$ and parallel thrust zones with direction to the east that are filled

with tectonic clay, while rocks in the vicinity are crushed (small black crosses on the Figure 2) and locally folded. In the region of tectonically crushed rocks in the top-heading at 1273.6 m, an overbreak of 30 m³ occurred on July 15th, 2005, when the excavation works were stopped for 6 days (Figure 2). Between 1284 and 1310 m shaly siltstone prevails over the sandstone. Thrusts in the top-heading have the direction 110°/5-15° and 40-50°/12-20°, faults have the direction 300-320°/40-60°, schistosity has the direction NE-SE/5-25°, while a system of cracks has the direction 280-290°/60-70° (6). In crushed rocks of the top-heading at 1301.1 m an overbreak of 13 m³ occurred on August 9, 2005, when the excavation works were stopped for 5 days.

The geotechnical model was made based on geological and geotechnical monitoring during the excavation of the exploration gallery and both main tubes of the tunnel. The purpose of the model was to foresee the geotechnical conditions for widening the caverns^[7,8]. This research showed

that the tectonic model of the rock mass is much more complex than foreseen. The accuracy of the predicted geological models was assessed in the range between 1 and 10, where the accuracy of the model 2002, known at the time of tender documents, was assessed as 3; accuracy of the geological model 2005, known after excavation of the exploration gallery, was estimated as 7; while accuracy of the model 2006, known after excavation of the main tubes, was estimated as 9.

ROCK MASS CATEGORIES: TENDER-ACTUAL

Based on the Austrian standard ÖNORM B 2203 it was foreseen in the tender documents that Šentvid tunnel would be excavated in rock mass category PC in the region of portals, SCC in the region of shallow cover class, B2 in the range where rock mass is strongly structurally damaged, C2 in the rock mass where increased stress-strain conditions occur during the excavation, and C3 in the rock mass where greatly increased stress-strain conditions

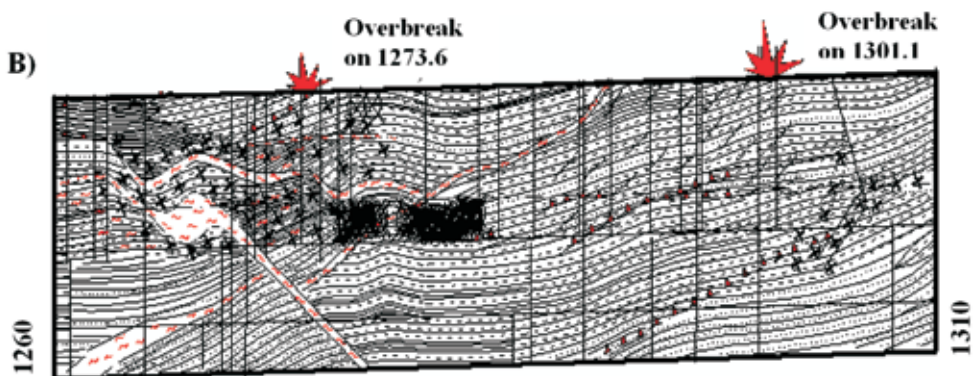


Figure 2. Actual geological composition in the left tube between 1260 and 1310 m (B)
Slika 2. Dejanska geološka zgradba v trasi leve predorske cevi na stacionažah med 1260 in 1310 (B)

occur during the excavation. A parking bay niche was designed in the two lane tube while, in the contact between the ramp tunnel and the main tube, a cavern was designed. Rock mass categories were adjusted according to actual geological conditions. Comparison between predicted and actual rock mass categories for the two- and three-lane tunnel is presented in Figures 3-6.

Rock mass category C2 in the two-lane tunnel was shortened from 49 % to 17 % of the tunnel length (status end of May 2006), (Figure 3 and 4). Rock mass category C3 was foreseen in 23 % of the tunnel length, and was installed in 18 % of the tunnel length whereas, in addition, in 33 % of the length much more reinforced C3 was installed – the so-called modified C3 category.

5 % of rock mass category B2 was foreseen in the tender documents in the two-lane tube, but it was not installed until the end of May 2007. Category PC was extended by 122 %. In 88 % of the parking bay niche a pipe roof was additionally installed. A pipe roof was foreseen only in the category PC (Figure 3), i.e. on 7 % of the tunnel length, but actually it was installed also in some parts of C2, C3 and the parking bay niche, altogether in 62 % of the tunnel length (status end of May 2006), (Figure 4).

C2 rock mass category in the three-lane tunnel (left and right tube together) was shortened by 7 % (Figures 5 and 6), whereas in an additional 13 % of the tunnel length much more reinforced C2 – modified category was installed. C3 category was shortened by 17 %, but an additional 8 % of much more reinforced C3

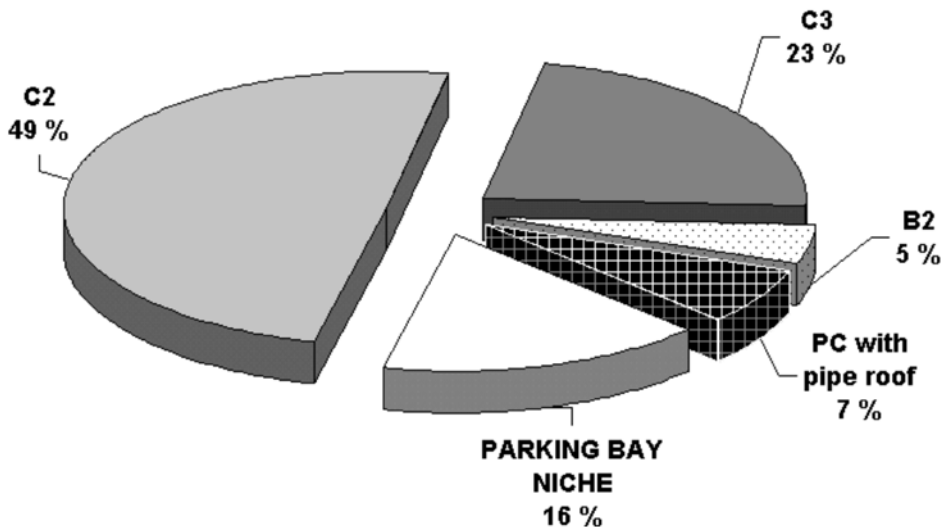


Figure 3. Rock mass categories in tender documents in 608 m of the two-lane tunnel (status end of May 2006). Netlike hatching indicates a pipe roof.

Slika 3. Hribinske kategorije po PZR na 608 m dvopasovnega predora (stanje do konca maja 2006). Mrežasta šrafura označuje cevni ščit.

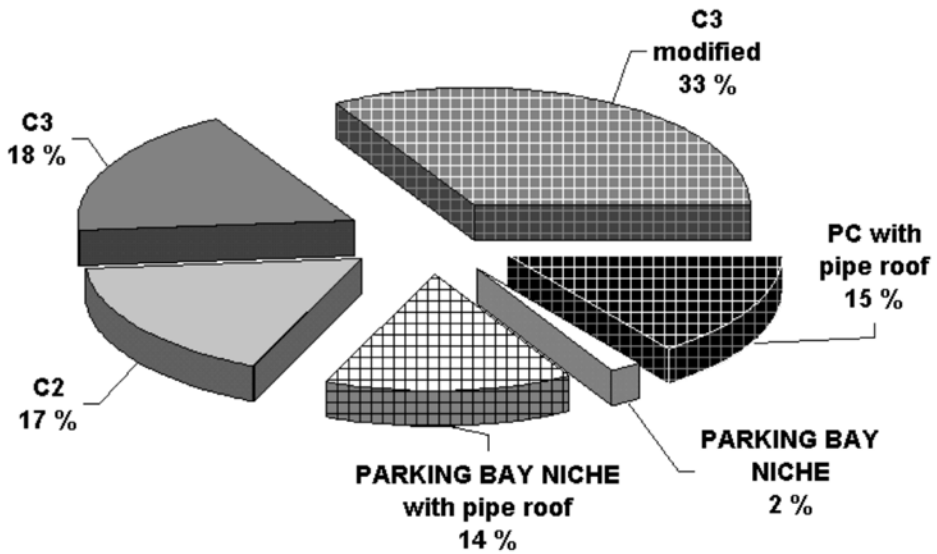


Figure 4. Actual rock mass categories in 608 m of the two-lane tunnel (status end of May 2006). Netlike hatching indicates a pipe roof.

Slika 4. Dejanske hribinske kategorije na 608 m dvopasovnega predora (stanje do konca maja 2006). Mrežasta šrafura označuje cevni ščit.

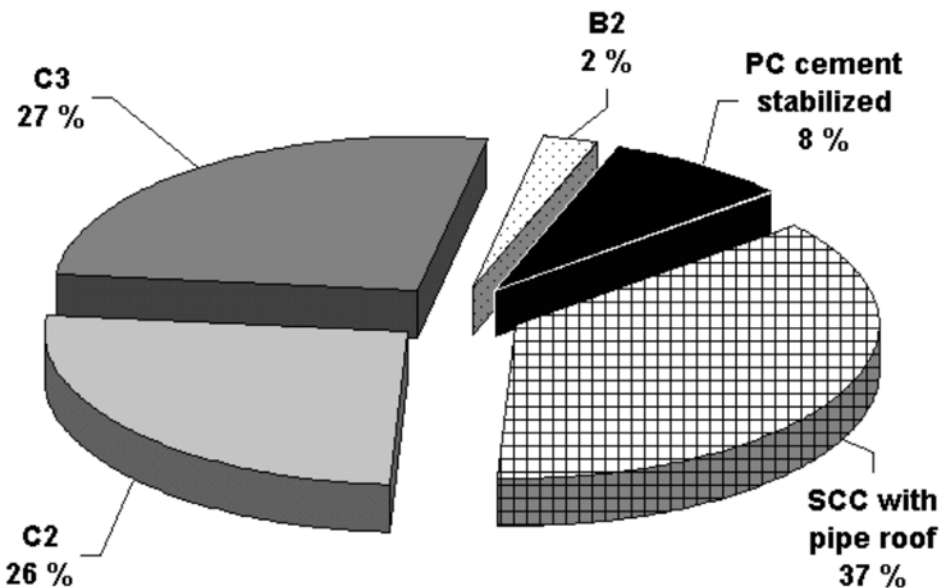


Figure 5. Rock mass categories in tender documents in 759 m of the three-lane tunnel (status end of May 2006). Netlike hatching indicates a pipe roof.

Slika 5. Hribinske kategorije po PZR na 759 m tripasovnega predora (stanje do konca maja 2006). Mrežasta šrafura označuje cevni ščit.

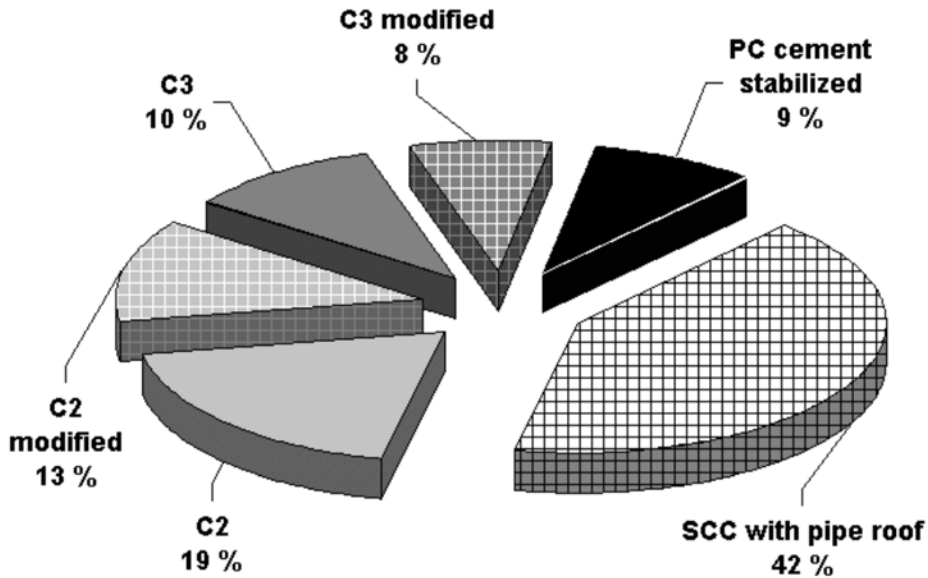


Figure 6. Actual rock mass categories in 759 m of the three-lane tunnel (status end of May 2006). Netlike hatching indicates a pipe roof.

Slika 6. Dejanske hribinske kategorije na 759 m tripasovnega predora (stanje do konca maja 2006). Mrežasta šrafura označuje cevni ščit.

modified category was installed. The B2 category foreseen in the tender documents in the three-lane tunnel was not installed until the end of the May 2006.

Category SCC with pipe roof was extended by 5 % and category PC by 1 %. Pipe roof was foreseen in the tender documents in the three lane tunnel only in the category SCC, i.e. on 37 % of the tunnel length, whereas it was actually installed also in the sections C2 and C3, altogether in 63 % of the tunnel length.

Substantial reinforced profiles were installed in 55 % of the two-lane tunnel length and in 26 % of the three-lane tunnel length, altogether in 39 % of the whole tunnel (status at the end of May 2006).

ADJUSTMENTS OF SUPPORT MEASURES AND METHODS OF CONSTRUCTION

Excavation of the tunnel in tectonized Permo-Carboniferous rocks was possible only with constant adjustments of the construction methods. Further, additional support measures were carried out according to geological conditions to achieve stability of the primary tunnel lining and the working face and to ensure safe working conditions. Comparison of the support measures foreseen in the tender documents with those that were actually installed was carried out on the basis of longitudinal profiles for both tubes. Support measures and construction methods were compared between each section of actual rock mass category and the corresponding section of the tender rock mass category.

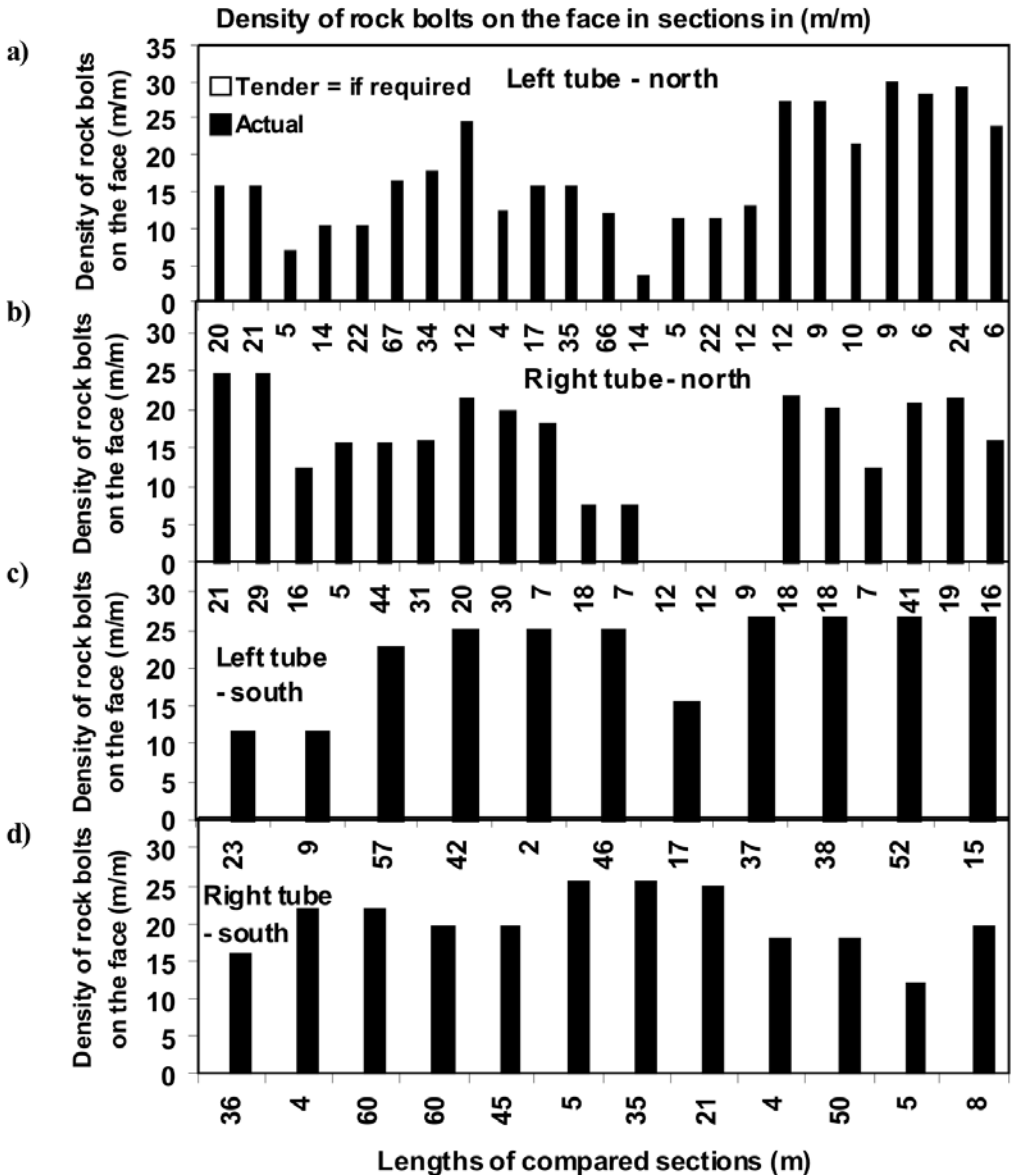


Figure 7. Actual density of rock bolts on the working face in sections. Face bolting in the tender documents was foreseen only »if required« with no given quantities: (a) left tube – north, (b) right tube – north, (c) left tube – south, (d) right tube – south

Slika 7. Dejanska gostota sider za varovanje izkopnega čela po odsekih: (a) leva cev – sever, (b) desna cev – sever, (c) leva cev – jug in (d) desna cev – jug

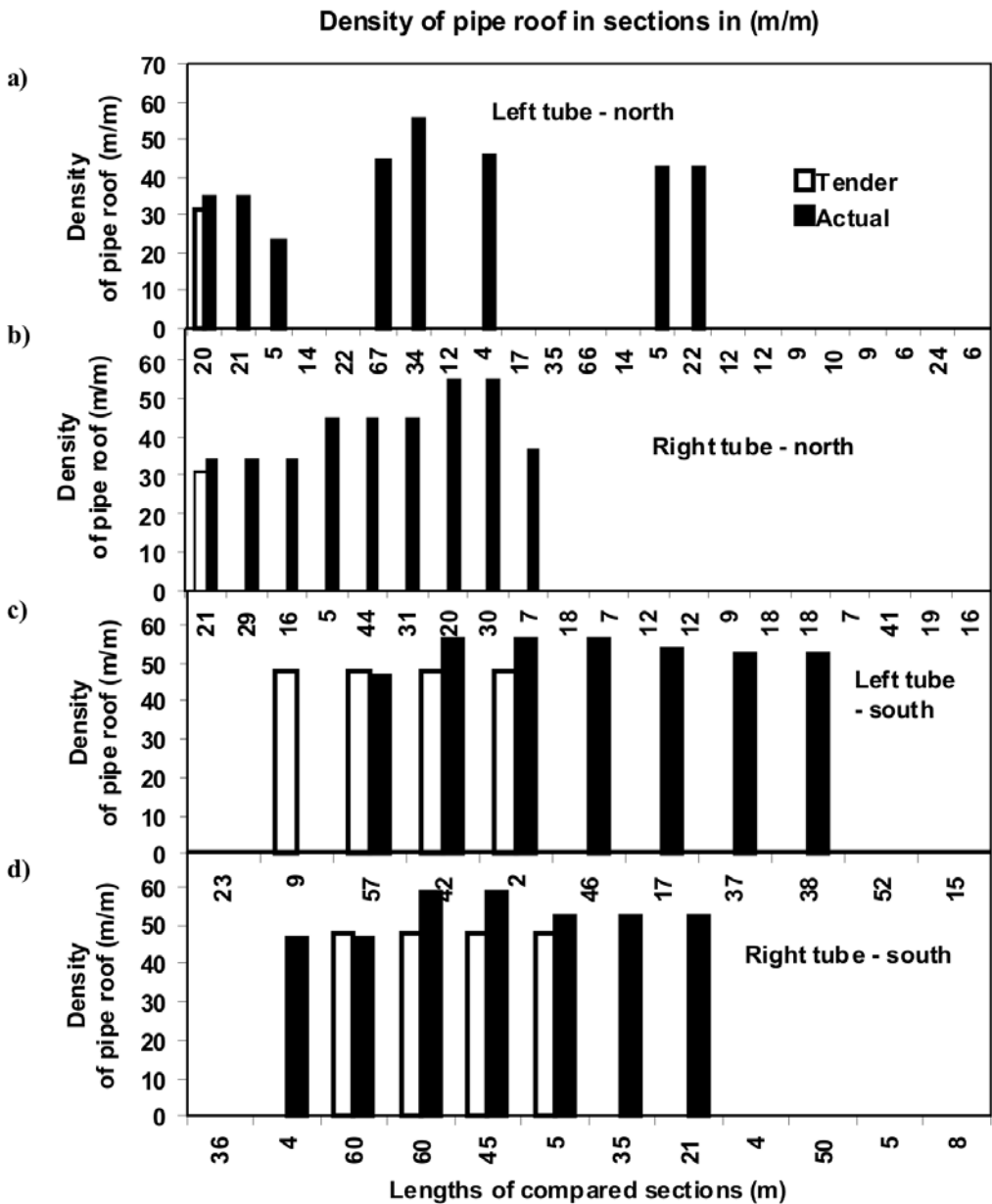


Figure 8. Actual sections with pipe roof (black columns) and those foreseen in the tender documents (white columns): (a) left tube – north, (b) right tube – north, (c) left tube – south, (d) right tube – south

Slika 8. Odseki s cevničnim ščitom (črni stolpci) in tisti predvideni po PZR (beli stolpci s črno obrobo): (a) leva cev – sever, (b) desna cev – sever, (c) leva cev – jug in (d) desna cev – jug

Table 1. Density of rock bolts in the caverns (m/m)**Tabela 1.** Gostota sider v kavernah (m/m)

Density of rock bolts in the cavern in tender (m/m)						Actual density of rock bolts in the cavern (m/m)					
left			right			left			right		
K-1A	K-2A	K-3A	K-1A	K-2A	K-3A	K-1A	K-2A	K-3A	K-1A	K-2A	K-3A
400.4	398.3	340	336.6	337.8	282.4	372	463.6	418.6	450.8	437.1	389.4
Difference in density of rock bolts: actual – tender in (m/m)						-28	65.3	78.6	114.2	99.3	107
Difference in density of rock bolts: actual – tender in (%)						-7	16	23	34	29	38

It was necessary to stabilize the working face systematically by a large number of rock bolts on 98 % of the excavated tunnel, whereas face bolting in the tender documents was foreseen only if required, without specifying the quantity (Figure 7).

Systematic rock bolting of the working face was carried out, even under the pipe roof. The average density of the rock bolts was 4–30 m/m. It was necessary to proceed the excavation with reinforced forepoling and pipe roof (Figure 8), or in some sections (C2, C3 and parking bay niche) also to replace forepoling pipes with pipe roof.

Pipe roof was foreseen in the tender documents only in the PC and SCC categories (Figures 3-6 and 8) over a length of 320 m, whereas it was actually installed also in sections C2, C3 and the parking bay niche; altogether over a length of 850 m (status end of May 2006).

Support for the primary tunnel lining was reinforced with additional rock bolts on 65 % of the tunnel's length (situation at the end of May 2006). Table 1 presents the

reinforcement of the primary tunnel lining in caverns. The density of rock bolts in the right cavern in all sections A (K-1A, K-2A and K-3A) was higher by up to 99-114 m/m, whereas in the left cavern it was higher in 70 % of its length by up to 65-79 m/m.

In the left tube – north, 18 % more rock bolts were installed than foreseen in the tender documents. In the right tube – north, 36 % more were installed and, in the right tube – south, 8 % more, whereas only in the left tube – south were fewer rock bolts installed than foreseen in the tender (Figure 9), (status end of May 2006).

In 34 % of the tunnel's length (status end of May 2006), increased deformation of the primary tunnel lining occurred, so that special measures were carried out to stabilize it using a large number of rock bolts, wire mesh and shotcrete.

Despite the pre-supporting measures ahead of the front associated with systematic face bolting and very careful sequences of excavation, frequent overbreaks occurred at

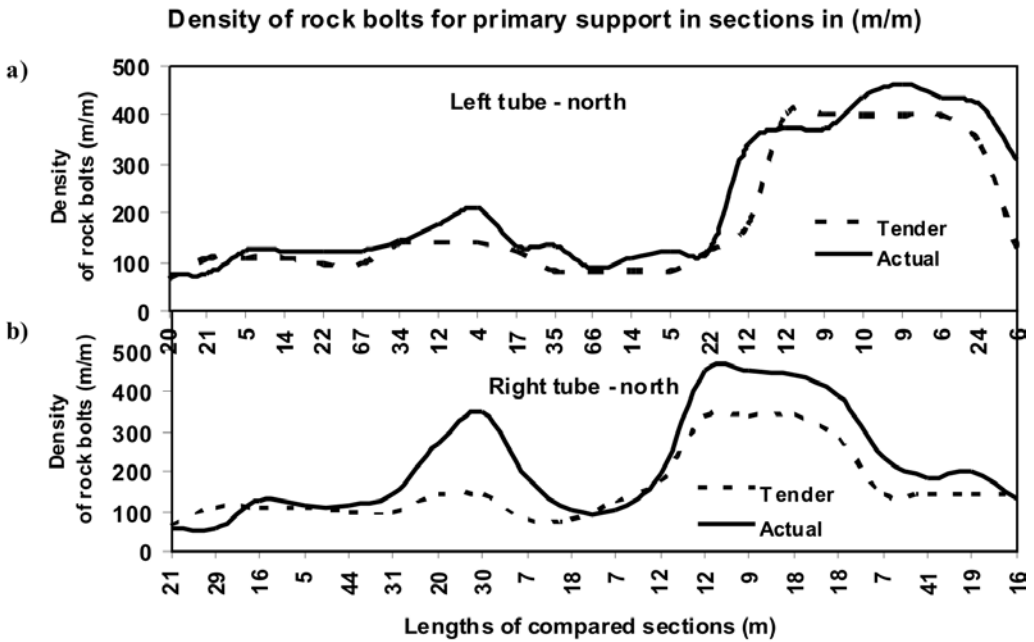


Figure 9. Comparison of tender and actual rock bolt density in particular sections: (a) left tube north and (b) right tube north

Slika 9. Primerjava dejanske in predvidene (PZR) gostote sider za primarno podgradnjo po odsekih: (a) leva cev sever in (b) desna cev sever

all four work sites, due to the very poor geological conditions, even under a pipe roof. Up to the end of May 2006; 14 overbreaks occurred in the left tube north (1 in the cavern), 4 in the right tube north (2 in the cavern), 4 in the left tube south and 5 in the right tube south. Special measures were carried out to stabilize the working face with additional installation of rock bolts, forepoling pipes, wire mesh, reinforcing steel bars, pipe roof and shotcrete.

Support measures and methods of construction were adjusted according to geological conditions in the rock mass. The consequence of these adjustments was the slower rate of the excavation works. Tunnel excavation in tectonized rock mass was

possible only in phases (Figure 10). Excavation works in the top heading of rock mass category PC, C2, C3, parking bay niche and cavern A was planned to be carried out in 3 phases and in rock mass category SCC in 2 phases, while the support body in all mentioned rock mass categories was planned to be excavated in 1 phase according to tender documents. In fact, excavation of the top heading was carried out in 94 % of the tunnel length and of the support body in 72 % of the tunnel length, in more phases than foreseen in the tender documents (status end of May 2006). Excavation of the top heading in rock mass category PC was carried out on average in 7 phases and of the support body in 3-5 phases. Excavation in SCC was carried out

on average in 11 phases and in the support body in 5-7 phases. Excavation in C2 of the two-lane tunnel was carried out on average in 7 phases, in rock mass category C2 with exploration gallery in 3 phases, and the support body was excavated in 4 phases. Excavation in category C2 of the three-lane tunnel was carried out in 4-9 phases and the support body was excavated in 2-6 phases. Excavation in the rock mass category C3 was carried out in 7-11 phases, in rock mass category C3 with the exploration gallery was carried out in 5-9 phases and the support body was excavated in 5-7 phases.

Round lengths in the invert were shortened in 67 % of the excavated tunnel; round lengths in the bench were shortened in 50 % of the excavated tunnel, while round lengths in the top-heading were shortened in 45 % of the tunnel length (status end of May 2006). Round lengths in the invert of the left tube north were on average 1.3 m

shorter (Figure 11a), in the right tube north on average 1.7 m shorter (Figure 11b) and, in both tubes south, on average 1.5 m shorter than those foreseen in the tender documents (Figure 11c and 11d).

Temporal invert was foreseen in the tender documents only in the categories PC and SCC of the three-lane tunnel (round length of the temporal invert for PC of the two-lane tunnel was not given in the tender), whereas actually it was installed in 344 m of the two-lane tunnel. Altogether it was installed in 390 m more of the temporal invert than was foreseen in the tender.

In the tender documents, the distance between the top heading and the invert in the rock mass category B2 was 200 m, in C2 150 m, and in SCC 60 m, while in category PC and C3 it was 30 m. These distances were shortened in 96 % of the tunnel length (status end of May 2006) because of unfavourable geological conditions (Figure

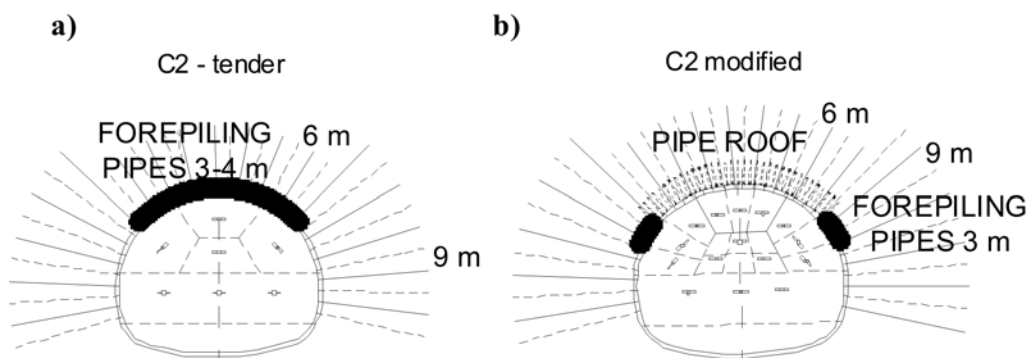


Figure 10. Excavation phases in the rock mass category C2 of the three-lane tunnel: (a) tender; 3 phases in the top heading and 1 phase for excavation of the support body, (b) actual; 9 phases in the top heading and 6 phases in the support body (drawing by Elea iC)

Slika 10. Izkopne faze kalote v hribinski kategoriji C2 tripasovnega predora: (a) PZR – 3 faze za izkop kalote in 1 faza za izkop podpornega jedra, (b) dejansko – 9 faz za izkop kalote in 6 faz za izkop podpornega jedra (avtor slike: Elea iC)

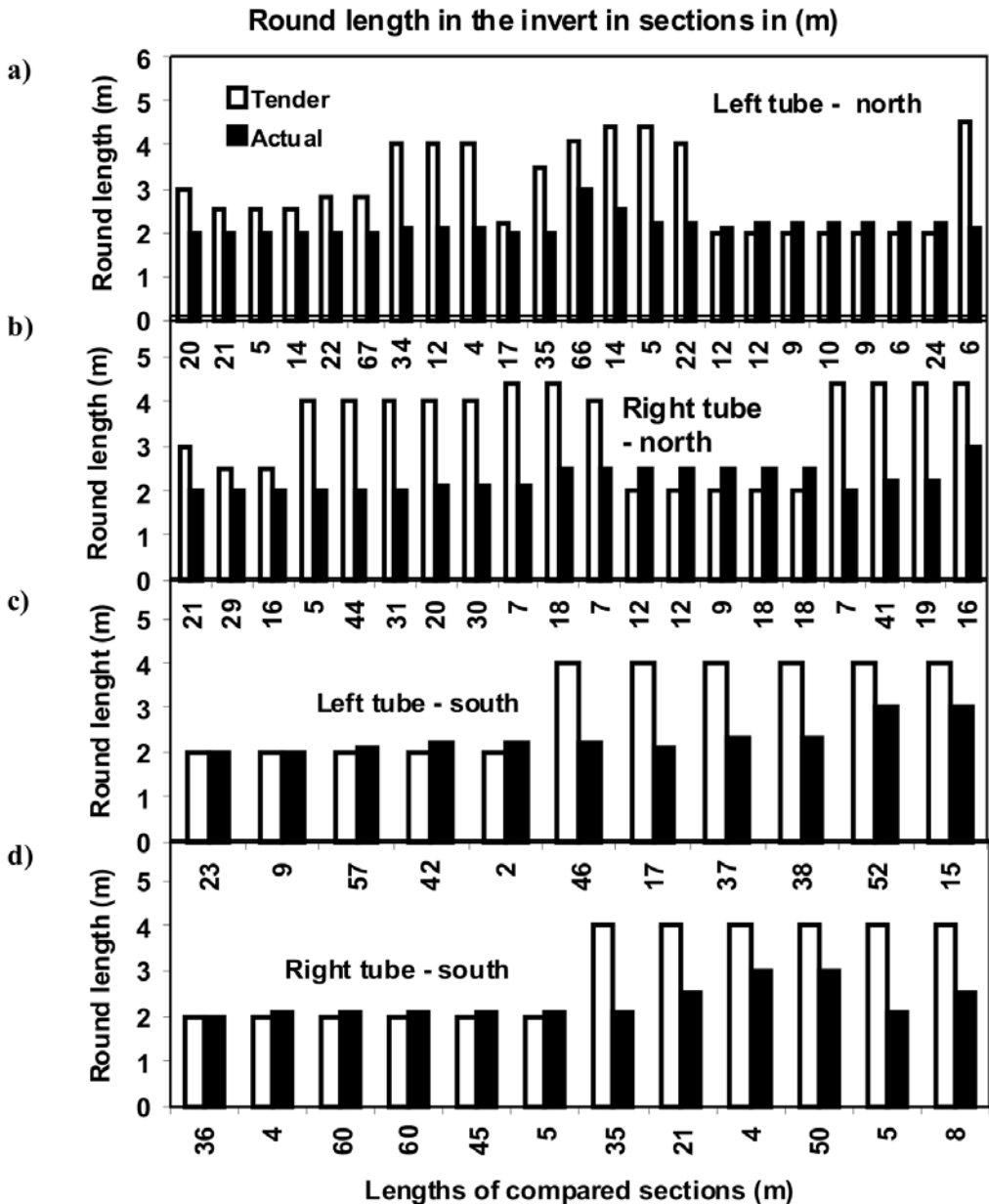


Figure 11. Round lengths in the invert (black columns) and those foreseen in the tender documents (white columns) in sections: (a) left tube north, (b) right tube north, (c) left tube south and (d) right tube south

Slika 11. Dolžine korakov v talnem oboku (črni stolpci) in dolžine predvidene po PZR (beli stolpci s črno obrobo) po odsekih: (a) leva cev – sever, (b) desna cev – sever, (c) leva cev – jug in (d) desna cev – jug

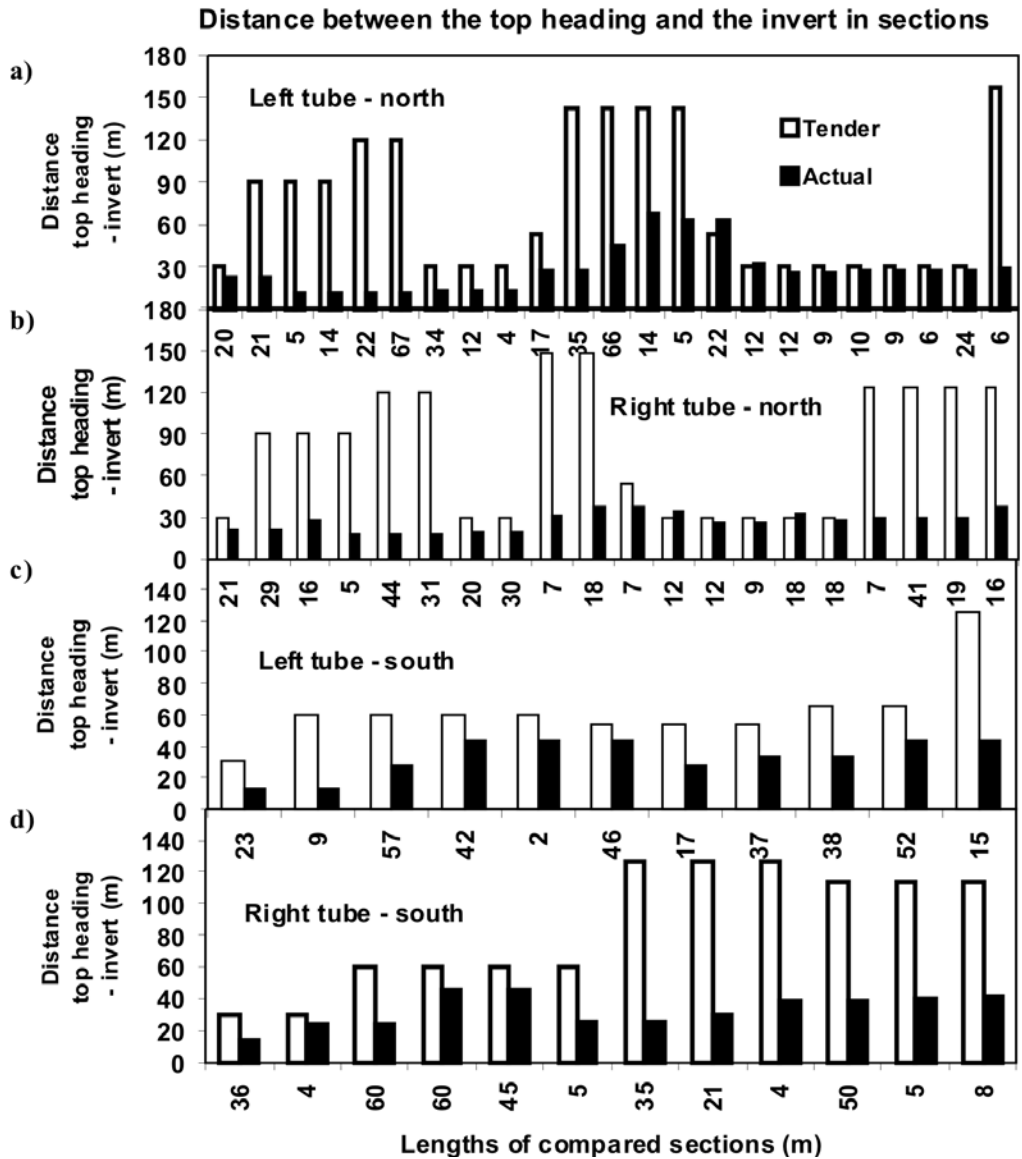


Figure 12. Actual distances between the top heading and the invert (black columns) and the distances foreseen in the tender documents (white columns) in sections: (a) left tube north, (b) right tube north, (c) left tube south and (d) right tube south

Slika 12. Dejanske razdalje kalota – talni obok (črni stolpci) in razdalje predvidene po PZR (beli stolpci s črno obrobo) po odsekih: (a) leva cev – sever, (b) desna cev – sever, (c) leva cev – jug in (d) desna cev – jug

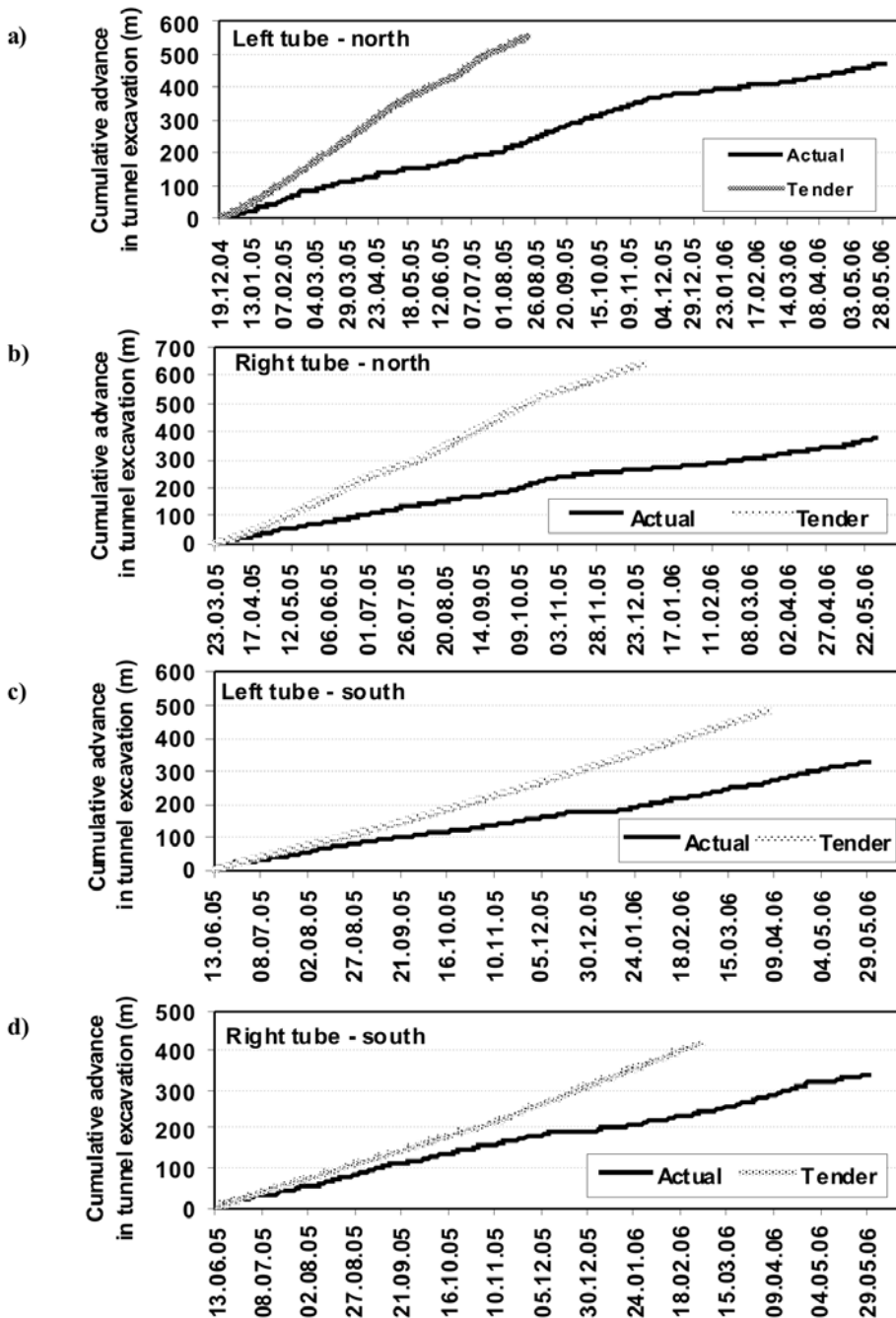


Figure 13. Cumulative advance in the Šentvid Tunnel: (a) left tube north, (b) right tube north, (c) left tube south and (d) right tube south

Slika 13. Kumulativni napredki izkopa predora Šentvid za vsa štiri napadna mesta: (a) leva cev – sever, (b) desna cev – sever, (c) leva cev – jug in (d) desna cev – jug

12). They were shortened by more than a half in 58 % of the tunnel length (status end of May 2006).

Constant adjustments of construction technology were carried out according to actual geological conditions. That is why the advance rate was less than that foreseen in the tender (Figure 13). Excavation of the tunnel with primary lining should have been finished in 8-10 months while, up to the end of May 2006, only 76 % of the left tube and 67 % of the right tube was excavated.

CONCLUSIONS

The constant adjustments in construction technology were due to the complex geological conditions in the rock mass. It was necessary to proceed excavation with reinforced forepoling and pipe roof (required only for some sections of SCC and PC) or even with substitution of the forepoling by a pipe roof in some sections of C2 and C3. Moreover, it was necessary to systematically stabilize the working face by a large number of rock bolts, even under a pipe roof. Despite the pre-supporting measures ahead of the front, associated with systematic face bolting and very careful sequences of excavation, frequent overbreaks due to the very poor geological conditions occurred in the four work sites. The number of excavation sequences in the top heading was increased; round lengths were

shortened as well as distances between the top-heading and the invert, the sections with temporal invert were extended. The support elements designed in the tunnel profiles needed reinforcing during execution of the works. The consequence was a general decrease of the rate of advance and a corresponding increase in construction delays.

POVZETEK

Gradnja predora Šentvid

Predor Šentvid je najzahtevnejši objekt na 5,5 kilometra dolgem avtocestnem odseku Šentvid-Koseze, ki bo povezal gorenjsko avtocesto z ljubljanskim avtocestnim obročem in s tem sklenil avtocestni križ na območju Ljubljane. Predorski cevi potekata med Šentvidom in Pržanjem v dolžini 1030 m (leva cev) in 1060 m (desna cev). Zaradi kompleksnih geoloških razmer je bilo treba stalno prilagajati tehnologijo gradnje predora. Za napredovanje izkopa je bilo potrebno ojačevanje stropa in bokov predora z vgradnjo sulic ali cevnega ščita in sistematično varovanje izkopnega čela z vgradnjo sider. Izkop smo izvajali v bistveno več fazah, podaljšali smo odseke z začasnimi talnim obokom, skrajšali korake napredovanja v kaloti, stopnici in talnem oboku ter skrajšali razdaljo kalota – talni obok in primarno podgradnjo ojačevali z dodatnimi sidri.

REFERENCES

- [¹] ZAG (2002): Dopolnilne geološko-geomehanske raziskave za PGD, PZI predora Šentvid. *Poročilo št. P0013.0112*.
- [²] ZAG iC (2003): Pregled geoloških in geomehanskih podatkov o trasi predora. *Poročilo št. P803-750-2*.
- [³] GORICKI, A., RACHANIOTIS, N., HOEK, E., MARINOS, P., TSOTSOS, S. and SCHUBERT, W. (2006): Support decision criteria for tunnels in fault zones. *Felsbau*. No. 5, pp. 51-57.
- [⁴] DARS (2004): Projekt za razpis za predor Šentvid. *PZR*.
- [⁵] Elea iC (2005): Predor Šentvid. Priključni kaverni. Študija izvedljivosti. *Poročilo št. 415484P*.
- [⁶] IRGO Consulting, Geoinženiring, Elea iC, (2005-2006): *Geološko-geotehnična poročila gradnje predora Šentvid*. pp. 1-75.
- [⁷] PÖSCHL, I., GENSER, W. and KLEBERGER, J. (2006): Development of a high-value geological model for cavern design in faulted rock mass. *Felsbau*. No. 5, pp. 28-32.
- [⁸] SCHUBERT, P., ŽIGON, A. and VERGEINER, R. (2006): Entscheidungskriterien für die planung zweier 360 m² kavernen in Slowenien. *Felsbau*. No. 5, pp. 38-43.

Strateški vidiki oskrbe centralne in jugovzhodne Evrope z električno energijo z oceno vloge premoga ter premogovnih tehnologij

Strategic aspects of electricity power supply in central and south - eastern Europe - The role of coal and coal technologies evaluation

MILAN MEDVED¹, EVGEN DERVARIC², GORAZD SKUBIN³

¹Premogovnik Velenje d.d., Partizanska cesta 78, SI-3320 Velenje, Slovenija;
E-mail: milan.medved@rlv.si

²Univerza v Ljubljani, Naravoslovnotehniška fakulteta, Aškerčeva cesta 12,
SI-1000 Ljubljana, Slovenija; E-mail: evgen.dervaric@ntf.uni-lj.si

³ENERGORA energetska svetovanje d.o.o., Sostrska cesta 43 a, SI-1261 Dobrunje,
Slovenija; E-mail: info@energora.si

Received: January 8, 2008

Accepted: June 3, 2008

Izvleček: Premog je vedno igral ključno vlogo pri proizvodnji električne energije in takšno vlogo bo vsekakor imel tudi v prihodnje. Nikjer na svetu v naslednjih desetletjih premoga ne bo mogoče nadomestiti. Podpora pri nadaljnji uporabi premoga, sprejemljivost na trgu in v okolju pa bo pomembna politična naloga za Evropo. Zaradi pomanjkanja primarnih energentov se morajo države Evropske Unije nenehno bojevati proti čedalje večji energetski odvisnosti od uvožene nafte in zemeljskega plina s strategijo varne in stabilne oskrbe. Ob racionalni rabi energije in povečani uporabi obnovljivih virov energije, je premog glavni doprinos k stabilnim cenam in varni oskrbi z električno energijo. Premog ima izredno dolgoročno perspektivo in dobro konkurenčno pozicijo za energetska oskrba Evrope. Dolgoročno spreminjanje cen elektrike temelji med drugim tudi na uporabi premoga in nuklearne energije. Do leta 2020, je prioriteta gradnja novih in modernizacija obstoječih termoelektrarn ter posledično s tem povečanje učinkovitosti. Uporaba premoga za pridobivanje električne energije bo v glavnem odvisna od cen plina in stroškov za izpust CO₂. Predvsem pa se bo položaj izboljšal zaradi dviga cen zemeljskega plina. Uvedba trgovanja z emisijami lahko močno spremeni strukturo proizvodnje elektrike v Evropi in s tem močno obremeni države, ki v glavnem uporabljajo premog.

Abstract: Throughout the world, coal cannot be replaced during the next decades. Facilitating further coal use, acceptable to the market and the environment, is an important political task for Europe. The EU must fight with deter-

mination against its increasing dependence on imported oil and gas with a strategy balanced between security of supply and sustainability. In addition to the rational use of energy and the increased use of renewable energies, coal makes a major contribution above all to stable prices and security of supply. Coal has outstanding long-term perspectives and a good competitive position for power generation in Europe. The moderate development of electricity prices in the long-term is the result of the use of coal and nuclear energy. Until 2020, the focus is on construction and modernization of existing power plants, and thereby improved efficiency. The use of coal for power generation will mainly be determined by the level of prices for gas and by CO₂ costs. Above all with rising prices for gas, the market position of coal for power generation continues to improve. The implementation of Emissions Trading can greatly change the structure of power generation in Europe and especially burden countries that use a lot of coal.

Ključne besede: premog, premogovne tehnologije, električna energija, energetske viri, konkurenčnost, varnost, zanesljivost

Key words: coal, coal technologies, electricity, energy sources, competitiveness, security, reliability

Uvod

Današnji svet se vse bolj sooča s skokovitim tehnološkim razvojem, poraba električne energije pa ob tem nezadržno narašča. Na drugi strani smo priča vse bolj zaskrbljujočemu zmanjševanju rezerv klasičnih primarnih energentov kot je to premog, surova nafta in zemeljski plin.

Obnovljivi viri energije kot so to voda, veter in sonce še zdaleč ne bodo pokrili vseh potreb človeštva po kvalitetni energiji kot je električna. Tako bo še dolgo eden izmed glavnih virov proizvodnje električne energije poleg plina in jedrske energije tudi premog. Na žalost pa je porazdelitev nahajališč premoga neenakomerna in na žalost v večini primerov ne sovпада z velikimi centri porabe električne energije.

V zadnjem obdobju pa smo priča tudi izjemno hitremu porastu porabe električne

energije na področju Jugovzhodne Evrope, ki sovпада z zastarelostjo voznega parka proizvodnih objektov in pomanjkanjem vlaganj v nove proizvodne objekte. Razmere glede pokritosti porabe električne energije z lastnimi proizvodnimi viri precej nihajo od države do države v regiji. Drug pomemben faktor pa je tudi struktura proizvodnih virov posamezne države. Poleg vodnih virov in manjšega dela nuklearne energije, bazira ves ostali del proizvodnje električne energije na premogu in tekočih ter plinastih gorivih.

VLOGA IN POMEN PREMOGA V PRIHODNOSTI EVROPE

Premog je vir energije, ki je vitalnega pomena za Evropo. Po podatkih Euracoal Market Report 2007 je v zadnjih petih letih poraba v EU 15 naraščala za ca. 1 % na leto in znaša trenutno povprečno 314 milijonov ton premoga (Mt). V novih državah članicah (EU

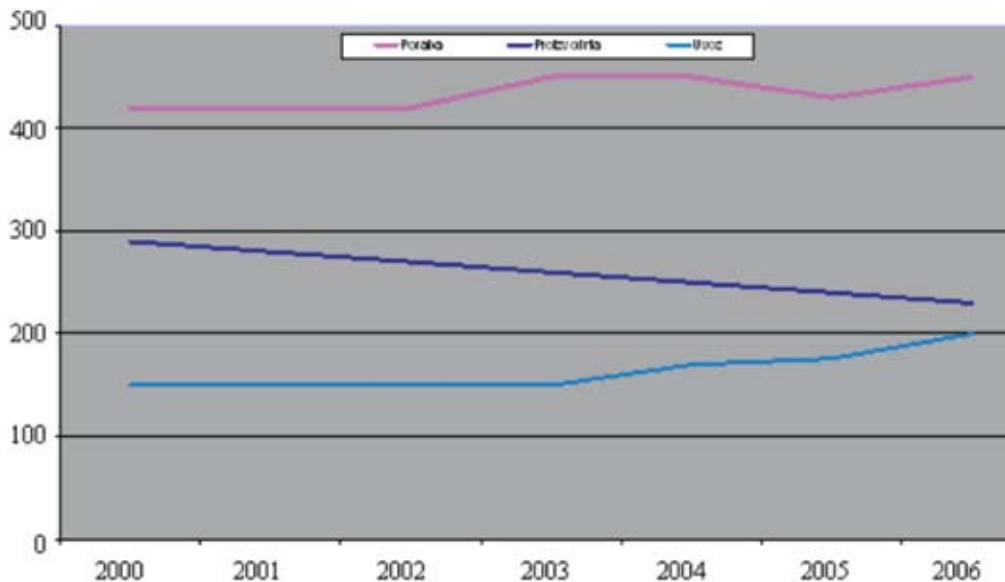
12), je poraba povprečno 145 Mt. V ostalih sosednjih evropskih državah predstavljajo potrebe okoli 60 Mt. Potrebe v Rusiji in drugih državah bivše Sovjetske zveze so okoli 250 Mt. S povprečno 750 Mt skupaj je Evropa, vključno z Rusijo tretji porabnik na svetu za Severno Ameriko in Kitajsko. Evropa predstavlja delež ca. 15 % svetovne porabe premoga. V EU 27 bo premog postopoma pokrival petino potreb po primarni energiji.

Največji porabnik premoga v EU je Nemčija, sledi pa ji Poljska. Evropa lahko pokrije velik delež potreb po premogu iz lastnih virov. Z letno proizvodnjo 315 Mt predstavlja Evropa (brez nekdanje Sovjetske zveze) 8 % svetovne proizvodnje. Ostale sosednje države proizvedejo enako količino kot Evropa. Tudi glede proizvodnje sta Poljska in Nemčija v vrhu EU. Skupaj imata dvotretjinski

delež celotne proizvodnje v EU. Češka republika, Grčija, Španija in Anglija prav tako spadajo med glavne proizvajalce premoga v EU. Pomembni proizvajalci na jugovzhodu Evrope so še Madžarska, Romunija in Bolgarija. Premog se, kakorkoli že, pridobiva tako v državah članicah EU kot v pridruženih članicah in tistih, ki še čakajo na pridružitve. Z deležem pod 5 % svetovnih zalog premoga, razpolaga Evropa z dovolj rezervami. Črni premog, lignit in rjavi premog je na voljo.

Vitalen pomen premoga za EU oskrbo z energijo se odseva tudi v povečevanju uvoza. Okoli 200 Mt premoga se za pokrivanje potreb letno uvozi predvsem iz Južne Afrike, Avstralije, Kolumbije pa tudi Rusije in Ukrajine.

Proizvodnja, uvoz in poraba premoga v EU 27 v Mt



Slika 1. Proizvodnja, uvoz in poraba premoga v EU 27 v Mt (World Coal Institute, 2005)

Figure 1. Production, import and consumption of coal in EU 27 in Mt (World Coal Institute, 2005)

Premog igra pomembno vlogo predvsem pri zagotavljanju varne in konkurenčne oskrbe elektrarn v EU. Več kot četrtina elektrike v EU je pridobljene iz premoga. Ob dinamičnem povečanju potreb za povprečno 2 % vsako leto je varna, konkurenčna in okolju prijazna proizvodnja energije velikega pomena za energetska politiko EU.

Potreba po električni energiji se nadpovprečno povečuje, predvsem v južnih državah članicah, letno do 5 %. Tehnološka in ekonomska integracija na evropski trg z električno energijo zahteva globalno strategijo za zagotavljanje zadostne oskrbe z električno energijo, ki temelji na zanesljivih in razpoložljivih virih energije. Uporaba premoga za elektrarne ostaja torej ključnega pomena za prihodnost Evropske unije.

Prihodnje odločitve evropske energetske politike igrajo glavno vlogo za prihodnjo strukturo evropske energetske proizvodnje. Evropska odvisnost od povečevanja uvoza nafte in plina terja odgovor. Tehnološka politika, ki promovira energijo brez emisij se že izvaja. V EU mnoge države članice podpirajo pospešen razvoj uporabe obnovljivih virov, neodvisnih od hidrologije, do leta 2020. To je zelo ambiciozen projekt, katerega posledica so velike spremembe v virih energije za oskrbo z elektriko v Evropi in ki zahteva nov pristop do varne oskrbe z električno energijo in nova omrežja. Skladno z evropsko shemo trgovanja z emisijskimi certifikati CO₂, se že kaže učinek truda za zmanjšanje emisij CO₂ v energetska ekonomiji.

Glavno breme glede zmanjševanja emisij pa nosijo termoelektrarne. Do leta 2020 bo manj tržno vodenih konstrukcij kakor je bilo pričakovano. Kombinacija premoga in plina zapolnjuje vrzel, ki je nuklearna energija in energija iz obnovljivih virov ne moreta zapolniti, glavna ovira pa je cena premoga, plina in CO₂.

REZULTATI ENERGETSKIH SCENARIJEV

Študija o bodoči vlogi premoga v Evropi (Euracoal, 2007), izdelana pod okriljem EURACOAL-a in ob pomoči mnogih evropskih podjetij in združenj ne predstavlja ciljnih vrednosti ali ponavlja poznane mnenja sektorja. Širok spekter različnih scenarijev je bil izbran kot metoda za analizo. Upoštevati je bilo možno širok spekter različnih faktorjev in njihov vpliv na trg z električno energijo, predvsem pa na premog, pri čemer so pristopi transparentni. Multifaktorski pristopi so obrazloženi in vplivajo na odločitve glede energetske politike ali na spremembe na mednarodnih trgih z električno energijo. EURACOAL predvideva, da bo ta analiza predstavljala v bodoče osnovo za mnoge razprave in konzultacije.

Osnovni scenarij: Karakteristika – visoke cene energije kakor tudi nizki stroški za CO₂, ki izhajajo iz mednarodnih odločitev in so koordinirani s strani klimatske politike. Osnovni ekonomski podatki kot predpostavke glede trendov cen in porabe energije temeljijo na napovedi "Trendi do 2030 (od 2005)" Evropske komisije, Direktorat za energijo in transport (EC – Directorate General for Energy and Transport, 2007).

Politika 15, 30, 45 scenarij: Temelji na predpostavki različne politike do klimatskih sprememb, različni stroški za CO₂ od 15, 30 ali 45 € za tono ogljikovega dioksida. Predvidene so visoke cene električne energije.

Politika nizkih cen energije 15, 30, 45 scenarij: Ta scenarij analizira dva različna klimatska pristopa z različnimi cenami energije.

Tehnološki 30 scenarij: Ta scenarij analizira pospešen tehnološki razvoj novih tehnologij elektrarn vključno z zajemom in skladiščenjem CO₂ (CCS) in relativno visoke stroške CO₂.

Tehnološki 45 scenarij: Ta scenarij temelji na predpostavki ambiciozne tehnološke strategije za določene zmožljive termoelektrarne brez emisij in razvoju nuklearne energije z visokimi cenami za CO₂.

Analiza predpostavk, ki se nanašajo na bodoče cene energije temelji na raziskavi "Trendi do 2030 (od 2005)" v EU (EC – Directorate General for Energy and Transport, 2007). Današnja pričakovanja, ki se nanašajo na razvoj cen v prihodnje so višja kot je napoved.

Analize vseh scenarijev pripeljejo do zaključka, da bo evropska energetika leta 2030 še vedno odvisna od fosilnih goriv. In sicer zaradi cene in varne oskrbe bodo nujno potrebni vsi viri energije. Razlika v ceni med plinom in premogom bo odločala o bodoči vlogi termoelektarn znotraj Evrope. Različni stroški za CO₂ imajo z ekonomskega vidika visok vpliv zaradi ob-

veze zmanjševanja emisij zaradi klimatske zaščite.

Relativno visoke cene energije povzete v osnovnem scenariju v povezavi z nizkimi cenami CO₂ povečujejo delež premoga pri uporabi v termoelektarnah. Glede na to, da ostajajo cene plina visoke je uporaba tega goriva na evropskem trgu edina konkurenčna s cenami za CO₂ več kot 30 € na tono. Za večji padec izpusta CO₂ bi morala biti cena najmanj 45 € na tono. Z novimi cenami zemeljskega plina ostaja premog konkurenčen dokler bo cena za CO₂ ostala na 15 € za tono. Ob povečanju cene za CO₂ bo premog izgubil prednost pred plinom. Pri ceni nad 30 € bo prednost na strani zemeljskega plina. Povečevanje potreb po plinu pa bo povišalo ceno le tega, to pa bo ponovno izravnalo razliko v konkurenčnosti.

KLIMATSKA ZAŠČITA OB UPORABI SODOBNIH TEHNOLOGIJ

V primerjavi izpusta CO₂ v evropskih termoelektarnah v letu 2005 in sicer 1.275 milijard ton je znižanje do 2030 možno doseči le z visokimi cenami za CO₂ in vplivom na ceno zemeljskega plina. Pomembno znižanje izpusta CO₂ okoli 774 Mt bi bilo recimo možno, če bi kombinirali uporabo CCS tehnologije (zajem in skladiščenje CO₂), z uporabo nuklearne energije. Po letu 2020, bodo elektrarne s CCS že na trgu, cene elektrike in CO₂ pa visoke. Če se bodo stroški za zaščito klime znižali se bo konkurenčnost klasičnih termoelektarn pokrila s ceno CO₂ pod 30 € (EC – Directorate General for Energy and Transport, 2007).

Po mnenju premogovništva in skladno z evropsko energetske politiko bi morale imeti termoelektrarne s CCS sistemom prednost pred zemeljskim plinom. Ne le, da se cene zemeljskega plina strmo dvigajo tudi stroški elektrarn se višajo, pri tem pa se povečuje riziko zagotavljanja dobav v EU. CCS (zajem in skladiščenje CO₂) tehnologija posledično tudi bistveno bolj zmanjšuje količine CO₂ kakor preklon na druga goriva z manjšo vsebnostjo CO₂. Analiza ne upošteva še dodatnega zmanjševanja CO₂, ki bi bilo posledica še večje uporabe obnovljivih virov energije kakor je to predvideno v osnovnem scenariju EU. Še več, posledice klimatske politike, ki mednarodno ni usklajena glede konkurenčnosti, zmanjševanja porabe in izpusta CO₂ še niso predvidene.

Da bi zagotovili trajne rešitve glede klimatskih pogojev in zmanjšali odvisnost od uvoženih virov energije po spremenljivih cenah je opcija uporaba vseh razpoložljivih alternativ za pridobivanje energije v Evropi. To pa vključuje tako racionalno rabo energije, izboljšan izkoristek v termoelektrarnah, nuklearno energijo, zajem in skladiščenje CO₂. Vse to pa zahteva intenzivno raziskavo in razvoj na vseh področjih, vključno s čistimi tehnologijami premoga.

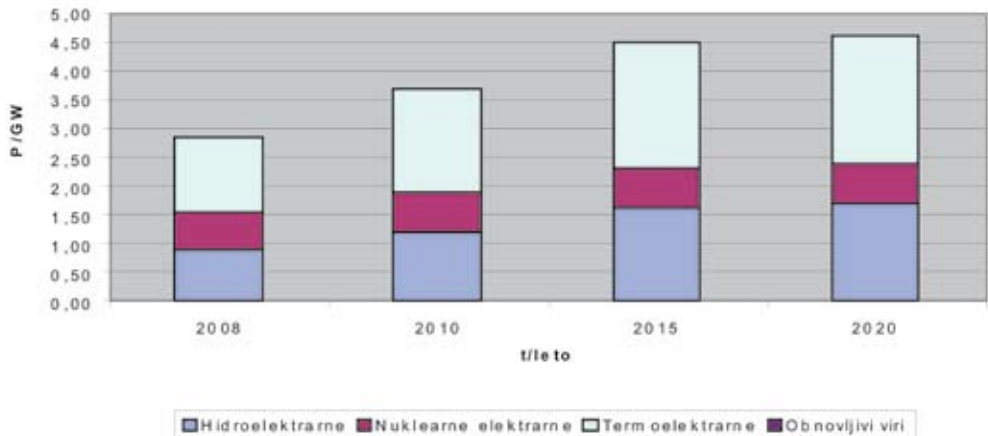
Že s cenami za CO₂ pod 30 € za tona, so termoelektrarne na premog s tehnologijo CCS konkurenčne na liberaliziranem trgu z električno energijo. Potrebno pa bo spodbujati CCS. Če se bo sistem CCS uporabljal v vseh elektrarnah na fosilna goriva po letu 2020, bodo elektrarne, ki uporabljajo črn premog in lignit mnogo doprinesle k oskrbi EU z električno energijo.

Cene elektrike v EU se bodo v obdobju do 2030 povečale zaradi povečevanja potreb, višjih cen goriv in kapitalno intenzivnejših tehnologij. Predviden dvig je med 0,4 in 1 % na leto glede na razvoj individualnih faktorjev. Za leto 2030 so predvideni stroški proizvodnje električne energije med 58 in 73 €/MWh. Pri tem je 2 € pa do 12 € še za kupone CO₂. Zelo pomembno je upoštevati da CCS tehnologija ne vpliva na najvišje cene elektrike. To dokazuje, da je v EU z reduciranjem emisij možno vplivati na ceno elektrike, brez da bi se morali odreči varni oskrbi in potencialu premoga.

PROIZVODNJA IN PORABA ELEKTRIČNE ENERGIJE V SLOVENIJI

V Sloveniji je trenutno instaliranih 2,77 GW proizvodnih zmogljivosti. V letu 2007 je bilo večino električne energije proizvedeno v nuklearni elektrarni Krško (NEK), ki je predstavlja kar 42 odstotni delež vse proizvedene energije v Sloveniji. Z 32 odstotki ji je sledila proizvodnja električne energije v termoelektrarnah (TE) ter s 26 odstotki proizvodnja hidroelektrarn. Višino instaliranih proizvodnih virov ter strukturo instalirane proizvodnje, od leta 2008 do 2020 prikazuje Slika 2.

Glede na obstoječe in predvidene objekte, ki so in bodo vključeni v elektroenergetsko omrežje (EEO), se v tej regiji še naprej predvideva negativna elektroenergetska bilanca. Tako bo Slovenija tudi v prihodnosti neto uvoznik z električno energijo s povprečnim letnim uvozom v višini 2,9 TWh.



Slika 2. Struktura proizvodnje v Sloveniji
Figure 2. Production structure in Slovenia

PREGLED STANJA NA PODROČJU OSKRBE Z ENERGIJO IN PREMOGOM V SLOVENIJI

Slovenija nima pomembnih primarnih energetskega virov. Edine domače dokazane energetske rezerve so 51,8 Mtce (Million tonnes coal equivalent) lignita. Od osamosvojitve leta 1991 je Slovenija zabeležila stalno gospodarsko rast in med leti od 1992 do 2002 se je državna poraba primarne energije povečala za več kot 25 % na okoli 8,5 Mtce. Nafta ima največji delež na tem trgu z 39 %, sledijo ji nuklearna energija z 21 %, premog z 19 % (uvožen premog 4 % in domač lignit 15 %) in zemeljski plin z 13 %.

Okoli 60 % državnih primarnih potreb po energiji je uvoženih. Skoraj tri četrtine teh uvoženih goriv je nafta in ena četrtina je plin. Uvoz je se je povečal za več kot 50 % od leta 1992 do leta 2002.

Nacionalna poraba elektrike je porasla na 13,29 TWh v 2006, kar predstavlja porast za 3,3 % glede na prejšnje leto. Nacionalna proizvodna moč glavnih elektrarn v letu 2006 je bila 10,8 TWh in sicer s proizvodnjo termoelektarn 7,2 TWh in hidroelektarn 3,6 TWh. Nuklearna elektrarna Krško ima predvideno proizvodnjo 700 MW, proizvedena pa je 5,2 TWh električne energije v letu 2006. Termoelektarni v Šoštanju in Trbovljah, obe uporabljata za gorivo domač premog in proizvedeta 3,5 TWh in 0,6 TWh.

Slovenija je sprejela nacionalni energetskega načrt, ki je oblikovan tako, da ščiti javne infrastrukture in podpira privatno vlaganje v izgradnjo energetskega objektov. Povečana energetska zmogljivost je ena od prioriteta tega načrta. Slovenija ima dve podzemni nahajališči lignita in rjavega premoga, eno v Velenju na severu države, in enega v

osrednji Slovenji, v Trbovljah. Ta dva premogovnika sta izkopala 4,6 Mt lignita in rjavega premoga v letu 2006.

Velenjski bazen pokriva območje 21 km². Debelina sloja lignita je od 20 do 160 m in na globini med 140 m in 500 m. Odkopavanje poteka po svetovno znani in inovativni Velenjski odkopni metodi. Premog je v celoti (4 Mt) namenjen termoelektrarni Šoštanj, ki ima zmogljivost 750 MW.

Rudnik Trbovlje je izkopal 0,6 Mt rjavega premoga v letu 2006, večina je bila porabljena v termo elektrarni Trbovlje.

PREGLED DOLGOROČNIH POTREB PO ELEKTRIČNI ENERGIJI IZ PREMOGA V EU

Večina evropskih držav (Euracoal, 2005) napoveduje do pet odstotno povečanje porabe električne energije do leta 2010 in do dvajset odstotno povečanje do leta 2020. Skladno z Evropsko direktivo ter emisijskimi standardi se do leta 2010 načrtuje ustavitve instaliranih proizvodnih termo enot, ki ne izpolnjujejo okoljevarstvenih standardov ter povišanje instaliranih proizvodnih enot z obnovljivimi viri. V Franciji imajo v planu izgradnjo vetrne elektrarne s skupno instalirano močjo 14 GW.

Zaradi velikega deleža hidroelektrarn je proizvodnja in pokrivanje porabe z lastnimi viri v Avstriji in Švici zelo odvisna tudi od vremenskih vplivov, kar lahko povzroči velike primanjkljaje in s tem povezan uvoz električne energije. Francoski in belgijski elektroenergetski sistem večino električne energije proizvedeta v nuklearnih elektrarnah. Ostale države v Evropski uniji po-

memben delež električne energije proizvedejo v termoelektrarnah, predvsem Grčija in Nizozemska z 90 odstotnim deležem. Slovenija, Hrvaška, Italija, Madžarska, Belgija in Nizozemska so uvozniki električne energije, medtem ko imajo Nemčija, Češka, Slovaška in Poljska strategijo pokrivanja porabe naravnano k pozitivni bilanci sistema, s čimer bodo te države do leta 2010 neto izvozniki z električno energijo. Bosna in Hercegovina je edina država na jugovzhodnem delu Evrope, ki še vedno izvažata precejšnje količine elektrike. V kolikor bi se v prihodnosti cena električne energije na evropskem trgu bistveno povečala, je Italija sposobna s svojimi proizvodnimi viri pokriti obremenitev v sistemu in postati izvoznik električne energije. Velika Britanija je eden največjih porabnikov elektrike v Evropi, ni pa sinhronizirana z evropskim omrežjem v okviru UCTE.

RAZPOLOŽLJIVE ZMOGLJIVOSTI TERMOELEKTRARN NA TRDA GORIVA

Instalirane moči elektrarn na premog se bodo po podatkih raziskave Coal – Secure Energy- WCI do leta 2020 predvidoma povečale v Avstriji iz 5,5 na 6,1 GW, v Bosni in Hercegovini iz 1,8 na 2,1 GW, v Nemčiji iz 45 na 51 GW, na Nizozemskem iz 3,31 na 4,72 GW, v Srbiji iz 5,65 na 6,8 GW, na Češkem iz 10 na 12 GW in v Bolgariji iz 6,47 na 7,07 GW. Odstotno največje povečanje moči elektrarn bodo dosegle Belgija (0,24 na 1,4 GW), Švica (0,7 na 1,6 GW), Hrvaška, Slovenija in Črna Gora, kar pa v številkah ne pomeni veliko v evropskem merilu. Približno na enaki moči nameravajo ostati v Španiji s 16 GW, v Grčiji s 4,81 GW, v Makedoniji, v Zahodni Ukrajini in v Romu-



Slika 3. Pregled proizvodnih zmogljivosti za proizvodnjo električne energije iz črnega premoga, lignita in rjavega premoga v Evropi (Energora, 2007)

Figure 3. Production capacities for electricity output from coal in Europe (Energora, 2007)

niji (5 GW). Zmanjšanje nameščene moči do leta 2020 pričakujejo v Franciji iz 8,21 na 5,82 GW, na Portugalskem, v Italiji, na Poljskem iz 29 na 18 GW in na Slovaškem. Skupno se bo v vseh obravnavanih državah nameščena moč termoelektrarn na premog predvidoma znižala iz 160 GW leta 2008 na 150 GW leta 2020.

REZERVE IN LETNI IZKOP PREMOGA V DRŽAVAH EU

Evropa lahko pokrije velik delež potreb po premogu iz lastnih virov. Premog se prid-

biva tako v državah članicah EU kot v pridruženih članicah in tistih, ki še čakajo na pridružitve. Z deležem pod 5 % svetovnih zalog premoga (Euracoal, 2004), razpolaga Evropa z dovolj rezervami. Poljska in Nemčija imata skupaj dvotretjinski delež celotne proizvodnje v EU. Češka republika, Grčija, Španija in Anglija spadajo med glavne proizvajalce premoga v EU, pomembni proizvajalci na jugovzhodu Evrope pa so še Madžarska, Romunija in Bolgarija. Pomen premoga za oskrbo z energijo v Evropi se odseva tudi v povečevanju uvoza, predvsem iz Južne Afrike, Avstralije, Kolumbije, Indonezije in Ukrajine.

V Avstriji ne obstajajo zaloge premoga, ki bi upravičevale komercialno izkoriščanje, zato tudi iz teh razlogov ne predvidevajo izgradnje termoelektarn, ki bi kot energent uporabljale premog. Slovenija nima pomembnih primarnih energetskih virov. Edine domače dokazane energetske rezerve so 51,8 Mtce lignita. Hrvaška, Italija in Švica prav tako ne razpolagajo z rezervami premoga. Francija je ekonomsko gledano peta največja industrijska država, zaloge fosilnih goriv pa ima zelo omejene. Tudi Madžarska in Grčija imata dokaj skromne energetske rezerve. Na Slovaškem, v Belgiji in na Nizozemskem ostaja uvožen premog pomemben energent. Srbija ima omejene vire energije, lignit pa predstavlja

stalen vir pri energetski oskrbi. Za elektrarne uporabljajo lasten premog v Bosni in Hercegovini. Nahajališča rjavega premoga in lignita so na različnih lokacijah. Na Češkem, v Španiji, Bolgariji in Romuniji ima premog precejšen pomen kot energent. Politika ravnanja s surovinami je usmerjena v učinkovito pridobivanje trdih goriv iz nahajališč, ki so trenutno aktivna.

Poljska ima zalog premoga za 10 milijard tce, glavna nahajališča črnega premoga pa so v gornji Šleziji in v bazenu Lublin. Rezerve lignita, ki se trenutno odkopavajo znašajo več kot 500 Mtce. Črni premog in lignit pokrivata 68 % poljskih potreb po primarnih surovinah. Izvoz črnega pre-



Slika 4. Pregled zalog črnega premoga, lignita in rjavega premoga v Evropi (Energora, 2007)

Figure 4. Coal reserves in Europe (Energora, 2007)



Slika 5. Letni izkop črnega premoga, lignita in rjavega premoga v Evropi (Energora, 2007)
Figure 5. Annual coal output in Europe (Energora, 2007)

moga iz Poljske znaša 21 Mt na leto, eno tretjino se ga pretransportira po železnici v sosednje države, dve tretjini pa se izvozi preko pristanišč v Baltiku.

Nemčija ima največje zaloge črnega premoga (21,6 Gtce) in lignita (12,8 Gtce) v Evropi in s tem je to tudi najpomembnejše gorivo za to državo. V letu 2004 je nemški trg porabil 66,5 Mtce. Pregled zalog premoga v posameznih državah je prikazan v Sliki 4.

VKLJUČITVE IN IZKLJUČITVE PROIZVODNIH VIROV V EU

Preprost pregled vključevanja in zausta-

vitev proizvodnih enot v oziroma iz prenosnega omrežja do leta 2010 prikazuje Tabela 1, v kateri so prikazane vsote moči proizvodnih virov, ki bodo zaustavljene ali pa priključene na elektroenergetsko omrežje.

Iz Tabele 1 je razvidno, da se v letu 2008 pričakuje veliko zaustavljanje proizvodnih enot, ko nameravajo v Nemčiji zmanjšati proizvodne zmogljivosti za 8300 MW. Sledita ji še Bolgarija in Romunija z zmanjšanjem proizvodnih zmogljivosti za 700 MW oziroma 600 MW. Trend vključevanja novih proizvodnih enot se bo nadaljeval v Italiji, kjer so v letih 2006 v obratovanje vključili za 1500 MW novih proizvodnih zmogljivosti, v letu 2007 pa 4700 MW no-

Tabela 1. Pregled vključevanja in zaustavitve instaliranih proizvodnih enot v GW
Table 1. Inclusion and exclusion review of production capacities in GW

Država	2008	2009	2010
Avstrija	-	-	-
Slovenija	0,2	0,1	0,1
Hrvaška	-	-	-
Italija	3,9	0,9	0,9
Švica	-	-	-
Nemčija	-8,3	2,9	2,8
Češka republika	0,1	-0,1	-0,1
Slovaška	-0,2	-0,2	-0,2
Poljska	0,7	0,3	0,3
Madžarska	0,1	0,1	0,1
Francija	0,4	0,4	0,3
Španija	3,3	0,8	0,8
Portugalska	0,8	1	1
Belgija	-	0,1	-
Nizozemska	0,2	0,2	0,1
Bosna in Hercegovina	-	-	-
Srbija in ČG	-	-	0,1
Make donija	-	-	-
Grčija	0,6	-0,1	-0,1
Romunija	-0,6	-0,3	-0,3
Bolgarija	-0,7	0,1	-

vih proizvodnih zmogljivosti. V letu 2008 planirajo povečanje instaliranih proizvodnih zmogljivosti za 3900 MW ter povečanje za 900 MW v letih 2009 in 2010. Poleg Italije so predvidene vključitve večjih proizvodnih enot v obratovanje v Nemčiji, Španiji in na Poljskem. V Nemčiji tako pričakujejo vključitev v obratovanje 3800 MW instaliranih proizvodnih enot v letu 2008, 2900 MW instaliranih proizvodnih enot v letu 2009 in 2800 MW instaliranih proizvodnih enot v letu 2010. V Španiji se pričakuje vključitev v obratovanje za 3300 MW instaliranih proizvodnih enot v letu 2008 in 800 MW instaliranih proizvodnih enot v letih 2009 in 2010. Na Poljskem se

pričakuje nekoliko manjše vključevanje proizvodnih enot v obratovanje, saj predvidevajo v letu 2008 za 800 MW instaliranih proizvodnih enot ter v letih 2009 in 2100 za 1000 MW instaliranih proizvodnih enot.

RAZPOLOŽLJIVE KAPACITETE ZAUSTAVLJENIH ENOT V EU

Tabela 2 prikazuje pregled razpoložljivih instaliranih proizvodnih enot od leta 2008 do leta 2020 za vse obravnavane države. Iz tabele je razvidno, da ima na razpolago največ prostih proizvodnih zmogljivosti

Tabela 2. Pregled razpoložljivosti proizvodnje iz zaustavljenih proizvodnih enot v GW
Table 2. Availability review of excluded production capacities in GW

Država	2008	2010	2015	2020
Avstrija	2,90	2,90	2,90	2,90
Bosna in Hercegovina	0,70	0,70	0,70	0,70
Belgija	1,04	1,29	1,54	1,72
Švica	4,40	4,60	4,70	4,80
Nemčija	28,62	34,23	43,94	53,27
Francija	17,09	17,02	23,02	27,52
Hrvaška	0,20	0,20	0,20	0,20
Luxemburg	0,03	0,04	0,04	0,07
Nizozemska	2,79	3,37	6,45	7,52
Slovenija	0,30	0,45	0,45	0,45
Španija	25,48	30,54	34,32	40,20
Portugalska	3,55	4,63	5,84	6,35
Italija	15,60	20,30	22,40	23,90
Srbija	1,00	2,10	2,10	2,10
Črna Gora	0,20	0,20	0,30	0,30
Grčija	1,20	3,20	3,20	3,20
Makedonija	0,19	0,19	0,19	0,19
Češka	2,00	2,40	2,50	2,50
Madžarska	0,60	0,65	0,70	0,75
Poljska	2,40	3,80	4,80	4,60
Slovaška	1,90	1,94	1,90	1,99
Zahodna Ukrajina	0,28	0,14	0,09	0,04
Romunija	3,74	3,81	6,03	6,26
Bolgarija	2,10	2,10	2,10	2,10

Francija, ki je tudi največja izvoznica z električno energijo. Presežki proizvodnih zmogljivosti v Franciji so v glavnem v nuklearnih in klasičnih termoelektrarnah in se gibljejo med 10,3 in 12,3 GW. Sledijo ji Španija z 11 GW presežnih zmogljivosti, ki se nahajajo v klasičnih termoelektrarnah in hidroelektrarnah, Poljska z 8 GW presežnih proizvodnih zmogljivosti v termoelektrarnah in Nemčija z 9 GW presežnih zmogljivosti predvsem v dokaj starih termoelektrarnah na premog in v elektrarnah na veter. Italija ima prav tako na razpolago

veliko prostih proizvodnih zmogljivosti v termoelektrarnah na mazut, ki pa zaradi visokih proizvodnih stroškov večinoma ne obratujejo.

V kolikor se bodo pogoji na trgu spremenili, in bo cena električne energije dosegla lastno proizvodno ceno, lahko pričakujemo, da bo Italija bistveno povečala proizvodnjo v domačih elektrarnah in posledično zmanjšala njen uvoz. Veliko razpoložljivih proizvodnih kapacitet v hidroelektrarnah imajo tudi Avstrija (5

GW) in Švica (4 GW), katerima sledijo še Romunija s 3 GW presežnih proizvodnih zmogljivosti v termoelektrarnah in hidroelektrarnah, Češka z 2,5 GW presežkov v termoelektrarnah in Portugalska z 1,7 GW rezerv v dokaj dragih termoelektrarnah in hidroelektrarnah.

OCENA ZADOSTNOSTI OSKRBE Z ELEKTRIČNO ENERGIJO V EU

V tem poglavju bomo ugotavljali, kakšna je pričakovana zadostnost virov na območju jugovzhodne in centralne Evrope do leta 2020. Podatke o tem dobimo iz periodičnega poročila o zadostnosti oskrbe v kontinentalni Evropi, ki ga pripravlja združenje sistemskih operaterjev UCTE (Union of the Co-ordination of Transmission of Electricity). Vrednosti v nadaljevanju podajajo presežek proizvodnje v izbranih referenčnih urah v posameznem letu.

Tabela 3. Presežek proizvodnje
Table 3. Remaining capacity

GW	2007	2010	2015	2020
Presežek CE	41,77	45,06	46,93	37,81
Presežek JV	3,87	4,48	6,90	5,62

Presežek (Remaining capacity) v Tabeli 3 predstavlja razliko med zanesljivo razpoložljivimi proizvodnimi zmogljivostmi (Reliably available capacity) ter odjemom (Load) v skladu s študijo UCTE System Adequacy Forecast 2007 – 2020, scenarij B. Scenarij B je bil izbran zato, ker daje najboljši približek pričakovanih investicij v proizvodnjo za razliko od scenarija A,

ki upošteva le (danes) zanesljivo potrjene investicije.

Za izpeljavo ocene zadostnosti oskrbe v območjih CE in JV Evrope moramo presežek primerjati z referenčno vrednostjo zadostnosti (Adequacy Reference Margin), ki podaja oceno negotovosti obratovanja proizvodnje in odjema. Referenčno vrednost zadostnosti je UCTE definiral z vsoto dveh členov. Prvi je 5 % razpoložljive proizvodnje, drugi pa razlika med dnevnim končnim odjemom in odjemom v referenčni uri, t.i. Margin against Daily Peak Load.

Pri oceni zadostnosti na opisan način bi odštevanje odjema od presežka proizvodnje (dve veličini z veliko vrednostjo, ki tvorita malo razliko) ter nadaljnja primerjava te razlike z referenčno vrednostjo zadostnosti (ARM – majhna vrednost) predstavljalo kritično operacijo in s tem povezano veliko negotovost rezultata. Ob upoštevanju surovih podatkov iz UCTE poročila, bi ocena zadostnosti med letoma 2015 in letom 2020 preveč in neutemeljeno nihala, zato surove vrednosti zgladimo z linearno aproksimacijo. Takšen način obravnave rezultira v stabilnem trendu spremembe razmer na področju zadostnosti oskrbe saj nas ne zanimajo razmere v ozki časovni periodi v prihodnosti, ampak stremimo k dolgoročno stabilnemu trendu napovedi.

Ob primerjavi linearizirane relativne ocene zadostnosti za območje CE in JV Evrope ugotovimo, da se bo relativna ocena zadostnosti v CE zmanjšala iz 59,10 % na 27,94 %, to je za 31,16 % (-). Pri JV se bo relativna ocena zadostnosti povečala iz -7,96 % na 11,26 %, to je za 19,22 % (+).

Tabela 4. Zadostnost oskrbe v centralni Evropi**Table 4.** Adequacy reference margin in CE

CE	Enota	2007	2010	2015	2020
Razpoložljiva proizvodnja (AC)	GW	396,37	415,80	448,17	480,54
Zanesljivo razpoložljiva proizvodnja (RAC)	GW	280,52	288,44	301,65	314,85
Odjem (LOAD)	GW	235,95	244,71	259,31	273,90
Razlika med koničnim in referenčnim odjemom (MADPL)	GW	8,19	8,14	8,06	7,98
Presežek proizvodnje (RC)	GW	44,56	43,73	42,34	40,95
Referenčna vrednost zadostnosti (ARM)	GW	28,01	28,93	30,47	32,01
Absolutna ocena zadostnosti (RC – ARM)	GW	16,55	14,80	11,87	8,94
Relativna ocena zadostnosti (RC – ARM)/ARM	%	59,10	51,14	38,95	27,94

Tabela 5. Zadostnost oskrbe v JV Evropi**Table 5.** Adequacy reference margin in SE Europe

JV Evropa	Enota	2007	2010	2015	2020
Razpoložljiva proizvodnja (AC)	GW	52,19	55,34	60,59	65,84
Zanesljivo razpoložljiva proizvodnja (RAC)	GW	33,39	36,18	40,82	45,47
Odjem (LOAD)	GW	29,17	31,46	35,27	39,07
Razlika med koničnim in referenčnim odjemom (MADPL)	GW	1,97	2,08	2,27	2,46
Presežek proizvodnje (RC)	GW	4,21	4,72	5,56	6,40
Referenčna vrednost zadostnosti (ARM)	GW	4,58	4,85	5,30	5,75
Absolutna ocena zadostnosti (RC – ARM)	GW	-0,36	-0,13	0,26	0,65
Relativna ocena zadostnosti (RC – ARM)/ARM	%	-7,96	-2,70	4,87	11,26

SPREMEMBA STRUKTURE PROIZVODNJE

Prav tako očitne razlike med območjema CE in JV nastopijo, če ugotavljamo delež posameznih virov v bodoči strukturi proizvodnje v teh območjih.

Predvideno gibanje deležev proizvodnje po posameznih energentih v centralni Evropi v prihodnjih 15 letih je prikazano v Tabeli 6.

Tabela 6. Predvideno gibanje deležev proizvodnje v centralni Evropi

Table 6. Production structure in CE

	2006	2010	2015	2020
Hidro	0,19	0,18	0,17	0,17
Jedrske	0,26	0,23	0,21	0,18
Premogovne	0,26	0,24	0,23	0,20
tekoča fosilna	0,19	0,21	0,21	0,24
Obnovljivi	0,08	0,12	0,16	0,19

Predvideno gibanje deležev proizvodnje po posameznih energentih v jugovzhodni Evropi v prihodnjih 15 letih je prikazano v Tabeli 7.

Tabela 7. Predvideno gibanje deležev proizvodnje v JV Evropi

Table 7. Production structure in SE Europe

	2006	2010	2015	2020
Hidro	0,32	0,31	0,31	0,31
Jedrske	0,06	0,06	0,09	0,10
Premogovne	0,33	0,29	0,28	0,28
Tekoča fosilna	0,16	0,18	0,18	0,17
Obnovljivi	0,01	0,03	0,03	0,03

Zelo negotov dejavnik pri napovedovanju proizvodne cene elektrarn je postala cena emisij CO₂, ki lahko v veliki meri zmanjša konkurenčno prednost, ki jo imajo na trgu elektrarne na fosilna goriva. Predvideni stroški proizvodnje elektrarn z različnimi vrstami energentov, v odvisnosti od vrednosti emisij CO₂, so prikazani v Tabeli 8.

Tabela 8. Stroški obratovanja na MWuro
Table 8. MWh production costs

Cena CO ₂	CO ₂ nič	CO ₂ srednje	CO ₂ drago
	€/MW/uro	€/MW/uro	€/MW/uro
Hidro	12	12	12
Jedrske	33,5	33,5	33,5
Premogovne	36,5	54,75	73
Tekoča fosilna	32,1	40,05	48
Obnovljivi	54	54	54

Uporabljene enote €/MW/uro so prilagojene podatkom iz napovedi zadostnosti oskrbe, ki podajajo moč v MW. Stroški investicije, kapitala, obratovanja in drugi stroški elektrarn so preračunani na inštalirano velikost elektrarn. Ne glede na dejansko dinamiko proizvodnje mora elektrarna v svoji življenjski dobi v vsaki uri za vsak MW moči pokriti stroške v višini, ki jo podaja zgornja tabela.

Povprečne stroške obratovanja sistemov JV Evrope in CE v odvisnosti od vrednosti emisij CO₂ v prihodnjih 15 letih prikazuje Tabela 9. Cena je v JV manjša kot v CE zaradi večjega deleža hidroelektrarn v strukturi proizvodnje. Razlika v ceni med CE in JV Evropo se pri nižji vrednosti emisij povečuje, pri veliki in srednji vrednosti emisij CO₂ se razlika zmanjšuje. Do tega pride,

ker je v CE predvideno veliko zmanjšanje proizvodnje iz elektrarn na fosilna goriva, v JV Evropi se delež teh elektrarn ohranja. Ob povečanju cene emisije CO₂ se tako cena energije v JV Evropi poveča bolj kot v CE.

Tabela 9. Povprečni stroški obratovanja sistemov JV Evrope in centralne Evrope

Table 9. Average production costs in SEE and CE

CO ₂ srednja	2006	2010	2015	2020
Cena JV	23,6	30,7	30,8	31,0
Cena CE	31,1	37,8	38,7	39,2
% Razlika	0,0	-8,8	-6,0	-5,4

CO ₂ brez	2006	2010	2015	2020
Cena JV	23,6	23,9	24,3	24,5
Cena CE	31,1	31,8	32,8	33,6
% Razlika	0,0	0,7	2,5	3,9

CO ₂ drago	2006	2010	2015	2020
Cena JV	23,6	37,5	37,2	37,4
Cena CE	31,1	43,8	44,6	44,8
% Razlika	0,0	-18,2	-14,5	-14,6

Rast cen električne energije v JV Evropi je ocenjena na 31 %, rast v CE Evropi pa 26 %. To pomeni, da bo zaradi okoljskih vplivov rast cene električne energije v JV Evropi za 5 % večja od rasti cene v CE.

SKLEPI

Nikjer na svetu v naslednjih desetletjih premoga ni mogoče nadomestiti. Podpora pri nadaljnji uporabi premoga, sprejemljivost na trgu in v okolju je pomembna politična naloga za Evropo.

EU se mora bojevati proti čedalje večji odvisnosti od uvožene nafte in zemeljskega plina s strategijo varne in stabilne oskrbe. Ob racionalni rabi energije in povečani uporabi obnovljivih virov energije, je premog glavni doprinos k stabilnim cenam in varni oskrbi.

Premog ima izredno dolgoročno perspektivo in dobro konkurenčno pozicijo za energetske oskrbo Evrope. Dolgoročno spreminjanje cen elektrike temelji med drugim tudi na uporabi premoga in nuklearne energije. Do leta 2020, je prioriteta gradnja in modernizacija obstoječih termoelektarn in posledično s tem povečanje učinkovitosti.

Uporaba premoga za pridobivanje električne energije bo v glavnem odvisna od cen plina in stroškov za izpust CO₂. Predvsem pa se bo položaj izboljšal zaradi dviga cen zemeljskega plina. Implementacija trgovanja z emisijami lahko močno spremeni strukturo proizvodnje elektrike v Evropi in s tem močno obremeni države, ki v glavnem uporabljajo premog.

Prihodnost premoga v Evropi bo odvisna tudi od tehnološkega pristopa do klimatskih sprememb. S CCS (zajem in skladiščenje CO₂) tehnologijo je možno sistemsko bistveno zmanjšati količine CO₂ ob sprejemljivih stroških, to pa lahko postane del resničnosti po letu 2020.

CCS tehnologija omogoča reduciranje stopnje CO₂, cene elektrike pa bi ostale v razumljivih mejah. V tem kontekstu ostaja premog konkurenčen vir energije za termoelektrarne. Da bi se izognili velikim

razlikam v konkurenčnosti, mora Evropa odigrati glavno vlogo skupaj z ostalimi industrijsko razvitimi narodi, najprej v smislu učinkovitosti, zatem s tehnologijo CCS, prav tako pa tudi pri trgovanju z emisijskimi kuponi.

SUMMARY

Strategic aspects of electricity power supply in central and south-eastern Europe - The role of coal and coal technologies evaluation

Throughout the world, coal cannot be replaced during the next decades. Facilitating further coal use, acceptable to the market and the environment, is an important political task for Europe.

The EU must fight with determination against its increasing dependence on imported oil and gas with a strategy balanced between security of supply and sustainability. In addition to the rational use of energy and the increased use of renewable energies, coal makes a major contribution above all to stable prices and security of supply.

Coal has outstanding long-term perspectives and a good competitive position for power generation in Europe. The moderate development of electricity prices in the long-term is the result of the use of coal

and nuclear energy. Until 2020, the focus is on construction and modernisation of existing power plants, and thereby improved efficiency.

The use of coal for power generation will mainly be determined by the level of prices for gas and by CO₂ costs. Above all with rising prices for gas, the market position of coal for power generation continues to improve. The implementation of Emissions Trading can greatly change the structure of power generation in Europe and especially burden countries that use a lot of coal.

The future of coal in Europe will also be determined by technological responses to climate issues. With CCS (Carbon Capture and Storage), technology is available that, if developed systematically within an appropriate framework, makes a wide-ranging avoidance of CO₂ output at acceptable costs become a reality in the future, i.e. after 2020.

CCS technology makes possible ambitious objectives to reduce CO₂ with electricity prices remaining at a reasonable level. In this context, coal remains a competitive source of energy for power generation. In order to avoid major competition distortions, Europe should play the leading role together with other major industrialized nations, first in matters of efficiency, later for CCS technology but also for Emissions Trading.

VIRI

- EC – Directorate General for Energy and Transport (2007): *European Energy and Transport-Trends to 2030 (Update 2005)*. http://ec.europa.eu/dgs/energy_transport/figures/trends_2030_update_2007/energy_transport_trends_2030_update_2007_en.pdf
- Energora (2007): *Strateška vloga premoga kot energenta na področju JV Evrope*. Energora.
- European Association for Coal and Lignite - Euracoal (2004): *EU Statistics 2004*. Euracoal, Brussels.
- European Association for Coal and Lignite - Euracoal (2005): *Coal Industry Across Europe*. Euracoal, Brussels.
- European Association for Coal and Lignite - Euracoal (2007): *Euracoal Market Report 2/2007*. Euracoal, Brussels.
- European Association for Coal and Lignite - Euracoal (2007): *The Future Role of Coal in Europe*. Euracoal, Brussels. http://www.worldcoal.org/assets_cm/files/PDF/thecoalresource.pdf
- Union for the Co-ordination of Transmission of Electricity (2005): *System Adequacy Forecast 2008-2020*. Brussels.
- Union for the Co-ordination of Transmission of Electricity (2005): *System Adequacy Retrospect 2005*. Brussels.
- Union for the Co-ordination of Transmission of Electricity (2006): *Memo 2000-2005*. Brussels.
- Union for the Co-ordination of Transmission of Electricity: *Statistical yearbooks 2000-2005*. Brussels.
- World Coal Institute (2005): *Coal: Secure Energy*. http://www.worldcoal.org/assets_cm/files/PDF/wci_coal_secure_energy_2005.pdf
- World Coal Institute (2005): *The Coal Resource – A Comprehensive Overview of Coal*.

Author's Index, Vol. 55, No. 2

Bizjak Milan	milan.bizjak@ntf.uni-lj.si	163
Bombač David	david.bombac@ntf.uni-lj.si	173
Bratuš Vitoslav	vito.bratus@hidria.com	163
Brojan Miha	miha.brojan@fs.uni-lj.si	173
Česnik Damir	damir.cesnik@hidria.com	163
Dervarič Evgen	evgen.dervaric@ntf.uni-lj.si	277
Fazarinc Matevž	matevz.fazarinc@guest.arnes.si	147
Jerolimov Vjekoslav	jerolimov@sfgz.hr	191
Kosec Borut	borut.kosec@ntf.uni-lj.si	163
Kosel Franc	franc.kosel@fs.uni-lj.si	173
Kugler Goran	goran.kugler@ntf.uni-lj.si	147
Medved Milan	milan.medved@rlv.si	277
Miklavič Blaž	blaz.miklavic@gmail.com	199
Monticelli Franco	franco.monticelli@riotinto.com	225
Oggeri Claudio	claudio.oggeri@polito.it	225
Oreste Pierpaolo	pierpaolo.oreste@polito.it	225
Pavlin Martin	martin.pavlin@triera.net	191
Peila Daniele	daniele.peila@polito.it	225
Polizza Sebastiano	sebastiano.polizza@polito.it	225
Popit Andreja	andreja.popit@sct.si	259
Rant Jože	joze.rant@sct.si	259
Rozman Janez	janez.rozman@guest.arnes.si	163
Rožič Boštjan	bostjan.rozic@ntf.uni-lj.si	199
Rudolf Rebeka	rebeka.rudolf@uni-mb.si	191
Skubin Gorazd	info@energora.si	277
Stevanovič Lidija	lidijas@gmail.com	237
Terčelj Milan	milan.tercelj@ntf.uni-lj.si	147
Večko Pirtovšek Tatjana	tpirtovsek@metalravne.com	147
Videnič Tomaž	tomaz.videnic@fs.uni-lj.si	173
Viršek Sandi	sandi.virsek@gov.si	215
Vižintin Goran	goran.vizintin@ntf.uni-lj.si	215,237
Vukelič Željko	zeljko.vukelic@ntf.uni-lj.si	237

INSTRUCTIONS TO AUTHORS

RMZ-MATERIALS & GEOENVIRONMENT (RMZ- Materiali in geokolje) is a periodical publication with four issues per year (established 1952 and renamed to RMZ-M&G in 1998). The main topics of contents are Mining and Geotechnology, Metallurgy and Materials, Geology and Geoenvironment.

RMZ-M&G publishes original Scientific articles, Review papers, Technical and Expert contributions (also as short papers or letters) **in English**. In addition, evaluations of other publications (books, monographs,...), short letters and comments are welcome. A short summary of the contents in Slovene will be included at the end of each paper. It can be included by the author(s) or will be provided by the referee or the Editorial Office.

** **Additional information and remarks for Slovenian authors:***

*English version with extended »Povzetek«, and additional roles (in Template for Slovenian authors) **can** be written. Only exceptionally the articles in the Slovenian language with summary in English will be published. The contributions in English will be considered with priority over those in the Slovenian language in the review process.*

Authorship and originality of the contributions. Authors are responsible for originality of presented data, ideas and conclusions as well as for correct citation of data adopted from other sources. The publication in RMZ-M&G obligate authors that the article will not be published anywhere else in the same form.

Specification of Contributions

Optimal number of pages of full papers is 7 to 15, longer articles should be discussed with Editor, but 20 pages is limit.

Scientific papers represent unpublished results of original research.

Review papers summarize previously published scientific, research and/or expertise articles on the new scientific level and can contain also other cited sources, which are not mainly result of author(s).

Technical and Expert papers are the result of technological research achievements, application research results and information about achievements in practice and industry.

Short papers (Letters) are the contributions that contain mostly very new short reports of advanced investigation. They should be approximately 2 pages long but should not exceed 4 pages.

Evaluations or critics contain author's opinion on new published books, monographs,

textbooks, exhibitions...(up to 2 pages, figure of cover page is expected).

In memoriam (up to 2 pages, a photo is expected).

Professional remarks (Comments) cannot exceed 1 page, and only professional disagreements can be discussed. Normally the source author(s) reply the remarks in the same issue.

Supervision and review of manuscripts. All manuscripts will be supervised. The referees evaluate manuscripts and can ask authors to change particular segments, and propose to the Editor the acceptability of submitted articles. Authors can suggest the referee but Editor has a right to choose another. **The name of the referee remains anonymous.** The technical corrections will be done too and authors can be asked to correct missing items. The final decision whether the manuscript will be published is made by the Editor in Chief.

The Form of the Manuscript

The manuscript should be submitted as a complete hard copy including figures and tables. The figures should also be enclosed separately, both charts and photos in the original version. In addition, all material should also be provided in electronic form on a diskette or a CD. The necessary information can conveniently also be delivered by E-mail.

Composition of manuscript is defined in the attached Template

The original file of Template is temporarily available on E-mail addresses:

peter.fajfar@ntf.uni-lj.si,

barbara.bohar@ntf.uni-lj.si

References - can be arranged in two ways:

- first possibility: alphabetic arrangement of first authors - in text: (Borgne, 1955),
or

- second possibility: ^[1] numerated in the same order as cited in the text: example^[1]

Format of papers in journals:

Le Borgne, E. (1955): Susceptibilite magnetic anomale du sol superficiel.
Annales de Geophysique, 11, pp. 399-419.

Format of books:

Roberts, J. L. (1989): Geological structures, *MacMillan, London*, 250 p.

Text on the hard print copy can be prepared with any text-processor. The electronic version on the diskette, CD or E-mail transfer should be in MS Word or ASCII format.

Captions of figures and tables should be enclosed separately. **Figures (graphs and photos)** and tables should be original and sent separately in addition to text. They can be prepared on paper or computer designed (MSExcel, Corel, Acad).

Format. Electronic figures are recommended to be in CDR, AI, EPS, TIF or JPG formats. Resolution of bitmap graphics (TIF, JPG) should be at least 300 dpi. Text in vector graphics (CDR, AI, EPS) must be in MSWord Times typography or converted in curves.

Color prints. Authors will be charged for color prints of figures and photos.

Labeling of the additionally provided material for the manuscript should be very clear and must contain at least the lead author's name, address, the beginning of the title and the date of delivery of the manuscript. In case of an E-mail transfer the exact message with above asked data must accompany the attachment with the file containing the manuscript.

Information about RMZ-M&G:

Editor in Chief prof. dr. Peter Fajfar (tel. ++386 1 4250-316) or
Secretary Barbara Bohar Bobnar, un. dipl. ing. geol. (++386 1 4704-630),
Aškerčeva 12, Ljubljana, Slovenia

or at E-mail addresses:

peter.fajfar@ntf.uni-lj.si,
barbara.bohar@ntf.uni-lj.si

Sending of manuscripts. Manuscripts can be sent by mail to the **Editorial Office** address:

- RMZ-Materials & Geoenvironment
Aškerčeva 12,
1000 Ljubljana, Slovenia

or delivered to:

- **Reception** of the Faculty of Natural Science and Engineering (for RMZ-M&G)
Aškerčeva 12,
1000 Ljubljana, Slovenia
- E-mail - addresses of Editor and Secretary
- You can also contact them on their phone numbers.

TEMPLATE

**The title of the manuscript should be written in bold letters
(Times New Roman, 14, Center)**

NAME SURNAME¹, , & NAME SURNAME^X
(TIMES NEW ROMAN, 12, CENTER)

^xFaculty of ... , University of ... , Address..., Country, e-mail: ...
(Times New Roman, 11, Center)

THE LENGTH OF FULL PAPER SHOULD NOT EXCEED TWENTY (20, INCLUDING FIGURES AND TABLES) PAGES (OPTIMAL 7 TO 15), SHORT PAPER FOUR (4) AND OTHER TWO (2) WITHOUT TEXT FLOWING BY GRAPHICS AND TABLES.

Abstract (Times New Roman, Normal, 11): The text of the abstract is placed here. The abstract should be concise and should present the aim of the work, essential results and conclusion. It should be typed in font size 11, single-spaced. Except for the first line, the text should be indented from the left margin by 10 mm. The length should not exceed fifteen (15) lines (10 are recommended).

Key words: a list of up to 5 key words (3 to 5) that will be useful for indexing or searching. Use the same styling as for abstract.

INTRODUCTION (TIMES NEW ROMAN, BOLD, 12)

Two lines below the keywords begin the introduction. Use Times New Roman, font size 12, Justify alignment.

There are two (2) admissible methods of citing references in text:

1. by stating the first author and the year of publication of the reference in the parenthesis at the appropriate place in the text and arranging the reference list in the alphabetic order of first authors; e.g.:
“Detailed information about geohistorical development of this zone can be found in: Antonijević (1957), Grubić (1962), ...”
“... the method was described previously (Hoefs, 1996)”

2. by consecutive Arabic numerals in square brackets, superscripted at the appropriate place in the text and arranging the reference list at the end of the text in the like manner; e.g.:
“... while the portal was made in Zope^[3] environment.”

MATERIALS AND METHODS (TIMES NEW ROMAN, BOLD, 12)

This section describes the available data and procedure of work and therefore provides enough information to allow the interpretation of the results, obtained by the used methods.

RESULTS AND DISCUSSION (TIMES NEW ROMAN, BOLD, 12)

Tables, figures, pictures, and schemes should be incorporated in the text at the appropriate place and should fit on one page. Break larger schemes and tables into smaller parts to prevent extending over more than one page.

CONCLUSIONS (TIMES NEW ROMAN, BOLD, 12)

This paragraph summarizes the results and draws conclusions.

Acknowledgements (Times New Roman, Bold, 12, Center - optional)

This work was supported by the ****.

REFERENCES (TIMES NEW ROMAN, BOLD, 12)

In regard to the method used in the text, the styling, punctuation and capitalization should conform to the following:

FIRST OPTION - in alphabetical order

Casati, P., Jadoul, F., Nicora, A., Marinelli, M., Fantini-Sestini, N. & Fois, E.
(1981): Geologia della Valle del'Anisici e dei gruppi M. Popera - Tre

Cime di Lavaredo (Dolomiti Orientali). *Riv. Ital. Paleont.*; Vol. 87, No. 3, pp. 391-400, Milano.

Folk, R. L. (1959): Practical petrographic classification of limestones. *Amer. Ass. Petrol. Geol. Bull.*; Vol. 43, No. 1, pp. 1-38, Tulsa.

SECOND OPTION - in numerical order

^[1] Trček, B. (2001): *Solute transport monitoring in the unsaturated zone of the karst aquifer by natural tracers*. Ph.D. Thesis. Ljubljana: University of Ljubljana 2001; 125 p.

^[2] Higashitani, K., Iseri, H., Okuhara, K., Hatade, S. (1995): Magnetic Effects on Zeta Potential and Diffusivity of Nonmagnetic Particles. *Journal of Colloid and Interface Science* 172, pp. 383-388.

Citing the Internet site:

CASREACT-Chemical reactions database [online]. Chemical Abstracts Service, 2000, updated 2.2.2000 [cited 3.2.2000]. Accessible on Internet: <http://www.cas.org/CASFILES/casreact.html>.

POVZETEK (TIMES NEW ROMAN, 12)

A short summary of the contents in Slovene (up to 400 characters) can be written by the author(s) or will be provided by the referee or by the Editorial Board.

TEMPLATE for Slovenian Authors

**The title of the manuscript should be written in bold letters
(Times New Roman, 14, Center)**

Naslov članka (Times New Roman, 14, Center)

NAME SURNAME¹,..., & NAME SURNAME^X (TIMES NEW ROMAN, 12, CENTER)
IME PRIIMEK¹, ..., IME PRIIMEK^X (TIMES NEW ROMAN, 12, CENTER)

^XFaculty of ... , University of ... , Address..., Country; e-mail: ...
(Times New Roman, 11, Center)

^XFakulteta..., Univerza..., Naslov..., Država; e-mail: ...
(Times New Roman, 11, Center)

THE LENGTH OF ORIGINAL SCIENTIFIC PAPER SHOULD NOT EXCEED TWENTY (20, INCLUDING FIGURES AND TABLES) PAGES (OPTIMAL 7 TO 15), SHORT PAPER FOUR (4) AND OTHER TWO (2) WITHOUT TEXT FLOWING BY GRAPHICS AND TABLES.

DOLŽINA IZVIRNEGA ZNANSTVENEGA ČLANKA NE SME PRESEGATI DVAJSET (20, VKLJUČNO S SLIKAMI IN TABELAMI), KRATKEGA ČLANKA ŠTIRI (4) IN OSTALIH PRISPEVKOV DVE (2) STRANI.

Abstract (Times New Roman, Normal, 11): The text of the abstract is placed here. The abstract should be concise and should present the aim of the work, essential results and conclusion. It should be typed in font size 11, single-spaced. Except for the first line, the text should be indented from the left margin by 10 mm. The length should not exceed fifteen (15) lines (10 are recommended).

Izvleček (TNR, N, 11): Kratek izvleček namena članka ter ključnih rezultatov in ugotovitev. Razen prve vrstice naj bo tekst zamaknjen z levega roba za 10 mm. Dolžina naj ne presega petnajst (15) vrstic (10 je priporočeno).

Key words: a list of up to 5 key words (3 to 5) that will be useful for indexing or searching. Use the same styling as for abstract.

Ključne besede: seznam največ 5 ključnih besed (3-5) za pomoč pri indeksiranju ali iskanju. Uporabite enako obliko kot za izvleček.

INTRODUCTION – UVOD (TIMES NEW ROMAN, BOLD, 12)

Two lines below the keywords begin the introduction. Use Times New Roman, font size 12, Justify alignment. All captions of text and tables as well as the text in graphics must be prepared in English and Slovenian language.

Dve vrstici pod ključnimi besedami se začne Uvod. Uporabite pisavo TNR, velikost črk 12, z obojestransko poravnavo. Naslovi slik in tabel (vključno z besedilom v slikah) morajo biti pripravljene v slovenskem in angleškem jeziku.

Figure (Table) X. Text belonging to figure (table)

Slika (Tabela) X. Pripadajoče besedilo k sliki (tabeli)

There are two (2) admissible methods of citing references – obstajata dve sprejemljivi metodi navajanja referenc:

1. by stating the first author and the year of publication of the reference in the parenthesis at the appropriate place in the text and arranging the reference list in the alphabetic order of first authors; e.g.:
 1. z navedbo prvega avtorja in letnice objave reference v oklepaju na ustreznem mestu v tekstu in z ureditvijo seznama referenc po abecednem zaporedju prvih avtorjev; npr.:

“Detailed information about geohistorical development of this zone can be found in: Antonijević (1957), Grubić (1962), ...”

“... the method was described previously (Hoefs, 1996)”

or/ali

2. by consecutive Arabic numerals in square brackets, superscripted at the appropriate place in the text and arranging the reference list at the end of the text in the like manner; e.g.:
 2. z zaporednimi arabskimi številkami v oglatih oklepajih na ustreznem mestu v tekstu in z ureditvijo seznama referenc v številčnem zaporedju navajanja; npr.:

“... while the portal was made in Zope^[3] environment.”

MATERIALS AND METHODS (TIMES NEW ROMAN, BOLD, 12)

This section describes the available data and procedure of work and therefore provides enough information to allow the interpretation of the results, obtained by the used methods.

Ta del opisuje razpoložljive podatke, metode in način dela ter omogoča zadostno količino informacij, da lahko z opisanimi metodami delo ponovimo.

RESULTS AND DISCUSSION – REZULTATI IN RAZPRAVA (TIMES NEW ROMAN, BOLD, 12)

Tables, figures, pictures, and schemes should be incorporated (inserted, not pasted) in the text at the appropriate place and should fit on one page. Break larger schemes and tables into smaller parts to prevent extending over more than one page.

Tabele, sheme in slike je potrebno vnesti (z ukazom Insert, ne Paste) v tekst na ustreznem mestu. Večje sheme in tabele je potrebno ločiti na manjše dele, da ne presegajo ene strani.

CONCLUSIONS – SKLEPI (TIMES NEW ROMAN, BOLD, 12)

This paragraph summarizes the results and draws conclusions.
Povzetek rezultatov in zaključki.

Acknowledgements – Zahvale (Times New Roman, Bold, 12, Center - optional)

This work was supported by the
Izvedbo tega dela je omogočilo

REFERENCES - VIRI (TIMES NEW ROMAN, BOLD, 12)

With regard to the method used in the text, the styling, punctuation and capitalization should conform to the following:

Glede na uporabljeno metodo citiranja referenc v tekstu upoštevajte eno od naslednjih oblik:

FIRST OPTION (recommended) – PRVA MOŽNOST (priporočena) – in alphabetical order (v abecednem zaporedju)

Casati, P., Jadoul, F., Nicora, A., Marinelli, M., Fantini-Sestini, N. & Fois, E. (1981): Geologia della Valle del'Anisici e dei gruppi M. Popera – Tre Cime di Lavaredo (Dolomiti Orientali). *Riv. Ital. Paleont.*; Vol. 87, No. 3, pp. 391-400, Milano.

Folk, R. L. (1959): Practical petrographic classification of limestones. *Amer. Ass. Petrol. Geol. Bull.*; Vol. 43, No. 1, pp. 1-38, Tulsa.

SECOND OPTION – DRUGA MOŽNOST - in numerical order (v numeričnem zaporedju)

^[1] Trček, B. (2001): *Solute transport monitoring in the unsaturated zone of the karst aquifer by natural tracers*. Ph.D. Thesis. Ljubljana: University of Ljubljana 2001; 125 p.

^[2] Higashitani, K., Iseri, H., Okuhara, K., Hatade, S. (1995): Magnetic Effects on Zeta Potential and Diffusivity of Nonmagnetic Particles. *Journal of Colloid and Interface Science* 172, pp. 383-388.

Citing the Internet site:

CASREACT-Chemical reactions database [online]. Chemical Abstracts Service, 2000, updated 2.2.2000 [cited 3.2.2000]. Accessible on Internet: <http://www.cas.org/CASFILES/casreact.html>.

Citiranje Internetne strani:

CASREACT-Chemical reactions database [online]. Chemical Abstracts Service, 2000, obnovljeno 2.2.2000 [citirano 3.2.2000]. Dostopno na svetovnem spletu: <http://www.cas.org/CASFILES/casreact.html>.

POVZETEK – SUMMARY (TIMES NEW ROMAN, 12)

An extended summary of the contents in Slovene (from one page to approximately 1/3 of the original article length).

Razširjeni povzetek vsebine prispevka v Angleščini (od ene strani do približno 1/3 dolžine izvirnega članka).

Rešitve za opazovanje premikov in deformacij

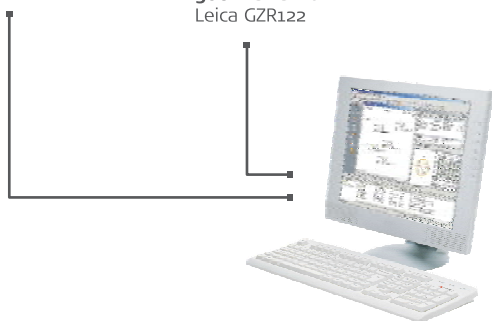


GNSS senzor
Leica GMX902 GG

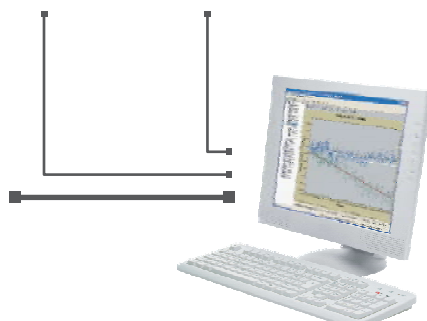
GPS senzor
Leica GMX901
in 360° reflektor
Leica GZR122

Nagibni senzor
Leica NIVEL200

Samodejni tahimeter
Leica TCA1201 M



Programska oprema
Leica GNSS Spider



Programska oprema
Leica GeoMoS



Geoservis, d.o.o.
Litjiska cesta 45, 1000 Ljubljana
t. (01) 586 38 30, i. www.geoservis.si

■ Authorized Leica Geosystems Distributor

- when it has to be **right**

Leica
Geosystems

Skupina **hse**



PREMOGOVNIK VELENJE

je pomemben in zanesljiv člen
v oskrbi Slovenije
z električno energijo.

Zavedamo se odgovornosti do
lastnikov, zaposlenih in okolja.



ČUT ZA PRIHODNOST



RTH

ŠTORE Q STEEL



INVESTOR IN PEOPLE

ISO 9001
ISO 14001
OHSAS 18001
BUREAU VERITAS
Certification



N. 214241 / N. 220242 / N. 224312

Železarska cesta 3, 3220 Štore, Slovenia
Phone: ++386 3 78 05 100
Fax: ++386 3 78 05 384
www.store-steel.si

prof. dr. Andrej Paulin

Tehniški metalurški slovar (CD-ROM za WINDOWS)

slovensko - angleško - nemški

Technical metallurgical dictionary (CD-ROM for WINDOWS)

Slovenian - English - German

Več kot 10.000 gesel s področij:

- metalurgije,
- tehniških materialov,
- tehnike površin,
- analiznih metod,
- strojništva,
- kemije,
- elektrotehnike,
- ekologije,
- standardizacije,
- predpisov,
- ekonomike in
- uporabe računalništva pri tehnoloških postopkih.

Osnovne značilnosti oz. prednosti elektronske različice slovarja so preprost in izjemno hiter dostop do iskanega gesla, besede ali zveze, tudi pri zahtevnejših pogojih, ter velika prilagodljivost vmesnika uporabnikovim potrebam in željam. Slovar uporablja pregledovalnik ASP32 in je združen s številnimi drugimi slovarji v tem sistemu.

Cenik elektronskega slovarja:

- Enuporabniška lokalna verzija - 58,00 EUR
- 5 licenc mrežna verzija - 390,00 EUR
- 10 licenc mrežna verzija - 535,00 EUR
- 20 licenc mrežna verzija - 680,00 EUR
- 30 licenc mrežna verzija - 825,00 EUR
- 40 licenc mrežna verzija - 970,00 EUR
- 50 licenc mrežna verzija - 1.115,00 EUR

Prices for the electronic dictionary:

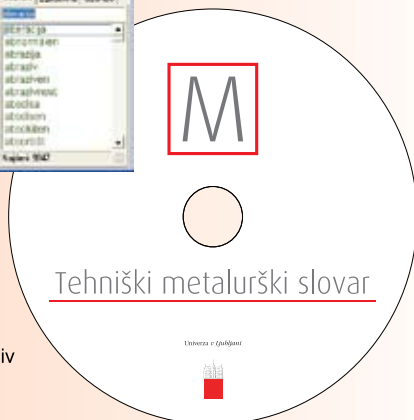
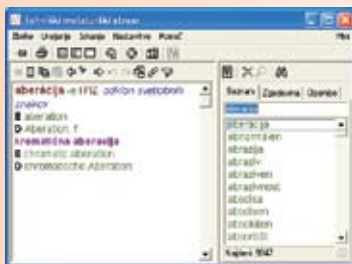
- Single user local version - 58,00 EUR
- 5 users network version - 390,00 EUR
- 10 users network version - 535,00 EUR
- 20 users network version - 680,00 EUR
- 30 users network version - 825,00 EUR
- 40 users network version - 970,00 EUR
- 50 users network version - 1.115,00 EUR

Basic characteristics or advantages, respectively, of electronic version of the dictionary is simple and very fast access to sought term, word or to complex term, also in more demanding conditions, and a great adaptability of the interface to user's needs and wishes. The dictionary uses ASP32 search system that is compatible to numerous other dictionaries in this system.

Za naročila in dodatne informacijas kontaktirajte preko e-pošte:

For orders and additional information please contact us by e-mail:

omm@ntf.uni-lj.si



Leto izdaje: 2007
Issued in 2007

More than 10 000 technical terms on:

- metallurgy
- technical materials
- surface engineering
- analytical methods
- mechanical engineering
- chemical engineering
- electrical engineering
- environmental engineering
- standardization
- technical regulations
- economics, and
- computer engineering in technological processes

RMZ - Materials and Geoenvironment

RMZ-M&G, Vol. 55, No. 2

pp. 147-306 (2008)

Contents

MATERIALS AND METALLURGY

Increasing of hot deformability of tool steels – preliminary results
VEČKO PIRTOVŠEK, T., FAZARINC, M., KUGLER, G., TERČELJ, M. 147

Heat treatment and fine-blankin Inconel 718
ČESNIK, D., BRATUŠ, V., KOSEC, B., ROZMAN, J., BIZJAK, M. 163

Shape memory alloys in medicine
BROJAN, M., BOMBAČ, D., KOSEL, F., VIDENIČ, T. 173

Artificial tooth and polymer-base bond in removable dentures: the influence
of pre-treatment on technological parameters to the bond's strength
PAVLIN, M., RUDOLF, R., JEROLIMOV, V. 191

GEOLOGY

The onset of Maastrichtian basinal sedimentation on Mt. Matajur, NW Slovenia
MIKLAVIČ, B., ROŽIČ, B. 199

Analytical surface water forecasting system for Republic of Slovenia
VIŽINTIN, G., VIRŠEK, S. 215

GEOTECHNOLOGY AND MINING

Rodoretto talc mine (To, Italy): studies for the optimization of the cemented backfilling
PEILA, D., OGGERI, C., ORESTE, P., POLIZZA, S., MONTICELLI, F. 225

Determination of environmental criteria for estimation of land development using GIS
VIŽINTIN, G., STEVANOVIČ, L., VUKELIČ, Ž. 237

Construction of the Šentvid tunnel
POPIT, A., RANT, J. 259

Strateški vidiki oskrbe centralne in jugovzhodne Evrope z električno energijo
z oceno vloge premoga ter premogovnih tehnologij
MEDVED, M., DERVARIČ, E., SKUBIN, G. 277

Author's Index, Vol. 55, No. 2 296

Instructions to Authors 297

Template 300